University of Southampton

Faculty of Medicine

Cancer Sciences Unit

Role of Stem-like Cells in Breast Cancer

By

Pardis Arvinrad

Thesis for the Degree of Doctor of Philosophy

September 2016

Acknowledgments

Through the difficulties, Up to the stars …

Undertaking this PhD has been a truly life-changing experience for me and it would not have been possible to do without the support and guidance that I received from many people in many countries, who so generously contributed to the work presented in this thesis. I can honestly say that doing this PhD has changed me for the better. I am using this opportunity to express my gratitude to everyone who reminded me in moments where I felt like nothing, that being here was already everything!

Firstly, I would like to express my sincere gratitude to my two supervisors Dr. Jeremy Blaydes and Dr. Franchesca Houghton for sharing their truthful views on this project and for their continuous support during the past four years. Jeremy has been a wonderful advisor and mentor and his insightful discussions helped me throughout research and writing of this thesis. Jeremy was always reachable and his emailed replies came back almost promptly. Franchesca has always come up with brilliant ideas and suggestions and tried to challenge me with her questions. Living abroad and being away from my loved ones has never been easy, especially during hard times when you need support; Franchesca provided me with much support throughout my PhD. My deep appreciation goes out to them for their patience, time, and effort they put into this project.

I am also very grateful to my supervisor Professor Paul Townsend for his scientific advice and constant encouragements. Although I met less regularly with Paul, he was always contactable by text and email, even late in the evening, at the weekend, or when he was on holiday. And when I met with him, I always left with optimism for the next experiments. I would also like to thank Ramsey Cutress for his help in putting all this together in the first place.

I would also like to express my gratitude to the people around the department and in the lab who made these years an unforgettable experience for me. I will forever be thankful to Matt Darley for his helpful guidance and friendly advice. Matt was so helpful when I first joined the lab and of course consistently during the three years of my lab

experience. Matt taught me most of the techniques I have used in this project. He was particularly patient and instrumental in helping me through the mistakes I repeatedly made! I would like to give my special thanks to lovely Samantha Larkin for her generosity with her time in kindly helping me to structure my thesis nicely.

I will forever be thankful to my former research advisor Dr. Khosro Jafari when I first started my University in Tehran. I still think warmly of my time as an undergraduate student in his lab. Four years of precious experience during my Bachelors degree was the main reason why I decided to pursue a career in research.

I am indebted to all my friends who have filled the last four years with amazing memories which helped me through the difficult moments I have had; mostly to my best friend Paria Sadeghi, without whom I would not have had the courage to cope with the challenges of this journey.

I would also like to say a heartfelt thank you to Daniele Barducci, who has been by my side throughout this PhD and encouraged me with his hopeful words when I was feeling disappointed. Without him, I would not have had the courage to making it possible and complete what I have started.

Words cannot express how grateful I am to my parents; my mum and dad who have sacrificed their lives and provided unconditional love and care and for helping me in whatever way they could during this challenging period. And my little sister Parmis, who has been my best friend all my life for always believing in me and encouraging me to follow my dreams. I love them so much, and I would not have made it this far without them. They are the most important people in my world and I dedicate this thesis to them.

Table of Contents

List of Figures

List of Tables

Declaration of Authorship

I, Pardis Arvinrad, declare that this thesis and the work presented in it are my own and has been generated by me as the result of my own original research.

Role of Stem-like Cells in Breast Cancer

I confirm that:

1. This work was done wholly or mainly while in candidature for a research degree at this University;
2. Where any part of this thesis has previously been submitted for a degree or any other qualification at this University or any other institution, this has been clearly stated;
3. Where I have consulted the published work of others, this is always clearly attributed;

4. Where I have quoted from the work of others, the source is always given. With the exception of such quotations, this thesis is entirely my own work;
5. I have acknowledged all main sources of help;
6. Where the thesis is based on work done by myself jointly with others, I have made clear exactly what was done by others and what I have contributed myself;
7. None of this work has been published before submission

Signed:

Date:

UNIVERSITY OF SOUTHAMPTON

ABSTRACT

FACULTY OF MEDICINE

Doctor of Philosophy

ROLE OF STEM-LIKE CELLS IN BREAST CANCER

By Pardis Arvinrad

Breast cancer is a leading cause of mortality in women worldwide, with a high incidence of tumour recurrence and metastasis, predominantly due to chemoresistance, key obstacles in the treatment of any cancer. Studies are emerging in support of the "cancer stem cells theory", which postulates that a small subset of cancer cells is exclusively responsible for the initiation and malignant behaviour of a cancer that are highly tumorigenic, resistant to therapeutic regimes, and responsible for treatment failure and disease relapse. The emergence of cancer is also accompanied by specific metabolic alterations; in particular, enhanced aerobic glycolytic activity which leads to rapid tumour progression. Our current conventional therapies are based on eliminating differentiated tumours, whereas identification of the factors that lead to cancer stem-like cells (CSLCs) maintenance in the tumour population, could lead to the development of more effective therapeutics. Therefore, this thesis aimed to investigate the effect of modulating tumour cell metabolism, using a variety of metabolic inhibitors, on the maintenance of the stem cell population of breast cancer cells, to stop or slow down CSLCs growth. Additionally, this thesis aimed to study the expression levels of the main stem cell markers SOX2, OCT4, and its most homologous pseudogene (OCT4 PG1), in breast cancer following metabolic treatments and to investigate the effect of reducing the expression of these markers on the mammosphere forming ability of MCF-7 cells.

We developed a cell line model of glycolytic vs. glycolysis restricted cells by adapting cells to fructose in the absence of glucose so that cells could grow at normal rates without being glycolytic. We then proceeded to characterise the stem cell population of breast cancer cells using the mammosphere assay. Strikingly, this study demonstrated that MCF-7 cells are able to adapt to fructose conditions, proliferate in a programmed manner as glucose adapted cells, and significantly form more mammospheres than more glycolytic cells. This indicates that the CSLCs do not require a high rate of glycolysis to survive as long as they have sufficient substrate to grow. Moreover, it was found that SOX2 is more highly expressed in glycolysis restricted conditions and OCT4A is not present in breast cancer cell lines. OCT4 PG1 was expressed in some breast cancer cell lines (MCF-7), implying a possible role in carcinogenesis. Additionally, targeting different metabolic pathways found that the use of oxamate to inhibit glycolysis showed that glycolysis is not a critical metabolic pathway for CSLC activity in fructose adapted cells. In conclusion this work shows important links between glycolytic metabolism and pluripotency, and pluripotency related genes in breast cancer.

Abbreviations

2D	Two-dimensional
2DG	2-Deoxy-D-glucose
3D	Three-dimensional
Acetyl-CoA	Acetyl coenzyme A
ADP	Adenosine diphosphate
AKT	Also known as Protein kinase B (PKB)
ALDH	Aldehyde dehydrogenase
AML	Acute myeloid leukaemia
ATP	Adenosine triphosphate
BSA	Bovine serum albumin
bCSLC	Breast cancer stem-like cell
CD24	Cellular adhesion molecule, heat stable antigen
CD44	Hyaluronic acid cell differentiation cluster 44
cDNA	Complementary DNA
CO_2	Carbon dioxide
CPT1	Carnitine palmitoyl transferase 1
CSLC	Cancer stem-like cell
Ct	Cycle threshold
CtBP	C-terminal binding protein

DAKO	Fluorescent mounting medium
DAPI	4'6'diamidino-2-phenylindole
DCA	Dichloroacetate
DCIS	Ductal carcinoma in situ
DMEM	Dulbecco's modified Eagle's medium
DMSO	Dimethyl sulfoxide
DNA	Deoxyribonucleic acid
dNTP	Deoxynucleotide
E-cadherin	CDH1
ECL	Enhanced chemiluminescence
ECM	Extracellular matrix
EDTA	Ethylenediaminetetraacetic acid
EMT	Epithelial to mesenchymal transition
ER	Estrogen
ESA	Epithelial surface antigen
ESC	Embryonic stem cell
F6P	Fructose-6-phosphate
FAO	Fatty acid oxidation
FAS	Fatty acid synthase
FCS	Foetal calf serum

G6P	Glucose-6-phosphate
GDH	Glutamate dehydrogenase
GLS	Glutaminase
GLUT	Glutamine transporter
HBSS	Hank's Balanced Salt Solution
HCC	Human hepatocellular carcinoma
HER	Human epidermal growth factor
hESC	Human embryonic stem cell
HIF	Hypoxia inducible factor
HK	Hexokinase
IDC	Invasive ductal carcinoma
ILC	Invasive lobular carcinoma
iPS	Induced stem cells
LCIS	Lobular carcinoma in situ
LDH	Lactate dehydrogenase
MCT	Monocarboxylate (lactate transporter)
MET	Mesenchymal to epithelial transition
MFE	Mammosphere forming efficiency
mRNA	messenger RNA
MTOB	2-keto-4-methyl-thiobutryate

mTOR	The mechanistic target of rapamycin
NAD	Nicotinamide adenine dinucleotide
NOD/SCID	Non-obesediabetic/severe combined immunodeficient
OCT1	Organic cation transporter 1
OCT4	Octamer-binding transcription factor 4 (POU5F1)
OXPHOS	Oxidative phosphorylation
PBS	Phosphate-buffered saline
PDH	Pyruvate dehydrogenase
PDK1	Pyruvate dehydrogenase kinase
PET	Positron emission tomography
PFK1	Fructose-1, 6-biphosphate
PG1	Pseudogene 1 (POU5F1B)
PI3K	Phosphoinositol 3 kinase
Polyhema	2-hydroxyethyl methacrylate
PPP	Pentose phosphate pathway
PR	Progesterone
qPCR	Quantitative (Real-Time) PCR
RNA	Ribonucleic acid
RT-PCR	Semi-quantitative reverse transcriptase polymerase chain reaction
SDS-PAGE	Sodium dodecyl sulphate polyacrylamide gel electrophoresis

SEM	Standard error of mean
siRNA	Small interfering RNA
SOX2	Sex determining region Y-related box 2
TAE	Tris base, acetic acid and EDTA
TCA	Tricarboxylic acid
TGF-β	Transforming growth factor- β
TNM	Tumour-lymph nodes-metastasis
USP22	Ubiquitin-specific protease 22
WHO	World health organisation

Chapter 1

Introduction

1.1 Cancer

One in two people will be diagnosed with cancer at some point in their life-time (1). Even though the five-year survival rate has improved, there is still an increase in the incidence of cancer in the entire population. Cancer is a broad term for a class of diseases characterised by uncontrolled cell growth and proliferation. Mutations can deregulate cell growth and differentiation in somatic cells, altering the properties of healthy cells such as cell-cell interaction, adhesion, specialisation, and controlled cell death, eventually leading to the formation of neoplasms (1) (2). To maintain cellular integrity, cells undergo apoptosis (programmed cell death). However, on some occasions in cancer cells, apoptosis is unable to be activated; cells accumulate and instead build up into a mass of cells or tissues commonly referred to as a tumour (3). Neoplasms are classified into three main groups according to the World Health Organisation (WHO): benign neoplasms, malignant neoplasms (cancers), and neoplasms of unknown source. The majority of lumps are benign (not generally cancerous) and not aggressive towards surrounding tissues. Benign tumours are less mobile and have lower proliferation rates. Malignant tumours in contrast, proliferate at high rates, move rapidly, and interfere with different organs of the body through either the blood or lymphatic system, invade the adjacent healthy tissues, and can become metastatic (4) (5).

1.1.1 Cancer initiation

Cancers are primarily considered as a disease of the DNA (6). In non-cancerous cells, DNA damage-repair enzymes, repair the errors introduced during DNA replication. However, when normal repair processes fail, and when cellular apoptosis does not occur, the damage to the DNA is not recoverable and mutation occurs (7). On such occasions cells may not function as originally intended. Two main gene categories that are affected by these changes consist of oncogenes and tumour suppressor genes. Tumour suppressor genes represent the oppose cell growth; they discourage cell proliferation and tumour development by repairing damaged DNA and regulating apoptosis. In certain circumstances oncogenes, such as BRCA1 and P53, may promote the malignant phenotype and cause cancer (7). Oncogenes are often over-expressed or mutated in cancers. Inappropriate alterations, such as those seen in cancer, promote genetic changes that affect the proper functioning of tumour suppressor genes. This may alter cell division, survival, or other properties of cancer cells. Typically, it has been proposed that for a cell to become

cancerous it must undergo mutations in genes regulating the cell cycle and differentiation (8).

1.1.2 Cancer development and metastasis

1.1.2.1 Cancer development

There are at least three main factors causing or triggering cancer progression:

- DNA alteration
- Metabolic alteration
- Cancer stem-like cells (CSLCs)

A change in DNA replication and metabolic alteration are both required for cancer development. An increased rate of glycolytic metabolism, despite the presence of oxygen for mitochondrial respiration (the Warburg effect), is characteristic of various cancer cells, including those from breast tumours. The most widely accepted view on carcinogenesis claims DNA alteration as the main cause of tumorigenesis. Mutations might occur in genes at many levels during mitosis and cause abnormalities which may lead to cancer (9).

An alternative view considers an association between DNA alteration and metabolic alteration, two essential factors for cancer initiation and progression (10). The latter (metabolic alteration of cancer cells) is not essentially induced by mutations in oncogenes and tumour suppressor genes, and provides the majority of the building blocks required for cell division (9). The excessive proliferation rate in cancer cells leads to an enhanced nutrient uptake from the blood for the purpose of forming new cells. To this end, the stimulation of glycolysis is necessary for cancer cells to provide most of the energy required for the synthesis of cellular components for cell proliferation (9). During early stages, a tumour gains its bulk mass through cellular proliferation. However, when becoming more mobile, instead of proliferation, metabolic energy is the main source of movement and invasion.

The most recent view highlights the critical role of a small population of cancer cells referred to as CSLCs in the initiation and development of cancer. Research in the field of stem cell biology is lending insight into where cancer originates from and will eventually yield new approaches to fight this disease. Therefore, this project emphasises the two latter key areas of research by focusing on targeting breast cancer stem-like cells (bCSLCs) through reprogramming metabolic pathways in this population.

1.1.2.2 Metastasis

Development of cancer is usually associated with metastasis which refers to an advanced stage of cancer where the tumour spreads to different part of the body from its origin site and accounts for the majority of cancer related deaths including breast (11) (12). Metastasis initiates with the local invasion of surrounding host tissues. During metastasis, cancer cells initially escape from the primary tumour (intravasation), then circulate into the bloodstream or lymphatic system (dissemination), and migrate to the secondary site (extravasation) in the body (13). At this stage, tumour cells continue to multiply and reproduce more metastatic forming tumours (Figure 1.1) (14).

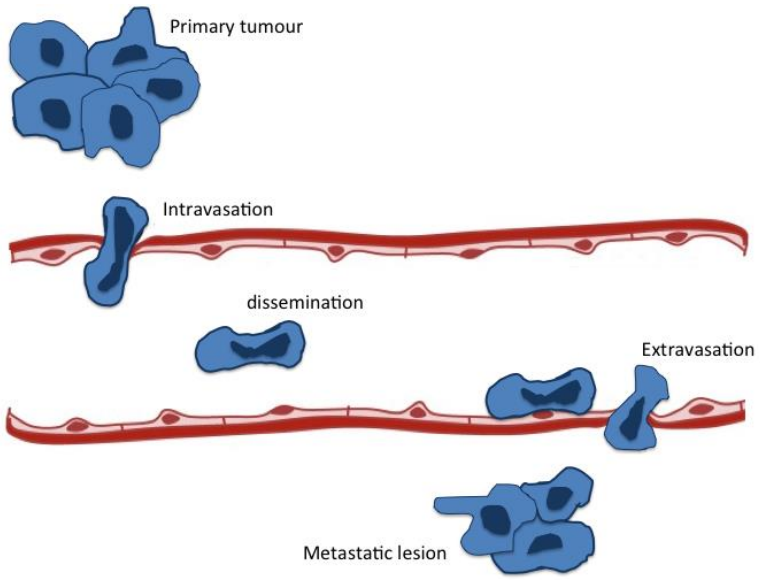

Figure 1.1 A schematic representation of metastasis. Metastatic cells initially break free from the primary tumour by losing adhesion to neighbouring cells and migrate into the bloodstream. They will then attach to the wall of the blood vessels, exit the blood stream to the second site, and become metastatic.

In the specific case of breast cancer, if a primary tumour is not treated, cancer progresses from a primary tumour to a secondary metastatic lesion mainly in the bone, brain, liver or lung (15). Several steps are needed for initiation of metastasis; gaining the ability to break away from their origin, attaching to the blood or lymph vessels wall, entering and settling into a new organ or tissue in a new environment. Moreover, while in the secondary site, cancer cells need to continue growing and avoiding the reactions from the immune system. Gaining these abilities gives them new characteristics different from those in the primary tumours which therefore make them more difficult to target and treat (15).

1.1.3 Epithelial-mesenchymal-transition (EMT) involvement in cancer progression

The metastatic spread of cancer cells requires high levels of flexibility in the adhesive properties of tumour cells and their interacting cells (15). To gain metastatic ability, cells often undergo the development of mesenchymal characteristics, such as a reduction in cell-cell adhesion. Epithelial to mesenchymal transition, EMT, is a reversible multi-step morphogenic process during which epithelial cancer cells lose adhesions with neighbouring cells, undergo remodeling and replacement of cytoskeletal components and turn from a well-differentiated adherent phenotype to invasive migratory mesenchymal cells (Figure 1.2) (16). EMT, most likely the first step in the metastatic cascade, is closely tied to cancer progression and metastasis. EMT rises with the loss of cellular polarity, the onset of cell migration (16). It drives cancer cells with a more motile and invasive phenotype which is important at the primary phase of the metastatic cascade when invasion occurs into the surrounding tissue and blood vessels through the basement membrane (17). The cellular process of EMT is important throughout embryonic development for organogenesis and resembles the development from a normal to transformed cell phenotype during cancer progression (18).

Moreover, cancer progression is associated with the cross-linking of proteins lying on the extracellular matrix (ECM). This leads to an increase in ECM density and cell-matrix adhesions creating an imbalance between cell-matrix and cell-cell adhesions (19). Such alterations in the density of ECM could trigger EMT and lead to metastasis (12).

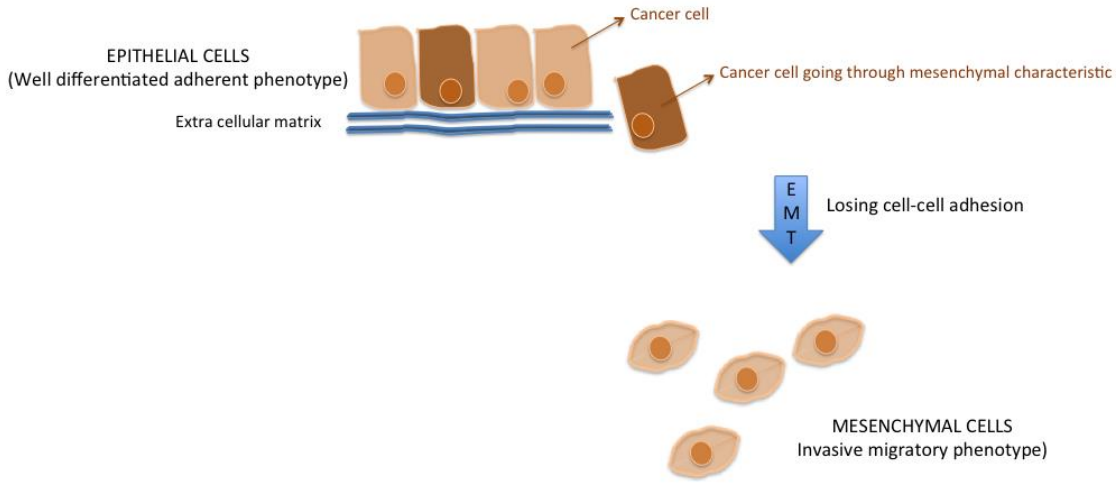

Figure 1.2 A schematic representation of EMT. Epithelial cells contain cancer cells that gain the ability to migrate freely, undergo EMT and transfer to mesenchyme cells.

Cell adhesion is mainly governed by the cadherin protein family. The cadherin family is known to play important roles in mediating cell-cell adhesion and breast cancer progression (15). E-cadherin (CDH1) maintains cell-cell adhesion, which retains the homeostasis and architecture of epithelial tissues. Therefore down-regulation of E-cadherin expression, well documented as a hallmark of EMT, results in the loss of cell-cell junctions, cell-matrix adhesion, and a change in cell polarity; this in turn assists the invasiveness of epithelial cells during tumorigenesis (EMT) and is a determinant in the outgrowth of metastatic breast cancer cells (20). Downregulation of E-cadherin is induced by transforming growth factor-β (TGF-β) followed by other molecular changes such as facilitating β1 integrin expression, a fundamental factor in metastasis (21).

According to the latest breast cancer studies, the plasticity of cancer cells allows the transformation of well-differentiated breast cancer cells to cancer stem-like phenotype (22). More recent data also revealed that EMT indicates an increased plasticity linked to cellular stemness and the ability to generate tumours (16). On the contrary, according to Dykxhoorn *et al.* the formation of some tumours at a secondary site could be related to and enhanced by the reverse process to that of EMT, called mesenchymal to epithelial transition (MET). This could therefore support the idea that a secondary tumour or a metastatic lesion may represent a similar phenotype (epithelial) to that of the primary tumour it originally initiated from (23).

1.1.4 Breast origins and anatomy

The breast is situated within the superficial fascia of the anterior thoracic wall between the clavicle and the sixth to eight ribs and develops from the mammary ridge in the embryo. Each breast or mammary gland consists of lobes that are formed from the tubuloalveolar type surrounded by fibrous connective tissue (24) (25). Each lobe branches into smaller lobules (milk-producing glands) which then divides into ducts that carry milk to the nipples (26) (Figure 1.4).

Stem cells have the ability to regenerate themselves and develop into a large range of tissues. Multipotent adult mammary/breast stem cells reside in the mammary gland and undergo self-renewal. They can differentiate into all specialised mammary epithelial cells. During asymmetric division, a stem cell or a progenitor cell undergoes mitosis and turns into two daughter cells (luminal progenitor cells and myoepithelial progenitor cells), one of which remains a stem/progenitor cell (luminal or basal-like cells), while the other becomes a more specialised cell such as milk-producing cells (Figure 1.3).

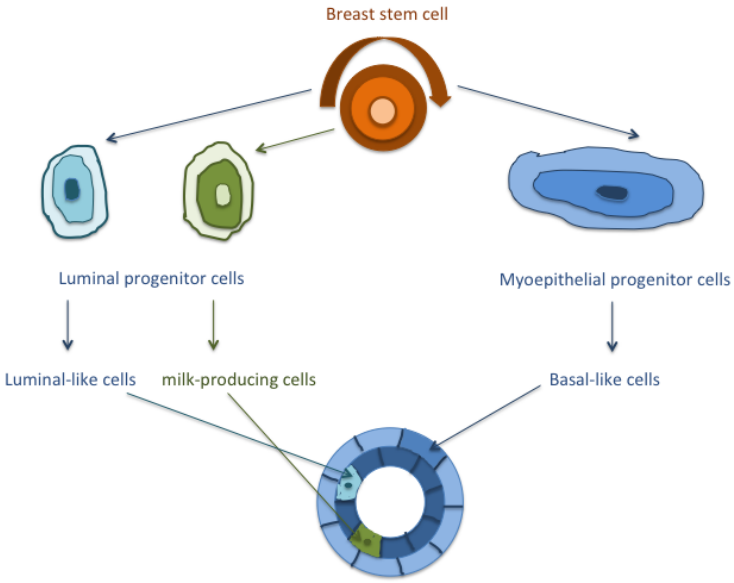

Figure 1.3 A schematic representation of breast cancer origin. During asymmetric division two daughter cells become either a stem/progenitor cell while the other becomes a more specialized cell.

Human breast tissues maintain their structure over time through a tightly regulated process sustained by a minority of tissue stem cells. During embryogenesis, the morphogenesis of mammary glands occurs from a thickening in the ventral skin. Subsequently, mammary ducts develop during the early pubertal period (27). The inner luminal and outer myoepithelium cell layers form the mammary epithelium. The identification of the luminal and myoepithelial stem/progenitor cells in each layer of the mammary epithelium provides the possibility of the involvement of distinct stem/progenitor cells in the initial development, homeostasis, and remodeling of the mammary epithelium (28) (Figure 1.4).

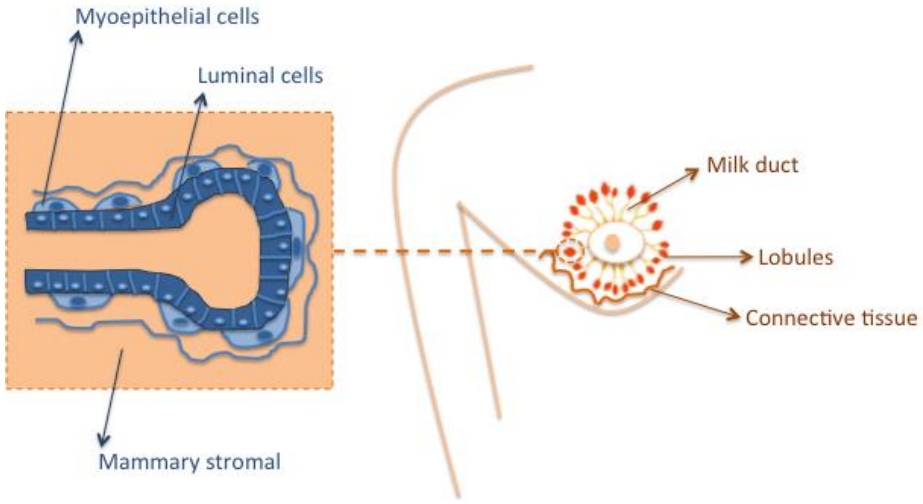

Figure 1.4 A schematic representation of breast anatomy (mammary gland and mammary epithelial cell structure). Breast is made of connective tissue and contains a complex network of ducts and lobules made of two layers of cells, epithelial cells and myoepithelial cells. Luminal epithelial cells surrounded by loose myoepithelial layer on basement membrane.

1.1.5 Breast cancer

Normal healthy cells can transform into a neoplasm in nearly any part of the body. When breast cells are diverted from the regular arrangement, a malignant neoplasm develops and breast cancer occurs (4). On such occasions, breast cells lose certain abilities, such as their adhesion properties, enabling them to escape from the primary site they have initiated from (breast). The breast cells can then easily spread throughout the body into distant tissues by traveling through blood or lymph vessels and establish secondary areas of growth i.e., they can metastasise (2) (29).

According to the WHO, breast cancer is one of the leading causes of cancer related-death worldwide (declining since about 1990, due to early detection and improvements in treatment). Breast cancer is the most common malignancy amongst women (30), claiming the lives of hundreds of thousands of patients each year mainly due to metastasis (31) (32). It is highly treatable when diagnosed at an early stage. However, it is an inherently challenging disease to treat due to its biological complexity and intra- and inter- tumour heterogeneity. Breast cancer could be a serious threat and result in death due to relapse and metastasis (31). Thus, in the battle against cancer, one of the main goals is to stop tumour cells from spreading to distant parts of the body from their tissue of origin.

1.1.5.1 Classification of breast cancer

Human breast cancer is a group of heterogeneous diseases at both the pathological and molecular level meaning that breast tumours can show distinct morphological and phenotypic profiles, including gene expression, metabolism, motility, proliferation, and metastatic potential (26). The classification of breast cancer relates to the differentiation state of cancer cells in tumour progression (33). Breast cancer is classified into different groups according to histopathology, grading and staging of tumour, receptor status, and protein and gene expression (34). Histological appearance of breast tissue in the tumour is most commonly used as the primary classification of breast cancer (4). Although breast cancer varies in histological type, transformation of epithelial cells lining the milk ducts or lobules most commonly develops into this disease (35).

Sarcomas are tumours that are generated from connective tissues whereas those originating from epithelial tissues are referred to as carcinomas (31). If the breast carcinoma emerges from the ducts and remains at the original site without evidence of invading through the basement membrane, it is called ductal carcinoma *in situ* (DCIS), whereas tumours spreading through the cells of the ducts and invading distant tissue are called invasive ductal carcinoma (IDC). Tumours arising from lobules and restricted to the milk producing glands or lobules are known as lobular carcinoma *in situ* (LCIS) and when spreading out of the lobules are called invasive lobular carcinoma (ILC) (34) (31) (35). IDC, DCIS, and ILC and LCIS account for 55%, 13%, and 5% of breast cancer cases respectively (36).

1.1.5.1.2 Breast cancer stage and grading

Breast cancer staging is based on the TNM system and describes the size of the tumour **(T)** and takes into account the extent that cancer has spread from the tumour primary location; such as adjacent lymph nodes **(N)** or to the distant part of the body when it has metastasized **(M)** (31) (37). Grading compares the appearance (differentiation) of breast cancer cells to that of normal breast tissue. It is an indicator of how fast a tumour is likely to grow and spread. If cancer cells look more like normal cells and tend to grow and spread more slowly than poorly differentiated or undifferentiated cancer cells, this results in a grading of cancer as "well differentiated" (low grade or grade 1). As tissue appears less differentiated and dissimilar to normal tissue, it is classified as moderately differentiated (intermediate grade or grade 2) and poorly differentiated (high grade or grade 3) (38).

1.1.5.1.3 Molecular profiling of breast cancer

In addition to the tumour staging and grading, molecular profiling of breast cancer, which is based on the variation of gene expression also determines, different subtypes of this disease. Breast cancer comprises at least two main biological types.

Luminal types: The luminal types are estrogen receptor (ER)–positive. The gene expression patterns of these cancers are similar to non-cancerous cells that line the breast ducts and glands. Luminal A tumours are ER positive, have high levels of the progesterone receptor (PR), and are HER2 (human epidermal growth factor) negative. They are low grade, tend to grow slowly, and have the best prognosis. Luminal B tumours are less common, ER positive, show different HER2 cluster expression, and have a higher expression of proliferation related genes (39). They grow faster than Luminal A and are often high grade with a worse prognosis. The two luminal subtypes (A and B) contain most ER-positive breast cancers and are characterized by a high expression of ER-related genes. The major biological difference between the two luminal types is an increased expression of proliferation genes, detected by proliferation markers such as Ki67 in luminal B subtype (40).

Basal types: In contrast with the luminal type, basal-like tumours tend to be negative for all three receptors (triple-negative) and express proliferation genes at higher levels (41). The terms basal-like and triple negative are not identical, however, they are often used interchangeably (40). Basal-like breast cancer is strongly associated with cancers arising in

the mutated breast cancer gene BRCA1 which has the worst prognosis among all types (33).

1.1.5.1.4 Receptor status of breast cancer

As well as molecular profiling, receptor status of breast cancer is another possible way to characterise this disease. Breast cancers display different subtypes according to their receptor status with different clinical outcomes (42). The origin of bCSLCs also differs according to the tumour subtypes (43). Comprehensive gene expression profiling revealed three main receptors in breast cancer: ER, PR, and HER2/neu.

1.2 Stem cells

Stem cells are a small population of cells accounting for ≤1% of cells in the body. They are undifferentiated unspecialised cells possessing two unique properties: self-renewal and differentiation (pluripotency). Stem cells are commonly defined as cells with a potentially unlimited capacity for self-renewal without senescence. They retain the ability to renew themselves through either symmetric (producing two identical stem cells) or asymmetric (producing one stem cell and one progenitor cell) division, preserving the stem cell pool (44). Stem cells can give rise and differentiate into a diverse range of specialised cell types found in mature tissues (45).

1.2.1 Potency

Cells with the most differentiation potential are termed totipotent. Pluripotency, multipotency, oligopotency, and finally unipotency show decreasing differentiation potential. Cell potency is the ability of a cell to differentiate into other cell types (46). **Totipotency** describes a cell with the ability to differentiate into all possible cell types in the body (e.g. Zygote). A **pluripotent** cell has the ability to differentiate into all derivatives of the three primary germ layers: endoderm, ectoderm, and mesoderm (e.g. embryonic stem cells) (46). **Multipotent** cells have the potential to differentiate into multiple, but limited cell types (e.g. haematopoietic cells).

1.2.2 Self-renewal

The most significant property of stem cells is the ability to self-renew (47). There are some similarities shared between stem cells and cancer cells through this self-renewal property:

- **The source of origin:** tumours may regularly arise from the transformation of normal stem cells.
- **Signaling pathways:** self-renewal may be regulated by similar signaling pathways in stem cells and cancer cells.
- **Cancer stem-like cells (CSLCs):** cancer cells may consist of rare cells with an unlimited self-renewal ability that drives tumorigenesis (47).

CSLCs (will be discussed in more depth later in section 1.2.5) divide into proliferative progenitor cells through asymmetric division. Unlike normal progenitor cells which lose their ability to differentiate after certain number of divisions, cancer progenitor cells

maintain this ability to higher levels which give rise to heterogeneous lineages of the cancer cells with enhanced tumorigenicity (48) (49) (Figure 1.5).

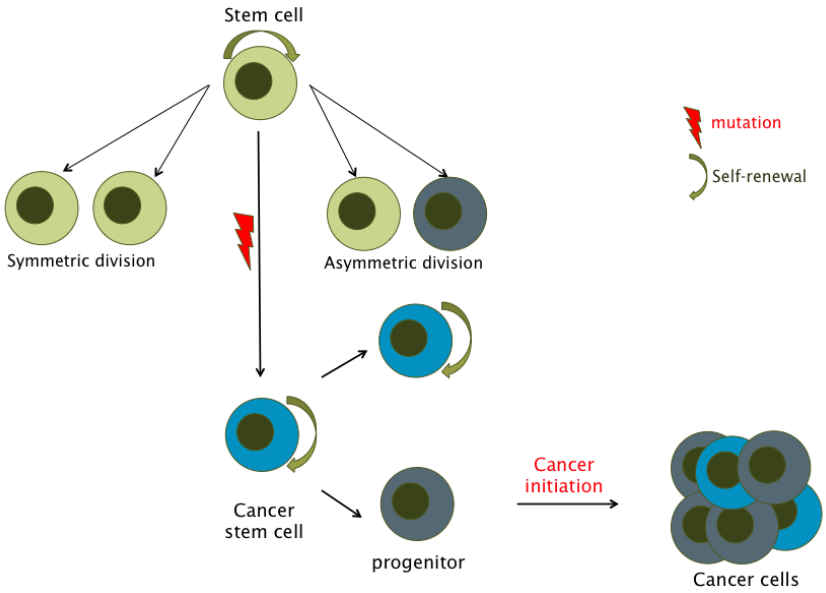

Figure 1.5 A schematic representation defining stem cell self-renewal (symmetric and asymmetric division). There is a subpopulation of stem cells known as cancer stem like cells (CSLCs) which possess the chemoresistance and an enhanced tumorigenicity by being involved in cancer initiation and development through the stem cell processes of self-renewal and differentiation.

1.2.3 Different types of stem cells

There are three main types of stem cells currently known; embryonic and adult stem cells (e.g. somatic stem cells) (50) and induced pluripotent (iPS) cells. iPS cells are a type of pluripotent stem cell that are produced in the lab by genetic reprogramming to create an embryonic stem cell (ES)–like state to express ES characteristics. The iPS cell technology was first announced by Takahashi *et al.* in 2006 showing that mature cells can be reprogrammed to pluripotent cells (51). Stem cells have unique biological properties such as potency that make them important for clinical research trials and a great future hope for modern medicine. During the past few years, there have been a number of novel innovations in stem cell research and regenerative medicine. Therefore, stem cell research has evolved into a rapidly developing research area which holds great promise for treating and perhaps curing certain diseases such as cancer.

1.2.3.1 Embryonic and adult stem cells

1.2.3.1.1 Embryonic stem (ES) cells

In 1981, Martin Evans and Matthew Kaufman first isolated ES cells from mouse embryos (52). In 1998, human ES cells (hESCs) were isolated by Thomson *et al.* from the inner cell mass of a blastocyst, the final stage of preimplantation embryo development (53). ES cells are capable of undergoing an unlimited number of symmetrical divisions without differentiating (long-term self-renewal) and are capable of differentiating into all cell types of the body (pluripotent) (50). The pluripotency of ES cells are governed by three main factors, OCT4, SOX2, and NANOG (Figure 1.6).

1.2.3.1.2 Adult stem cells

Adult or somatic stem cells are found throughout the body following embryonic development and can develop into a limited number of different tissue types (50). Potency distinguishes embryonic and adult stem cells (52). Unlike ES cells, adult stem cells are multipotent.

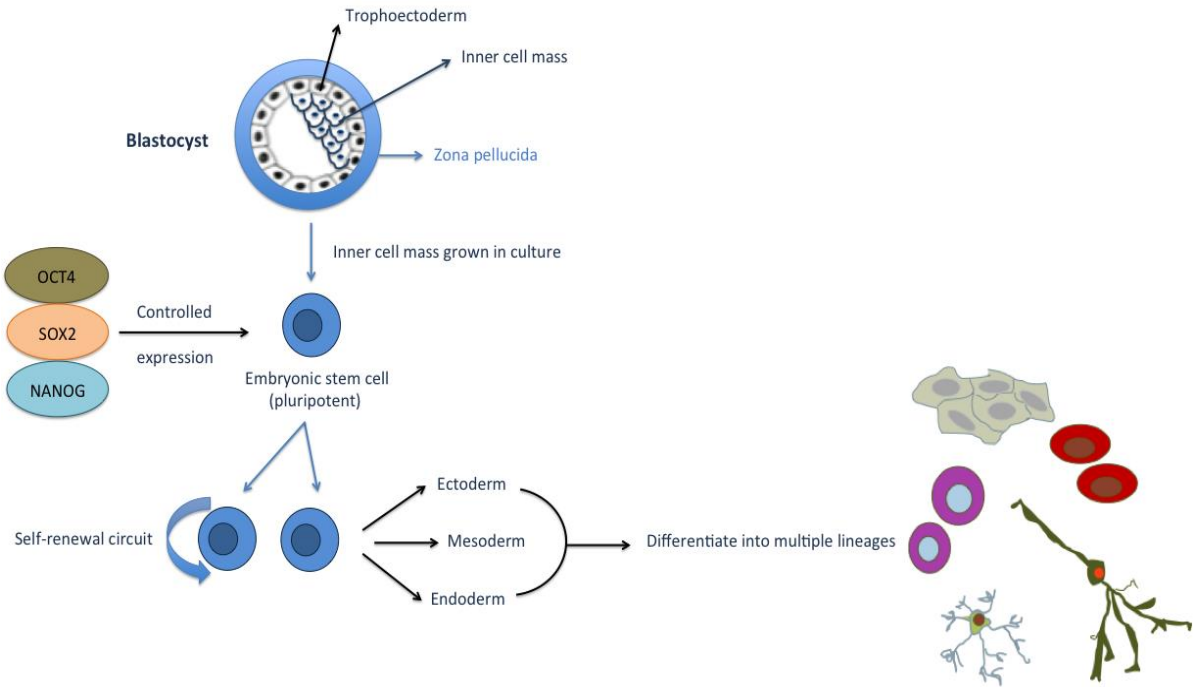

Figure 1.6 A schematic representation of embryonic stem cell origin and differentiation through controlled expression of key pluripotency markers.

1.2.4 Pluripotency/transcription factors

The unique feature of pluripotency in ES cells are that they display characteristics such as the ability to retain a non-differentiating state during *in vitro* culture by expressing specific pluripotency markers OCT4, SOX2, and NANOG (50). The individual loss of each results in the differentiation of ES cells, supporting the idea that these pluripotency markers are key factors in maintaining stem cell identity.

It was revealed in 2007 that iPS cells could be generated by the expression of a set of transcription factors, OCT4, SOX2, and NANOG, which regulate differentiation and pluripotency in their population (51) (54). Different expression levels of each have distinctive effects on differentiation in ES cells which makes them core regulators of pluripotency. Each of which induces its own expression and that of the two other genes (55). These set of transcription factors are able to change from the differentiated state into pluripotent cells without the need of an embryo, which may be useful for cell replacement therapies. Furthermore, expression of these markers is well documented to be critical for development of different human malignancies (54) (56). Mounting evidence demonstrated that OCT4 and SOX2 are highly expressed in different cancers and their expression could stimulate tumour development and promote anti-apoptotic and metastatic phenotype *in vitro* and *in vivo* emphasising their role in carcinogenesis (57). Recent evidence revealed that the expression of these transcription factors are strongly associated with CSLCs suggesting that downregulation of these genes could reduce tumour sphere formation and inhibit tumour initiation in xenograft tumour models (58). Moreover, interesting findings show that overexpression of SOX2, OCT4, and NANOG were significantly associated with high expression of N-cadherin promoting the induction of EMT (EMT is characterized by a switch from E-cadherin to N-cadherin expression) (59) (60) (61). It is noteworthy that SOX2 does not promote EMT. NANOG (pron. nanOg) is a homeobox domain transcription factor involved with self-renewal of undifferentiated ESCs in concert with other factors such as OCT4 and SOX2. It is known as a critical regulator of embryonic development and cellular reprogramming, which has been reported to be largely expressed in different human cancer types and is encoded by the *NANOG* gene. *NANOG* triggers tumorigenesis through the regulation of different aspects of cancer development, such as tumour cell proliferation, self-renewal, motility, EMT, immune evasion, and drug-resistance, which are all distinct features for CSLCs (237) (238). Therefore, NANOG could represent a novel therapeutic target for the diagnosis, prognosis, and treatment

outcome of cancer (238). According to different studies, NANOG could define CSLCs in different types of solid tumours, such as colorectal cancer. NANOG activity could determine cell fate in both embryonic and CSLCs in a time depending manner; inappropriate timing in activation of NANOG would result in CSLCs rather than normal pluripotent stem cells or differentiated somatic cells. Moreover, overexpression of NANOG in different cancers is associated with poor survival outcome of patients (237).

1.2.4.1 OCT4 (POU5F1) and its expression in cancer

Octamer-binding transcription factor 4 (POU5F1), OCT4, belongs to the octamer class of transcription factors and was the very first master gene discovered 25 years ago. OCT4, a member of the POU family of homeodomain transcription factors, interacts through two DNA binding-proteins and is the key regulator critical for the initial formation of a pluripotent cell in the mammalian embryo and aids the maintenance of the pluripotency and self-renewal of ES cells at its intermediate level of expression (62) (63) (64). The POU family of proteins binds to the octamer motif ATGCAAAT within their promoter or enhancer regions and regulates the expression of target genes (65). OCT4, also known as Oct-3, Oct-3/4, Otf3 or NF-A3, plays an important role in the reprogramming of differentiated cells into iPS cells (66) (63). OCT4 is known to be an essential factor for the stemness properties of ES cells and for the reprogramming of somatic cells (63). Due to the high expression of OCT4 in stem cells through development and a large number of tumours, it has become the most widely studied octamer-binding protein (67). With varying expression levels, OCT4 is able to have various functions including promoting the expression of genes involved in the maintenance of pluripotency in complex with several partners (SOX family, SOX2) depending on its post-translational modifications (63). The OCT4 gene consists of five exons and is located on the chromosome six in humans (68).

OCT4 encodes for two spliced variants through alternative splicing, OCT4A and OCT4B. In addition to the two main isoforms of OCT4, OCT4A and OCT4B, there is another known isoform OCT4B1 that its function is still unclear. OCT4B1 has been considered as a putative marker of stemness (69). These two isoforms (OCT4A and OCT4B) can be distinguished by their distinct subcellular localisation (70). Alternative splicing is a post-transcriptional regulatory process during gene expression in which introns are removed, remaining exons are spliced and translated into different protein isoforms that may affect

biological functions (71). There is evidence of OCT4 alternative splicing in ES cells, where OCT4A is more specifically expressed (72). OCT4A expression is restricted to ES and embryonal carcinoma (EC) cells, whereas OCT4B could be detected in different non-pluripotent cell types (70). OCT4A, the most common transcript of OCT4, is known to be a key pluripotency marker and has been confirmed as a transcription factor responsible for the stem-ness properties of the cells. OCT4A is activated during transactivation and translated into a full-length protein located in the nucleus and includes an N- and C-terminal transactivation domain. These two isoforms (OCT4A and OCT4B) can be distinguished by their distinct subcellular localisation (70). Among all OCT4 isoforms, OCT4A is the only one including exon 1 which makes this exon a good indicator of pluripotency (66). Alternatively, OCT4B contains the same downstream sequence as OCT4A with a shorter N-terminal domain due to its lack of exon 1 and extended exon 2. OCT4B is mainly located in the cytoplasm of the cells which therefore brings its function as a transcription factor into question. Moreover, OCT4B, contrary to OCT4A, lacks the ability to maintain the self-renewal capacity of ES cells and is more involved in the cellular stress response (62) (Figure 1.7).

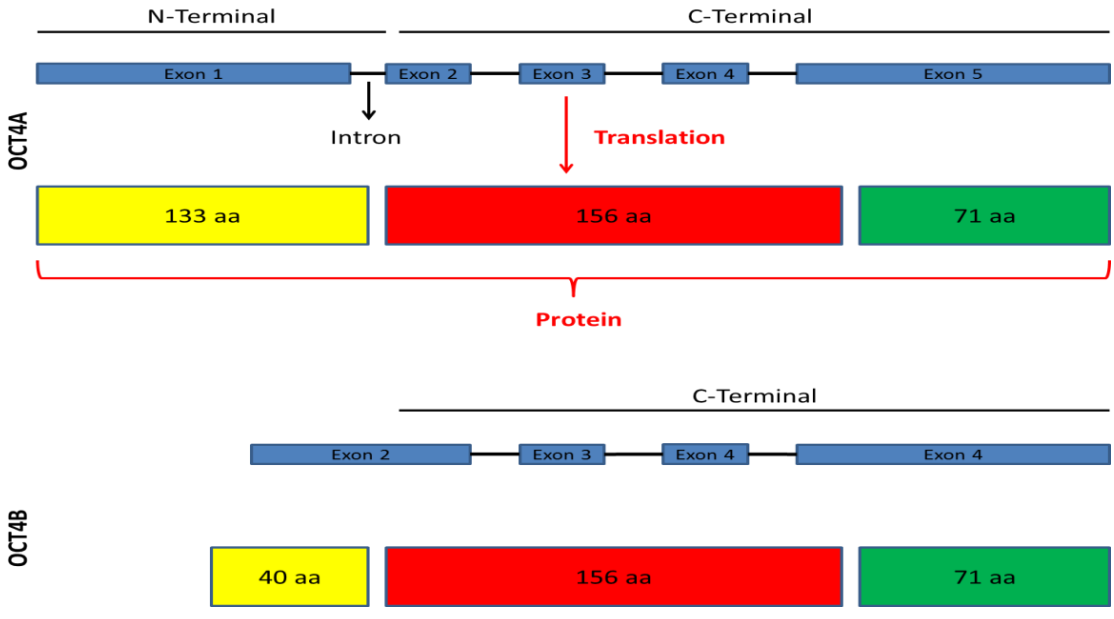

Figure 1.7 A schematic representation of the human OCT4 spliced variants showing OCT4A and OCT4B isoforms.

It has been proposed that OCT4 expression is required for CSLC survival (73); however, contradictory evidence has suggested that OCT4 is not expressed in somatic cancers comprising CSLCs (73). Moreover, other studies failed to confirm the latter observation and revealed the expression of OCT4 in different human cancers and pluripotent germ cell tumours, suggesting the role of OCT4 in tumorigenesis (74). Cancer cells with OCT4 expression are also likely to display characteristics of CSLCs. However, the heterogeneous nature of tumour tissues (presence of cells at different stages of maturation) may result in the misdetection of OCT4 in both Western blotting and immunochemistry in different cancer cell types (62). Therefore further interpretation of OCT4 gene transcription was required. This will lead to new insights into the pattern of OCT4 splice variants and their expression in different cell types. Recent contradictory reports on OCT4 expression in different tumour cells and tissues created the necessity to discriminate the expression of OCT4A from other variants as well as OCT4 pseudogenes.

1.2.4.1.1 OCT4 pseudogenes

Lack of distinction of OCT4 isoforms could lead to confusion and disagreements on the role of OCT4 in different tissues and cells. Many studies argued that detection of OCT4 in somatic cells due to false-positive signals from pseudogene transcripts and DNA contamination (75). Pseudogenes are defined as copies of genes lacking the ability of producing a full-length functional protein chain. They are distinguishable from disruptions to their apparent coding sequence. Pseudogenes are genomic DNA sequences similar to normal genes, lacking introns and a *5'* promoter (75). Since pseudogenes are structurally lacking the intervening sequences that exist in the functional counterparts, they are described as intron-less genes. Pseudogenes are generally located on a different chromosome to their functional counterpart and were primarily considered as non-functional genes lacking the ability to translate into functional proteins. By definition, pseudogenes lack a functioning gene product (76). However, they are now known to be functional and encode for functional proteins (77).

Pseudogenes are classified into two main groups: processed or retrotransposed pseudogenes (produced by reverse transcription from an mRNA) and non-processed or duplicated pseudogenes (76). In the retrotransposition process, a part of the mRNA transcript of a gene is naturally reverse transcribed back into DNA and added into chromosomal DNA. Processed pseudogenes generally create copies of themselves. However, it has been shown in an *in vitro* system that they can also create retrotransposed copies of random genes (78). These pseudogenes normally include a poly-A tail and have had their introns spliced out. Processed pseudogenes lack the upstream promoters of normal genes due to originating from a mature mRNA and becoming non-functional pseudogenes instantly following the retrotransposition process (79). An important process in the evolution of genomes is gene duplication. Gene duplication may result in a copy of a functional gene which might consequently undergo mutation. This may eventually lead to the formation of a nonfunctional gene. The loss of function usually does not severely impact the fate of organism due to the existence of a complete functional copy of the gene (80).

The OCT4 protein is related to multiple pseudogenes. There are several pseudogenes of OCT4 in human somatic tumours which could possibly cause uncertainty in the accuracy of OCT4 expression and functions in tumorigenesis (62). The OCT4 protein is related to

multiple pseudogenes. There are several pseudogenes of *OCT4* in human somatic tumours, which could possibly cause uncertainty in the accuracy of OCT4 expression and functions in tumorigenesis (62).

To this point, seven pseudogenes have been discovered for the human *OCT4* gene by bioinformatics and experimental analyses and shown to be processed and transcribed in different cancer cell lines and tissues (198). POU domain class 5 transcription factor 1B (*POU5F1B*), pseudogene 1, pseudogene 3 and pseudogene 4 have very similar exon structures to *OCT4A*, and therefore could mistakenly be detected as *OCT4A* (62). *OCT4* pseudogene 3 and *OCT4* pseudogene 4, were found to be expressed in human solid tumours, glioma, and breast carcinoma from which CSLCs had been isolated (62). *OCT4* pseudogene 4, is irregularly activated in hepatocellular carcinoma (HCC). Its expression level is positively correlated with that of *OCT4* gene. Additionally *OCT4* pseudogene 4 has been shown to promote growth and tumorigenicity of HCC cells, hence taking on an oncogenic role in hepatocarcinogenesis. Moreover, high levels of *OCT4* pseudogene 4 is significantly correlated with poor prognosis of HCC patients (62). Although the transcripts from pseudogene 1, pseudogene 3 and pseudogene 4 can translate into protein products, no transcript of *OCT4* pseudogene 3 was detected in MCF7 breast cancer cells. Moreover, *OCT4* pseudogene 3 was mainly localised in the cytoplasm and therefore does not possess stemness activity.

Consequently, among the above three pseudogenes, *OCT4* pseudogene 1 was chosen as a better model in this thesis.

1.2.4.1.1.1 OCT4 pseudogene 1 (POU5F1B)

POU domain class 5 transcription factor 1B (POU5F1B), pseudogene 1, and pseudogene 5 are thought to be associated with OCT4 gene regulation and involvement in carcinogenesis (62). POU5F1B is highly homologous to OCT4A and was recently shown to be transcribed in cancer cells. However, its clinical application and biological function is not yet entirely clear (81). The DNA copy number and mRNA abundance of OCT4 pseudogene 1 has shown that this pseudogene (not OCT4 gene) is regularly amplified in gastric cancer cell lines and clinical specimens. There is evidence that overexpression of OCT4 pseudogene 1 in gastric cancer cells induced colony formation *in vitro* as well as tumour growth *in vivo.* Additionally, silencing the expression of OCT4 pseudogene 1 further confirmed the involvement of OCT4 pseudogene 1 in the promotion of cancer cell growth *in vitro* and tumour growth *in vivo* (81). Therefore, the study of OCT4 pseudogenes and their role in carcinogenesis is of no less importance than the study of the OCT4 gene.

1.2.4.2 SOX2 and its contribution in cancer

SOX2 gene (sex determining region Y (SRY)-related box 2) is a member of the SOX family and encodes for a transcription factor associated with different stages of mammalian development which was discovered and characterized in humans in 1994 (82). SOX2 contains a high mobility group (HMG) which permits highly specific DNA recognition and binding. It encodes for a protein consisting of 317 amino acids (82). SOX2 is located on chromosome 3q26.3–q27 and is a fundamental ES cell gene critical for induced cellular reprogramming and functions as a regulator of gene transcription (82). SOX2 plays a critical role in the pluripotency of undifferentiated ES cells and maintaining their self-renewal capability (67). SOX2 is one of the two factors (SOX2 and OCT4) sufficient for generation of iPS cells from human blood cells (83).

A focus on SOX2 has been recently switched from its role in developmental and stem cell biology to the involvement in disease via its association and amplification in numerous types of cancer (84). SOX2, in some cases, has been referred to as an oncogene, and a factor that controls cancer cell physiology via promoting oncogenic signaling and in many cases maintaining CSLCs (82). SOX2 has been shown to be overexpressed in human breast cancer tissue and cell lines and the level of its expression is strongly allied with tumour grade, implying that SOX2 is highly expressed in invasive carcinoma (82). SOX2 amplification has been documented to be strongly associated with the following cancer

hallmarks: enhanced cell proliferation, evading apoptotic signals, colony formation, and metastasis in breast cancer. There are factors that suggest SOX2 is a key transcription factor in various cancers: SOX2 promotes cancer phenotypes by regulating (suppressing or activating) certain target genes, such as genes promoting EMT by binding to the promoter regions of SNAIL, SLUG and TWIST (transcription factors that regulate the expression of tumour suppressors such as E-cadherin) (82).

Moreover, deregulation of transcription factors including irregular functioning of SOX2 could cause defects in cell proliferation and therefore contribute to proliferation of breast cancer cells and lead to many other cancers (84). Sussman *et al.* revealed the importance of ubiquitin-specific protease 22 (USP22) in regulating the cellular transition from stemness towards differentiation. They also discovered that USP22 limits the ability of SOX2 promoter to control the ES cell transition from self-renewal to differentiation. Taken together, SOX2 is an essential stem cell marker and a critical factor for cellular differentiation and cancer progression. Thus, it is worth investigating its role in the stem cell population of breast cancer (85).

1.2.4.3 OCT4, SOX2, and their involvement in tumorigenicity

Recent studies revealed that OCT4 and SOX2 overexpression, individually or in collaboration, could lead to tumour initiation, progression, and metastasis in various cancer types (86). There is much evidence to suggest that OCT4 and SOX2 are highly overexpressed in less-differentiated cells and their expression levels lessen upon differentiation (63). Of interest, OCT4 is known to bind in partnership with SOX2 (59). Moreover, there are studies highlighting a link between these two markers showing that high expression of both was allied with higher histological grade or TNM stage ($p < 0.001$ for both factors). This therefore demonstrates a link between OCT4 and SOX2 and their involvement in tumour dedifferentiation. Additionally, high levels of SOX2 expression correlate with poor patient survival outcome ($p < 0.001$) (87).

The key role of OCT4 in the survival of prostate and breast cancer stem like cells (bCSLCs) was reported in different studies (88) (89). As previously mentioned, tumour recurrence and metastasis were reported to be highly dependent on the role of OCT4 in maintaining CSLCs. Moreover, it was shown that OCT4 expression increased the invasion and metastatic potential of breast cancer cell line MCF-7 (88) (89).

An in depth knowledge of stem cells is required to understand the mechanisms which regulate cellular transformation leading to cancer. This could be useful to develop a solution to prevent tumour initiation. Therefore it would be useful to further examine the expression levels of OCT4 and SOX2 in the CSLC population to see whether the formation of tumour initiating cells is the result of uncontrolled reprogramming of OCT4 and SOX2 genes regulating stemness.

1.2.5 Cancer stem cells (CSCs)/Cancer stem-like cells (CSLCs)

According to the classic models of carcinogenesis, cancer arises via a series of mutations such that any type of cell within an organ is able to initiate tumours containing similar malignant properties (90). However, recent novel investigations in the identification of CSLCs from several human cancers, including breast, support a different model for defining cancer initiation, maintenance, and progression according to the CSLC model (91) (92).

CSLCs possess both stem and cancer properties (phenotypically and functionally). This cell population has the capacity to self-renew, generate progeny with identical tumorigenic potential, and to differentiate into the bulk of cancer cells. CSLCs are known to be resistant to different therapeutic regimes and are therefore responsible for tumour recurrence, relapse, and ultimately metastasis (93). They can be identified by the expression of specific pluripotency markers, SOX2 and OCT4, and stem cell surface markers such as CD44 and CD24 (see section 1.2.5.1). CSLCs are also thought to display altered metabolic activity (94) (95). Investigating the accuracy of this allegation could be beneficial to prevent the initiation and progression of CSLCs (Figure 1.8).

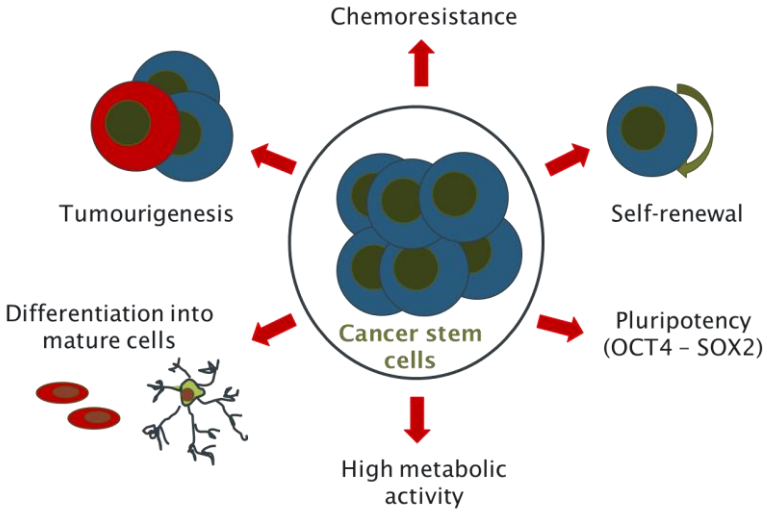

Figure 1.8 A schematic representation of CSLCs characteristics and role in tumorigenicity.

To explain how CSLCs could be responsible for tumour progression and recurrence, scientists proposed two models as follows:

- **Cancer stem cell model** is also known as hierarchical model of cancer stem cells suggesting that a rare subset of tumour cells with stem cell-like properties, called "cancer stem cells" (also referred to as tumour-initiating cells). They are critical for neoplastic progression and metastatic spread. Due to the quiescent properties of stem cells, they escape from different therapeutic methods and generate new tumours (tumour recurrence) (32).

- **Clonal evolution model** which is applicable to different solid tumours including breast, suggests that every single cell within a tumour is potentially capable of undergoing mutations. The most adaptive phenotype to the new situation will give rise to new tumours and lead to recurrence (32). This specific property of CSLCs is through the stem cell processes of self-renewal and differentiation through similar molecular mechanisms governing cellular reprogramming (96).

1.2.5.1 Identification and characterisation of breast cancer stem-like cells (bCSLCs) and their resistance to chemotherapy

1.2.5.1.1 Cell surface markers

An effective way to single out this minor subpopulation for better understanding is required. Breast cancer stem cells can be identified based on the expression levels of various markers. Two of the many markers to define stemness in breast cancer cells are the Hyaluronic acid receptor (CD44) and "cellular adhesion molecule, heat stable antigen" (CD24). $CD44^+/CD24^-$ phenotype demonstrates tumorigenicity by presenting in the CSLC population (97).

1.2.5.1.2 Aldehyde dehydrogenase (ALDH) activity

CSLCs have also been characterised based on their expression of aldehyde dehydrogenase (ALDH) activity. Overexpression of ALDH1, known as a functional marker of cancer stem and progenitor cells has also been reported in breast cancer cells (93). Ginestier *et al.* revealed ALDH1 as a marker of normal and malignant human mammary stem cells representing a poor clinical outcome (98). There is a higher rate of tumorigenicity in breast tumour cells positive for ALDH1 activity in NOD/SCID mice with phenotypic characteristics similar to the parental tumour (93). Breast stem cells express high levels of CD44 and ALDH1 and low levels of CD24 showing that tumorigenicity is at its highest level in breast cancer cells carrying the $CD44^+/CD24^-/ALDH^+$ phenotype (99) (49). This observation suggests that the $ALDH^+$ population consist of CSLCs (93). ALDH1 activity has been used as a tool to isolate populations with a high tumour-initiating ability and/or stem-like properties in normal mammary tissue in tumour transformation.

Additionally, human breast tumours and normal breast stem cells are characterized by high "epithelial surface antigen" (ESA). A specific antigenic phenotype $ESA^+/CD44^+/CD24^-$ has been identified as tumorigenic in primary tumours of breast cancer patients (100). These cells are highly enriched for CSLCs compared with the other cancer cells within the same tumours that only carry the $CD44^-/CD24^+$ phenotype (49). Taken together, these data demonstrate that a group of cells within breast tumours are more tumorigenic than the other cells and express stem cell markers, supporting the hypothesis that the presence of CSLCs could be associated with aggressiveness breast cancer (101).

1.2.5.1.3 Self-renewal pathways

One of the features shared by normal stem cells and CSLCs is the ability to self-renew. Deregulation of self-renewal pathways implicated in breast carcinogenesis such as Notch, Wnt, and Hedgehog might result in the transformation of stem and/or progenitor cells (102). This therefore suggests that targeting self-renewal pathways might provide a promising approach to eliminate CSLCs.

1.2.5.1.4 Tumorigenicity

The first experimental clues about the existence of CSLCs came from the observation that only a very small proportion of large numbers of tumour initiating cells (10^5-10^6) will go on to form metastatic cells (103). The hypothesis of the existence of CSLCs became a new era of research in the 1990s when their presence was proved experimentally. In 1994 Lapidot *et al.* first reported that hematopoietic stem cells of acute myeloid leukaemia (AML) could form tumours when transplanted into the mammary fat pad of NOD/SCID (non-obese diabetic/severe combined immunodeficient) mice (104). This observation was followed by more validations in solid cancers including breast. Only a small proportion of these so-called bCSLCs can fulfill two crucial criteria defining CSLCs - self-renewal and ability to form heterogeneous tumour cell population, and are able to grow tumours in breast (49). This population of cells were then used to classify breast cancer cells with a high rate of tumorigenicity (49). Accordingly, many tumours are thought to originate from a single cell (probably derived from normal stem cells or progenitor cells) that undergoes malignant transformation into a cancer-initiating cell (an alternative name for CSLC) with the capacity to proliferate and form tumours *in vivo* (105) (106) (Figure 1.9).

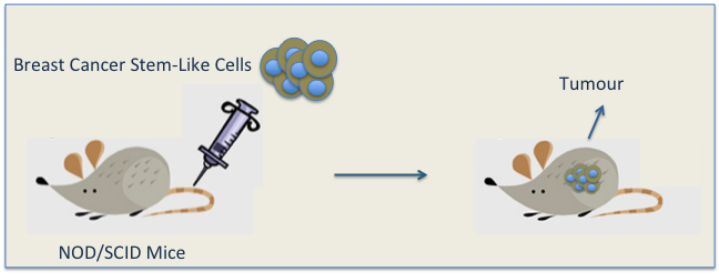

Figure 1.9 A schematic representation of tumorigenicity of cancer stem-like cells (CSLCs) when injected into NOD/SCID mice. Tumours originate from a single cell and undergo malignant transformation into a cancer-initiating cell to proliferate and form tumours in vivo.

Following the identification of stemness specific markers in hematopoietic tumours (AML), Al-Hajj *et al.* 2003 revealed the presence of a cell subpopulation in solid tissues and in pleural effusions of patients with advanced-stage metastatic breast cancer (97). This rare cell population displayed stem cell properties and were characterised by the cell surface marker profile $CD44^{+}/CD24^{-}$ with the enhanced ability to form tumours when xenotransplanted into NOD/SCID mice (49). This observation was further proof for the existence of CSLCs in the tumour population.

1.2.5.1.4.1 Common features between CSLCs and EMT

Tissue-specific stem cells retain their stemness in a certain microenvironment, called the stem cell niche (107). Likewise, different studies proposed specific microenvironments for the maintenance of CSLCs (107). CSLCs and ES cells are regulated by interactions of the components in their niche. Mesenchymal stem cells also follow the same rule and are considered to be resistant to apoptosis, therapeutic regimes, and associated with tumour progression, relapse, and metastasis via EMT (94) (108) (109). EMT is an important factor in the acquisition and maintenance of stem-like characteristics. Likewise, CSLCs often take up a mesenchymal phenotype and display EMT properties (109). These findings together underscore a tight link between EMT and CSLCs which might have several implications in tumour development that could be fundamental for cancer therapy (92). Hence, several studies have focused on discovering a link between EMT and CSLC and the existence of common molecules among these populations (110) (111, 112). Therefore, the challenge is to target factors that are involved in EMT initiation and identify CSLC properties to enable the development of new pathways to prevent metastatic spread.

1.2.6 Stem like-cell properties in sphere floating cells (mammospheres)

1.2.6.1 Two-dimensional (2D) vs. three-dimensional (3D) cell culture systems

There are different model systems for cancer investigation which have provided important information towards the advancement of cancer biology. However, some still have major problems to deal with. As convenient and valuable as the 2D culture models are for biological assays such as maintaining cells, they lack realistic complexity. 2D culture systems do not reflect the situation *in vivo* and their drawbacks are increasingly recognised as imposing unnatural geometric and mechanical limitations (113). According to Van der Worp *et al*. there were about 90% of preclinical drugs with successful results when applied in 2D tissue culture but failed to have promising outcomes in human trials. This could mislead investigators which is wasteful in terms of time and money (114). In addition to 2D cell culture models, there are animal models that rarely reflect human tumour biology. They also come with their own practical, financial, and ethical issues (115) (114). Therefore scientists have been artificially developing 3D tissue culture models, which provide a more accurate morphological representation of tumour development and the physiological environment to bridge the gap between *in vitro* (used for discovery and screening) and *in vivo* experiments (used for efficacy and safety assessment) before proceeding to clinical trials. The following paragraphs compare the advantages of 3D over 2D culture.

***In vivo*-like environment:** Studies indicate that research in the field of cell biology in just a 2D system has substantial limitations which may cause a misinterpretation in important biological experimental outcomes. This system mainly generates adherent 2D monolayer cells in the majority of cell-based assays cultured on flat plastic substrates (113) (91). As opposed to 2D culture, cells developing in 3D systems more closely mimic native *in vivo* biological systems in terms of cellular communication and more precisely mimic the actual microenvironment that cells encounter in tissues (91). Therefore, 3D culture is a more practical approach to bridge this gap (116) (117).

Proliferation rates: Another drawback of 2D culture is that the majority of cells in 2D culture are proliferating cells, while in 3D cultures there is combination of cells at different stages including more invasive migratory cells (the main focus of tumour biology) which are easily detached from the surface during medium change. Therefore more invasive cells

are not always accessible for experimental studies in 2D culture, whereas 3D model systems provided the optimum culture conditions for this purpose (118). In 2D monolayer culture, the flat surface provides an unnatural state for cells to grow and spread than they would *in vivo* giving them the ability to proliferate at a relatively similar rate across the surface. In contrast, 3D culture systems enable cells to proliferate at similar rates to those seen *in vivo* (119). Settings in 2D culture cause irregular interactions between cells and proteins and other cells in the culture. Such interactions allow cells to receive an equal amount of nutrients and growth factors from the medium during growth.

Cell-cell interaction: Cells in 3D culture undergo complex mechanical and biochemical interplay; they are permitted to interact with each other as well as to the cells in the surrounding environment and ECM in all three dimensions. ECM contains various proteins (collagen, elastin, integrins, and laminin) that provide cells with mechanical properties and assist the communication between surrounding cells in the matrix. By exerting forces on one another, cells in 3D culture attach together and migrate as they would *in vivo*. These connections and cell-cell signalling increases communication among cells, which is important for cell function. Through these natural cell-cell interactions, cells are able to communicate with each other similar to the pathological conditions seen in cancer (91).

Treatment: Another advantage of 3D culture to 2D is in the case of treatments, different doses of chemotherapeutic drugs may kill cancer cells in 2D culture system. The same dose of the same drug might have no effect on cancer cells grown in 3D just as has been found in the body (120). Cells in such environments (3D) gain enhanced resistance to chemotherapy compared with the same cells developed in monolayers possibly because cells growing in 3D form multi-layers of cells which makes the accessibility of drugs difficult to the cells on the inside of the spheroid structures (120). This cell structure mimics natural obstacles to drugs such as having to diffuse through multi-layers of cells to reach the inner target cells, which is more realistic compared with 2D cultures. Therefore, 3D culture is more valid for discovering and validating different drugs for specific types of cancer.

Stemness properties: Although there is no ultimate decisive proof of the presence of CSLCs in tumour population, recent observations have increased the possibility that *in vitro* 3D models could create a stem-like population similar to that of *in vivo*, which may be responsible for drug resistance (117).

To sum up, as 2D cultured cells may not behave as they would *in vivo*, there will be misleading data from the 2D cell culture system and non-predictive data for *in vivo* responses (117). Generally, replacing a standard 2D model system with 3D could be time saving by generating more significantly realistic results. Cancer treatment is moving toward targeted therapy and 3D cultures could be promising in finding new targets which were not available in the traditional 2D culture systems.

1.2.6.2 Mammosphere formation assay for isolation of stem cell population

Improvements in cell culture techniques have been a key factor in the identification and study of bCSLCs. Studies suggest that the majority of breast epithelial tumours are initiated and maintained by only a small percentage, (10%–25%), of breast tumour cells (bCSLCs) that undergo a total transition and may be the main source of cancer recurrence and actively metastatic cells (121) (122) (123). It is therefore important to identify an assay to classify this small population of cells to gain a better understanding of their properties and role in carcinogenesis from tumour initiation to a metastatic state; and eventually ceasing their growth rate (108). Eliminating this minor cell population could be the target to aim for to enable successful treatments. Thus, to isolate a mammary cell population that represent stem-like properties and to mimic *in-vivo* conditions, a non-adherent undifferentiated state (3D model system) was required to allow bCSLCs to grow with undifferentiated properties, while the rest of the population remain differentiated (116) (100). This 3D model system will allow cancer scientists to isolate CSLCs and investigate the mechanisms underlying cancer development together with responses to therapeutic agents in an environment that best mimics *in-vivo* conditions (122).

For the development of mammary epithelial cells the most widely used *in vitro* assay for enrichment, isolation, or identification of tumorigenic bCSLCs and their activity within tumour is the mammosphere assay. These cells are enriched in the stem cell phenotype CD44high/CD24low (124) (49) (125). Mammary epithelial stem and progenitor cells are capable of proliferating in a non-adherent manner (polyhema coated wells which provide a neutral charge and are highly hydrophobic, avoiding cell attachment) and form floating spherical colonies referred to as mammospheres (100). The dimension of mammospheres varies from 40 to 110 µm. However, the dimension of their initiator cells (stem/progenitor cells) may vary from 2 to 15 µm. With regard to the size of spheres, it is generally believed that larger spheres (≥50 µm) could possibly be generated by stem cells which are the main

focus of this particular research project, while the origin of smaller spheres (<50 µm) might be progenitor cells which lose self-renewal ability (126). Therefore, in respect to dimension and structure, mammospheres could represent the cellular heterogeneity and thus display different cellular properties and mimic a more realistic tumour model (44).

One of the key objectives in mammosphere generation is to evaluate the gene expression analysis of pluripotent transcription factors (OCT4 and SOX2) in this population to investigate whether the expression levels of these stem cell markers play a role in the elimination of CSLCs and development of carcinogenesis (88) (100).

1.3 Cell metabolism

1.3.1 Cell metabolism in non-cancerous (normal) cells

Cellular metabolism is a set of controlled biochemical reactions (metabolic pathways) within the cells of living organisms, involved in maintaining the living state of the cell. It is required for energy production to run cellular processes or is utilized for macromolecular synthesis (127). There are two major types of metabolic pathways: glycolysis and mitochondrial oxidative phosphorylation (OXPHOS). In normal conditions, both pathways contribute to generating energy and are required to maintain cellular energetic balance (128). In most cells, 70% of the energy is provided by OXPHOS, while glycolysis supplies the rest of the energy by metabolizing the glucose in the cytoplasm (129).

1.3.1.1 Glycolysis (in the anaerobic metabolic pathway)

Glycolysis occurs in the cytoplasm of cells where sugars such as glucose and fructose are metabolised. Glucose initially enters the cytosol by passing through any glucose transporters (GLUTs) and phosphorylated into an intermediate product, glucose-6-phosphate (G6P) by hexokinase enzymes (HKII). HKII catalyses the first irreversible step of glycolysis. This reaction requires energy and therefore results in the hydrolysis of adenosine triphosphate (ATP) to adenosine diphosphate (ADP) (130). G6P lies at the start of two metabolic pathways; it can either exit glycolysis to enter the pentose phosphate pathway (PPP), an alternative route for glucose breakdown, or be metabolized via glycolysis. The cytoplasmic concentration of $NADP^+$ plays a key role in determining which pathway G6P goes through.

When Oxygen (O_2) is limited (hypoxia), cells sustain their viability through glycolysis (131). G6P targeted for glycolysis undergoes isomerisation by phosphoglucose isomerase to fructose-6-phosphate (F6P), which is then converted to fructose-1,6-bisphosphate by phosphofructokinase 1 (PFK1). PFK1 is converted into two intermediary molecules of pyruvic acid (pyruvate). Lactate dehydrogenase (LDH) catalyses the conversion of pyruvate to lactic acid (lactate) and back, as it converts nicotinamide adenine dinucleotide (NAD^+) to NADH. The energy released in glycolysis is used to produce two ATP and two NADH molecules (Figure 1.10) (103) (127). In an attempt to compensate for the deficiency of ATP generation through glycolysis (2 ATP), cancer cells upregulate GLUTs and take more glucose into the cells. Inefficient ATP production only causes a problem

when there is not enough energy source for cells; this is not the case for proliferating cells such as cancers which have a constant supply of blood sugar and nutrients (130). Cancer cells need ATP for their maintenance rather than proliferation. Therefore, the ATP formed through glycolysis is sufficient for this purpose (132).

Going through the PPP, G6P is converted into ribose-5-phosphate while producing two molecules of NADPH for nucleotide synthesis (130). The accumulation of glycolysis intermediates promotes PPP which helps the biosynthesis of lipids and nucleic acids, providing benefit to cancer cells (132).

Glycolysis is regulated by multiple genes including oncogenes; RAS, c-Myc, and HKs (133). In addition to oncogenes, tumour suppressor genes such as P53 also regulate glycolysis. P53 inhibits GLUT1 and GLUT4 and therefore reduces glucose uptake into the cells (133).

Moreover, signaling kinases including AMP, AKT, and PAK1 are also involved in glycolytic pathways by upregulating glucose transporters such as GLUT1 (133). Aerobic glycolysis is mainly regulated by phosphoinositol 3 kinase (PI3K) signaling pathway (134). PI3K is a major activator of metabolism which is activated by growth factors resulting in activation of AKT and mTOR signaling pathways (135). Activation of PI3K/AKT pathway results in the upregulation of HKs and PFK1, leading to enhanced glycolytic flux (133).

1.3.1.2 Tricarboxylic acid (TCA) cycle and OXPHOS

During oxidative phosphorylation (a more efficient pathway compared with the cytoplasmic glycolysis), glucose is oxidised to carbon in the presence of O_2 (136). The free electrons are transferred from electron donors to electron acceptors such as O_2, in redox reactions (136). In non-cancerous cells, the majority of the pyruvate is transported into the mitochondria to be further metabolised by pyruvate dehydrogenase (PDH). It is then transformed into acetyl coenzyme A (acetyl-CoA) and carbon dioxide (CO_2), and fed into the Krebs' cycle, now known as TCA cycle. Acetyl-CoA is then converted to malonyl coenzyme A (malonyl-CoA) by acetyl-CoA carboxylase, and they are both used by fatty acid synthase (FAS) for the synthesis and elongation of fatty acid chains (127). PDH is one of the major regulators of mitochondrial function which plays a critical role in controlling the irreversible conversion of pyruvate to acetyl-CoA, CO_2, and NADH. The majority of NADH resulting from glycolysis, fatty acid oxidation

(FAO), and the TCA cycle is used to provide the energy for ATP synthesis via OXPHOS (127). The complete aerobic oxidation of glucose is coupled to the generation of up to 36 molecules of ATP mainly through the complete catabolism via the TCA cycle and OXPHOS (Figure 1.10) (137) (103).

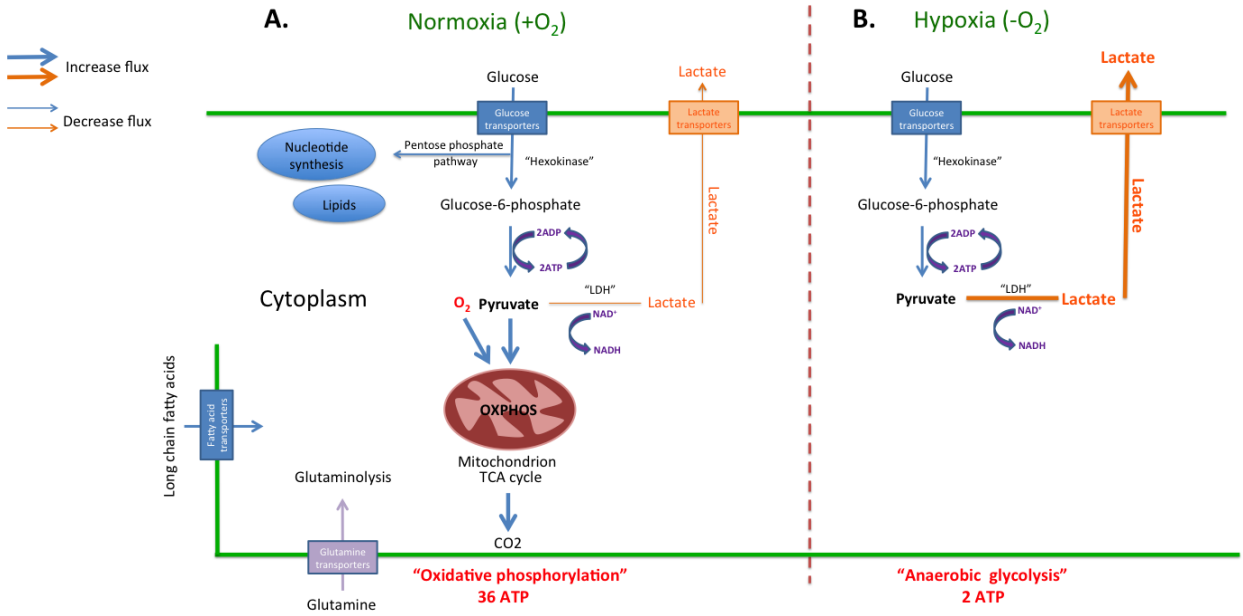

Figure 1.10 A schematic view of metabolic differences between oxidative phosphorylation under normoxia and anaerobic glycolysis under hypoxic conditions. Differentiated cells favour (A) oxidative phosphorylation in the presence of O_2 and (B) anaerobic glycolysis in the absence of O_2. Normal cells initially metabolize glucose to pyruvate for growth and survival followed by completing the process of oxidizing pyruvate to CO_2 through the TCA cycle and the OXPHOS in the mitochondria generation of 36 ATPs (A). When O_2 is limited in anaerobic condition, pyruvate is metabolised to lactate, resulting in the generation of 2 ATPs (B).

1.3.2 Cancer cell metabolism (aerobic glycolysis)

Throughout the transition from “normal” to cancerous cells, one of the key features affected is the cellular energy metabolism which could be the main cause of uncontrolled cell proliferation and cell death if dysregulated. As previously mentioned, enhanced proliferative activity is one of the major hallmarks of cancers and is critical for cancer cells to resist oxidative stress and adapt to hypoxic conditions (138) (139). This increase in glucose metabolism by cancer cells has now been confirmed by positron emission tomography (PET) imaging (136). PET analyses also confirmed that tumour invasion in cancer cell lines correlates with higher glycolytic rates. For instance, non-invasive MCF-7 breast cancer cells consume much less glucose in comparison with invasive MDA-MB-231 breast cancer cell line (134). Undergoing rapid proliferation, every cancer type including breast, adjust their metabolic pathways and use aerobic glycolysis over OXPHOS to fuel macromolecules for the synthesis of nucleotides, fatty acids, and amino acids (127) (133) (140).

In more differentiated cells, the energy metabolism shifts from glycolysis to OXPHOS, whereas, in cancer cells and throughout reprogramming to pluripotency, the metabolic shift is towards glycolysis (141). This reversed metabolic pathway is known as the Warburg effect and was first introduced by Nobel Prize winning biochemist Otto Warburg (The metabolism of tumours in the body). The Warburg effect is described as the exclusive conversion of glucose to lactic acid even in the presence of O_2 (Figure 1.11) (140).

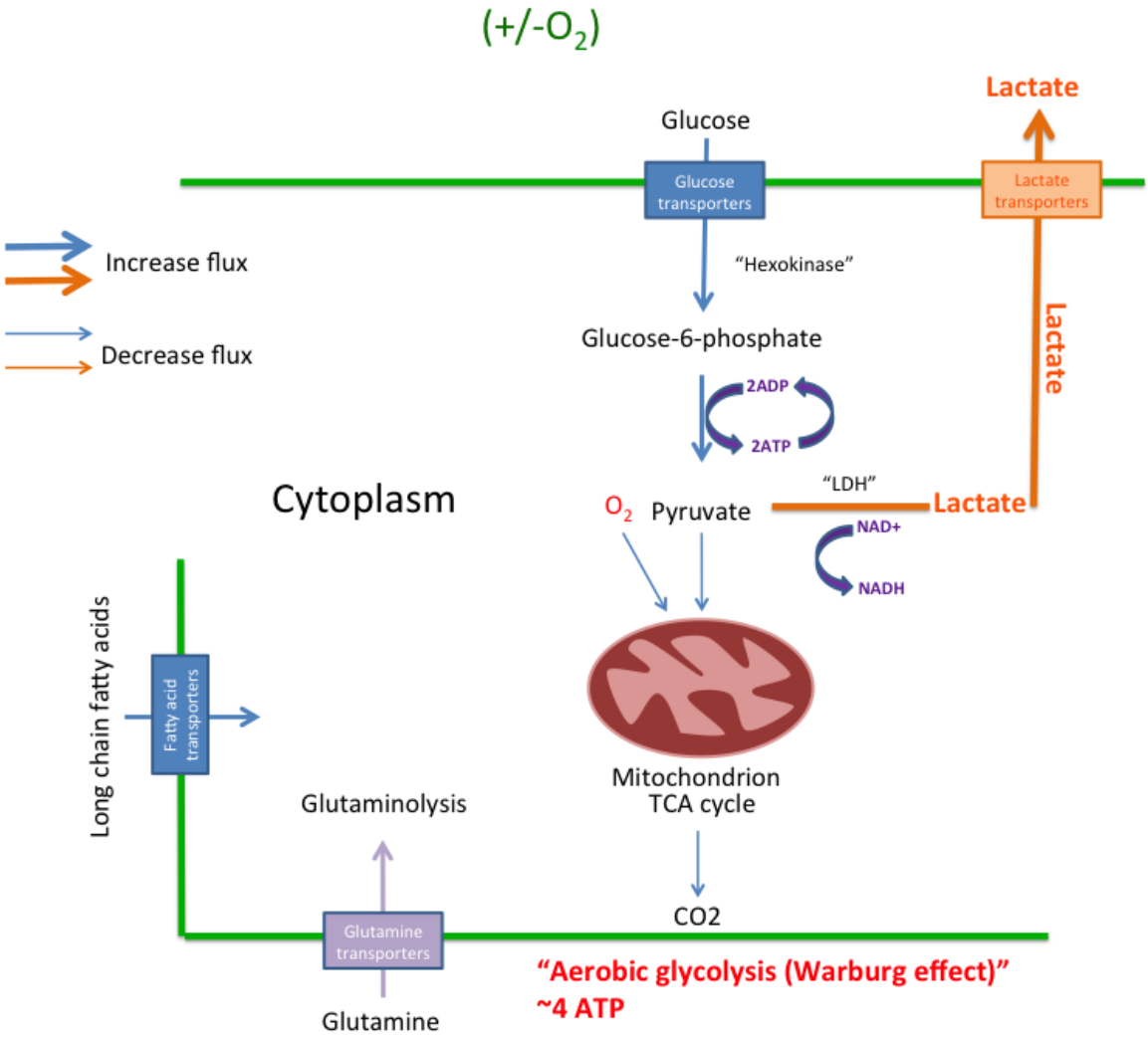

Figure 1.11 A schematic view of cancer metabolism, an aerobic glycolysis in the presence of oxygen (Warburg effect). Even in the presence of sufficient oxygen, cancer cells convert most glucose to lactate in the cytosol to accelerate cell proliferation by generating ~4 ATP per glucose. On the contrary, cancer cells convert glucose to lactate (Warburg effect) generating only two ATPs per glucose.

A metabolic shift to enhanced glycolysis occurs at early stages during tumorigenesis. As in cancer cells, ES cells also favour an alternative metabolic pathway, that is, they share a common metabolic shift towards a high glycolytic phenotype with a reduced use of the TCA cycle (133). In glycolytic metabolism of cancer cells, PDH activity is blocked by the hypoxia-driven enzyme, pyruvate dehydrogenase kinase (PDKI), and glucose-derived pyruvate is predominantly synthesised into lactate by LDH rather than being transported into mitochondria (Figure 1.11) (134). Lactate levels indicate the prevalence of the glycolytic phenotype (142). Lactate enters and exits the cell through lactate transporters, monocarboxylate (MCTs), which are overexpressed in most tumours (142). The accumulation of lactate contributes to an acidic extracellular pH and further alterations in gene expression. This damages the adjacent population of cells and as lactate aggregates in the microenvironment of the tumour increases in acidity occur which degrades the ECM of the cells (143). This upregulation of lactate within the tumour microenvironment is associated with tumour recurrence and thus, promotes angiogenesis and invasion leading to metastasis. Contrary to normal cells, cancer cells adapt to acidity and survive by inhibiting DNA repair system and resisting apoptosis (142).

1.3.3 Metabolic manipulation as a target for cancer treatment

Recent therapeutic efforts have focused on the development of new therapies to treat cancers. Despite this, cancer still remains as one of the leading causes of mortality in patients. Recently, metabolic modulation therapy was introduced to cancer therapy (144). Metabolic balance is an important factor in cell survival. There is mounting evidence that alterations in cellular metabolism are among the most consistent emerging hallmarks of cancer (144) (145). Metabolic properties of cancer cells are considerably different from those of normal cells (144). Tumour cells exhibit enhanced metabolic independence compared with normal cells, taking up nutrients and metabolizing them in pathways that support high growth rates and proliferation (146). This metabolic shift has been observed comprehensively during carcinogenesis and has always been considered a reliable biomarker for malignant transformation. Breast cancer is metabolically a heterogeneous disease which can be classified into different metabolic phenotypes (147). As well as glycolysis, cancer cells share other metabolic characteristics such as increased fatty acid synthesis and high rates of glutamine metabolism (144). These common characteristics in cancer cells are linked to therapeutic resistance in cancer treatment.

Aiming to target pathways involved in cancer metabolism may lead to promising treatments for an extensive range of human cancers (132) (148). Modulation of cancer metabolism through the targeting of different metabolic enzymes such as hexokinase, lactate dehydrogenase, pyruvate dehydrogenase kinase, fatty acid synthase, and glutaminase could possibly improve outcome by reducing the growth rate of CSLCs and therefore lessening the probability of cancer initiation (149).

1.3.3.1 Inhibiting glycolysis, a central energy source for cells

Glucose metabolism counts as a major energy source for cells and more specifically highly proliferating cells such as cancer cells. There are several enzymes such as LDH and HK contributing to the series of reactions which are critical for the breakdown of glucose in glycolysis. Targeting and inhibiting these enzymes could be used as an anticancer strategy to trap glycolysis and therefore suppress the main source of energy for cancer cells and stem cells.

The inhibition of the two main enzymes, HK and LDH, in the glycolytic pathways is discussed below.

1.3.3.1.1 Targeting HK

2-Deoxy-D-glucose (2DG), a compound known to inhibit the first step of glycolysis:

One possible way to target glycolysis is through the enzyme HKII which is highly expressed in tumours and facilitates high rates of glucose catabolism (150). HK inhibitors such as **2DG** have been used in pre-clinical trials. It is therefore important to assess the impact of this inhibitor on cancer cell survival and stem cell populations by analysing the growth rate of bCSLCs (mammosphere assay) (149). 2DG is a glucose analog; it enters the cytosol through the same transporters as glucose (GLUTs) and is phosphorylated by HK to 2DG-6-phosphate (Figure 1.12). Due to the low levels of intracellular phosphatase, 2DG-6-phosphate is stored and trapped in the cytoplasm and is incapable of being further metabolized. This in turn leads to suppression of HK activity and therefore inhibition of glucose metabolism, impairing PPP and nucleotide synthesis (151).

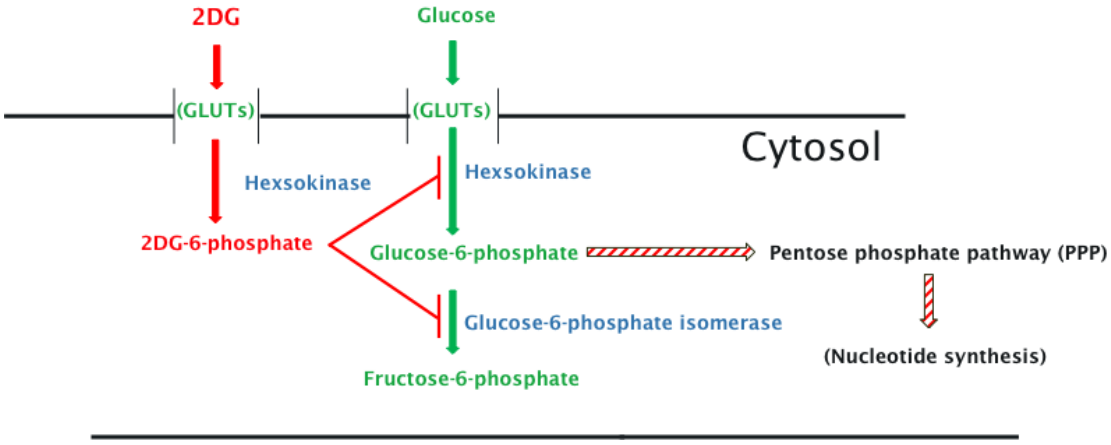

Figure 1.12 A schematic representation of glycolysis inhibition by 2-deoxy-D-glucose (2DG). 2DG is phosphorylated by HK and accumulates in the cytoplasm. It is then unable to undergo further metabolism. This reduces HK activity and inhibits glucose metabolism. HK suppression leads to reduced glucose-6-phosphate production which in turn results in impaired PPP and nucleotide synthesis.

1.3.3.1.2 Targeting LDH

Sodium oxamate, a compound known to inhibit the last phase of glycolysis:

One of the other approaches to inhibit glycolysis is to reduce the LDH activity which is known as an efficient antitumour strategy (152). LDH is known as an essential factor in facilitating tumour maintenance. Breast cancer cells are well documented to be sensitive to glucose deprivation as well as increased LDH activity (152). Reducing LDH activity in tumour cells reduces lactate production. Reduced lactate levels leads to increased oxygen consumption, enhanced mitochondrial respiration, and eventually reduced glycolysis (152). Thus, using LDH inhibitors such as **sodium oxamate** could be an efficient step towards limiting CSLC activity and suppressing tumorigenicity. Sodium oxamate is a structural analog of pyruvate, a classic inhibitor of LDH and glycolysis. Oxamate disrupts the entire gluconeogenic pathway and is well-known as an anticancer compound (153) (Figure 1.13).

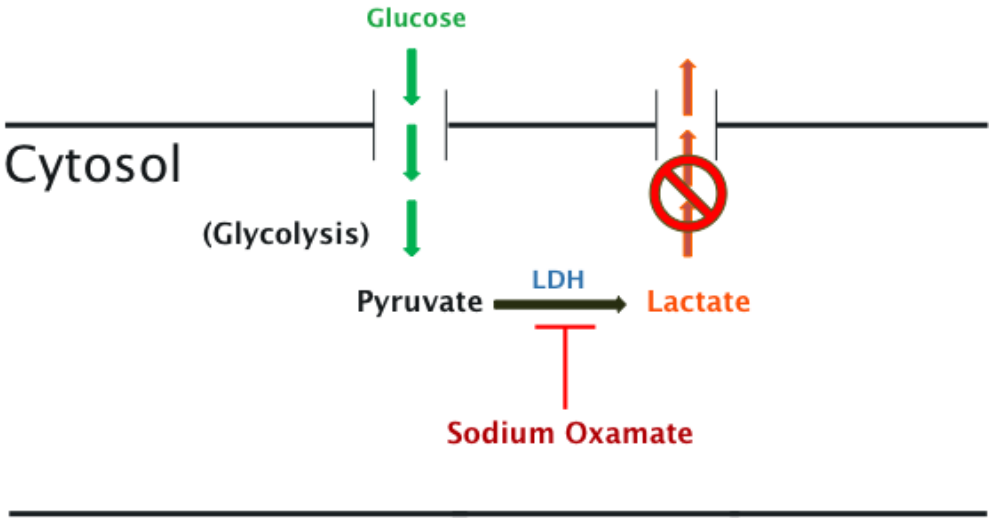

Figure 1.13 A schematic representation of glycolysis inhibition by sodium oxamate. Sodium oxamate inhibits LDH activity and catalyses the final step of glycolytic pathway that converts pyruvate into lactate. This results in the inhibition of glycolysis.

1.3.3.2 Glutamine starvation

Sugars and amino acids are essential substrates for cellular homeostasis. Together with glucose, the critical role of glutamine, the most abundant amino acid, is well documented in cell growth and energy metabolism (OXPHOS) (154) (155) (131). Glutamine supplies carbon (in the form of mitochondrial oxaloacetate), nitrogen (protein and nucleic acid production), and free energy to maintain citrate production in the mitochondria and supports cell growth and division. In order for a cell to engage in replicative division and macromolecular biosynthesis, extracellular nutrients such as glucose and glutamine are required (127) (130). Cancer cells take up glutamine at high rates through the glutamine transporter where it is partially metabolized via glutaminolysis (130). Glutaminolysis consists of two steps: Firstly, the catalysis of glutamate from glutamine through the enzyme glutaminase (GLS) for the maintenance of the TCA cycle. Secondly, the conversion of glutamate to α-ketoglutarate (a key intermediate in the TCA cycle) by glutamate dehydrogenase (GDH) (149). The majority of cancer cells survive and grow via aerobic glycolysis while some cancers prefer glutamine even though it is not an essential amino acid. According to metabolic flux analysis, cancer cells that display Warburg-like metabolism rely on glutamine as the main source of carbon to use in TCA cycle (146). Glutamine is capable of providing energy through the first step of the TCA cycle independently of glucose. Consequently, in the event of glutamine deprivation, the TCA cycle would be impaired and result in reduced energy production. Glutamine is catabolised in considerable amounts and is mainly used to maintain the membrane potential in the mitochondria in cancer cells along with regulating NADH production for fatty acids and macromolecule synthesis (156). Furthermore, glutamine regulates the activity of several genes involved in the metabolism, cell proliferation, and cell repair (157). Among those genes, the c-Myc oncogene has been observed in tumours which are more sensitive to glutamine withdrawal. Genes involved in glutamine metabolism are directly or indirectly under the transcriptional control of Myc proteins (130). Glutamine withdrawal from Myc transformed cells suffer extensive loss of TCA cycle which results in cell death (130). In glutamine starvation, glutaminolysis will not take place and the lack of glutamate in the mitochondria reduces amino acid formation and gluconeogenesis (less glucose formation) (Figure 14). Moreover, cancer cells cannot proliferate properly in culture without glutamine. Instead, the accessibility of glutamine to cancer cells results in enhanced

production of byproducts necessary for rapidly proliferating cells, such as stem cells and cancer cells (148).

In addition to TCA cycle impairment, limiting glutamine synthesis has an extreme impact on cancer cell proliferation reducing the growth rate in tumours, both *in vitro* and *in vivo* (135). Hence, the glutamine balance must be maintained to retain the metabolic equilibrium in cells.

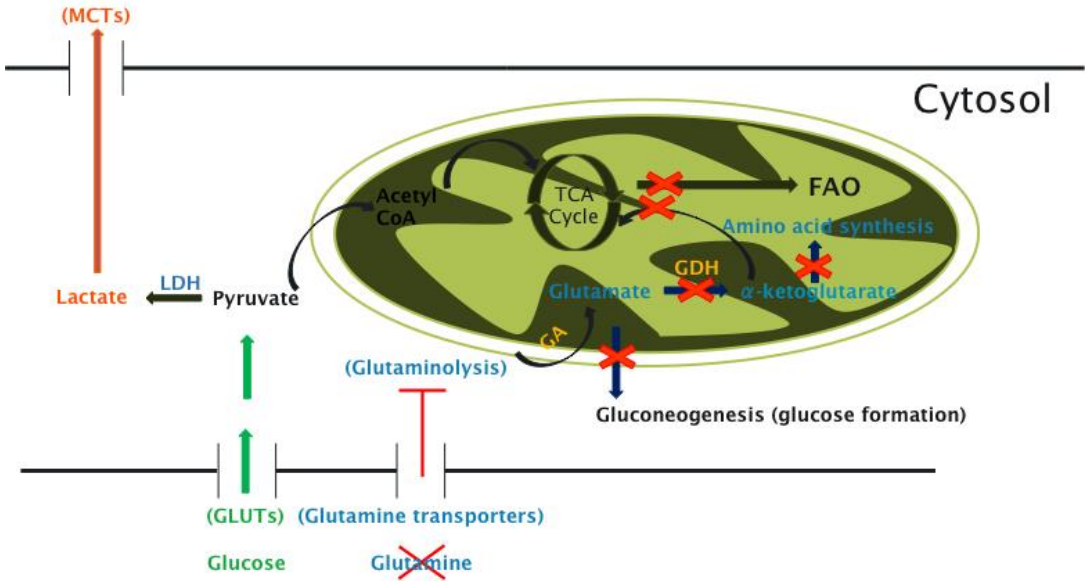

Figure 1.14 A schematic representation of the effect of glutamine starvation on mitochondrial function. In many cancer cells glutamine maintains the TCA cycle via glutaminolysis through the GA enzyme which converts glutamine to glutamate. Glutamate is then converted to α-ketoglutarate via GDH, a key TCA cycle intermediate. In the incidence of glutamine starvation, the TCA cycle is impaired which results in reduced fatty acid oxidation. In the absence of glutamine, glutaminolysis will not take place and therefore there will be no glutamate in the mitochondria to be used for amino acid formation and gluconeogenesis (less glucose formation).

1.3.3.3 Mitochondrial respiration, a more effective pathway for energy production

1.3.3.3.1 Targeting pyruvate dehydrogenase kinase (PDK):

One of the key factors leading to altered energy metabolism is the activity of HIF-α factor (HIF-1α). HIF target genes strongly correlate with those associated with dysregulated tumour metabolism. HIF-1 transcription factor is induced by low levels of O_2 within the tumour (158). As well as stimulating glycolysis, HIF-1 also actively suppresses mitochondrial function (OXPHOS) by transactivating the PDK1 (159). PDK1 phosphorylates PDH and inhibits it from using pyruvate to fuel the mitochondrial TCA cycle. This results in disconnection of the TCA cycle from glycolysis and reduces the mitochondrial O_2 consumption causing an increase in intracellular O_2 tension (159). This reduction is partly facilitated through the induction of PDKs (HIF-1 dependent) within the tumour cells and a reduction in pyruvate oxidation within the mitochondria (158). In cancers, mitochondrial glucose oxidation is suppressed and cytoplasmic glycolysis compensates in terms of energy production. Therefore, reactivating mitochondrial metabolism could delay cancer cells switching to glycolysis (149).

Inhibiting mitochondrial function is as important as enhanced glycolysis in promoting the Warburg effect. Targeting PDH controls the entry of carbons derived from carbohydrates into the mitochondria and therefore creates a glycolytic shift in glucose metabolism. This reaction has a major impact on the regulation of mitochondrial energy-producing pathways (TCA and OXPHOS) and has an important role in the generation of biosynthetic intermediates (154). **Dichloroacetate (DCA)**, a small molecule drug, stimulates mitochondrial function by inactivating PDK, leading to enhanced PDH activity and a metabolic switch from glycolysis to mitochondrial respiration. This leads to increased TCA cycle and glucose oxidative metabolism by promoting the influx of acetyl-CoA into the mitochondria and the TCA cycle. This therefore increases the NADH supply to complex l of the electron transport chain (149). By blocking PDK, DCA induces cancer cells into aerobic metabolism (glucose oxidation) in the mitochondria, resulting in glycolysis suppression. The increase in glucose oxidation following DCA use could also be obtained by inhibiting mitochondrial FAO levels (160). Cancer cells naturally have a poor supply of O_2 compared with normal tissues so if aerobic metabolism in tumours is delayed, the lack of O_2 may lead to apoptosis (Figure 1.15). The preclinical trials on DCA have shown its

effects via the induction of apoptosis in different cancer tissues such as lung, breast, and glioblastoma by shifting cellular metabolism from aerobic glycolysis to glucose oxidation (161).

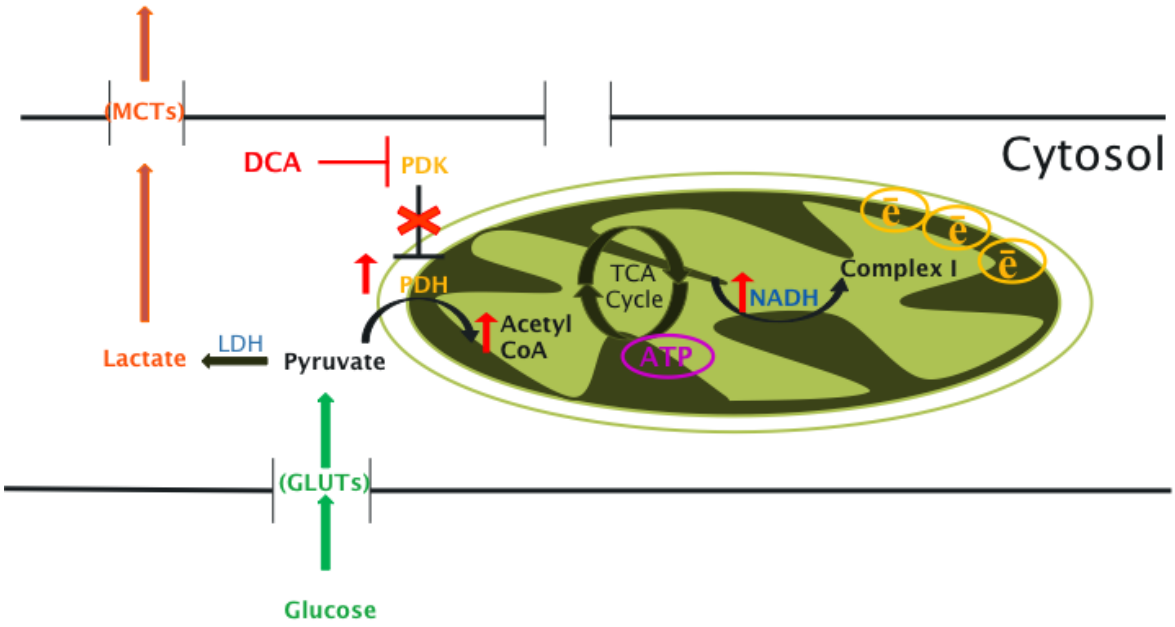

Figure 1.15 A schematic representation of cellular consequences of DCA action. In the last step of glycolysis, pyruvate is transported to the mitochondria and converted into Acetyl-CoA through PDH. Acetyl-CoA then enters into the TCA cycle for ATP production. In the incidence of cancer, where mitochondrial oxidation is limited, DCA inhibits PDK and triggers PDH activity which induces cancer cells to utilise aerobic metabolism in the mitochondria. This compensates for the TCA cycle by increasing the influx of acetyl-CoA into the mitochondria and therefore NADH is supplied to complex I of the electron transport chain.

1.3.3.3.2 Blocking mitochondrial respiration:

Metformin is found to be one of the most effective therapeutic agents in the treatment of diabetes. There is great interest to use metformin for cancer prevention or treatment (106). Metformin inhibits metabolism from different aspects. It was evident in studies that metformin treated cells that became energetically inefficient, for instance when displaying increased aerobic glycolysis and reduced glucose oxidation in the mitochondria (106). The inhibitory role of metformin on glucose metabolism is an outcome of a combination of effects on glycolysis, FAO, and signalling pathways. One aspect is that metformin impairs glycolysis by inhibiting the enzymatic activity of HKII, resulting in less pyruvate production (162).

In addition, metformin could directly target cancer cells by reducing the energy supply from the mitochondria. Studies have demonstrated that cancer cells with mitochondrial dysfunction such as complex I (the first component of the mitochondrial electron transport chain) mutations displayed more sensitivity to the action of metformin (163) (164). Metformin enters the cell through the organic cation transporter 1 (OCT1) and enters the mitochondria where it inhibits complex I, resulting in decreased NADH oxidation, impaired TCA cycle, and less mitochondrial ATP synthesis. These actions result in decreased gluconeogenesis (less glucose formation from pyruvate) and increased glycolysis (more pyruvate formation from glucose) (Figure 1.16) (162). The effects of metformin depend on glucose availability to cells. Metformin reduces the cell division in cancer cells in the presence of abundant amounts of glucose, leading to reduced tumour growth (106).

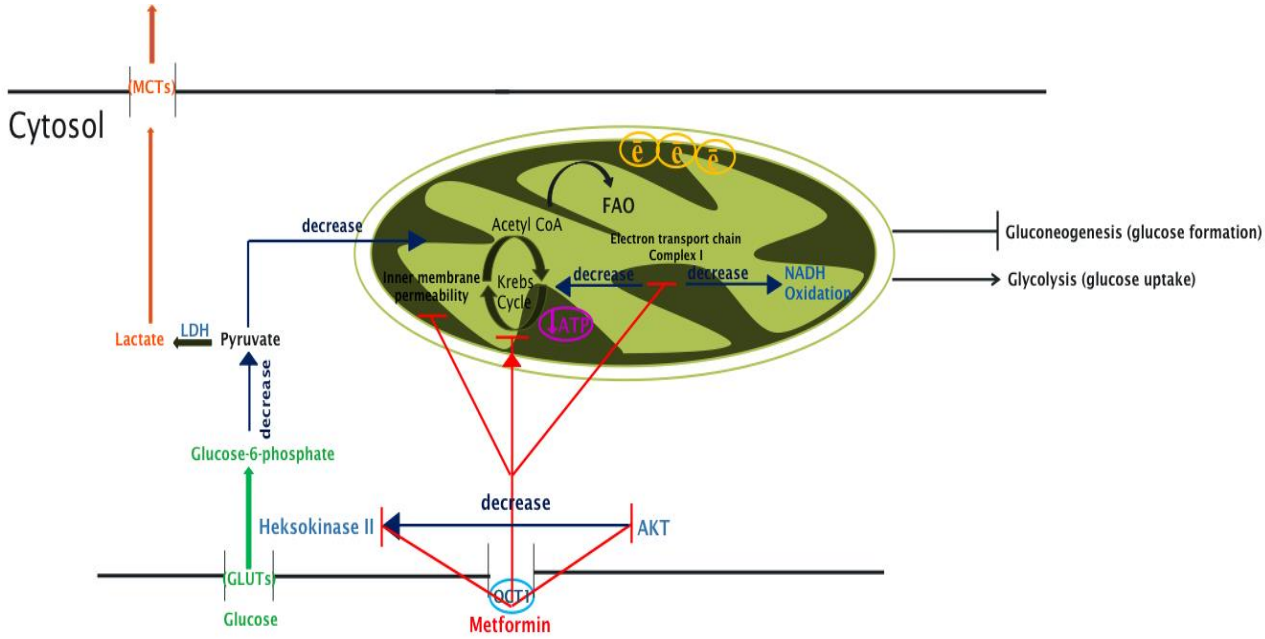

Figure 1.16 A schematic representation of metformin on cellular metabolism. Metformin enters the cell via the OCT1 transporter. Metformin directly and indirectly reduces HKII activity and mitochondrial interaction. Metformin inhibits complex l of the electron transport chain and reduces TCA activity. These actions decrease gluconeogenesis and stimulate glycolysis.

1.3.3.4 Inhibition of fatty acid oxidation (FAO)

Fatty acids flow across the cell membrane by passing through malonyl-CoA and fatty acid protein transporters located on the cell surface (165). Malonyl-CoA regulates FAO by controlling the uptake of fatty acids into the mitochondria through the inhibition of Carnitine palmitoyl transferase 1 (CPT1). A CoA group is added to fatty acids and forms a long-chain acyl-CoA. The CPT1 site on the outer mitochondria membrane allows the transportation of acyl-CoA into the mitochondrial membrane and fatty acid β-oxidation pathway, resulting in the production of one acetyl-CoA. Acetyl-CoA enters the TCA cycle and is used in fatty acid β-oxidation. The electron transport chain utilizes the energy produced by fatty acid β-oxidation and the TCA cycle to produce ATP (165).

A reasonable approach to reduce energy sources for cancer cells is to inhibit FAO. **Etomoxir** acts as a strong inhibitor of mitochondrial CPT1 on the outer face of the inner mitochondrial membrane. Inhibition of CPT1 reduces the ratio of fatty acid flux into the mitochondria and inhibits FAO (131). This step is essential to the production of ATP from FAO. Therefore, using direct inhibitors for FAO, such as etomoxir, could prove promising in reducing cancer growth (Figure 1.17).

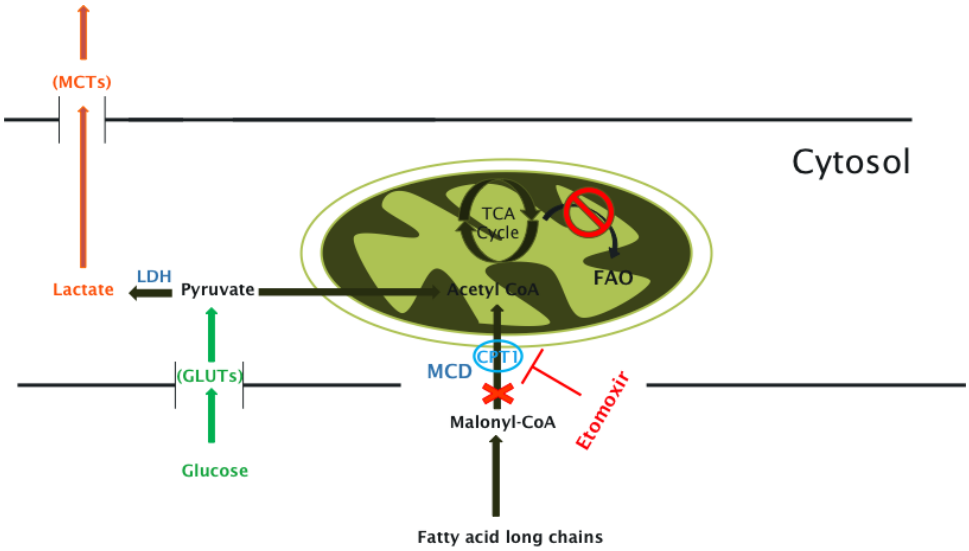

Figure 1.17 A schematic representative of etomoxir in fatty acid oxidation. Long chain fatty acids enter mitochondria through the CPT1 proteins and are then transformed into acetyl-CoA to take part in the TCA cycle and fatty acid oxidation.

In summary, altering glucose metabolism and FAO in cancer cells opens new insights to cancer treatment. The potential of targeting the CSLC population by metabolic modulation therapy to promote glucose oxidation rates, reducing FAO, or inhibiting glycolysis is a promising avenue for cancer biology.

1.3.4 The role of C-terminal binding proteins (CtBP1/2) in cancer

The CtBP1/2 proteins are a dimeric family of proteins that in mammals consist of two members; CtBP1 and CtBP2. CtBP1 is encoded by genes located on chromosome 4 and CtBP2 on chromosome 10. According to genetic studies in *Drosophila* and mice, both members are highly expressed throughout development (166). CtBP1 was discovered as a cellular protein that interacted with the C-terminus of adenovirus E1A proteins (167). CtBPs are well-characterised transcriptional co-repressors with important roles in tumorigenesis (168). Co-repressors are capable of combining with a specific repressor molecule and activating it, thus blocking gene transcription. CtBPs have been associated with various biological processes including development, proliferation, differentiation, and transformation through their association with a wide range of transcription factors. CtBPs directly and indirectly supress the expression levels of a range of tumour suppressor and EMT-related genes such as E-cadherin (167) (169) (170). Loss of E-cadherin is associated with promoting mesenchymal (stem-like) features, which leads to a more metastatic phenotype (171) (Figure 1.18).

1.3.4.1 CtBP, an NADH dependent transcriptional factor

CtBPs have a unique redox-sensing ability capable of sensing the NAD^+/NADH ratio and detecting enhanced levels of free nuclear NADH in cancer cells based on the metabolic environment of cells (hypoxia). The enhanced levels of NADH stimulate CtBP dimerization promoting CtBP recruitment to the E-cadherin promoter (167) (172). Hypoxia inhibits the expression of E-cadherin, leading to enhanced tumour migration (Figure 18) (166). Pyruvate, the product of glycolysis, could prevent this action by inhibiting the NADH increase and therefore CtBP function (167). In total, CtBPs are well documented as key regulators of metabolic states in cancer cells.

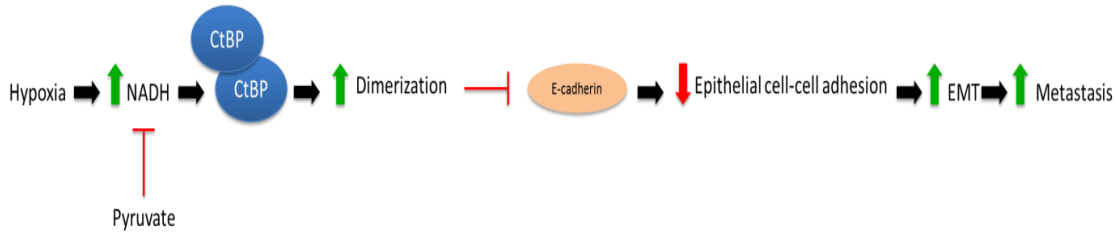

Figure 1.18 CtBP triggers tumorigenicity by inhibiting EMT-related genes (E-cadherin) and promoting metastasis.

1.3.4.2 Regulation of CtBP by glucose and glutamine

Carbon sources in glucose and glutamine are essential for ATP generation and biosynthesis in cancer cells (139). Many cancer cells including MCF-7 breast cancer cells rely on glutamine for their growth. In general, tumour cells primarily rely on glycolysis for their energy metabolism, which is often incomplete resulting in the accumulation of acidic metabolites such as pyruvate and lactate within the cytosol (173). To lessen intracellular acidification and stabilise pH levels, cancer cells rely on ammonia, the product of glutaminolysis, which plays an important role in resisting the cytoplasmic acidification caused by glycolysis (173). CtBPs have shown to be critical in stimulating glutaminolysis by repressing SIRT4 (a glutaminolysis inhibitor). By stimulating glutaminolysis, CtBPs promote tumorigenicity in breast cancer patients (173).

1.3.4.3 4-methylthio-2-oxobutyric acid (MTOB), a CtBP inhibitor

Loss of CtBP results, in intracellular acidification, leading to the induction of apoptosis in breast cancer cells (173). Inhibition of CtBP family proteins reduces the growth and self-renewal of CSLCs, whereas overexpression of CtBPs has increases CSLC population (174) (172). Therefore, targeting CtBPs and inhibiting their activity may present a promising therapeutic approach in breast cancer treatment. Straza *et al*. showed a compound in the methionine salvage pathway (MTOB) that strongly inhibited spheroid growth and self-renewal in a dose dependent manner (172). MTOB is a CtBP dehydrogenase substrate, proven as a direct inhibitor of repressive function of CtBP at high concentrations, resulting in cancer cell death and inhibition of engrafted tumour growth (171). CtBP targets pro-apoptotic factors such as Bik. MTOB competes with CtBP for binding to the Bik promoter, leading to cell apoptosis and decreased cell survival through displacement of CtBP2 from the Bik promoter (172) (Figure 1.19).

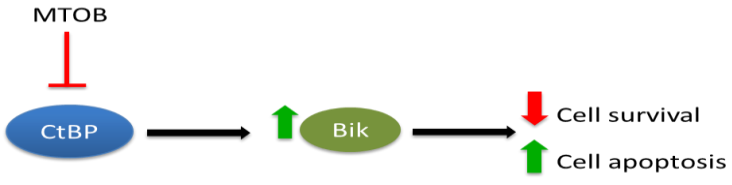

Figure 1.19 MTOB facilitates Bik expression by inhibiting the CtBP regulation leading to cell apoptosis.

Further studies have proposed that MTOB application to breast cancer MCF-7 cells enhanced the acidification of culture medium and cytoplasm. This highlights the capability of MTOB disrupt the pH homeostasis of cancer cells (173). In addition, MTOB application showed antitumour effects in xenograft models and apoptosis *in vitro*, but only at high concentrations. This suggests that MTOB might selectively target CSLCs in the tumour population. This is in agreement with the observation that MTOB was more effective at the inhibition of spheroid formation than at killing cells in monolayer cultures (174). Therefore, such molecules (MTOB) may be beneficial in cancer therapy (172).

Taken together, extensive profiles of CtBP-target genes in breast cancer regulate stem cell related genes, EMT, and cancer cell metabolism, suggesting that CtBPs could be potential therapeutic targets for breast cancer treatment (171).

1.5 Aims

This thesis aims to exploit the 3D mammosphere assay to address key current questions regarding the role of CSLCs in breast cancer. Based on evidence from hESC, it is hypothesized that changes in glycolytic metabolism will affect stem cell characteristics. Furthermore, it is assumed that pluripotency factors such as OCT4 and SOX2 might be involved in this observation.

The specific aims of this thesis are:

- To investigate the role of key transcription factors OCT4 and SOX2 in tumorigenicity of breast cancer.
- To characterise the expression of OCT4 pseudogene 1 in breast cancer cells and its role in tumorigenicity.
- To examine whether glycolysis restriction would impact on cell proliferation and CSLC populations in breast cancer cells.
- To investigate whether modulation of tumour cell metabolism using different metabolic inhibitors in stem-like population of breast cancer cell lines stop or slow down CSLCs growth.
- To characterise the effect of CtBP inhibition in CSLC population of breast cancer cells in different metabolic conditions using CtBP siRNA and the CtBP inhibitor, MTOB.

Chapter 2

Material and Methods

2.1 Cell culture procedures

All steps of cell culture were performed in sterilised laminar flow hoods cleaned with 70% ethanol. Reagents were warmed to 37°C in a water bath and cleaned with ethanol prior to use in the hood.

2.1.1 Cell lines

The carcinoma cell lines listed in Table 2.1 were cultured in the growth medium, Dulbecco's modified Eagle's medium (DMEM), supplemented with 10% foetal calf serum (FCS), 1% Penicillin/Streptomycin, and 2 mM L-Glutamine. Cell lines were maintained as a monolayer in sterile T75 cell culture flasks in humidified incubators with 10% CO_2 at 37°C.

Table 2.1 Description of cell lines

Cell lines	Origin	Description
MDA-MB-231	**ATCC®HTB-26™**	**Mammary gland, breast, derived from metastatic site: pleural effusion**
MCF-7	**ATCC®HTB-22™**	**Mammary gland, breast, derived from metastatic site: pleural effusion**
SkBr-3	**ATCC®HTB-30™**	**Mammary gland, breast, derived from metastatic site: pleural effusion**
Ntera-2	**ATCC®CRL-1973™**	**Testis, derived from metastatic site: lung**
T-47D	**ATCC® HTB-133™**	**Mammary gland, breast, derived from metastatic site: pleural effusion**
BT-474	**ATCC® HTB-20™**	**Mammary gland, breast, derived from solid, invasive ductal carcinoma of the breast**

2.1.2 Passaging cells

To subculture cells, the spent culture media was aspirated from the cell culture vessels and cells were washed with Hank's Balanced Salt Solution (HBSS) to remove any traces of growth factors and serum. HBSS was then aspirated and 1-2 ml per 25 cm^2 of 0.05% trypsin/5 mM EDTA solution (PAA) was added to the cells for three to five minutes in the incubator to be detached. Detached cells were then re-suspended in 9 ml fresh media. Cells were passaged at different ratios depending on the growth rate of each cell line.

2.1.3 Cell counting

A haemocytometer was used in order to determine the number of cells. The surface and the coverslip were cleaned with ethanol and the coverslip placed over the counting surface prior to the addition of the cell suspension. Following trypsinisation, the cells were collected in 15 ml falcon tubes and centrifuged at 1300 rpm for three minutes at room temperature. The supernatant was removed and the pellet was re-suspended in fresh media. A total of 15 µl of the cell suspension was transferred to a chamber on the haemocytometer. Cell counting was repeated three times using three different squares of the haemocytometer.

2.1.4 Maintenance of cell stocks

2.1.4.1 Freezing

To maintain stocks, cells were seeded in culture flasks and fed one day before confluency. 24 hours after changing the media, cells were washed with HBSS, trypsinised, re-suspended in media, transferred to a sterile centrifuge tube, and centrifuged at 200 g at 4°C for three minutes. The supernatant was then removed and cell pellets were quickly re-suspended in 10ml media/freezing media (5 ml media, 1 ml dimethyl sulfoxide [DMSO] and 4 ml FCS per cryovial). DMSO prevents ice crystal formation upon freezing, and hence avoids cell rupture. The vials were transferred to a cell freezing container, stored at -80°C overnight for gradual cooling, and were transferred to a liquid nitrogen tank for long-term storage.

2.1.4.2 Thawing

Cryovials were removed from the liquid nitrogen tank and thawed rapidly at 37°C. The cells were re-suspended into a 15 ml falcon tube in 10 ml fresh medium. The suspension was centrifuged at 1300 rpm for three minutes at room temperature. The supernatant was aspirated off and the cell pellet re-suspended in 10 ml fresh media. The cells suspension was transferred into a T75 tissue culture flask and placed in a 10% CO_2 humidified incubator at 37°C.

2.2 *In vitro* cell culture assays

2.2.1 Protein knockdown with small interfering RNA (siRNA)

Cells were seeded in 60 mm dishes at a concentration of 250,000 per 3 ml growth medium and allowed to adhere overnight. The cells were transfected the following day: OPTIMEM reduced-serum medium (GIBCO), 25 nM siRNA, and INTERFERin™ (Cat No 409-10), were mixed and incubated for 10 minutes at room temperature. A total of 400 µl of media was aspirated off each dish and replaced with the siRNA mixture. The cells then incubated at 37°C for 4 hours. The transfection procedure was stopped by replacing the spent media with 3 ml fresh media and transfected cells were transferred to humidified incubator at 37°C for 72 hours. Details of all siRNA sequences are stated in the Table 2.2.

Table 2.2 Description of siRNA reagents and sequences

Protein target	Sequence (5' → 3')	Source	Reference
CtBP1	ACGACUUCACCGUCAAGCATT UGCUUGACGGUGAAGUCGUTT	QIAGEN	
CtBP2	GCGCCUUGGUCAGUAAUAGTT CUAUUACUGACCAAGGCGCTT	QIAGEN	
CtBP1/2	GGGAGGACCUGAGAAGUUUTT AACUUCUCCAGGUCCUCCCTT	Applied Biosystems	
Control siRNA	NA	Applied Biosystems	
Hs_POU5F1_2	TGGGATTAAGTTCTTCATTCA	QIAGEN	Sl00690382
Hs_POU5F1_10	AGGGAAGGTGAAGTTCAATGA	QIAGEN	Sl04153835
SOX2	CAGUAUUUAUCGAGAUAAATT UUUAUCUCGAUAAAUACUGTA	ThermoFisher Scientific	4392420
OCT4 full length	GUCCGAGUGUGGUUCUGUATT UACAGAACCACACUCGGACCA	ThermoFisher Scientific	4392420
OCT4 AB	GGGUUUUUGGGAUUAAGUUTT AACUUAAUCCCAAAAACCCTG	ThermoFisher Scientific	AM16708
POU5F1B	GCCCGAAACCCACACUGCAGAUCAG CUGAUCUGCAGUGUGGGUUUCGGGC	Invitrogen	10620318 10620319

2.2.2 Protein analysis

2.2.2.1 Western blotting

Urea whole cell lysis: Cells were washed with ice-cold phosphate-buffered saline (PBS) followed by the addition of 1 ml ice-cold PBS and cells were collected with a cell scraper into a 1 ml microcentrifuge tube and centrifuged at 900 g for five minutes at 4°C. PBS was removed and cells were lysed in two volumes ice-cold Urea lysis buffer (Table 2.4) for 15 minutes on ice. The pellet was then vortexed to break it up. The cell lysates were centrifuged at 10500 g at 4°C for 10 minutes to pellet cell debris. The protein suspension was transferred to a 0.5 ml microfuge tube, snap frozen in liquid nitrogen, and stored at -20°C.

Protein quantification: The protein concentration was analysed using the Bradford Assay from Biorad (Cat No. 500-0006). The quantification was performed as per the instructions. Briefly, a 1:5 dilution of the stock Bradford reagent (BIO-RAD) was made up in distilled water. Cell lysate (1 µl) was added to 1 ml diluted reagent and mixed in disposable plastic cuvettes. The absorbance was read at 595 nm using a spectrophotometer.

Sodium dodecyl sulphate polyacrylamide gel electrophoresis (SDS-PAGE): A 10% polyacrylamide resolving gel was prepared (see recipe in Table 2.3) and poured to a depth of 3.2 ml in-between a glass and a spacer plate (0.75 mm). The top of the gel was overlaid with distilled water in order to obtain a straight edge. The gel was then allowed to polymerise for 45 minutes at room temperature. The water was replaced with 2 ml of stacking gel (see recipe in Table 2.3). A well-comb was inserted between the two glass plates and the stacking gel allowed to polymerise. After casting, the gel was placed in an electrophoresis tank filled with running buffer and the comb was removed carefully. A total of 20 µg of protein from cell lysates (detailed in Table 2.4) were diluted in SDS-loading buffer heated for two minutes at 95°C in a heat block. Proteins were loaded into each well of the gel and separated at 150 V for approximately 1 hour. Empty wells were loaded with SDS-sample buffer (Figure 2.1).

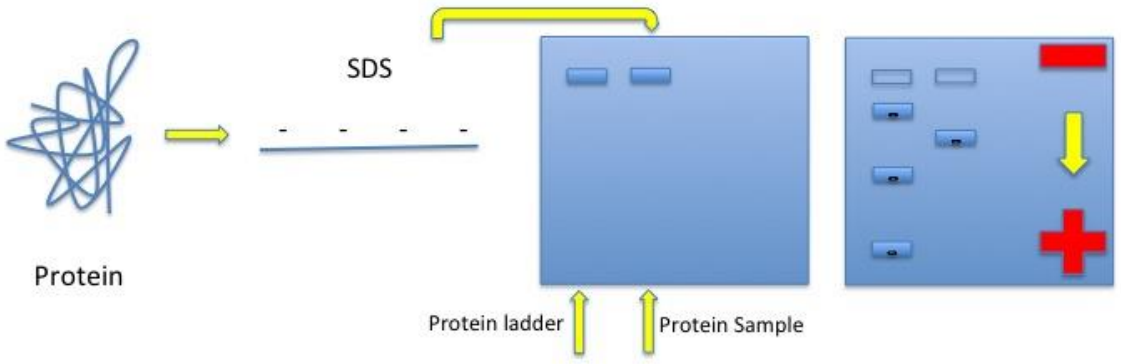

Figure 2.1 Gel Electrophoresis Process. Protein samples were resolved on a 10% polyacrylamide gel alongside the protein ladder. Proteins with negative and positive charges travel together through the gel towards the positively charged electrode. Proteins with less mass travel more quickly.

Hybond C (Amersham) and Whatman filter paper was cut to the size of the gel and rinsed in PBST (PBS with 0.1% Tween). After running, the gel was removed from the glass plates, placed on the membrane, and sandwiched between two stacks of Whatman filter paper. All bubbles were removed and the membrane was assembled in a clamp apparatus and transferred overnight at 20 mA in transfer buffer. The following day the membranes were removed from the apparatus and kept wet in 0.1% PBST. In order to verify the efficiency of transfer, membranes were stained with 1:1000 Indian Ink/ 0.1% PBST for 10 minutes on a roller (until bands were visible) and rinsed with 0.1% PBST until the stain was clear. Blots were blocked in 5% non-fat dried milk diluted in 0.1% PBST for 1 hour on a roller at room temperature. Blots and were probed with primary antibody (detailed in Table 2.5), diluted in blocking solution (3% non-fat dried milk, 0.1% 20/PBST) overnight at 4°C. After three washes with 0.1% PBST, each for ten minutes, the blots were incubated in HRP-conjugated secondary antibodies in blocking solution (detailed in Table 2.6) for one hour at room temperature. Blots were subjected to three washes, each for 10 minutes with 0.1% PBST prior developing. Blots were developed in supersignal solution (1:1 luminol enhancer and peroxide) which is part of the supersignal west pico chemilluminescent substrate reagent and were visualised using BioRad FluoroS Multimager. SuperSignal West Femto Substrate was used to enable detection of low concentration proteins which were not visible with typical enhanced chemiluminescence (ECL) substrates.

Table 2.3 The concentration of resolving and stacking gels used for running proteins

Resolving gel	Stacking gel
40% Acrylamide-Bis	40% Acrylamide-Bis
Water	Water
1.5M Tris pH 8.8	0.5M Tris pH 6.8
10% SDS	10% SDS
10% Ammonium Persulphate (APS)	10% Ammonium Persulphate (APS)
TEMED	TEMED

Table 2.4 Description of Urea Lysis Buffer

Urea Lysis Buffer	Final concentration
Urea	7 M
Triton x-100	0.05%
NaCl	25 mM
HEPES pH 7.6	20 mM
DTT	100 mM

Table 2.5 Description of Primary Antibodies

Primary Antibodies	Application/Final concentration	Source
OCT4 (Sc-5279)	IF (1:100), 2 µg/ml – WB (1:500), 0.4 µg/µml	Santa Cruz
OCT4A/B (Ab19857)	IF (1:100), 0.05 µg/ml – WB (1:500), 0.002 µg/ml	Abcam
SOX2 (Ab5603)	IF (1:700) – WB (1:1500) (2 µg/ml)	Milliopore
CtBP1-E12 (sc-17759)	IF (1:250), 0.8 µg/ml	Santa Cruz
CtBP2 (612044)	IF (1:200), 1.25 µg/ml	BD biosciences
β-actin (A5060)	WB (1:10000), 1.4 µg/ml	Sigma
OCT4 (MAB1759)	IF (1:500), – WB (1:2000)	R&D systems
E-cadherin (610181)	WB 250 µg/ml	BD biosciences
SOX2 (MAB2018)	WB (1:1500)	R&D systems

Table 2.6 Description of Secondary Antibodies

Secondary Antibodies	Application/Final concentration	Source
Goat Anti-Rabbit, IgG, A11008	IF (1:700), 2.85 µg/ml	LifeTechnologies
Goat Anti-Mouse, IgG, A11029	IF (1:250), 8 µg/ml	Invitrogen
Sheep Anti-Mouse, IgG, NA931	WB (1:2000), 0.265 µg/ml	GE Healthcare
Goat Anti-Rabbit, IgG, P0449	WB (1:2000)	DAKO
Rabbit Anti-Rat, IgG, P0450	WB (1:2000)	DAKO
Goat Anti-Rat, IgG, A11081	IF (1:250), 8 µg/ml	Invitrogen

2.2.2.2 Immunofluorescence

Round glass coverslips (13 mm diameter) were sterilised in 70% ethanol prior to use. To maintain consistency, cells were fed the day before any experiment. Cells were plated onto coverslips for approximately 48 hours prior to experiments. Coverslips were transferred into 12 well plates and rinsed once with PBS. Cells were fixed with 4% paraformaldehyde (PFA) in PBS for 15 minutes at room temperature. After one wash with PBS, cells were incubated with 10 mM glycine in PBS to quench any remaining formaldehyde. Cells were permeabilised in 0.2% Triton X-100 in PBS for 10 minutes. To avoid non-specific binding, cells were blocked in 10% FCS in PBS for 30 minutes. Samples were then incubated with primary antibodies (listed in Table 5) in 0.6% bovine serum albumin (BSA) (fraction V, protease free, catalogue No 700-10-1P) in PBS, kept in a humidified container in the dark at room temperature for 90 minutes. After two washes with PBS, cells were incubated with fluorophore-conjugated secondary antibody (listed in table 2.6), in 0.6% BSA in PBS, with 1 μg/ml DAPI counterstain (4',6'-diamidino-2-phenylindole) in a humidified container in the dark for 60 minutes. Cells were washed twice with PBS and once with distilled water. Coverslips were mounted on a glass slide using fluorescent mounting medium (DAKO) and were kept in the dark overnight. Cells were visualised using an Olympus IX81 microscope and images were taken using an Orca-ER digital camera. All steps were performed at room temperature.

2.2.3 DNA-RNA analysis

2.2.3.1 Semi-quantitative reverse transcriptase polymerase chain reaction (RT-PCR)

RNA extraction: Total RNA was extracted using an RNase mini Kit (QIAGEN, catalogue No 74104) according to the manufacturer's instructions. DNaseI was added to the total RNA to eradicate contaminating genomic DNA. The nucleic acid concentration was measured using a thermo scientific-nanodrop-1000 and labtech software V3.6.0.

cDNA synthesis: Once the mRNA was isolated, complementary DNA (cDNA) was synthesized using the Reverse Transcription System (Promega) to reverse transcribe RNA into cDNA (Table 2.7). Deoxynucleotides (dNTPs), oligo dT primers, and reverse transcriptase (a DNA polymerase) was added to mRNA and allowed the polymerase to make cDNA. The mRNA was removed and the second strand of DNA was synthesised.

Table 2.7 Composition of cDNA master-mix

Reagents	Final Concentration (40 µl)
5× RT Buffer (mmlv)	**1×**
Oligo dT	**0.5 µg**
dATP	**0.25 mM**
dTTP	**0.25 mM**
dCTP	**0.25 mM**
dGTP	**0.25 mM**
MMLV RT	**150 unit**

PCR procedure: A master-mix containing all components except for DNA template and GoTaq polymerase was prepared in 0.5 ml PCR tubes for the reaction (Table 2.8). GoTaq polymerase was added during the initial denaturation step to minimise primer dimer formation. The necessary amount of cDNA was added to the mix to reach the final reaction volume. PCR conditions were; an initial denaturation of 94°C (180 seconds) followed by 35 cycles of denaturation at 94°C (30 seconds), annealing at 60°C (30 seconds), and extension at 72°C for 1 minute. The final extension was set at 72°C for 1 cycle (120 seconds). The PCR products were held at 4°C (Table 2.10). Different PCR primer sets and conditions are described in table 2.9 and 2.10 respectively.

Table 2.8 Description of PCR master-mix

Reagents	Final Concentration (50 µl)
5× Go Taq Buffer	1×
$MgCl_2$	1.5 mM
dATP	0.2 mM
dTTP	0.2 mM
dCTP	0.2 mM
dGTP	0.2 mM
Forward Primer	0.4 mM
Reverse Primer	0.4 mM
DNA template	25 ng
GoTaq DNA Polymerase	0.5 unit
Nuclease- free water	-

Table 2.9 List of PCR primer sets used in RT-PCR

RNA target	Sequence 5' → 3'
OCT4 full length	**CATGGCGGGACACCTGGCT** **CCTCAGTTTGAATGCATGGGAG**
OCT4A **Discriminate between isoforms A and B**	**CTTCTCGCCCCCTCCAGGT** **AAATAGAACCCCCAGGGTGAGC**
OCT4-PG1 (POU5F1B)	**AGGCCGATGTGGGGCTCAT** **CCAGAGTGATGACGGAGACT**
SOX2	**ACCTACATGAACGGCTCGC** **ACCTACATGAACGGCTCGC**
OAZ1	**GGCGAGGGAATAGTCAGAGG** **GGACTGGACGTTGAGAATCC**
β-actin	**CTCAGGAGGAGCAATGATCTTG** **CTGGGCATGGAGTCCTGTGG**

PCR programmes:

Table 2.10 PCR program for the housekeeping gene β-actin, OAZ1, and genes of interest OCT4, OCT4-PG1, and SOX2

PCR program for β-actin			
Steps	**Temperature (°C)**	**Time (sec)**	**Cycles**
Initial denaturation	**94**	**180**	**×1**
Denaturation	**94**	**30**	**×25**
Annealing	**64**	**30**	
Extension	**72**	**60**	
Final extension	**72**	**120**	**×1**
Hold	**4**	∞	**×1**

PCR program for OAZ1			
Steps	**Temperature (°C)**	**Time (sec)**	**Cycles**
Initial denaturation	**94**	**180**	**×1**
Denaturation	**94**	**60**	**×30**
Annealing	**58**	**60**	
Extension	**72**	**60**	
Final extension	**72**	**600**	
Hold	**4**	∞	

PCR program for OCT4, OCT4-PG1, and SOX2			
Steps	**Temperature (°C)**	**Time (sec)**	**Cycles**
Initial denaturation	**94**	**180**	**×1**
Denaturation	**94**	**30**	**×35**
Annealing	**60**	**30**	
Extension	**72**	**60**	
Final extension	**72**	**120**	
Hold	**4**	∞	

Agarose gel electrophoresis: A 2% agarose gel was prepared by heating 2 grams agarose powder in 100 ml Tris base, acetic acid and EDTA (1× TAE) buffer in the microwave. Red safe DNA stain (cat No 21141; 2.5 µl) was added to the solution to bind and visualise the DNA (with 302 nm UV light). The melted agarose solution was poured into the assembled casting tray with a well-comb added to the solution, and allowed to cool until solid. The gel was placed in the electrophoresis chamber, covered with TAE buffer and the comb was removed. Upon the completion of PCR run, 20 µl of each sample was added to 5 µl orange G and was run alongside a DNA ladder (10 µl of 100 and/or 1000 bp according to the PCR product size). PCR products were run for approximately one hour at 100 V. Amplicons of PCR reactions were separated on the 2% agarose gel according to their weight. The DNA was visualized and imaged using Gel Doc software (Bio Rad).

2.2.3.2 TaqMan® Real-Time polymerase chain reaction (qPCR)

To perform the qPCR reaction, total RNA was obtained from desired cell lines using the RNase mini Kit (QIAGEN) following the manufacturer's instructions. Extracted RNA was used for synthesizing cDNA as explained previously in section 2.2.3.1. For the housekeeping gene β-actin, a reaction mix consisting of TaqMan® Universal Master PCR Mix, 20× predesigned validated TaqMan β-actin probes (including forward and reverse primers), and nuclease- free water was added in duplicate to a 96-well PCR plate followed by 5 µl of cDNA (5 ng/µl) to reach the final reaction volume of 20 µl (Table 2.11). To prepare the reaction mix for the gene of interest, a universal master-mix containing a universal probe library set (04683633001 Roche), forward and reverse primer set (designed using Roche software), and nuclease- free water was added in duplicates to a 96-well PCR plate followed by 5 µl of cDNA (5 ng/µl) to reach the final reaction volume of 20 µl (Table 2.11). The plate was sealed to avoid contamination and was centrifuged at 3000 rpm for 1 minute at 4°C to remove any air bubbles. The 96-well plate was placed into a 7900 HT fast real time PCR system. As the PCR progresses, the number of cycles and detected fluorescence increases until the reporter dye signal is sufficiently high to cross a threshold value and is visible above the background, known as the cycle threshold (Ct) value (linear part of the curve). To acquire the relative expression of the target gene in different samples, the abundance of the mRNA of interest was normalized relative to the β-actin housekeeping gene (Applied Biosystems 4326315E-1307025) and was calculated using the ΔΔCt method as follows.

$\Delta Ct = \bar{x}$ Ct (gene of interest) - $\bar{x}$ Ct (housekeeping gene)

$\Delta\Delta Ct = \Delta Ct$ sample 1 – ΔCt calibrator (a sample that all other samples are compared to)

Table 2.11 Description of reaction mix for qPCR

Housekeeping Gene (β-actin)	**Gene of interest (SOX2)**
Reagent	**Reagent**
Universal qPCR mix (2×)	**Universal master-mix**
Probe (20×)	**Probe (10 µM)**
cDNA (5 ng)	**cDNA (5 ng)**
Nuclease- free water	**Reverse Primer (10 µM)**
-	**Forward Primer (10 µM)**
-	**Nuclease- free water**

2.2.4 Mammosphere formation assay

All breast cancer cell lines were cultured in DMEM which was used for routine cell culture, supplemented with 25 mM glucose and/or 10 mM fructose. These concentrations were used for the following reasons:

Since cancer cells prevalently consume more glucose, culturing cancer cells *in vitro* within physiological glucose levels (i.e. around 4-5 mM) would result in severely low glucose conditions and an associated energy crisis. Consequently, culturing in 25 mM glucose provides cancer cells with adequate glucose to proliferate and survive in the laboratory system without requiring a frequent change of media. To develop a glucose restricted condition, fructose was chosen as a favourable substrate to replace glucose as it is utilised almost 100 times slower than glucose, and hence specifically lowers the glycolytic pathway. 10 mM fructose approximately provides a physiological equivalent of low glucose conditions where cells maintain proliferation and growth, yet without much dependency on glucose.

To provide non-adherent plates, 12 well-plates were coated with 350 µl of 12 mg/ml polyhema (2-hydroxyethyl methacrylate) per well for 48 hours at 40°C in a dry incubator. Cells were trypsinised and detached at 70-80% confluency and were centrifuged at 900 g for five minutes. Supernatant was removed and cells were re-suspended in 2 ml cold HBSS. Single cell suspensions were cultured in conditioned medium at a density of 5000 cells per well on a 12 well-plate dish coated with polyhema in triplicate and were induced to form spheres. Media from the 2D culture, to a confluence of 70-80%, was used as conditioned media for mammosphere formation (media was changed one day prior to collection). Plates were placed in a humidified incubator at 37°C in 10% CO_2 for five days without being disturbed and changing media. Cells which were able to survive and proliferate in such conditions and formed distinct clusters of cells termed mammospheres. After the culture period, the number of mammospheres ≥50 µm in diameter were counted at 20X magnification using an Olympus IX81 microscope fitted with a graticule (G23 Thompson 24 mm, order number 01A24056). The eyepiece graticule allowed the size of a mammosphere to be measured more accurately. Images were taken using an Orca-ER digital camera (Figure 2.2).

Mammosphere forming efficiency (MFE%) was calculated using the following equation:

MFE (%) = (Number of mammospheres per well ÷ number of cells seeded per well) × 100

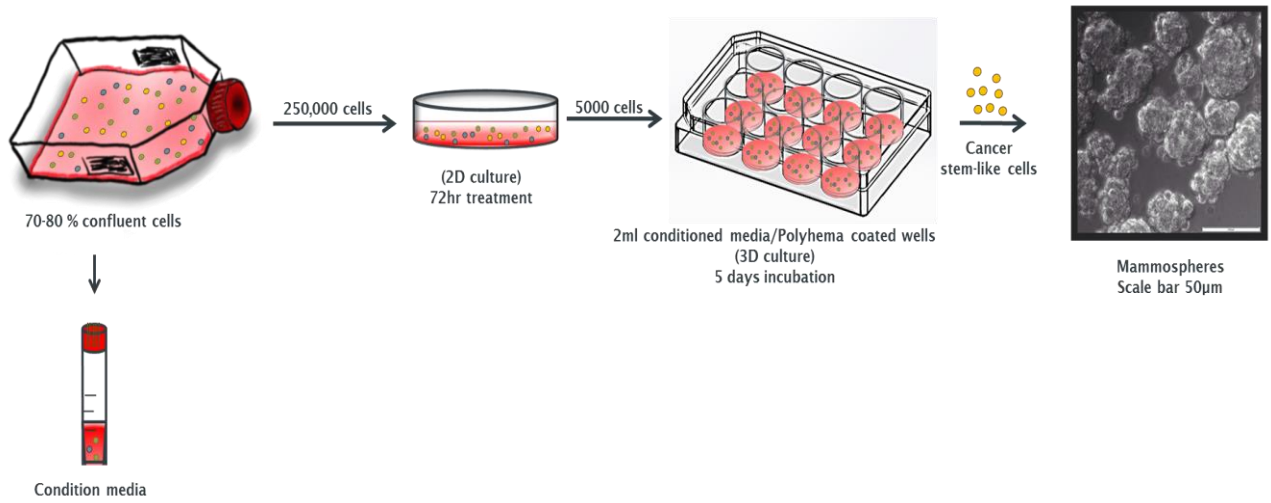

Figure 2.2 Mammosphere formation assay. MCF-7 cells have been cultured in 2D culture for a period of time suitable for cells to reach to a confluence of 70-80%. The media was collected to be used as mammosphere media which was proven to be an effective nutrition to enrich cancer stem-like cells. For this assay, to provide a non-adherent condition (3D), 12 well-plates were coated with Polyhema. 5000 cells were cultured in conditioned media for 5 days to form mammospheres. Mammospheres ≥50 µm was counted under the microscope and MFE was evaluated in the population as the number of counted spheres divided by the original number of single cells seeded and was expressed as a percentage. In the matter of treatments, cells were seeded at a density of 250,000 cells per 60 mm dish and left for 72 hours prior plating for mammosphere formation.

2.3 Statistical analysis

Unless it stated otherwise, all data were obtained from three biological repeat experiments, each consisting of technical triplicates and were shown as means ± SEM. Two-tailed Student's t-test was used to assess the difference between two groups. $p<0.05$ was considered to be statistically significant. Statistical analysis was performed using GraphPad Prism software by one-way analysis of variance (ANOVA).

Chapter 3

Mammospheres, as a model system for identification of human breast cancer stem-like cells

3.1 Introduction

The cancer stem cell model is supported by the hypothesis that only a specific subset of cancer cells within the tumour hold stem-like properties such as self-renewal and tumorigenicity suggesting their involvement in carcinogenesis from tumour initiation to a metastatic state (175). Current conventional therapies are based on eliminating more differentiated cancer cells, while development of more effective therapeutics may actually entail targeting CSLCs with specific metabolic phenotypes (176). An optimum method to investigate human cancer *in vitro* is essentially reliant on the use of established culture environments that resemble *in vivo*-like growth conditions. Studying cell biology in 2D systems has substantial limitations. The plastic surface of 2D cell culture provides an unnatural state for cells to grow and spread which in turn causes irregular cell attachments to proteins and other cells in the culture (91). To reduce the drawbacks of 2D culture, development of new cell culture environments was required to closely simulate the multicellular tumour microenvironment.

3D construction profits from certain properties that distinguish mammospheres from 2D culture. Due to the cellular heterogeneity of cells developing in 3D, they better resemble tumours and more closely mimic native *in vivo* biological properties (91). The stem-like cells of the 2D cell population are able to form multi-layers of cells when cultured under 3D conditions (177). The most widely used *in vitro* assay for mammary cells to enrich and identify CSLCs is the mammosphere assay (125). The non-adherent 3D spherical clusters of the breast cancer cells or mammary cells are known as mammospheres. Mammospheres express different markers presenting tumorigenic phenotypes. Taking this into account, the mammosphere assay was chosen as a suitable tool to measure the proportion of cells in a 2D culture that have stem-like characteristics.

3.1.1 The effects of reprogramming metabolism on breast cancer stem cells

In healthy cells glucose contributes to energy metabolism through glycolysis by converting to pyruvate and then lactate. Pyruvate enters mitochondria to be further metabolized in TCA and OXPHOS; whereas in cancer cells glucose predominantly participates in lactate production through a high rate of glycolysis (135). It has been shown that in addition to cancer cells, stem cells also rely on glycolysis (135). Similar to normal stem cells, CSLCs also exhibit glycolytic phenotypes with an overexpression of most glycolytic enzymes. The glucose transporters, LDH, and oncogene c-Myc are

upregulated in hypoxia, and regularly overexpressed in CSLCs which divert glucose from oxidative metabolism to glycolysis showing the high glycolytic activity of CSLCs (135). High glycolytic cancer cells are more affected in conditions with reduced or no glucose available. To examine the role of glycolysis in bCSLCs and to measure the ability of mammosphere formation in different growth conditions, a model system was required where glycolysis could be stably manipulated; a cell line model of glycolytic vs. less-glycolytic states was developed. It was hypothesised that removing glucose form the media could affect the cell survival and reduce the mammosphere formation. Moreover, it was predicted that addition of glucose to the fructose media might increase glucose uptake by cells and lead them to revert to a higher glycolytic state from being less glycolytic. Therefore, to assess the capability of breast cancer cells to re-adapt to glucose, glucose was added to the media containing fructose and cells were adapted to this condition prior to experiments.

3.1.2 Aims

The specific aims of this chapter are:

- To isolate small number of cells that can recapitulate breast tumour and to assess the ability of breast cancer cells to form mammospheres for the purpose of isolating mammary stem cells.
- To evaluate the ability of breast cancer cells to grow in low glycolytic conditions, and to see whether they are capable of re-adapting to glucose
- To investigate the effect of restricted glycolysis in breast cancer stem cell population

3.1.3 Experimental outline

It is possible that not all subtypes of breast cancer behave equally; therefore, multiple breast cancer cell lines representative of various subtypes were used in this experimental model; MDA-MB-231 (ER^-), SkBr-3 (ER^-), MCF-7 (ER^+), and T-47D (ER^+). MCF-7 cell line was used throughout the thesis due to its high ability to form robust and structured mammospheres.

In the cell line model of glycolytic vs. less-glycolytic, glucose was removed from the media and fructose was used as an alternative substrate. Fructose was used as it is taken

up slowly, before entering glycolysis (178). Glucose-containing media was chosen as a standard control condition (corresponding control). For adaptation, MCF-7 cells were cultured and adapted in DMEM supplemented with 10 mM fructose in the absence of glucose and cells treated with media containing 25 mM glucose were used as a control. Approximately three weeks were required for cells to develop fructose adaption. During the initial adaptation, fructose adapted cells were proliferating at a lower rate compared with the corresponding control cells (Figure 3.4). However, the rate of proliferation became more similar for both groups as fructose adaption developed.

Following adaptation, cells were detached, counted and diluted in conditioned medium before plating. According to established methods, single cell suspensions were then seeded at a cellular density of 5000 cells per well in polyhema-coated 12-well plates and allowed to form mammospheres. Spheres ≥50 μm were counted on day five (125). The non-adherent conditions prevent cells from attaching to the surface and differentiating; therefore, allowing the stem or progenitor cells to self-renew, whilst the bulk population die by anoikis. Media from the 2D cultures (being kept for long enough to be suitable for cells to reach a confluence of 70-80%) was proven to be an effective condition to enrich CSLCs (125). Hence, it was used in this experimental model as conditioned media. This work focused on optimising a 3D culture protocol with a well-known breast cancer cell line (MCF-7 cells).

3.1.4 Results

3.1.4.1 Morphology of breast cancer cell lines

In order to confirm whether different subtypes of breast cancer display distinctive morphological features, various breast cancer cell lines were cultured and phase contrast images taken (Figure 3.1). Epithelial cell lines like MCF-7 maintained spherical cell morphology and tightly cohesive structures displaying robust cell–cell adhesions (Figure 3.1, A) similar to that of T-47D (Figure 3.1, B). More aggressive basal-like breast cancer cell lines such as SkBr-3 had a rounded structure (Figure 3.1, C) while MDA-MB-231 displayed elongated and spindly appearance; more like fibroblast structure (Figure 3.1, D). The morphology of different subtypes were similar to those previously reported (179).

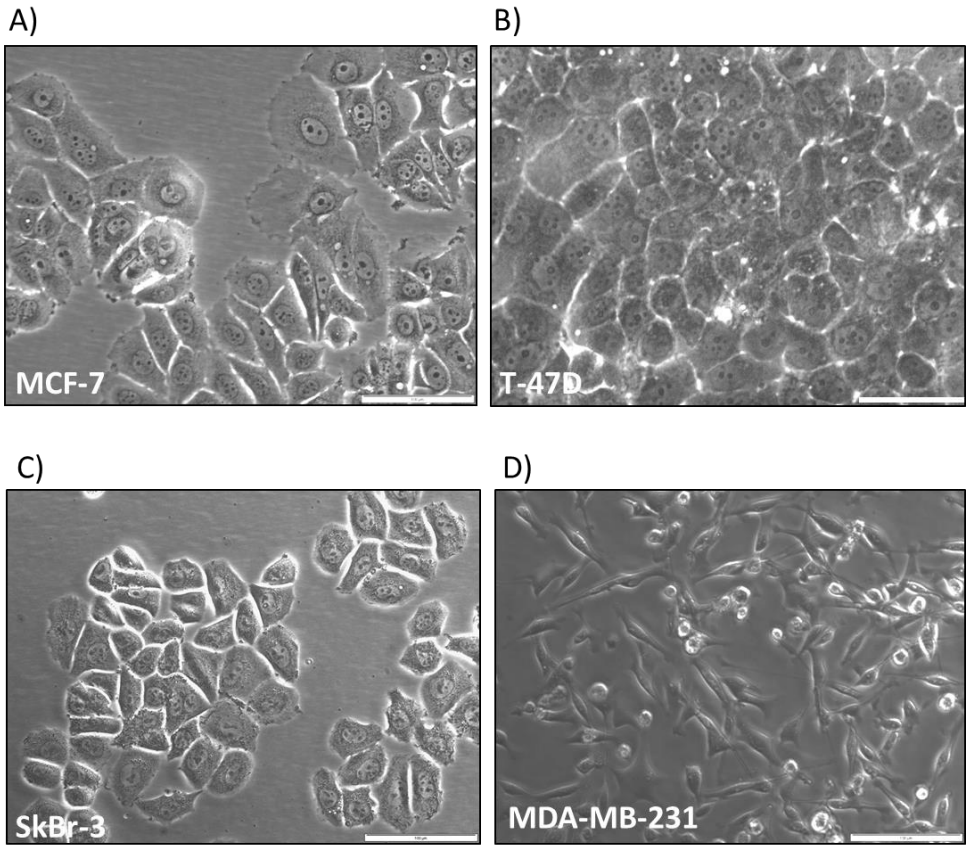

Figure 3.1 Representative phase contrast images of various subtypes of breast cancer cell lines. Cells were plated at sub-confluent density allowed to grow for 48 hours prior to imaging. **(**A) MCF-7. (B) T-47D. (C) SkBr-3. (D) MDA-MB-231. Scale bar shows 100 µm.

3.1.4.2 Optimisation of mammosphere cultures of human breast cancer cell lines

To determine the growth ability of breast carcinoma cells in non-adherent conditions and to measure the proportion of cells in the 2D cultures with stem-like properties, the mammosphere assay was performed as previously described. There were morphological differences and variations in the size and shape of mammospheres generated from various breast cancer subtypes. Therefore, four human breast cancer cell lines were selected to represent the major molecular subtypes of breast cancer. MCF-7 (Figure 3.2A) and T-47D (Figure 3.2B) formed more solid, rounded and defined spheroid shapes with tightly cohesive phenotype. SkBr-3 formed loose bunch of grape-like clumps of cells (Figure 3.2C) and MDA-MB-231 presented small structures (<50 µm) (white arrow) and single cells (black arrow) (Figure 3.2D). Since determining the number of mammospheres ≥50 µm was the main objective of this part of the project, luminal cell lines MCF-7 and T-47D, which displayed a better structural shape, were chosen as a model for our experiments.

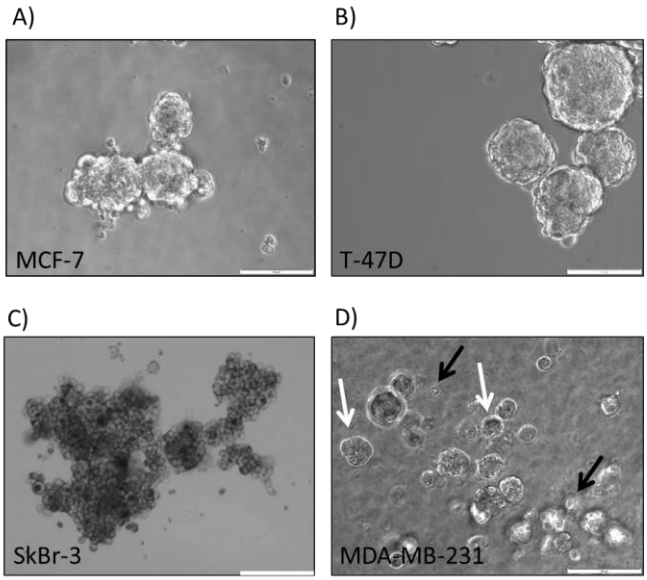

Figure 3.2 Representative images of human breast cancer cell lines mammospheres in 3D culture. 5000 cells were plated in polyhema-coated 12-well plates and then imaged on day 5. (A) MCF-7. (B) T-47D. (C) SkBr-3. (D) MDA-MB-231. White arrows represent small structures and black arrows show single cells. Scale bar shows 100 µm.

3.1.4.2.1 Optimisation of factors to consider for mammosphere assay

It is critical to establish consistency within methods to ensure mammosphere forming efficiency (MFE) remains constant between experiments. Therefore the following factors must be considered to ensure assay consistency.

3.1.4.2.1.1 Cell number

In order to determine the appropriate cell number for the mammosphere assay, MCF-7 cells were seeded at different densities; 5000, 10,000, 25,000, and 100,000 cells per 6-well plates under mammosphere culture conditions and the MFE was calculated. In this experiment 5000 cells gave 0.99% MFE; 10,000 cells 1.2% MFE; 25,000 cells resulted in 0.19% MFE, and 100,000 cells gave 0.31% MFE (Table 3.1).

Table 3.1 Mammosphere forming efficiency (MFE) depends on number of cells plated in 6 well plate

Cells seeded in 3D culture	**MFE (%) in 3D culture**
5000	**0.99**
10,000	**1.2**
25,000	**0.19**
100,000	**0.31**

As the results show, multiplying the number of cells by a factor did not increase the MFE by the same ratio. The number of cells seeded did not determine the number of mammospheres obtained. Moreover, with higher cell densities, more mammosphere congestion was observed which caused difficulty in counting (Figure 3.3). According to the obtained results, the optimum density will be one which is high enough to generate an adequate number of mammospheres, yet not so high as to result in aggregation. Out of different cell numbers, mammospheres generated from approximately 5000 to 10,000 cells presented the best possible proportion and spherical structures.

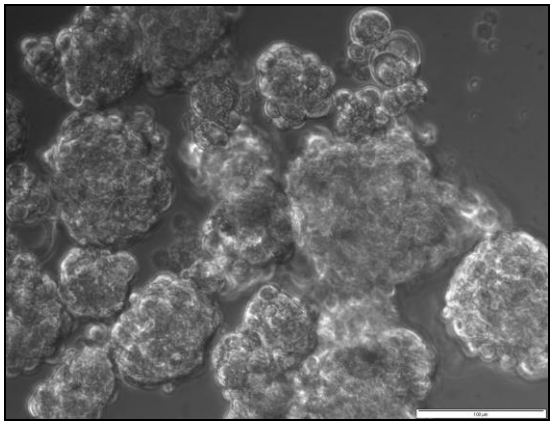

Figure 3.3 Representative image of MCF-7 mammosphere. 100,000 cells were plated in polyhema-coated 12-well plates and then imaged on day five. Scale bar shows 100 µm.

3.1.4.2.1.2 Cell culture plates

It is important to select the appropriate culture plates for mammosphere assays; for this reason, wells with the same diameter as the microscope field of view were considered ideal. This minimises the visual error when counting the mammospheres in the field. Therefore, 12-well plates were selected as the best option for this assay. Based on the results from Table 3.1, 5000 was chosen as the optimum cell number.

3.1.4.2.1.3 Eyepiece graticule

The main factor that needed to be considered in the assay was evaluating the number of spheres ≥50 µm in diameter. Therefore, another objective to consider was to calibrate an appropriate eyepiece graticule for the microscope to allow the accurate measurement of the diameter of mammospheres.

Taking everything into account, 5000 cells and 12-well plates coated with polyhema were taken together with a G23 Thompson 24 mm graticule as optimal for the mammosphere assay throughout the entire experiments.

3.1.4.2.2 Fructose adaption of breast cancer cell lines

3.1.4.2.2.1 Impact of fructose adaption on the growth rate of MCF-7 cells

To investigate whether fructose was an adequate nutrient for MCF-7 cells to grow in the absence of glucose, cells were cultured in separate conditions: standard medium including glucose, or medium containing fructose independent of glucose. Under both conditions, MCF-7 cells appeared morphologically similar (Figure 3.4). Moreover, observation of the cultures suggested a slower growth rate under fructose conditions during adaptation (Figure 3.4). Therefore, the growth rate was quantified formally using cell counts (Figure 3.5).

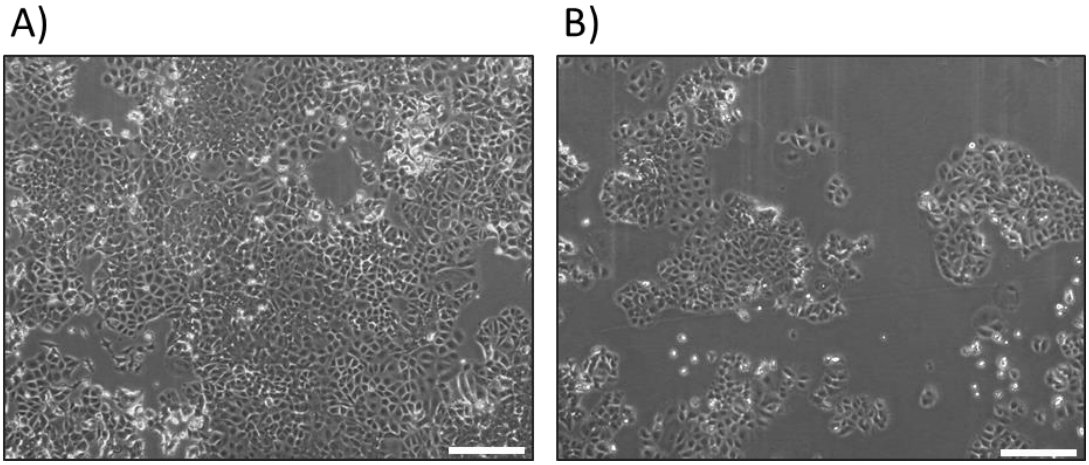

Figure 3.4 Representative phase contrast images of MCF-7. MCF-7 cells were exposed to either 25 mM glucose (A) or in the absence of glucose and the presence of 10 mM fructose (B), approximately for 2-3 weeks for adaptation. Scale bar shows 20 μm.

Having adapted the cells to either glucose or fructose for approximately 2-3 weeks, further experiments were done on the adapted cultures. Adapted cultures were frozen down into the multiple vials and used as stocks for future experiments.

To compare the proliferation rate under fructose and glucose conditions, MCF-7 cells were seeded at an initial density of 50,000 cells per well in 6-well plates in duplicate, two and five weeks after thawing. Cells were counted daily, using a haemocytometer for four consecutive days. Fresh media was added to the cells on day three.

Two weeks adaptation: during the first two days of the assay, fructose adapted cells maintained a lower growth rate compared with cells under glucose conditions which aligned with the initial hypothesis that cancer cells struggle in conditions with reduced or low glucose availability. Surprisingly by day three, the growth rate had risen considerably under fructose conditions; (could possibly be due to high ability of cancer cells to adapt to unusual conditions) while under glucose conditions, the growth rate raised steadily during the four days (Figure 3.5A).

Five weeks adaptation: Under both conditions (fructose and glucose), the growth rates followed a similar pattern (cancer cells in glycolytic restriction condition, were already adapted to the new condition and adjusted their growth rate similar to that of glycolytic cells) and had risen gradually until the fourth day where the increase was the greatest for the fructose adapted cells (Figure 3.5B).

Results demonstrating that following fructose adaptation, MCF-7 cells were not dependent on glucose to grow as long as they had sufficient sugar (fructose).

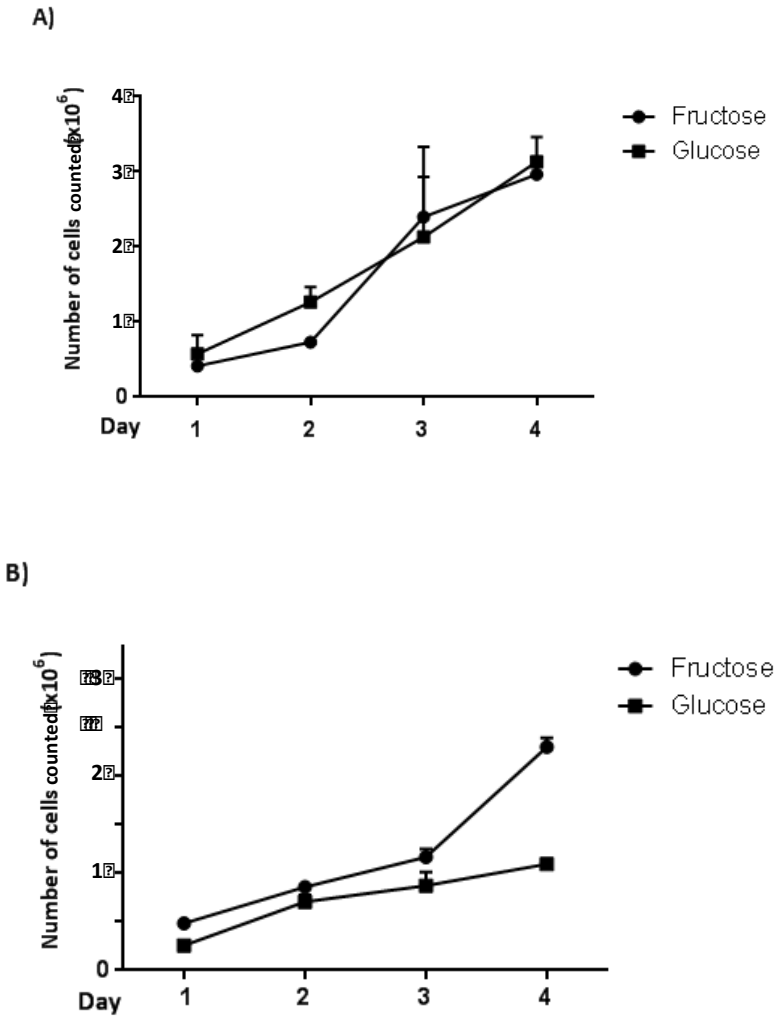

Figure 3.5 Representative graph of MCF-7 growth rate following fructose adaptation. MCF-7 cells adapted to grow in either 25 mM glucose or 10 mM fructose for two weeks (A) and ~ five weeks prior to starting the assay (B). Cells were counted on each day for four consecutive days. Results are presented as mean ± standard error of the mean (SEM).

3.1.4.2.2.2 Optimisation of MFE in MCF-7 cells following fructose adaptation

To investigate the effect of reducing glycolysis (replacing glucose with fructose in the media) on the mammosphere forming ability, previously adapted MCF-7 cells were cultured in media containing either fructose or glucose. Conditioned media were taken from both sets of cultures and put back on the cells in 3D culture relevant to the designed conditions (Table 3.2, conditions 1 and 2).

Table 3.2 Representative conditions of MCF-7 cell in 2D and 3D conditions

Condition	Media in the 2D culture	Media in the 3D culture
1	25 mM Glucose	25 mM Glucose
2	10 mM Fructose	10 mM Fructose
3	10 mM Fructose	25 mM Glucose
4 (Figure 3.8 only)	Fructose + Glucose	Fructose + Glucose

Mammospheres formed under both conditions and displayed similar morphology regardless of their culture adaptations. However, compared with mammospheres in glucose culture, under fructose conditions, mammospheres appeared larger (Figure 3.6).

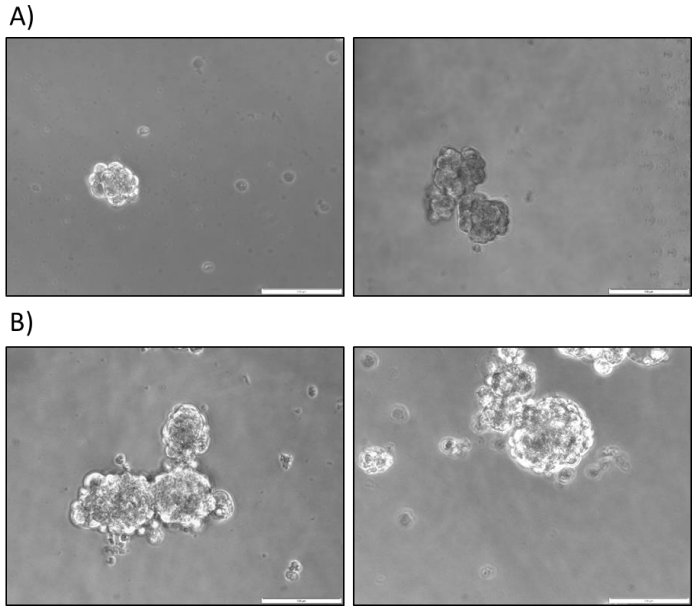

Figure 3.6 Representative images of MCF-7 mammospheres in 3D culture. 5000 cells were plated in polyhema-coated plates and then imaged on day five. (A) Glucose adapted MCF-7 cells in glucose conditioned medium. (B) Fructose adapted MCF-7 cells in fructose conditioned medium. Scale bar shows 100 µm.

Since the main aim of performing the mammosphere assay was to measure the number of stem cells in 2D population, it was important to keep the culture conditions of the mammospheres the same between 2D and 3D cultures. Therefore, the third condition used was mammospheres forming from fructose adapted cells grown in the same media as the corresponding control (Table 3.2, conditions 1 and 3).

3.5% MFE was obtained under standard glucose conditions (condition 1). Surprisingly, under fructose conditions (condition 2) MFE significantly increased by ~1.6 fold to 6%. This significant increase under fructose conditions was consistent through all experiments over the entire duration of thesis (Figure 3.7).

Under glucose conditions in 3D culture (condition 3), fructose adapted cells formed ~1.4 fold more mammospheres with a MFE of ~5% compared with glycolytic cells and no significant difference was observed between conditions 2 and 3. Results confirmed that the presence of fructose in the conditioned media was not the reason behind this significant increase in MFE. Therefore, it was necessary to have the 3rd condition

(condition 3). Results confirmed that the difference was caused by the fructose in the 2D culture where cells were adapted. Having shown that both fructose adaptation conditions (Table 3.2, conditions 2 and 3) represented higher MFE than the corresponding control (Table 3.2, condition 1) the third condition was considered unnecessary in the future experiments (Figure 3.7).

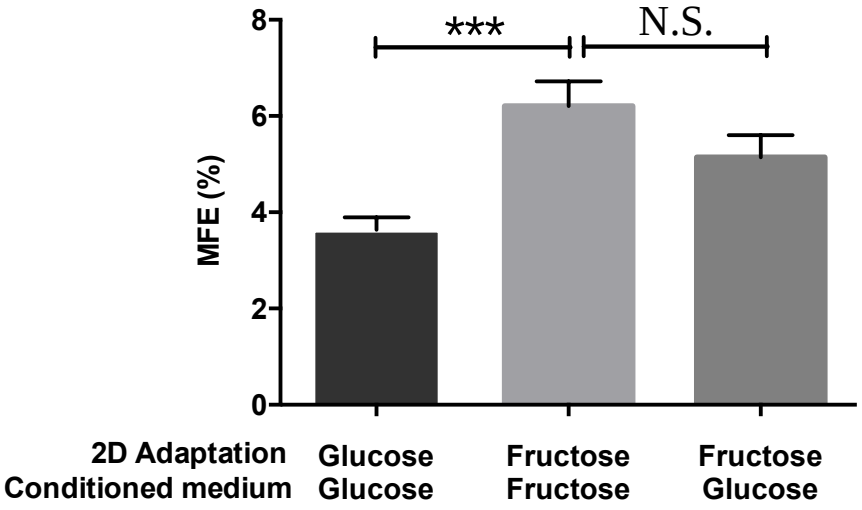

Figure 3.7 Representative graph of MFE (%) of MCF-7 cells adapted in different conditions. 25 mM glucose was replaced with 10 mM fructose in the media and MCF-7 cells were adapted for 30 days to this condition prior to mammosphere formation. MCF-7 cells were plated at an initial density of 5000 cells per well in non-adherent culture for 5 days to form mammospheres. Spheres ≥50 μm were counted. The graph shows a combination of three independent experiments, each of which was performed in triplicate. Results are presented as mean ± standard error of the mean (SEM). *** $P \leq 0.001$**.** n=3

To investigate whether adding glucose to fructose cultured cells could reverse the growth rate back to the more glycolytic state; initially, MCF-7 cells were counted and plated at a same initial plating density. Subsequently, glucose was added to the media containing fructose in the 2D culture and cells were adapted to all three conditions for approximately two weeks. Phase contrast images were taken on day sixteen of adaptation (Figure 3.8, A, B, and C).

Following two weeks adaptation, cells were seeded at the same initial plating density of 250,000 cells per 60 mm dishes and left for 48 hours prior counting. Fructose adapted cells that were re-adapted to fructose and glucose (Figure 3.8C) appeared morphologically similar to the other two conditions (Figure 3.8, A and B). Under fructose conditions, cells displayed a slower growth rate during the initial phase of adaptation compared with glucose adapted cells (Figure 3.8D). However, adding glucose

to the media containing fructose, the growth rate displayed an increased trend which can be possibly explained by the fact that fructose and glucose together could provide a better energy source and increase the growth rate.

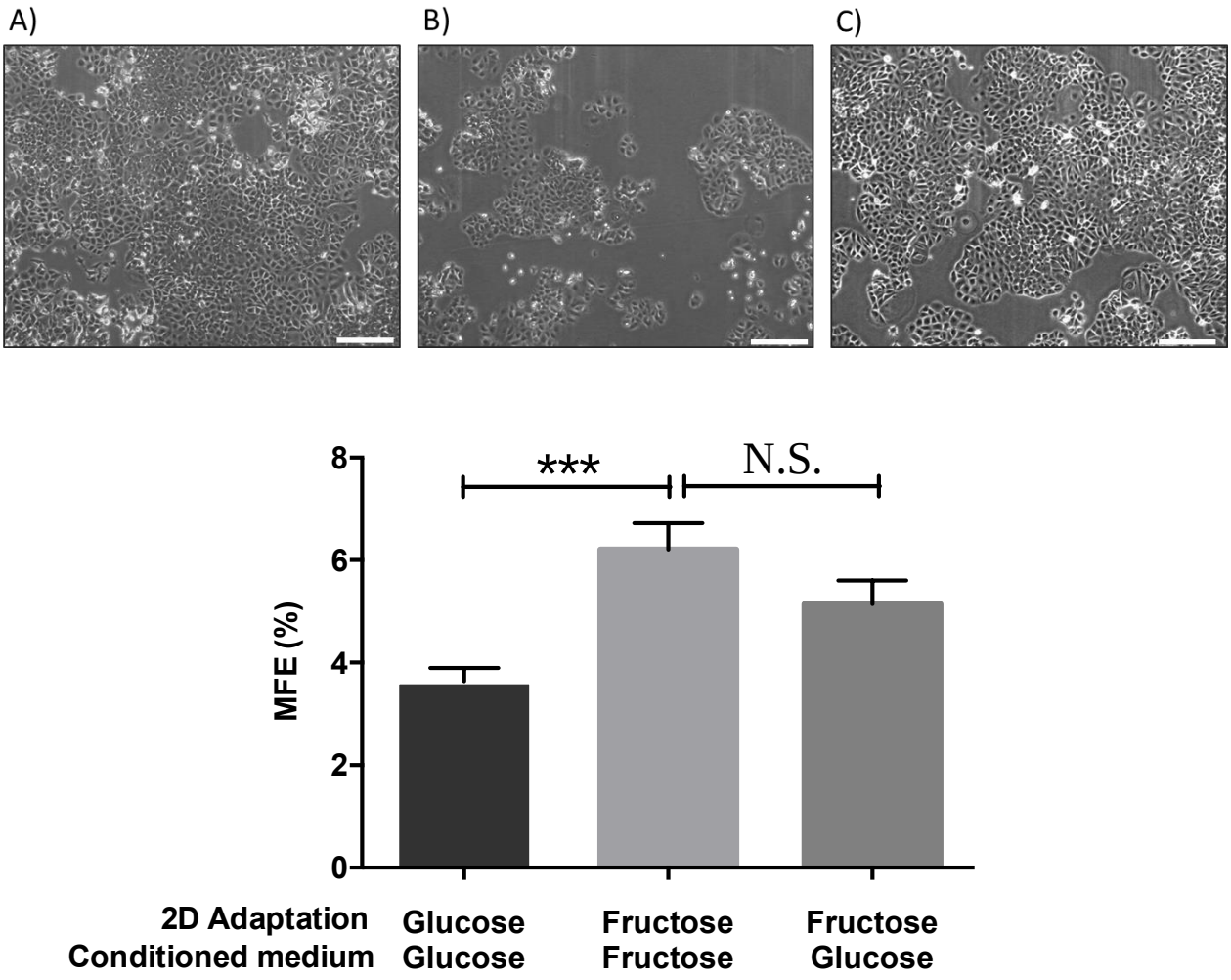

Figure 3.8 Representative phase contrast images and 2D cell count of MCF-7 cells under different culture conditions. MCF-7 cells adapted to grow in either 25 mM glucose (A) or 10 mM fructose (B) as previously shown in Figure 4. Under 2D conditions, 25 mM glucose was added to the fructose media and cells were allowed to adapt to this condition for two weeks (C). Following two weeks adaptation, cells were seeded at same initial plating density of 250,000 cells per 60 mm dishes and left for 48 hours prior counting. The graph shows a combination of three independent experiments (D). Results are presented as mean ± SEM. Scale bar shows 20 µm.

Following adaptation to all three conditions in 2D culture, MCF-7 cells were seeded at a density of 5000 cells per 12-well in polyhema-coated plates and were allowed to form mammospheres. Following five days under mammosphere culture conditions, MFE was calculated. Consistent with the previous data (Figure 3.7), MFE was significantly higher under fructose conditions compared with the corresponding control by ~1.2 fold increase (Figure 3.9, middle bar). Contrary to the hypothesis that the addition of glucose back to the media including fructose (Table 3.2, condition 4) may increase the glycolytic state of fructose adapted cells, findings showed that not only did this alteration not reduce the MFE to the same level as that of glucose adapted cells, it also significantly increased it (~1.3 fold) with respect to the corresponding control group (Figure 3.9, right bar). The increase in MFE following the addition of glucose was not significant between the two groups (Figure 3.9, middle and right bar).

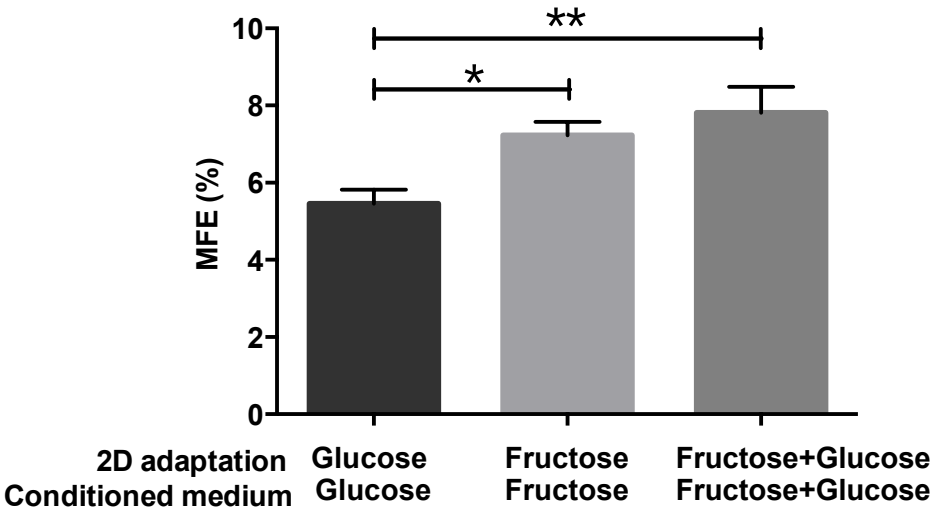

Figure 3.9 Representative graph of MFE (%) from MCF-7 cells under different culture conditions. MCF-7 cells adapted to grow in either 25 mM glucose or 10 mM fructose. Under 2D conditions, 25 mM glucose was added to the fructose media and cells were allowed to adapt to this condition for two weeks. MCF-7 cells were counted and seeded at density of 5000 cells per well in polyhema-coated 12-well plates for five days. Spheres ≥50 μm were counted. The graph shows a combined of three independent experiments, each of which was performed in triplicates. Results are presented as mean ± SEM. * $P \leq 0.05$, ** $P \leq 0.01$. n=3

3.1.4.2.2.3 Optimisation of fructose adaptation in T-47D cells

The unexpected increase in MFE in MCF-7 cells under fructose conditions was intriguing. To further investigate whether the fructose response was common among other breast cancer cell lines. T-47D cells were adapted to either 25 mM glucose or 10 mM fructose as previously described. Following adaptation, cells were plated at a same initial plating density of 250,000 cells per 60 mm dishes and counted after 48 hours. The growth rate was calculated in both conditions. Unlike MCF-7 cells, T-47D cells did not adapt to fructose conditions by not reaching to the similar growth rate of glucose adapted cells. When glucose was eliminated from the medium, cell proliferation slowed significantly compared with the control group. T-47D cells proliferated at higher rates under glucose conditions compared with fructose adapted cells (Figure 3.10).

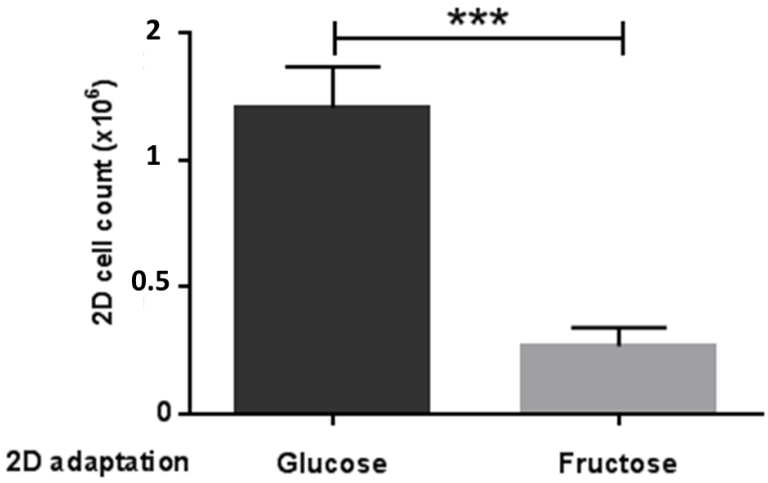

Figure 3.10 Representative of 2D cell count of T-47D cells in different conditions. T-47D cells adapted to grow in either 25 mM glucose or 10 mM fructose for three weeks. Following three weeks adaptation, cells were seeded at same initial plating density of 250,000 cells per 60 mm dishes and left for 48 hours prior counting. The graph shows a combined of three independent experiments. Results are presented as mean ± SEM. *** P≤ 0.001. n=3

Previously adapted T-47D cells were plated in non-adherent cultures (5000 cells per well) and allowed to form mammospheres. Results from counting mammospheres after five days showed no significant difference in MFE between glucose and fructose adapted cells. Although MCF-7 cells favoured fructose over glucose in forming larger and more mammospheres (Figure 3.6 and 3.7) in T-47D cells, MFE was not affected by fructose adaptation in this cell population (Figure 3.11).

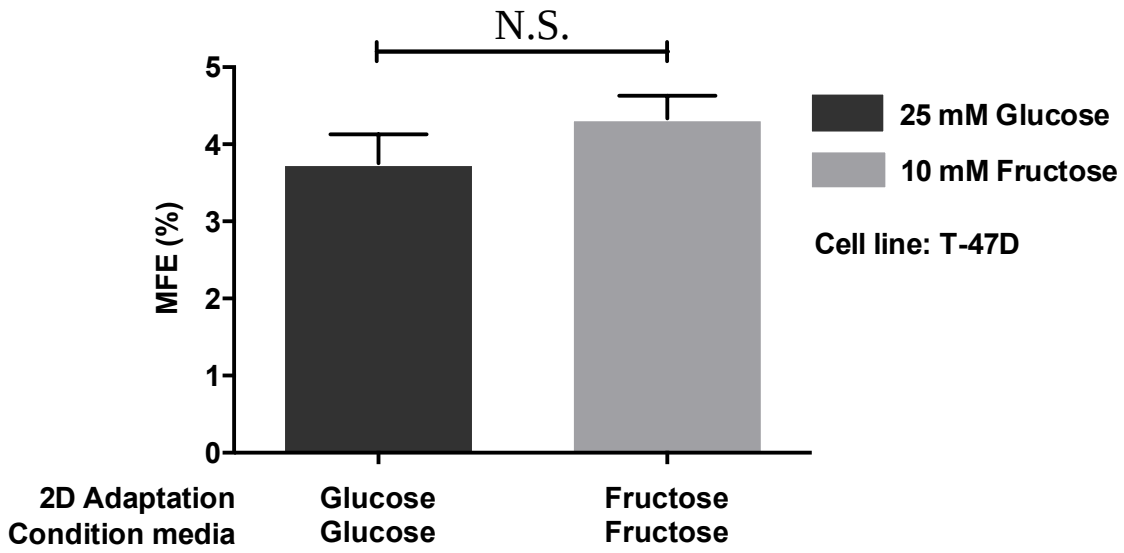

Figure 3.11 Representative graph of MFE (%) from T-47D cells under fructose conditions. T-47D cells adapted to grow in either 25 mM glucose or 10 mM fructose approximately for three weeks prior to mammosphere formation. T-47D cells were plated at an initial density of 5000 cells per well in polyhema-coated 12-well plates for 5 days to form mammospheres. Spheres ≥50 μm was counted at day five. The graph shows a combination of three independent experiments, each of which was performed in triplicate. Results are presented as mean ± SEM.

3.1.5 Discussion

Metabolism is fundamental in cellular homeostasis. Our knowledge about cancer cells displaying the glycolytic phenotype is growing day by day. Cancer scientists have long known that tumours participate in an altered metabolism. Similar to cancer cells, ES cells express the aerobic glycolytic phenotype (135). In accordance with published data, this high glycolytic phenotype is shared between several immortalized cells including cancer cells (135).

Cancer cells alter their metabolism and increase their uptake of glucose which facilitates rapid tumour growth. They also use glucose to fight against programmed cell death (apoptosis) (180). Therefore, a glucose restricted condition is an attractive approach for cancer treatment, aiming to inhibit proliferation and eliminate tumours. The truth is not quite this simple as cancer cells can utilise alternative energy sources. Furthermore, a rare population of cells within tumour, CSLCs, display phenotypical and functional features of stem-like cells with tumour initiating and mammosphere forming abilities. It was therefore important to investigate whether glucose starvation could impact the growth efficiency of this small population.

Fructose and glucose are two similar monosaccharaides contributing evenly to aerobic glycolysis and TCA cycle. However, according to Haibo *et al*. (181) cancer cells metabolise fructose and glucose through different metabolic pathways. They also reported that fructose makes a bigger contribution to nucleic acid synthesis than glucose and that cancer cells favour fructose over glucose to facilitate increased proliferative capacity, well known as a hallmark of cancer (181). Results from Haibo *et al*. (181) led us to study glycolytic vs. low-glycolytic (glucose restricted condition) environments for breast cancer cells by adapting them to fructose in the absence of glucose. Introducing fructose to the growth medium surprisingly increased the growth rate in MCF-7 breast cancer cells and enabled them to proliferate more efficiently in the absence of glucose. The fructose-containing medium proved to be preferred over glucose in MCF-7 cells. Subsequent experiments were performed to optimise the mammosphere forming ability under both glycolytic conditions.

With the growing evidence that cells holding stem-like properties are involved in tumour recurrence and metastasis of breast cancer (182), it was important to this project to use methodological approaches to specifically enrich for cancer stem cells. It was shown by

Dontu *et al*. (100) that cancer cells with stem-like characteristics are greatly enriched in mammospheres. Mammospheres have been shown to express OCT4 and display a high tumorigenic capacity in NOD/SCID mice. However, it may be that the mammosphere assay might not detect all quiescent stem cells (123). Though, in agreement with the principles described in this project (125), the mammsophere assay is still considered a valuable tool for the quantification of breast stem cells and therefore was used in this project as a reporter of cancer stem cell activity.

Mammospheres with different morphologies could be formed from various subtypes of breast cancer cell lines MCF-7, T-47D, MDA-MB-231, and SkBr-3. MCF-7 and T-47D cells formed more robust rounded mammospheres compared with those in basal-like cells which was consistent with the literature (124) (125) (183). Surprisingly, fructose cultured MCF-7 cells formed a higher number of larger mammospheres compared with those adapted to glucose conditions, suggesting that MCF-7 cells were more likely to display stemness properties in the presence of fructose. Here, a question arises regarding fructose adapted cells being able to revert to a glycolytic state in terms of mammosphere forming ability by adding glucose back into their growth media. Despite what was hypothesised, MCF-7 cells that were adapted to fructose were not able to use glucose and re-adapt in the presence of fructose. This observation was supported by the MFE obtained from MCF-7 cells under different conditions (Figure 3.9). The addition of glucose to the fructose-containing media may underlie the increase in MFE levels. This may have been due to better growth conditions as more sugar was present for metabolic consumption by cancer stem cells. In a different cell line (T-47D) which formed tightly rounded mammospheres in both glycolytic conditions, fructose presence did not equate to a higher MFE than their corresponding control group. It is worth mentioning that T-47D cells were not able to adapt to fructose conditions in the 2D culture as well as in the 3D culture (Figure 3.10) which may explain the mammosphere result (Figure 3.11).

Chapter 4

Expression of pluripotency-associated genes in breast cancer cell lines

4.1 Introduction

OCT4 and SOX2 are two critical transcription factors that are expressed in both CSLCs and ES cells. These transcription factors have important roles in maintaining the pluripotency and self-renewal of both groups (184) (185). Considering the many similarities shared by cancer cells and early embryonic cells, there is increasing interest to study the implication of embryonic genes in human cancer, specifically OCT4 and SOX2. Importantly, OCT4 and SOX2 are promising factors for clinical applications due to their expression levels in cancers that may induce tumour growth and development. In fact, together these transcription factors could prove useful predictors of the presence of different carcinomas in clinical settings.

The human OCT4 gene is now well documented as a master regulator for the pluripotency and self-renewal of ES cells with three known isoforms: OCT4A, OCT4B, and OCT4B1 (69) (70). There is a possibility that OCT4 has different transcript variants, protein isoforms, and pseudogenes. Therefore, a more in depth analysis would be required for a better understanding of the functional role of OCT4 in human cancer (186). OCT4 is expressed by CSLCs and its expression is associated with tumour progression (187). OCT4 expression increases CSLC characteristics in a mouse model of breast cancer (188). Additionally, false-positive signals from OCT4 in different breast cancer cell lines led to the investigation of the role of different OCT4 isoforms. Recent studies revealed the expression of OCT4 in various cell types and somatic tumours such as breast (189). However, at the time, the possibility of the transcription of OCT4 pseudogenes was not taken into account. Moreover, other studies reported that it is still unclear as to whether OCT4 is expressed in cancer cells (190) (62). Hence, investigating the role of OCT4 and its PGs is of importance in carcinogenesis as they may play a role in regulating OCT4 gene activity.

Different pseudogenes are suggested to regulate their genes of origin with OCT4 PG1 having the highest homology to OCT4A. This high homology led to the hypothesis that OCT4 PG1 may possess stemness potential. However, there was evidence against this hypothesis: compared with OCT4A, OCT4 PG1 was found to have a lower transcriptional activity, overexpression of OCT4 PG1 did not confer a stem-like phenotype in sphere assays and nor did it enhance the expression of stem cell markers (81). The amplification of OCT4 PG1 was, for the first time, reported to be associated

with an increased abundance of the corresponding mRNA and said to confer a malignant phenotype in cancer cells. Moreover, the same study showed that overexpression of OCT4 PG1 induced cell growth *in vitro* and increased tumour growth *in vivo* (81). Therefore, this project aimed to test and identify the role of OCT4 PG1 in a breast cancer stem cell population.

In addition to the aberrant expression of OCT4 in breast tumours and its activation in breast cancer stem cells, the induction of SOX2 expression has been reported in normal mammary stem cells, which is then lost as the cells differentiate and tumours progress towards advanced stages *in vivo* (191) (58). Further experiments would be needed to clarify the role of SOX2 in the generation of CSLCs and its contribution to mammosphere formation. Moreover, we previously found (chapter 3) that depriving glucose from the growing medium in 2D culture created a better condition for the stem cell population to form as mammospheres. This may explain relationship between metabolism and stem cells in breast cancer. Therefore, it was felt important to compare the expression levels of OCT4 and SOX2 in both glycolytic conditions.

This chapter summarises the role of two main pluripotency markers in breast; OCT4 and SOX2. However, the role of NANOG was not considered in this thesis at this point, due to the lack of information on its role in breast cancer.

4.2 Aims

Work in this chapter aimed to:

- Investigate the expression levels of the pluripotency markers OCT4 and SOX2 in breast cancer cell lines. In addition to OCT4A, the expression levels of OCT4B and pseudogene 1 and their role in tumorigenisis were also investigated.

- Assess the impact of different expression levels of OCT4 and SOX2 on the stem cell population of breast cancer cells under different metabolic conditions via the mammosphere formation assay.

4.3 Results

4.3.1 Expression levels of SOX2 in breast cancer cell lines

The role of SOX2 in stemness is worth mentioning. SOX2 along with OCT4 and c-MYC transcription factors are thought to induce pluripotency (192). Moreover, various studies have revealed an aberrant expression of SOX2 in breast tumours and its activation in breast cancer stem cells. Accordingly, SOX2 expression levels were investigated in breast cancer lines. The expression of SOX2 mRNA was assessed by RT-PCR. The mRNA expression of SOX2 was detected at ~197 bp in all cell lines including MCF-7, SkBr-3, and MDA-MB-231 at different levels. Higher levels of SOX2 mRNA were evident in the epithelial MCF-7 cells. SOX2 mRNA appeared weaker in basal-like breast cell lines, MDA-MB-231 and SkBr-3. The human embryonic teratocarcinoma cell line NT2 which has similar properties to ES cells was used as a positive control throughout the experiments (Figure 4.1).

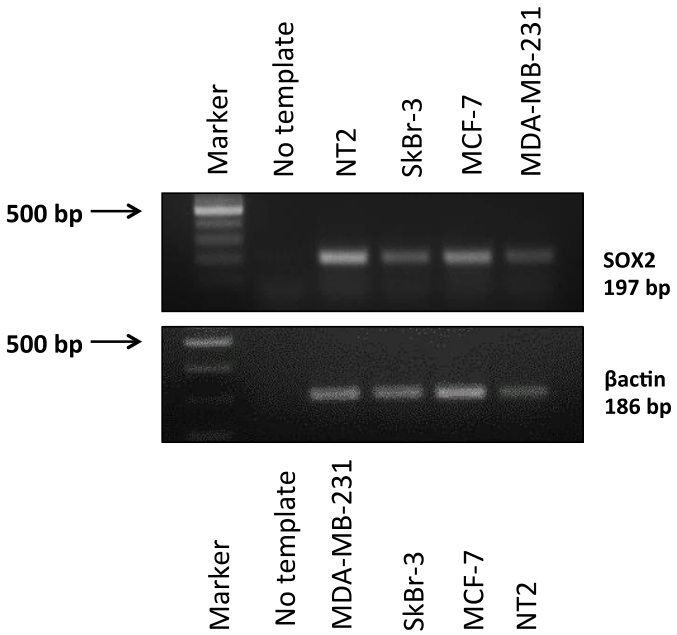

Figure 4.1 The expression levels of SOX2 in human breast cancer cell lines. The PCR image shows the SOX2 mRNA expression in NT2 cells (positive control) and three breast cancer cell lines SkBr-3, MCF-7, and MDA-MB-231detected using a SOX2 primer set. The extent of mRNA expression was normalised to β-actin, used as an internal control. PCR products separated on a 2% agarose gel and run at 36 cycles. 100-bp DNA ladder was used as size marker.

The expression levels of SOX2 were further examined by qPCR in different breast cancer lines. Data were normalized to the expression level of βactin, the housekeeping gene. The positive control NT2 was set equal to 1 to obtain a relative SOX2 expression. There was a two fold decrease in mRNA abundance in MCF-7 cells compared with NT2 cells. The graph indicates a decrease in the mRNA abundance of SOX2 in basal-like breast cancer cell lines in comparison with epithelial MCF-7 and T47D cells (Figure 4.2).

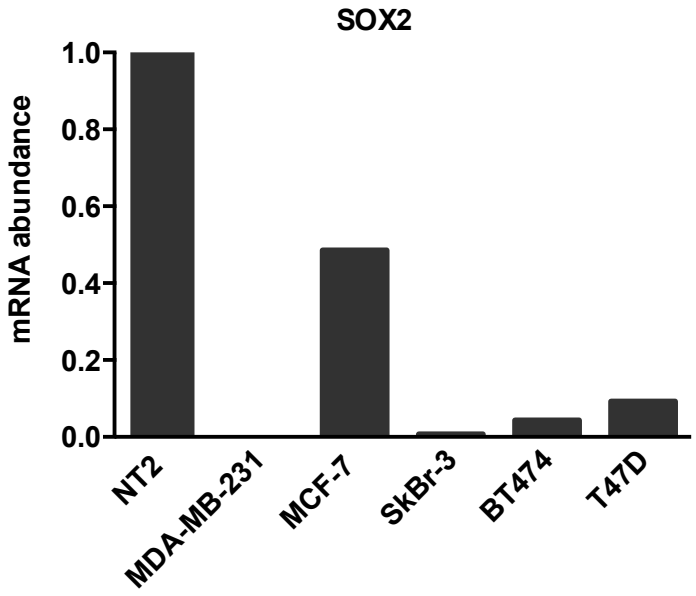

Figure 4.2 SOX2 mRNA abundance in breast cancer lines. SOX2 mRNA expression levels were assessed by qPCR in several breast cancer cell lines. The Ct obtained for each cell line was normalised against the housekeeping gene β-actin. Relative mRNA abundance was calculated by normalising to βactin. n=1

Genomic DNA contamination is a problem during RNA purification that may cause non-specific amplification and unusual results in RT-qPCR. RT-qPCR assays for single-exon genes, such as SOX2, will readily amplify contaminating genomic DNA. Moreover, it was practically difficult to entirely eliminate genomic DNA from SOX2 RNA preparations due to low levels of genomic DNA contamination. Therefore, it was essential to include general methods of controlling and correcting for gDNA contamination, such as a no reverse transcriptase (RT) control, (No-RT control), in the experiments for accurate measurements of gene expression. A No-RT control involves carrying out the reverse transcription step of a RT-qPCR experiment in the absence of reverse transcriptase. This control evaluates the amount of DNA contamination present in an RNA preparation. In this technique, all the RT-PCR reagents were present except for the reverse transcriptase enzyme. Therefore, any detected products were due to the presence of contaminating DNA, and it should be assumed that the same amount of genomic DNA is also present in the experimental samples. Thus, a No-RT experiment was designed to verify the accuracy of the detected mRNA. The Ct values were obtained at similar levels when SOX2 was measured in samples (with and without RT). However, the Ct values in the No-RT condition were higher compared to the control group when measuring actin. Most importantly, there was a clear difference in the Ct values for SOX2 under fructose conditions with and without RT (Figure 4.3).

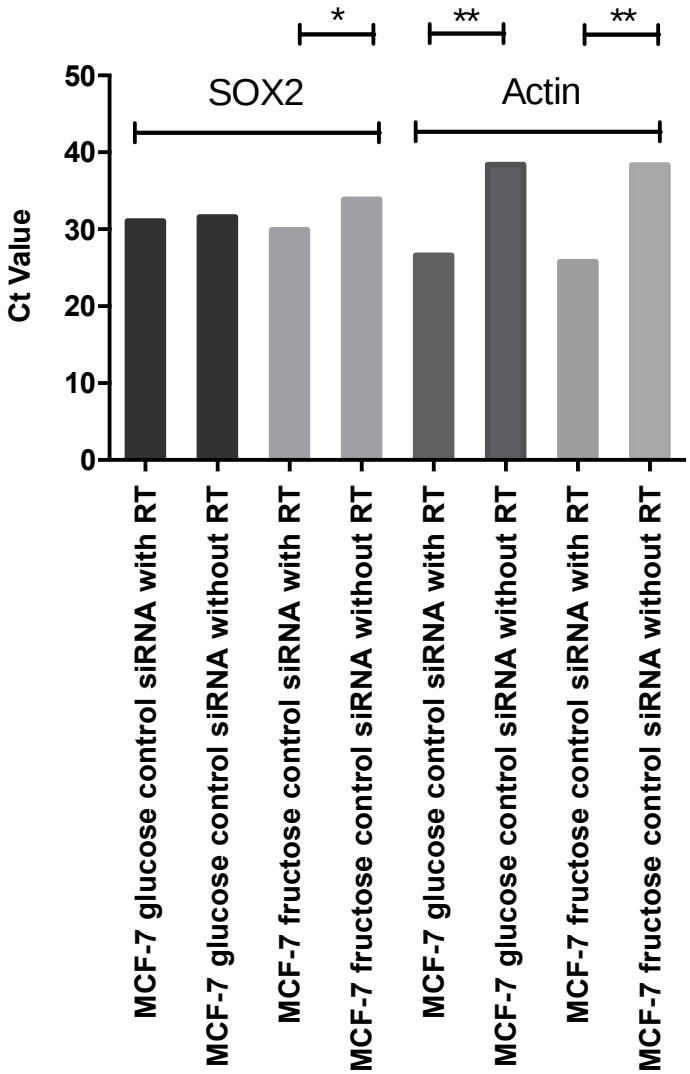

Figure 4.3 The evaluation of Ct value in SOX2 including a No-RT Control in MCF-7 cells. The Ct value was compared in glucose and fructose cultured cells with and without RT. n=3

The expression of the SOX2 protein was further assessed by immunocytochemistry in breast cancer cell lines. Individual cells were fixed, permeabilised, and blocked using 4% paraformaldehyde, 0.2% Triton X-100, and 10% FCS respectively. Samples were incubated with polyclonal SOX2 primary antibody overnight followed by the secondary antibody. The subcellular localisation of SOX2 revealed both nuclear and cytoplasmic staining in NT2 and all tested breast cancer cell lines. Together with mRNA expression, immuno-staining data confirmed a higher nuclear expression of SOX2 in the MCF-7 epithelial breast cancer cell line (Figure 4.4B) compared with the more aggressive MDA-MB-231 and SkBr-3 cells (Figure 4.4, C, D).

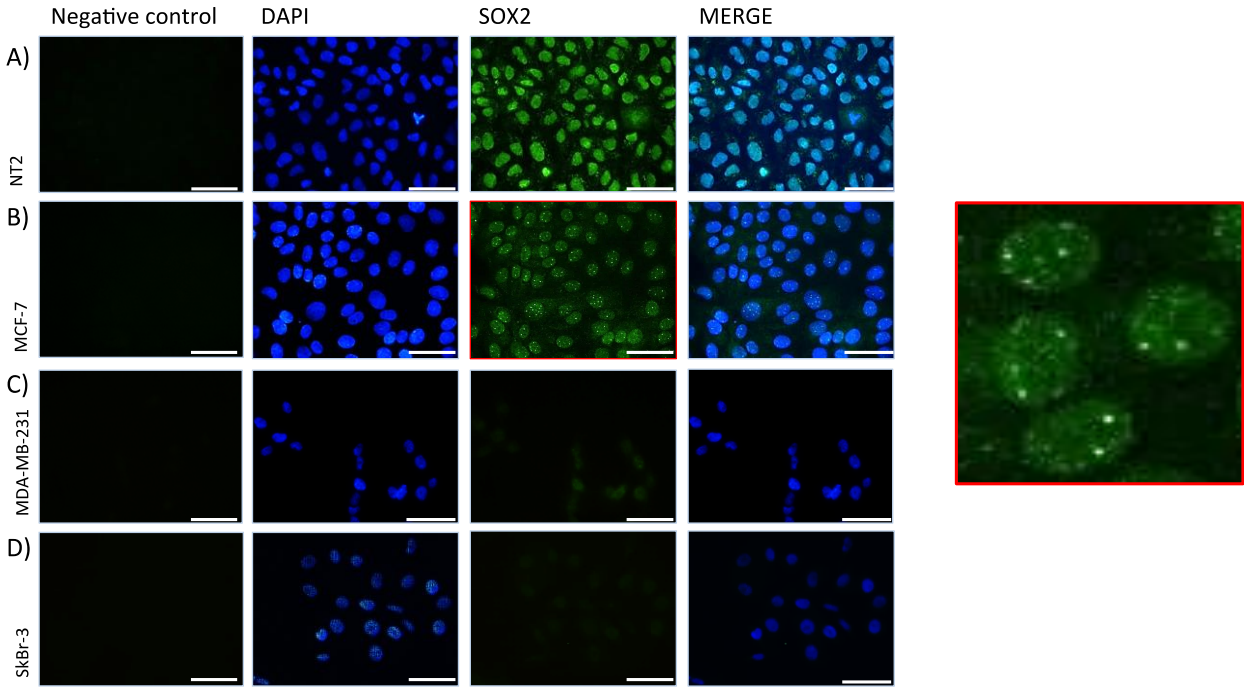

Figure 4.4 Characterisation of the intracellular localisation of SOX2 in several breast cancer cell lines. Immunofluorescence images showing the expression of SOX2 protein (green) in NT2 cells (A) and staining in three breast cancer cell lines, MCF-7, MA-MB-231, and SkBr-3 (B-D), detected using a polyclonal anti-SOX2 antibody. Nuclear and cytoplasmic expression of SOX2 was detected in all cells lines. Nuclei of cells were stained with DAPI, presented in blue. The negative control was secondary antibody only. Scale bar represents 20 μm.

Additionally, Western blot analysis was also performed to measure the protein expression of SOX2 in MCF-7 cells. MCF-7 and NT2 cells were transfected with SOX2 specific siRNA for 48 hours and subsequently probed with SOX2 polyclonal antibody over-night at 4°C. Blots were exposed using BioRad Multimager and protein expression was evaluated. SOX2 protein was highly expressed in NT2 and untransfected cells. Weaker signals in SOX2 siRNA transfected cells confirmed the accuracy of the siRNA transfection.

Moreover, OCT4 was silenced using OCT4 specific siRNA and transfected cells were probed with SOX2 antibody in order to evaluate the relationship between OCT4 and SOX2. SOX2 expression appeared weaker in NT2 cells silenced with OCT4 siRNA. A positive correlation was detected between OCT4 knockdown and SOX2 expression in NT2 cells (Figure 4.5A). However, this reduction in SOX2 expression following OCT4 siRNA transfection was less obvious in MCF-7 cells (Figure 4.5B).

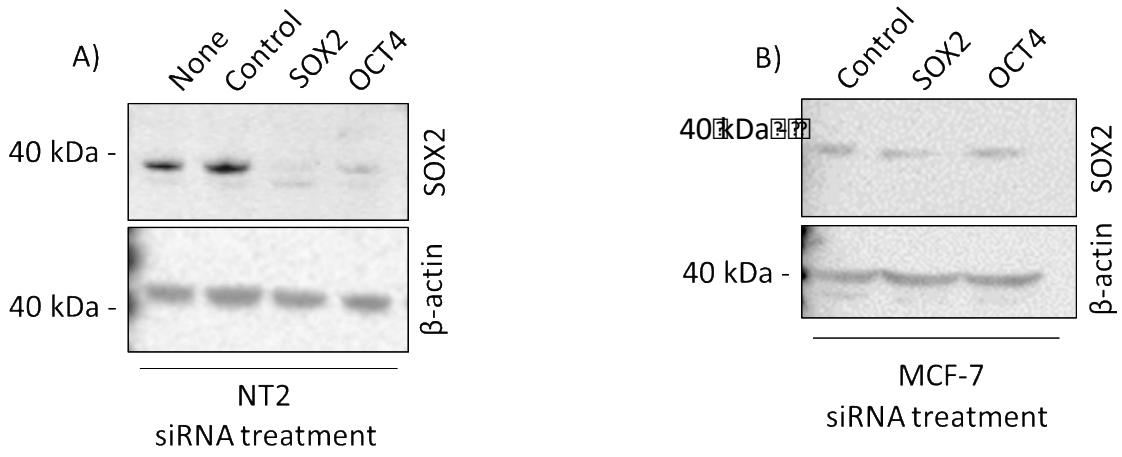

Figure 4.5 Characterisation of SOX2 protein expression in NT2 (A) and MCF-7 cells (B) by Western blot analysis. SOX2 was detected using a SOX2 antibody. β-actin was used as a loading control. Blots were exposed using BioRad FluoroS Multimager. The experiment is representative of three separate experiments.

4.3.1.2 The effect of glucose restricted conditions in the expression levels of pluripotency markers SOX2 and OCT4 in MCF-7 cells

Glucose is known to be a key metabolic substrate on which cancer cells thrive and fuel their growth. Moreover, recent studies revealed the high affinity of stem cells for glucose in energy production. Therefore, to investigate whether glucose has an impact on the expression levels of SOX2 and OCT4, the expression levels of these two stem cell markers were assessed in both groups (glucose vs. fructose adapted cells). To that end, 25 mM glucose was replaced with 10 mM fructose in the medium to starve cells of glucose.

4.3.1.2.1 Detection of SOX2 in MCF-7 breast cancer cell line under different glycolytic conditions (glucose and fructose):

To investigate differences in the expression levels of SOX2 in both metabolic groups, MCF-7 cells were cultured and adapted in DMEM supplemented with 10 mM fructose in the absence of glucose and cells treated with medium containing 25 mM glucose were used as a control as previously detailed in chapter 3. Following adaptation, SOX2 expression was assessed both at the mRNA and protein levels.

Immunostaining:

As Figures show, SOX2 protein (green) was more visible in the nuclei of fructose adapted cells (Figure 4.6B). Lower levels of SOX2 expression were visible in the nuclei of MCF-7 under glucose conditions (Figure 4.6B) (A). The negative control consists of a secondary antibody only where cells incubated in 0.6% BSA only (Figure 4.6).

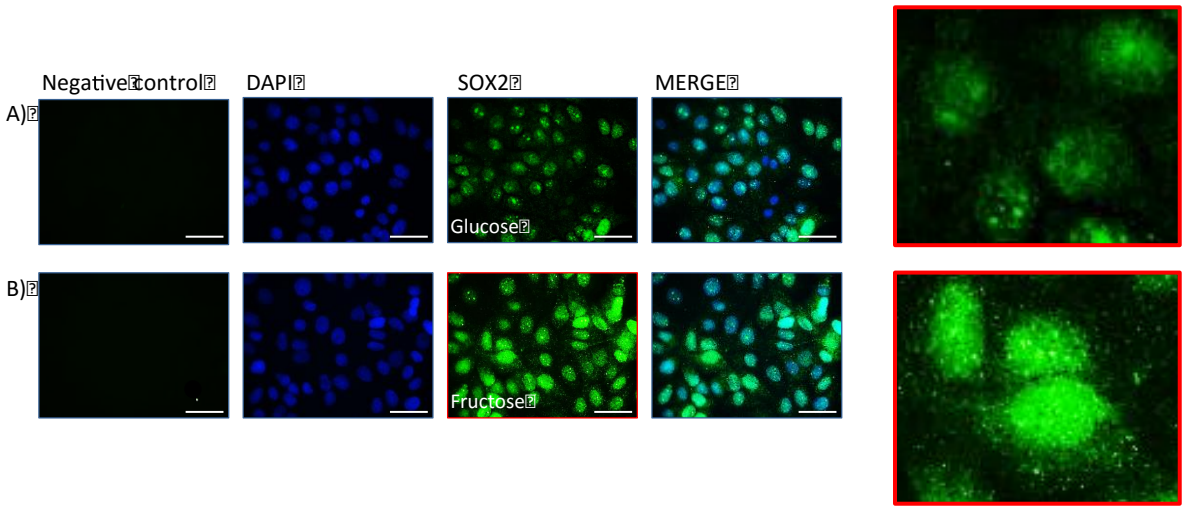

Figure 4.6 Characterisation of different expression levels of SOX2 under fructose and glucose conditions. Immunofluorescence images showing the nuclear and cytoplasmic expression of SOX2 protein (green) in MCF-7 cells under either glucose (A) or fructose (B) conditions, detected using a polyclonal anti-SOX2 antibody. Nuclei of cells were stained with DAPI, presented in blue. The negative control was secondary antibody only. Scale bar represents 20 μm.

Western blot analysis:

The expression of SOX2 under fructose and glucose conditions was determined in MCF-7 cells by Western blot analysis. β-actin served as loading control. From the blot it appears that the SOX2 protein was more highly expressed in MCF-7 cells under fructose conditions (Figure 4.7 C and D) (Figure 4.7).

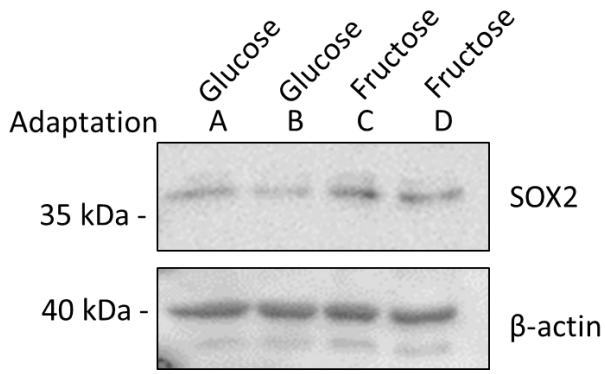

Figure 4.7 Characterisation of SOX2 protein expression in MCF-7 by Western blot analysis. SOX2 was detected in MCF-7 cells adapted in either glucose (A, B) or fructose (C, D), using SOX2 specific polyclonal antibody. β-actin was used as a loading control. Blots were exposed using BioRad FluoroS Multimager. The experiment is representative of three separate experiments.

qPCR analysis:

qPCR was performed as an efficient and more reliable sensitive technique for gene expression to determine absolute levels of SOX2 mRNA in MCF-7 cells in both metabolic groups. Results show that SOX2 mRNA abundance was significantly higher by ~1.5 fold under fructose conditions compared with glucose (** $P \leq 0.01$) (Figure 4.8).

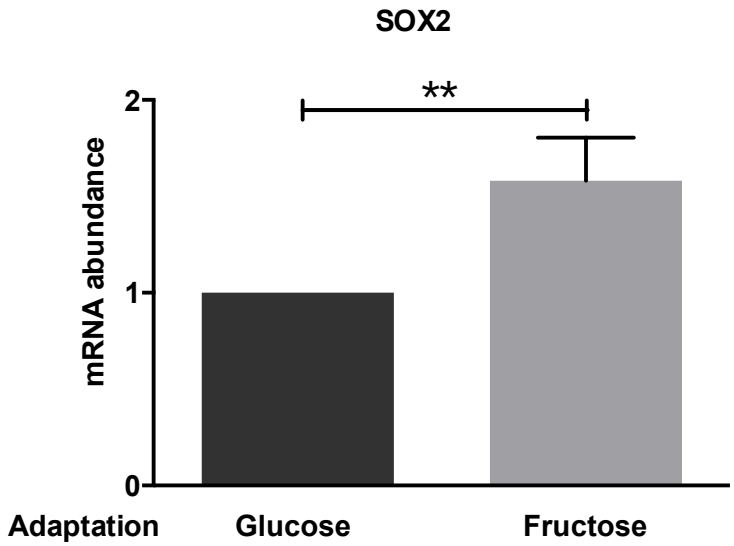

Figure 4.8 qPCR analysis of SOX2 mRNA abundance in MCF-7 breast cancer cell line under fructose and glucose conditions. The Ct obtained for each cell line was normalised against the housekeeping gene βactin. Relative mRNA abundance was calculated by normalising to β-actin. Results are presented as mean ± SEM. ** $P \leq 0.01$ n=4

To investigate differences in the expression levels of SOX2 under fructose and glucose conditions, SOX2 mRNA abundance was compared in MCF-7 cells adapted in both glycolytic groups and NT2 cells as a positive control cell line. SOX2 was silenced in all samples and the mRNA expression level of SOX2 was evaluated accordingly. The SOX2 mRNA abundance was higher in non-transfected cells and in the positive control cell line, NT2, compared with fructose adapted MCF-7 cells. Silencing SOX2 reduced SOX2 mRNA expression in all samples compared with relative control siRNA. Moreover, data confirmed higher abundance of SOX2 mRNA in MCF-7 control samples under fructose adaptation (Figure 4.9).

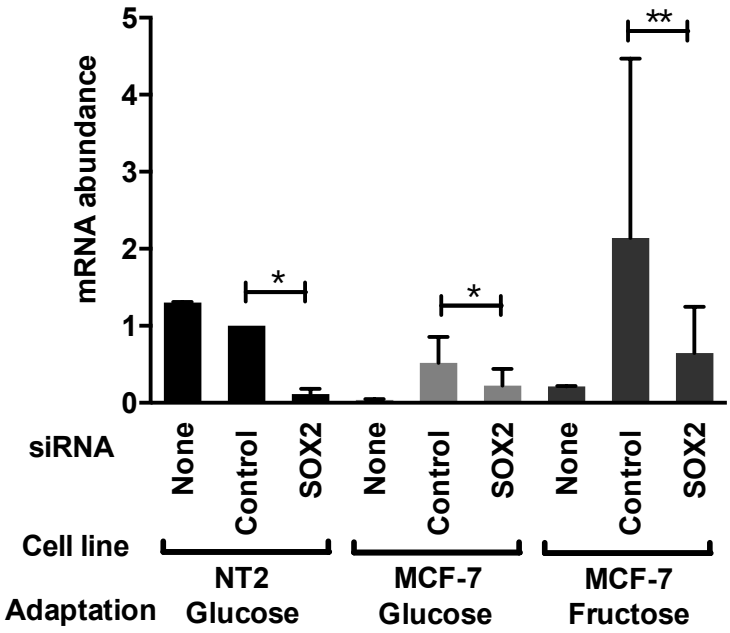

Figure 4.9 qPCR analysis of SOX2 mRNA abundance in MCF-7 breast cancer cell line under fructose and glucose conditions after selective knockdown of SOX2. The positive control NT2 (control siRNA) was set equal to 1 to obtain a relative SOX2 expression. The Ct obtained for each cell line was normalised against the housekeeping gene βactin. Relative mRNA abundance was calculated by normalising to β-actin. Each value represents the mean of ± SEM of three independent experiments.

4.3.2 The expression of OCT4 in breast cancer cell lines

The identified OCT4-positive cells in cancers are likely to represent CSLCs (184). However, there is ample evidence suggesting that OCT4 is not expressed in somatic cancers. According to the cancer stem cell concept, the expression of such genes may be associated with tumorigenesis. Several tumour cells possess stem-like properties and OCT4 is considered as a marker of stem-like cells in cancer. Thus, the potential expression of OCT4 in the cancer stem cell population of breast cancer cells was investigated in this part of the study.

The presence of OCT4 splice variants and highly homologous transcribed pseudogenes has confused breast cancer research. The OCT4A isoform contributes to the stem-ness properties of cells and OCT4 PG1 encodes a putative protein similar to OCT4A. Taking this into consideration, this project more specifically looked at the expression levels of OCT4A and OCT4 PG1 in breast cancer cell lines and how they might play a role in tumorigenicity.

Initially the expression of full length OCT4 was investigated at RNA and protein levels in different breast cancer lines, MCF-7, and more invasive SkBr-3, and MDA-MB-231. The NT2 cell line was used as a positive control for OCT4 expression.

OCT4 full-length primers were designed to amplify the entire coding sequence of the OCT4 gene including transcripts of OCT4A, POU5F1B, POU5F1P3, and POU5F1P4. Using OCT4 full-length primers, the predicted 1086 bp PCR products were detected in NT2 positive cell line and breast cancers of various subtypes (MDA-MB-231, SkBr-3, and MCF-7). The PCR data revealed an increased abundance of OCT4 mRNA in the NT2 cell line compared with those in breast cancer lines (Figure 4.10). The OAZ1 primers were designed to cross an intron and were used to identify DNA contamination. The expected size (with only cDNA and no DNA contamination) would be a single band product of 122 bp long. In the case of genomic DNA contamination, a band at 373 bp was expected to be detected.

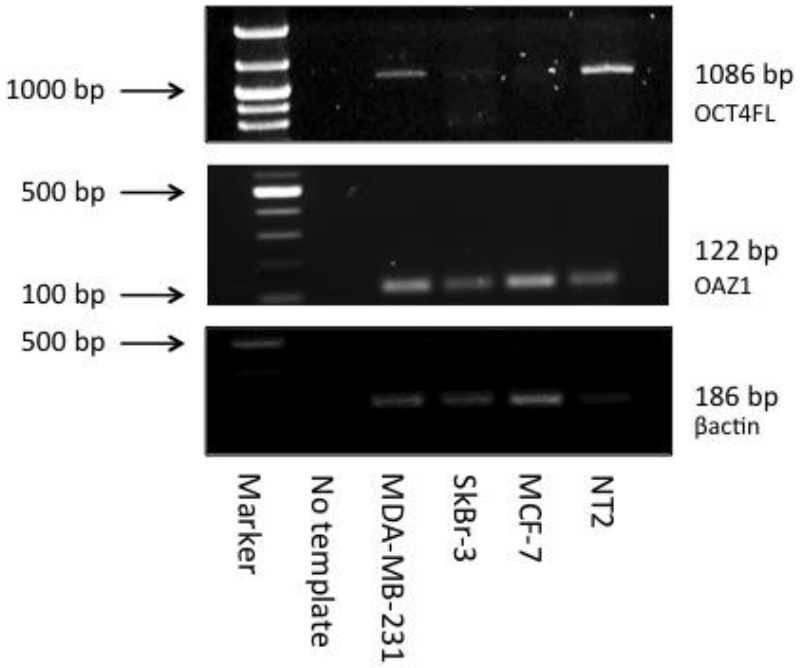

Figure 4.10 Expression levels of OCT4 full length in human breast cancer cell lines. OCT4 mRNA was detected in NT2 and breast cancer cell lines using a full length OCT4 primer set. The housekeeping gene OAZ1 was used as a loading control to identify genomic contamination. The bands were visualized at 122 bp indicating that samples were purely cDNA. The extent of mRNA expression was normalized to βactin, used as an internal control. PCR products separated on a 2% agarose gel. 100-bp DNA ladder used as size marker.

As explained in experiment 4.3, it was essential to include general methods of controlling and correcting for gDNA contamination, such as a No-RT control in the experiments for accurate measurements of gene expression. For the detection of OCT4 it is necessary to ensure that the detected signals are not false positive results. Thus, a No-RT experiment was designed to verify the accuracy of the detected mRNA. The Ct values for OCT4 PG1 obtained were similar between with and without RT in both glycolytic conditions. However, the Ct values for actin were higher in the No-RT condition compared with the control groups (4.11).

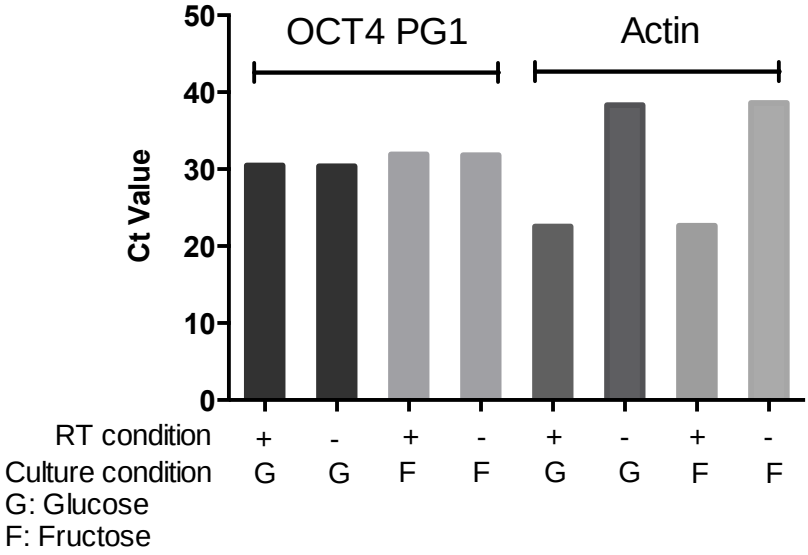

Figure 4.11 The evaluation of Ct value in (POU5F1B) OCT4 PG1 including a No-RT Control in MCF-7 cells. The Ct value was compared in glucose and fructose cultured cells with and without RT.

To qualitatively detect OCT4A expression at the mRNA level in breast cancer cells, an OCT4A specific primer set was used for RT-PCR (detailed in the methods section). This primer set specifically amplifies a fragment of the OCT4A transcript and is not able to amplify OCT4B and OCT4 PG1. OCT4A mRNA was not detected in breast cancer cell lines. The predicted 495 bp PCR product (OCT4A) was only detected in NT2 cells which was included as a positive control. βactin was used as an internal control (Figure 4.12).

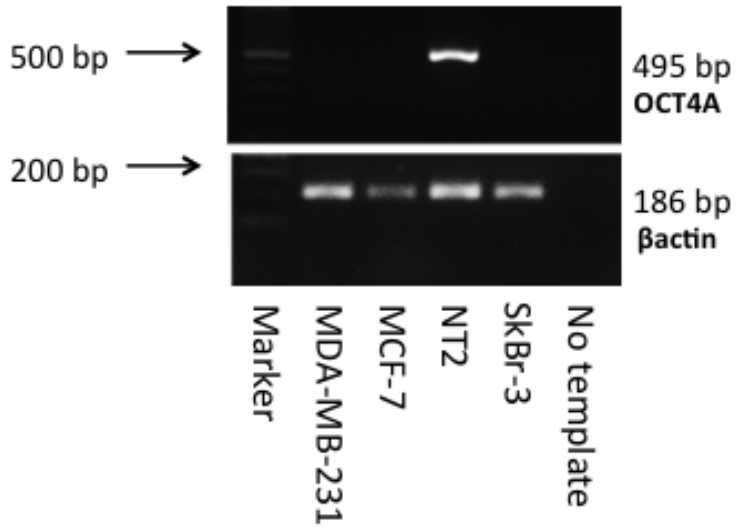

Figure 4.12 The expression levels of OCT4A in human breast cancer cell lines. The extent of mRNA expression was normalized to βactin used as an internal control. PCR products separated on a 2% agarose gel. 100-bp DNA ladder used as size marker.

To confirm the RT-PCR data, the expression of OCT4A was further examined at the protein level by Western blot and immunocytochemistry analysis using a Mouse monoclonal antibody (Sc-5279) raised against the N-terminal domain of OCT4 to recognise only the OCT4A isoform. Data revealed that OCT4A was only expressed in the nuclei of the positive control NT2 cells (Figure 4.13A) and was not expressed in breast cancer cell lines (Figure 4.13, B-C-D).

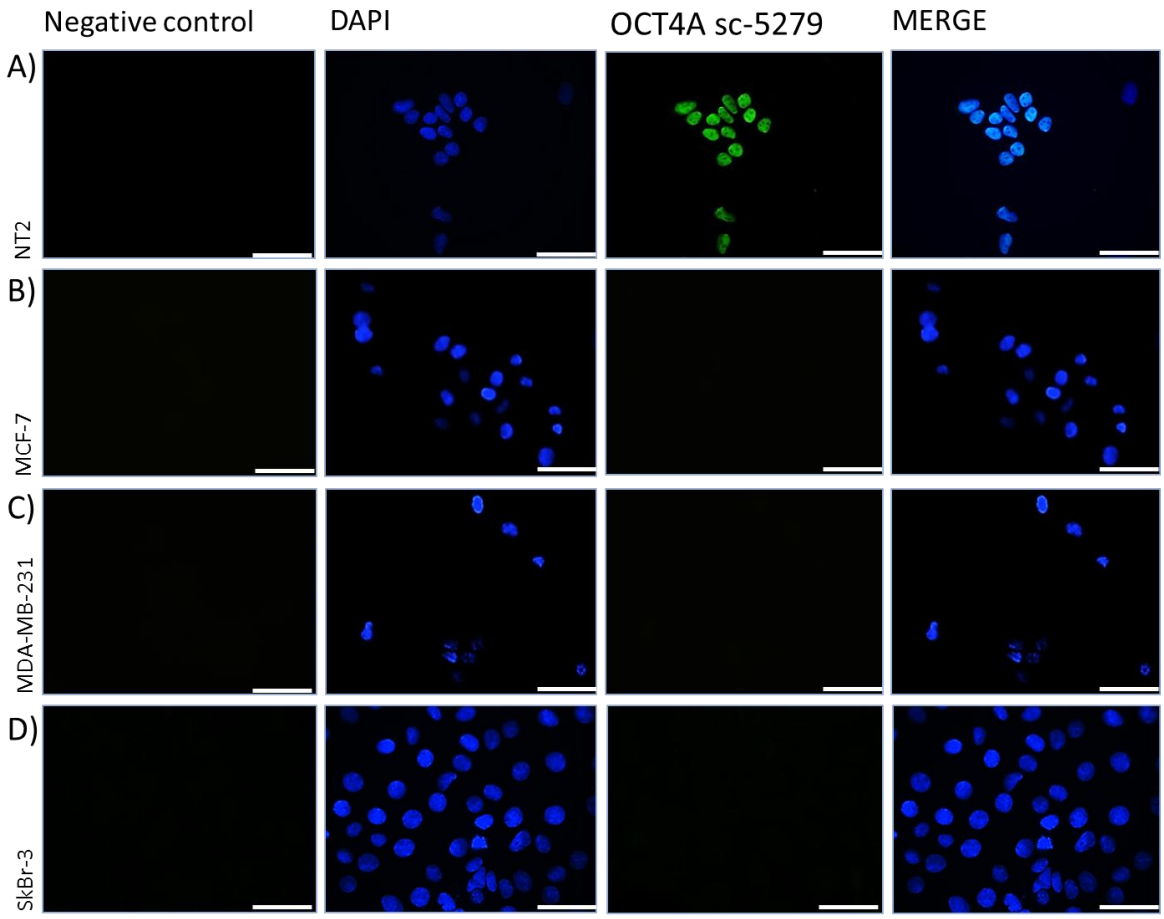

Figure 4.13 Characterisation of the intracellular localisation of OCT4A in several breast cancer cell lines. Immunofluorescence images showing the expression of OCT4A protein (green) in an embryonic carcinoma cell line NT2 (positive control) (A) and in three breast cancer cell lines, MCF-7, MDA-MB-231 and SkBr-3, (B, C, and D) detected using a monoclonal anti-OCT4 antibody (Sc-5279) directed against the N-terminus recognizing only OCT4A. Nuclei of cells were stained with DAPI, presented in blue. The negative control was with secondary antibody only. Merge represents merge images of DAPI and FITC (green). Scale bar represents 20 μm. The experiment is representative of three separate experiments.

As previously described, total protein lysates were prepared from siRNA transfected cells and Western blot analysis was performed to assess protein expression of OCT4A in breast cancer cell lines. As is shown in Figure 4.14, Western blot data further confirmed that the OCT4A specific antibody (Sc-5279) reacted exclusively with a single band of approximately 43 kDa in the positive control NT2 cell line; this band was absent from breast cancer cell lines (Figure 4.14).

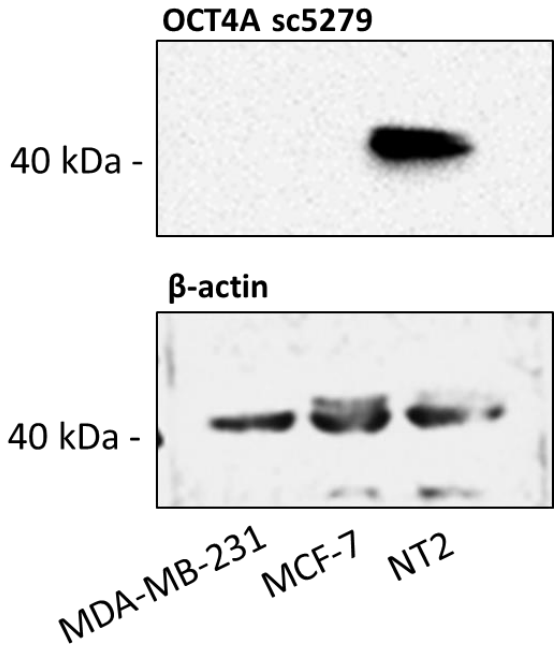

Figure 4.14 Characterisation of OCT4A protein expression in NT2 and MCF-7 cells by Western blot analysis. NT2 is served as positive control for OCT4 expression. β-actin was used as a loading control. Blots were exposed using BioRad FluoroS Multimager. The experiment is representative of three separate experiments.

Following the confirmation of the absence of OCT4A in breast cancer cells, the expression of the OCT4B isoform in breast cancer was assessed by Western blot and immunocytochemistry using a Rabbit polyclonal antibody (Ab19857), generated against the C-terminal part of the human OCT4, common to both OCT4A and OCT4B. OCT4AB is localised not only in the nucleus but also in the cytoplasm. Immunocytochemistry results showed a strong nuclear signal of OCT4 in NT2 cells using OCT4 (Ab19857) antibody which was comparable with the staining seen with Sc-5279 antibody recognising only OCT4A. Additionally, very weak staining was visible in the cytoplasm of NT2 cells (Figure 4.15A). In the invasive breast cancer cell lines,

SkBr-3 and MDA-MB-231, in addition to the slightly weaker nuclear staining, a strong staining was visible in the cytoplasm (Figure 4.15, C and D); whereas MCF-7 cells demonstrated only cytoplasmic staining with the Ab19857 antibody (Figure 4.15B).

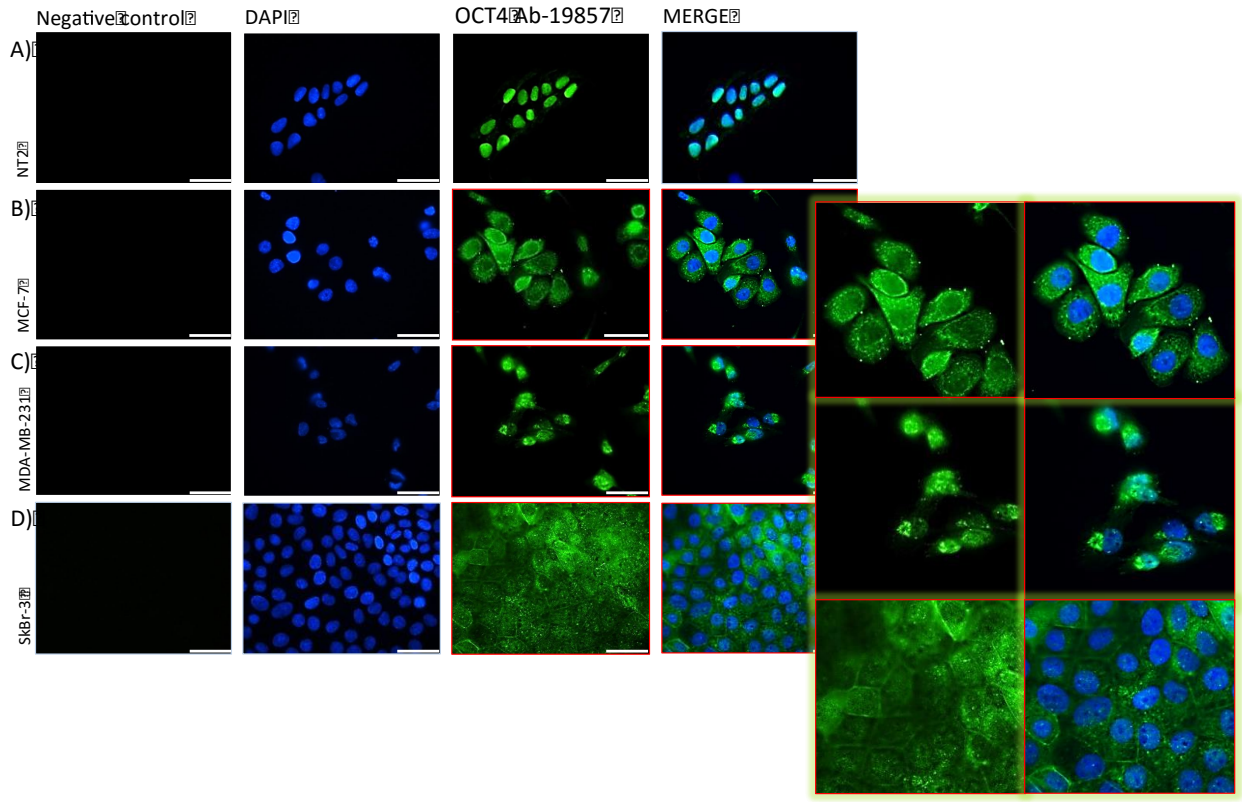

Figure 4.15 Characterisation of the intracellular localisation of OCT4 in breast cancer cell lines. Immunofluorescence images showing the nuclei expression of OCT4 protein (green) in NT2 cells (positive control) and cytoplasmic staining in three breast cancer cell lines, MCF-7, MDA-MB-231 and SkBr-3, detected using a polyclonal anti-OCT4 antibody (Ab-19857) directed against the C-terminus recognising OCT4A and OCT4B. Nuclei of cells were stained with DAPI, presented in blue. The negative control was with secondary antibody only. Merge represents merge images of DAPI and FITC (green). Scale bar represents 20 μm.

Total protein lysates were prepared form NT2, MCF-7, and MDA-MB-231 cells and Western blotting was performed to identify different OCT4 isoforms, using specific OCT4 antibodies, (Sc-5279) and (Ab19857). As it was also proved previously, OCT4A protein was only detected in NT2 cell line at about 43 kDa protein size (Figure 4.16A). The thicker band (43-45 kDa) detected in NT2 cells, using OCT4 (Ab19857) antibody is larger than OCT4B and therefore it cannot be assigned to this protein and it is thought to be related to OCT4A (Figure 4.16B).

There are bands detected in all samples which appeared larger than OCT4A in NT2 cells (~48 kDa). These bands appeared with higher intensity in breast cancer cell lines MCF-7 and MDA-MB-231compared with the signal in NT2 positive control which was only weak. The OCT4 (Ab19857) antibody also showed an additional band at ~50 kDa in NT2 cells (Figure 4.16B).

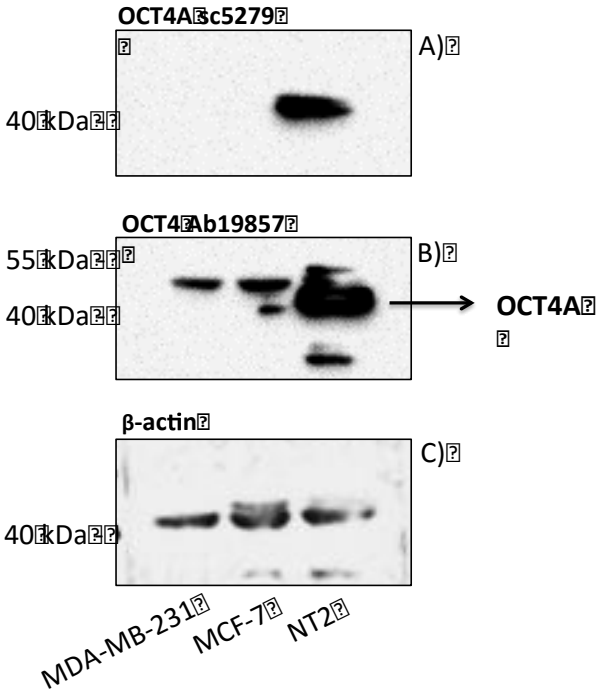

Figure 4.16 Characterisation of OCT4 protein expression in NT2 and MCF-7 cells by Western blot analysis. Immunoblotting was performed from three different cell lines: NT2, MCF-7, and MDA-MB-231. Blots were probed with appropriate antibodies; OCT4 sc5279 (A) and OCT4 Ab19857 (B). β-actin was used as a loading control (C). Blots were exposed using BioRad FluoroS Multimager. The experiment is representative of three separate experiments. Blots A and C are the same as Figure 3.23.

Findings from Western blot analysis using the OCT4 (Ab19857) antibody required further analysis to identify the additional observed bands. Therefore, to investigate which OCT4 isoform was expressed in MCF-7 cells and which in NT2, two different siRNAs targeting OCT4A and OCT4 PG1 was used to silence OCT4. The blot was separately probed with OCT4 (Ab19857) and OCT4 (MAB1759) antibody. The OCT4 (MAB1759) antibody was raised against full length OCT4.

In NT2 cells, where the blot was probed with the OCT4 (MAB1759) and OCT4 (Ab19857) antibody, protein expression did not change using either siRNAs, OCT4-2 or OCT4-10 columns (Figure 4.17 A and B).

In MCF-7 cells, OCT4-10 siRNA reduced the OCT4 protein level when probed with OCT4 (MAB1759) antibody, last column (Figure 4.17B). However, bands in MCF-7 cells remained unaffected using OCT4 (Ab19857) antibody (Figure 4.17A).
No loading control is provided for these gels, as the blotting failed.

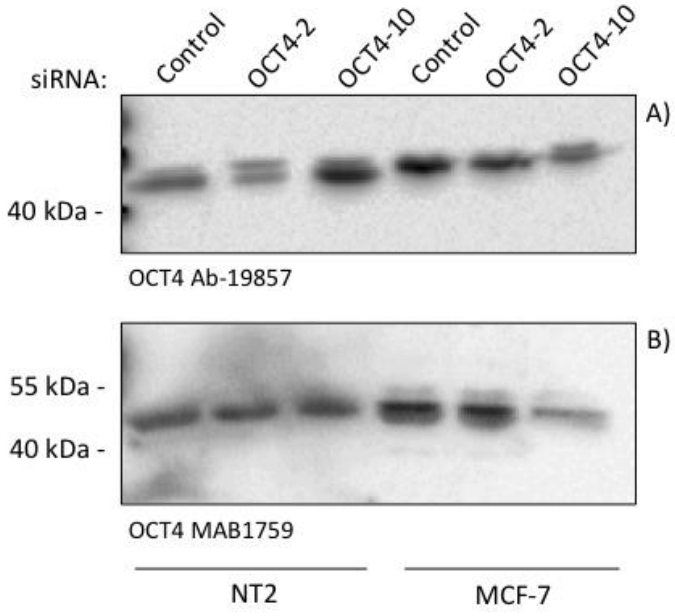

Figure 4.17 Characterisation of OCT4 protein expression in NT2 and MCF-7 cells by Western blot analysis. Cells were transfected with OCT4 siRNAs 2 and 10 (targeting OCT4A and OCT4 PG1) detected using polyclonal OCT4 Ab-19857 antibody (A) and polyclonal OCT4 MAB1759 antibody (B). Blots were exposed using BioRad FluoroS Multimager.

To further assess the OCT4 PG1 expression in breast cancer cell lines, initially, the mRNA expression of OCT4 PG1 was examined using a specific PCR primer set. Results indicated a higher expression of OCT4 PG1 in breast cancer cell lines and lower expression in NT2 cell line (Figure 4.18).

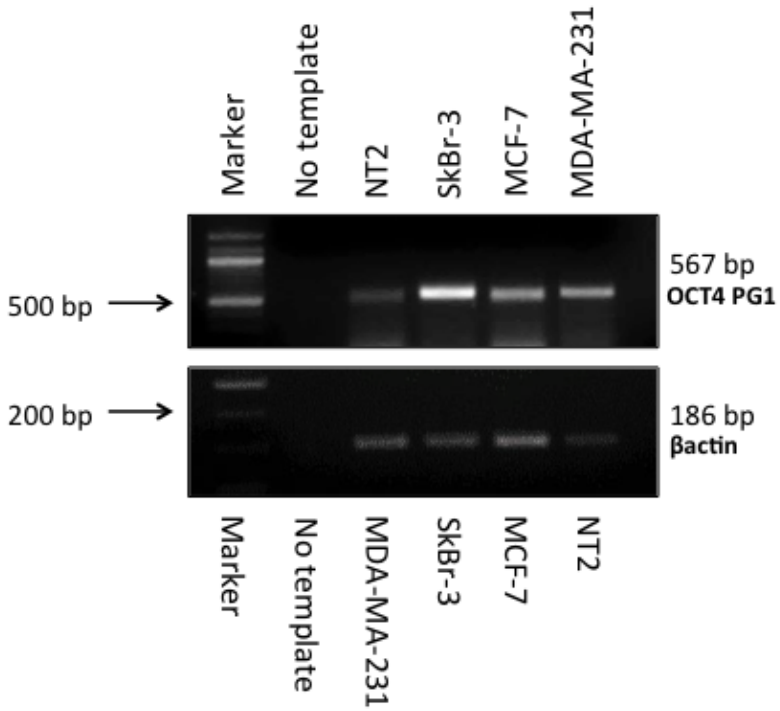

Figure 4.18 The expression levels of OCT4 PG1 mRNA in human breast cancer cell lines. PCR data show the OCT4 PG1 mRNA expression in NT2 and three breast cancer cell lines; SkBr-3, MCF-7, and MDA-MB-231, detected using an OCT4 PG1 specific primer pair. The control line represents control siRNA. The extent of mRNA expression was normalized to βactin, used as an internal control. PCR products separated on a 2% agarose gel. 100-bp DNA ladder used as a size marker.

4.3.2.1 The effect of glucose restricted conditions on the expression of OCT4 in MCF-7 cells

It was concluded that the expression of SOX2 increased upon fructose adaptation (Figure 4.8). To determine whether fructose had a similar impact on OCT4 expression, the expression level of OCT4 was investigated under fructose conditions (glucose restriction) and was compared with glucose adapted cells. Total RNA was extracted from cells and mRNA transcripts were analysed by RT-PCR using an OCT4 PCR primer set (targets the whole gene). The mRNA expression levels of OCT4 were stronger in NT2 cells compared with MCF-7 cells. Results showed no particular reduction upon OCT4 and OCT4 PG1 silencing in NT2 cells; however, consistent with previous data from PCR and Western blot analysis, a reverse correlation was detected between SOX2 knockdown and OCT4 expression showing a higher expression of OCT4 mRNA upon SOX2 knockdown in NT2 cells (Figure 4.19). Under glucose conditions in MCF-7 cells, OCT4 mRNA was reduced in OCT4 siRNA transfected cells, while this reduction was more obvious upon SOX2 and OCT4 PG1 siRNA transfection. Comparing the expression level of OCT4 under either glucose or fructose adaptation, an OCT4-related mRNA was more highly expressed under glucose conditions in MCF-7 cells (Figure 4.19).

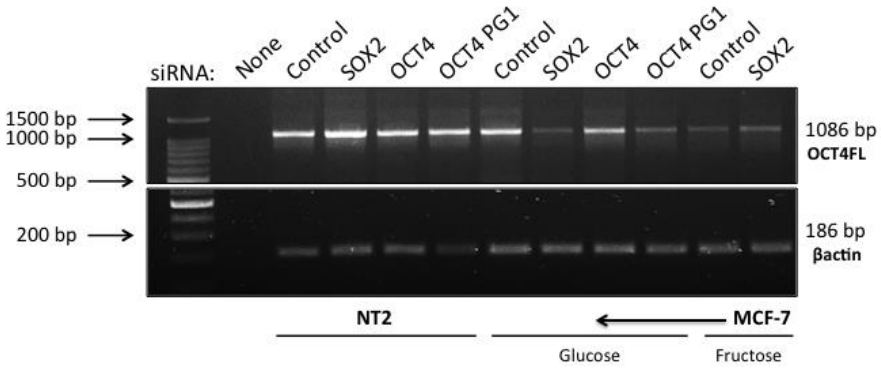

Figure 4.19 The expression levels of OCT4 mRNA in MCF-7 cells. PCR data show the OCT4 mRNA expression in NT2 cells (positive control) and MCF-7cells under either glucose or fructose conditions, detected using a primer set targeting the whole OCT4 gene. The control line represents control siRNA and the None line represents no siRNA. The extent of mRNA expression was normalized to βactin used as internal control. PCR products separated on a 2% agarose gel. 100-bp DNA ladder used as a size marker.

Consistent with the previous results, both at mRNA and protein levels, OCT4A was only detected in NT2 cell line (Figure 4.20). OCT4A mRNA levels were reduced using siRNA against OCT4 in NT2 cells while this level appeared higher in SOX2 siRNA transfected cells. Western blot and RT-PCR analysis once again proved that OCT4A mRNA (Figure 4.20A) and protein (Figure 4.20B) were not expressed in MCF-7 cells under either metabolic conditions.

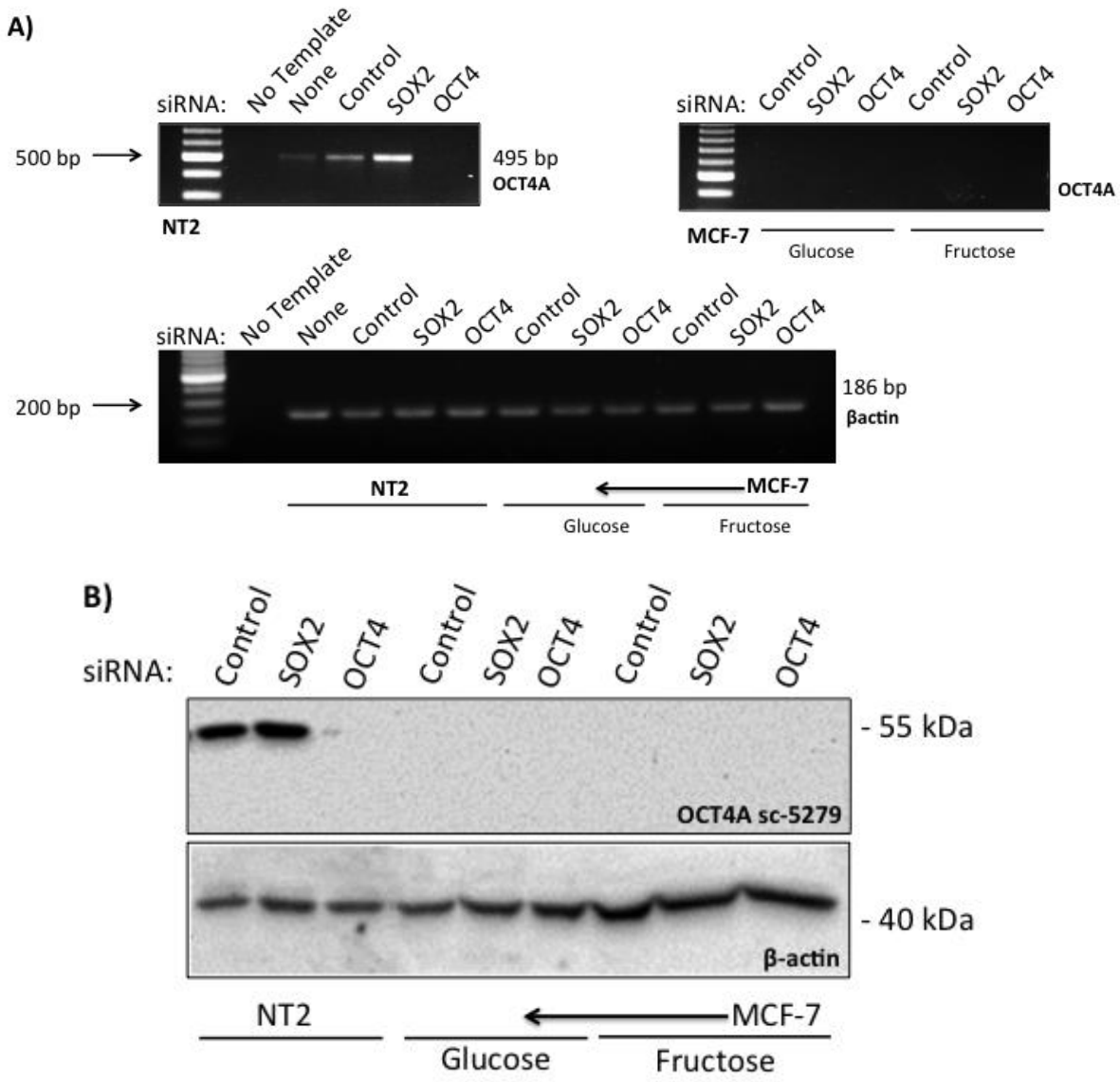

Figure 4.20 Characterisation of OCT4 expression in NT2 and MCF-7 cells by RT-PCR (A) and Western blot analysis (B). The extent of mRNA expression was normalized to β-actin, used as an internal control. The control line represents control siRNA and the None line represents no siRNA. PCR products separated on a 2% agarose gel. 100-bp DNA ladder used as a size marker. The Western blot experiment is representative of three separate experiments. β-actin was used as a loading control. Blots were exposed using BioRad FluoroS Multimager.

To understand which isoform/pseudogene was responsible for the signals in the previous RT-PCR result (Figure 4.18), the mRNA expression of OCT4 PG1 was further investigated in NT2 and MCF-7 cells. Cells were separately transfected with SOX2 and OCT4 siRNA (targets the full OCT4 gene and pseudogenes), and cDNA was synthesized for PCR analysis. RT-PCR was performed using OCT4 PG1 specific primers. Blast analysis confirmed the primers specificity for OCT4 PG1.

Consistent with the previous PCR data, OCT4 PG1 mRNA was less expressed in NT2 cells compared with glucose adapted MCF-7 cells, detected using an OCT4 PG1 specific primer set. The expression level of OCT4 PG1 mRNA was reduced following OCT4 siRNA transfection in NT2 cells, whereas the level of OCT4 PG1 mRNA was increased in SOX2 siRNA transfected cells.

The OCT4 PG1 mRNA was more highly expressed in MCF-7 cells under glucose conditions compared with those adapted to fructose. Following OCT4 siRNA transfection in MCF-7 cells, the expression level of OCT4 PG1 mRNA remained unaffected. However, the expression level of OCT4 PG1 mRNA was reduced following SOX2 siRNA transfection in MCF-7 cells only under glucose condition. Conversely, following SOX2 siRNA transfection in fructose adapted cells, the expression level of OCT4 PG1 mRNA remained unaffected. βactin was used as a loading control (Figure 4.21).

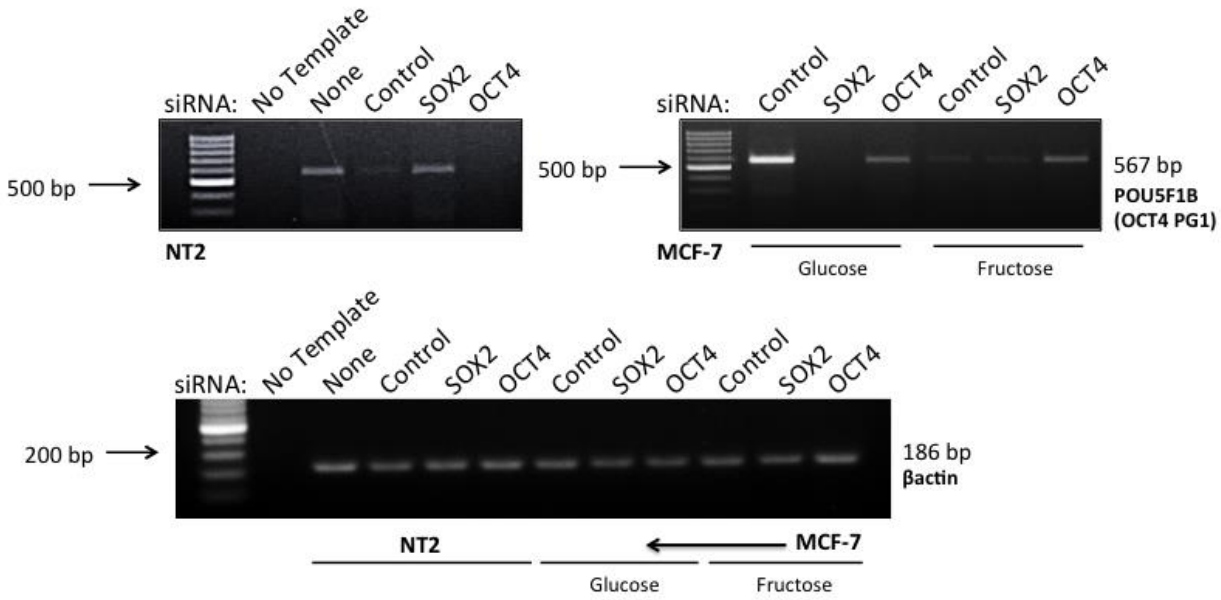

Figure 4.21 The expression levels of POU5F1B (OCT4 PG1) mRNA in human breast cancer cell lines. The extent of mRNA expression was normalized to β-actin used as an internal control. The control line represents control siRNA and the None line represents no siRNA. PCR products separated on a 2% agarose gel. 100-bp DNA ladder used as a size marker. n=3

To investigate the OCT4 isoforms and/or pseudogenes in MCF-7 breast cancer cells, and to determine the effect of glycolysis restriction, the expression levels of OCT4 were further assessed in MCF-7 cells under glucose and fructose conditions. Cells were initially fixed, permeabilised, and incubated independently with OCT4 MAB1759 (raised against the full length OCT4) and OCT4A Sc-5279 (specific to OCT4A) for immunocytochemistry analysis as described before. Individual cells were visualized using an Olympus IX81 microscope and images were taken using an Orca-ER digital camera. The cell nuclei were stained using DAPI.

Nuclear expression of OCT4 was detected in both cell lines (NT2 and MCF-7). A nuclear localisation of OCT4 was clearly determined in MCF-7 cells for the first time. However, the intensity of staining appeared stronger in the nuclei of NT2 cells. There was a higher intensity of perinuclear protein visible in fructose adapted cells. OCT4 protein was more highly expressed in fructose adapted MCF-7 cells (Figure 4.22).

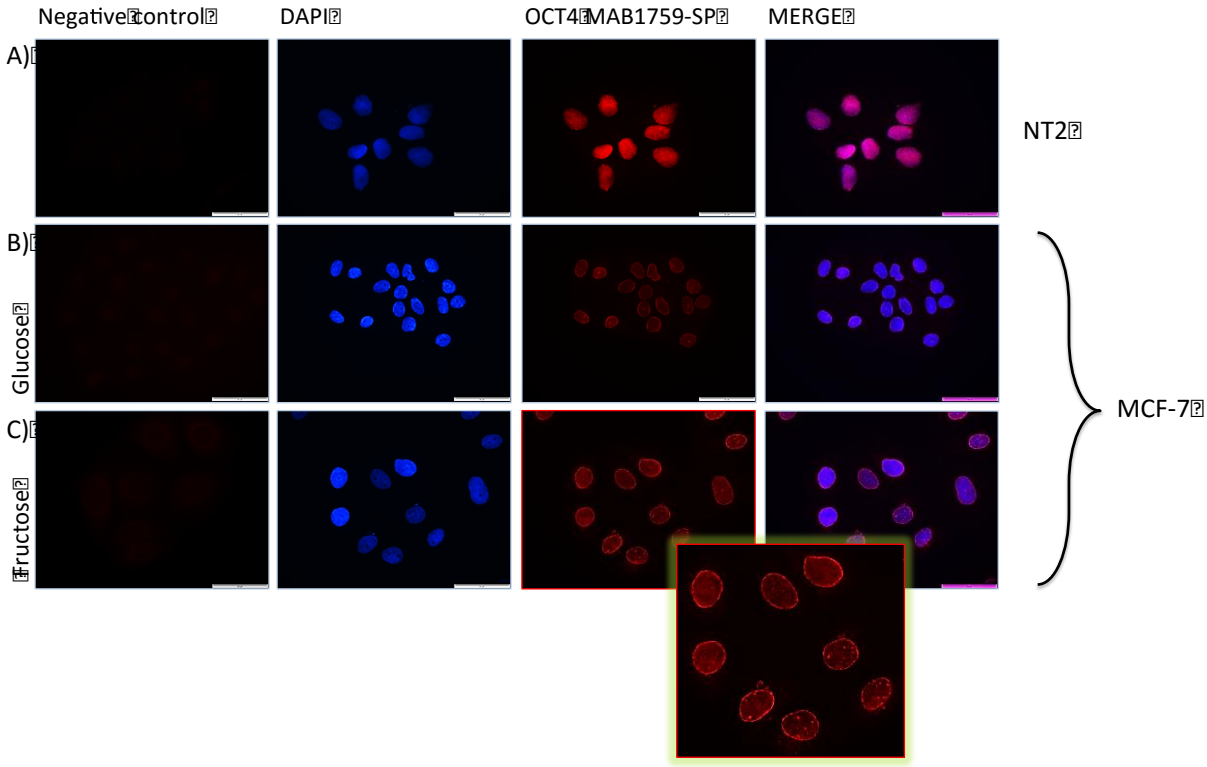

Figure 4.22 Characterisation of the intracellular localisation of OCT4 in fructose and glucose adapted MCF-7 cells. Immunofluorescence images showing expression of OCT4 protein (red) in NT2 cells (positive control) (A) and MCF-7 breast cancer cell line under glucose (B) or fructose conditions (C), detected using a monoclonal anti-OCT4 antibody raising against the full length OCT4. Nuclei of cells were stained with DAPI, presented in blue. The negative control was with secondary antibody only. Scale bar represents 20 μm.

To further confirm the absence of OCT4A in the MCF-7 breast cancer cell line and to better understand which OCT4 isoform was expressed in MCF-7 cells, OCT4 was silenced using two different siRNAs targeting the full length OCT4 and OCT4 PG1 separately. Cells were stained separately for OCT4A (Sc-5279) and OCT4 (MAB1759) antibody. OCT4A was expressed in the nuclei of NT2 cells (Figure 4.23, A-a). OCT4A was not detected in NT2 cells following silencing the full length OCT4, using OCT4 specific antibody (Figure 4.23, A-b). However, following OCT4 PG1 siRNA transfection, OCT4 was detected with the same intensity as appeared in controls (Figure 4.23, A-c). Consistent with the previous data, results demonstrating that OCT4A isoform was not expressed under either conditions in MCF-7 cell line (Figure 4.23 B, a-b-c).

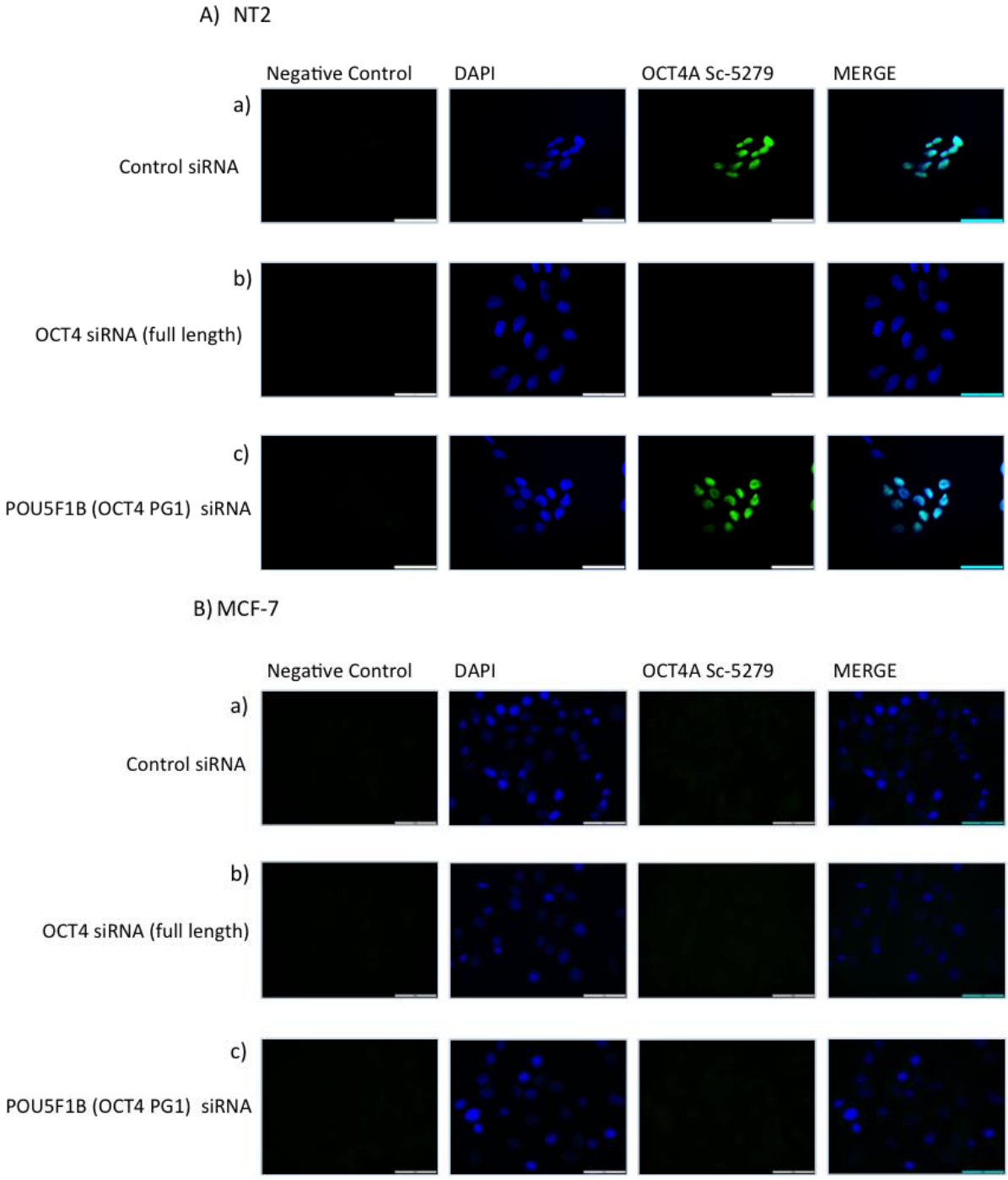

Figure 4.23 Characterisation of the intracellular localisation of OCT4 in NT2 and MCF-7 cell lines. OCT4 was silenced using two different siRNAs**.** One siRNA targeted against regions of the full length target mRNA of OCT4 (A-B, b), the other targeted the POU5F1B (OCT4 PG1) (A-B, c). Immunofluorescence images showing the nuclear expression of OCT4 protein (green) in the nuclei of NT2 cells when used as a control (A-a) and transfected with OCT4 PG1 siRNA (A-c), detected using a monoclonal anti-OCT4 antibody (OCT4A specific). Nuclei of cells were stained with DAPI, presented in blue. The negative control was with secondary antibody only. Scale bar represents 20 μm.

The OCT4 protein was detected using OCT4 (MAB1759) antibody in the nuclei of NT2 cells (Figure 4.24, A-a). A large percentage of cells were silenced using the siRNA targeted against the full gene, detected using OCT4 (MAB1759) antibody compared with the corresponding controls and OCT4 PG1 siRNA transfected cells (Figure 4.24, A-b). By applying OCT4 PG1 specific siRNA, OCT4 was detected in almost the entire cell population using OCT4 (MAB1759) antibody, suggesting that OCT4 PG1 is poorly expressed in NT2 cells (Figure 4.24, A-c).

Compared with the strong nuclear expression of OCT4 in NT2 cells, MCF-7 cells displayed a much weaker nuclear expression, using OCT4 (MAB1759) antibody. A similar pattern of cell membrane staining was observed in the MCF-7 control group (Figure 4.24 B, a). In MCF-7 cells, the OCT4 protein was silenced with a similar ratio following transfection with either siRNAs, using OCT4 (MAB1759) antibody (Figure 4.24 B, b and c).

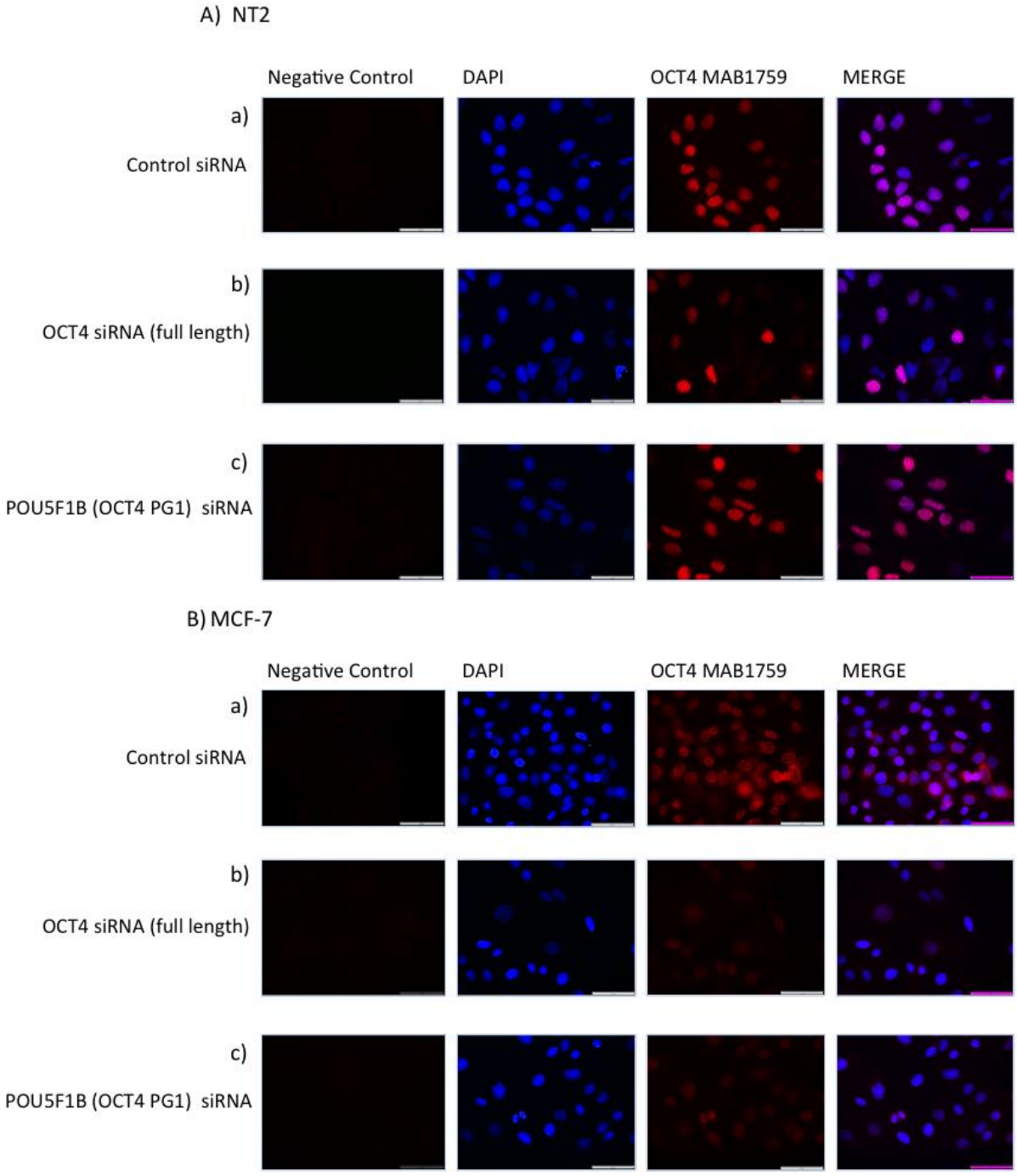

Figure 4.24 Characterisation of the intracellular localisation of OCT4 in MCF-7 cell line. OCT4 was silenced using two different siRNAs. One siRNA targeted against regions of the full length target mRNA of OCT4 and OCT4 PG1; the other targeted only the OCT4 PG1. Immunofluorescence images showing the expression of OCT4 protein (Red) in NT2 (A) and MCF-7 cells (B) detected using a polyclonal anti-OCT4 antibody targeting the full length OCT4 and OCT4 PG1. Nuclei of cells were stained with DAPI, presented in blue. The negative control was with secondary antibody only. Scale bar represents 20 μm.

To better clarify the identity of the detected OCT4 protein in MCF-7 cells, cells were separately transfected with OCT4 (target full length and OCT4 PG1) and OCT4 PG1 siRNA. 48 hour post siRNA transfection, cells were lysed for protein extraction. Equal concentrations of protein samples were loaded into wells and analysed by SDS-PAGE as previously described. Blots were probed with OCT4 (MAB1759) antibody (raised against all isoforms and pseudogenes) overnight and one hour with the secondary antibody.

An OCT4-related protein at about 48-50 kDa was detected for the first time in MCF-7 breast cancer cell line. A clean protein knockdown was observed following OCT4 siRNA transfection in NT2 cells when probing with OCT4 (MAB1759) antibody. However, the protein remained unaffected in NT2 cells when silenced with OCT4 PG1 siRNA (Figure 4.25A). OCT4 protein was silenced following OCT4 siRNA transfection against the full length OCT4 and OCT4 PG1 in MCF-7 cells under glucose and fructose conditions, detected using OCT4 (MAB1759) antibody. Additionally, under fructose conditions, OCT4 was silenced following OCT4 PG1 siRNA transfection, whereas in glucose adapted cells protein was remained unaffected (Figure 4.25, B and C).

It is clear that the additional bands (OCT4B variant) were only detected in MCF-7 cells at approximately 23 kDa, probing with OCT4 (MAB1759) antibody (Figure 4.25C). Similar silencing pattern to the series of bands at ~48-50 kDa was observed at about 23 kDa (Figure 4.25, B and C).

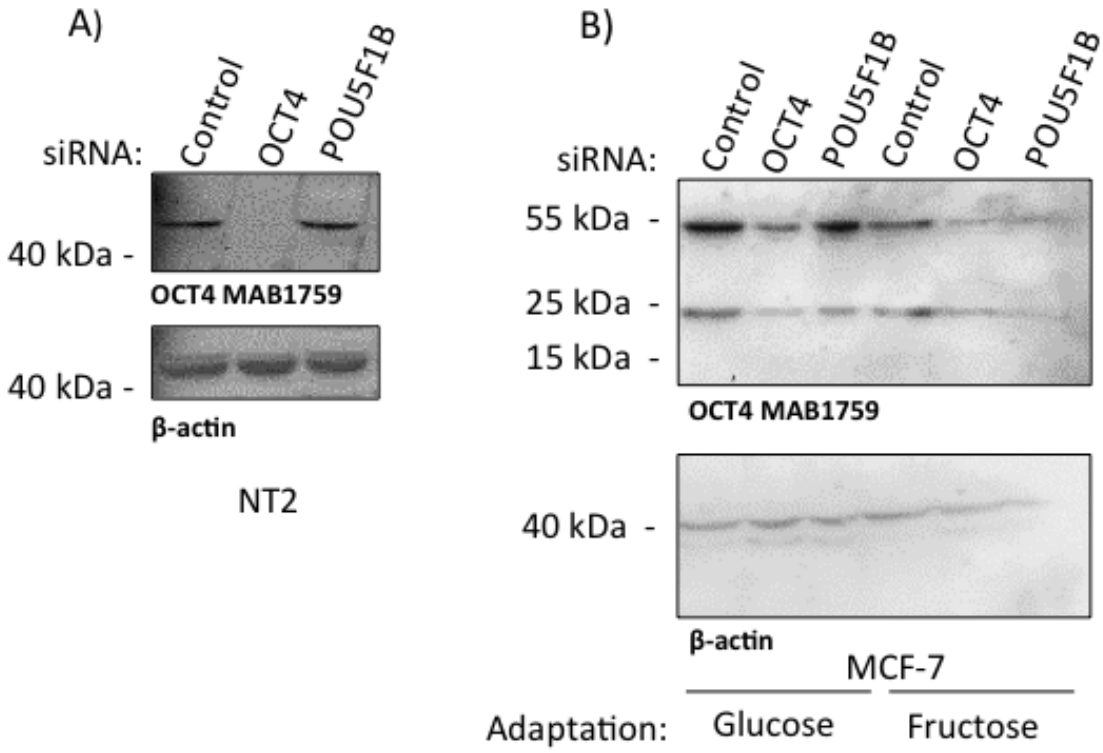

Figure 4.25 Characterisation of OCT4 protein expression in NT2 and MCF-7 cells by Western blot analysis. OCT4 protein was detected using a polyclonal OCT4 (MAB1759) antibody in NT2 (A) and MCF-7 cells (B, C). OCT4 protein was silenced using an siRNA against the full length OCT4 and OCT4 PG1, detected using OCT4 (MAB1759) antibody. β-actin was used as a loading control. Blots were exposed using BioRad FluoroS Multimager. Blot B and C are representative of two separate experiments.

To precisely target the specific OCT4 isoforms, an additional siRNA was used targeting against OCT4A and OCT4B in MCF-7 cells. Following siRNA transfection, different OCT4 antibodies were used to better investigate which isoforms were expressed in the population. Probing with OCT4 (MAB1759) antibody, a strong perinuclear staining was observed in the population of MCF-7 cells under both metabolic conditions (Figure 4.26).

Glucose adaptation – OCT4 MAB1759 antibody (targets OCT4A, OCT4B, and OCT4 PG1):

In the control group using control siRNA, a weak nuclear staining was observed in the population, with proportionally higher expression in some cells. Perinuclear staining was also detected as previously shown. In the group which was silenced with an siRNA against OCT4A and OCT4B, a similar expression pattern to that in control group was observed. In the other group, OCT4 was silenced using an siRNA against full length OCT4 including OCT4 PG1. Almost half of the cells showed that protein was silenced in the population. When OCT4 PG1 was silenced, an obvious difference was observed in the intensity of the protein expression. Almost all the cells in the population displayed a good knockdown following silencing with OCT4 PG1 specific siRNA, detected using OCT4 full antibody (Figure 4.26).

Fructose adaptation – OCT4 MAB1759 antibody (targets OCT4A, OCT4B, and OCT4 PG1):

In the control group, cells appeared larger under fructose conditions. Moreover, the intensity of the staining detected was higher under fructose conditions than in glucose adapted cells. Following OCT4A/B siRNA transfection, the protein expression was detected at higher levels compared with those in control population under fructose conditions. Moreover, the intensity of staining detected was higher in fructose adapted cells. Comparing the nuclear staining in the control group, siRNA transfected cells displayed weaker nuclear expression. Consistent with the results from glucose adapted cells, protein expression appeared weaker in MCF-7 cells transfected with PG1 siRNA (Figure 4.26).

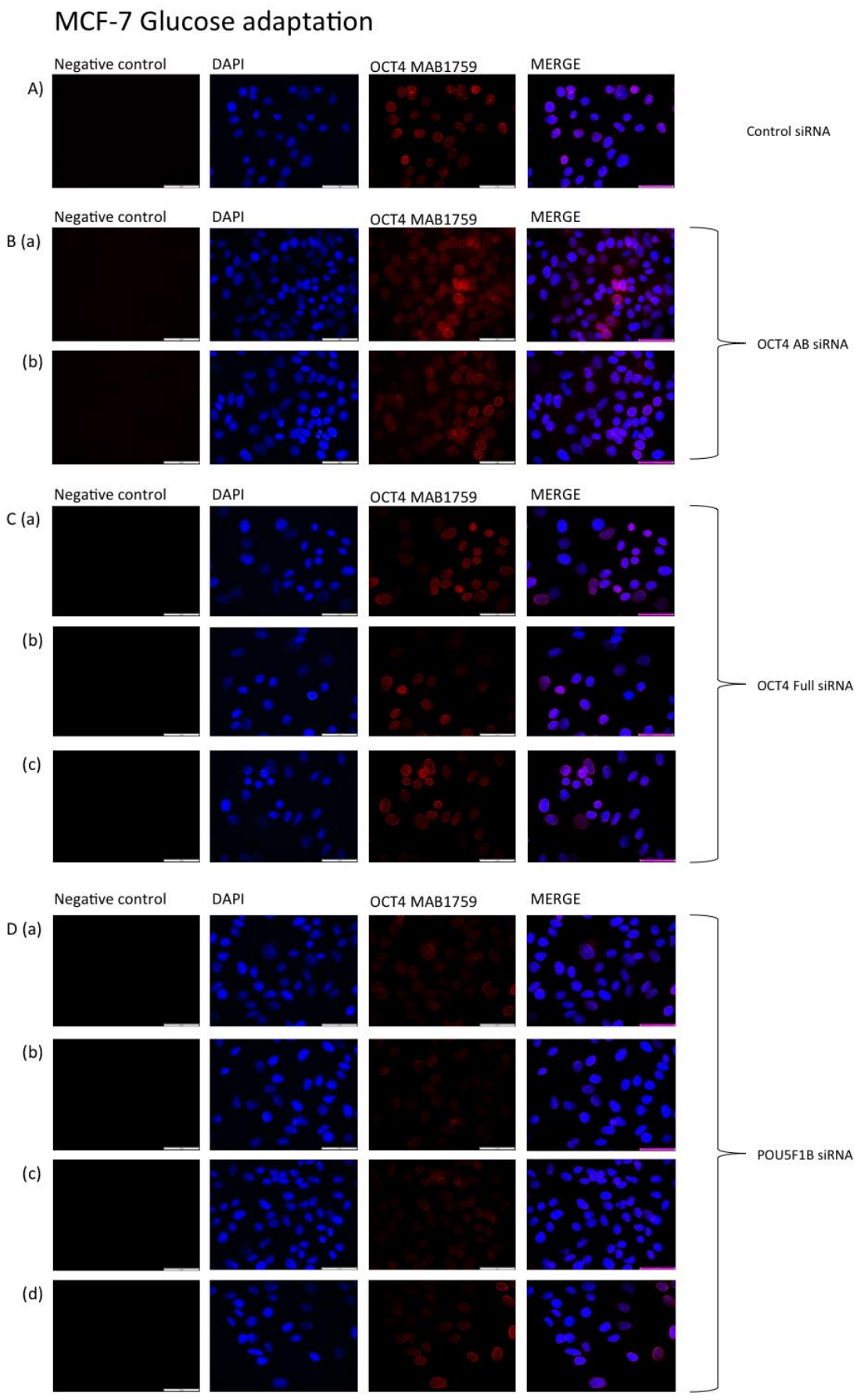
MCF-7 Glucose adaptation
Negative control
DAPI
OCT4 MAB1759
MERGE
A)
Control siRNA
B (a)
(b)
OCT4 AB siRNA
C (a)
(b)
(c)
OCT4 Full siRNA
D (a)
(b)
(c)
(d)
POU5F1B siRNA

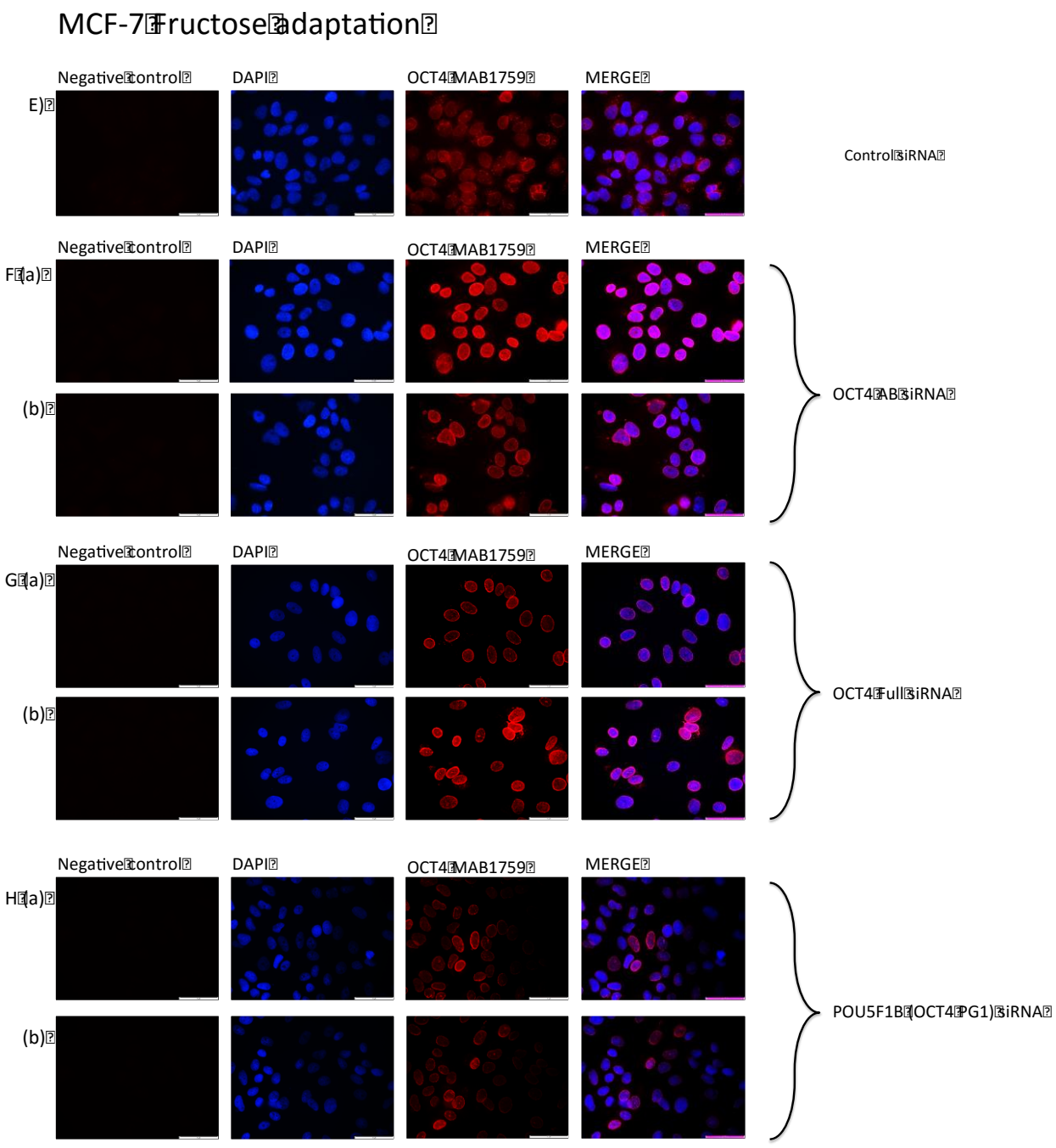

Figure 4.26 Characterisation of the intracellular localisation of OCT4 in MCF-7 cell line under glucose (A, B, C, and D) and fructose E, F, G, and H) conditions following transfection with different OCT4 siRNAs. OCT4 was silenced using three different siRNAs. One siRNA targeted against regions of the full length target mRNA of OCT4 and OCT4 PG1; the other targeted only the OCT4 PG1, and the last one target OCT4A and OCT4B only. Immunofluorescence images showing the expression of OCT4 protein (Red) detected using a polyclonal anti-OCT4 antibody targeting the full length OCT4 and OCT4 PG1 (OCT4 MAB1759). Nuclei of cells were stained with DAPI, presented in blue. The negative control was with secondary antibody only. Scale bar represent 20 µm.

4.3.3 The effect of OCT4 and SOX2 in mammosphere formation

4.3.3.1 SOX2 is not essential to represent stem-like properties and differentiation abilities

Knowing that OCT4 and SOX2 expression is relevant to pluripotency maintenance and may therefore affect the stemness potential, their role in the presence of CSLCs was investigated. Hence, a mammosphere formation assay was developed as an *in vitro* culture assay for tumour formation and the role of OCT4 and SOX2 expression in this population was investigated. SOX2 has been shown to be important in breast carcinoma and more notably in metastasis.

To study the role of SOX2 in mammosphere forming ability, SOX2 was silenced in MCF-7 cells adapted to either glucose or fructose conditions for 48 hours. siRNA transfected cells were plated to form mammospheres for five days. Spheres ≥50 were counted to measure the effect of SOX2 in CSLC. Consistent with previous data, MFE was significantly higher by about two fold under fructose conditions. Data revealed that SOX2 knockdown did not significantly reduce MFE in MCF-7 cells in both groups suggesting that SOX2 is not essential for stemness properties (Figure 4.27).

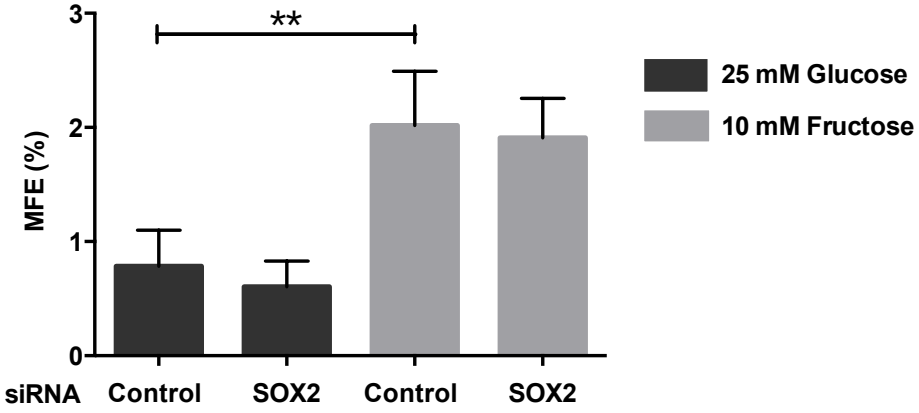

Figure 4.27 The evaluation of MFE following SOX2 silencing in MCF-7 cell line. MCF-7 cells were transfected with SOX2 specific siRNA for 48 hours. 5000 single cells were seeded to form mammospheres, cultured for five days under mammosphere conditions. Each experiment was repeated three times and performed in triplicate. Results were presented as mean ± SEM. Statistical analysis was performed using GraphPad Prism. ** $P \leq 0.01$. n=3

4.3.3.2 OCT4 is essential for retention of stemness in MCF-7 cells

The effect of OCT4 as a marker of CSLCs was examined in mammosphere formation in MCF-7 cells in different metabolic conditions, fructose and glucose. OCT4 was silenced using different siRNAs targeting against different variants.

4.3.3.2.1 Effect of silencing full length OCT4 in mammosphere formation

To investigate how OCT4 affects the stem cell population of MCF-7 cells, OCT4 was silenced using an siRNA targeting against the full length gene and OCT4 PG1. MFE was evaluated upon this siRNA transfection. The absence of OCT4 significantly reduced the number of stem cells in the population by a similar ratio in both glycolytic groups (Figure 4.28).

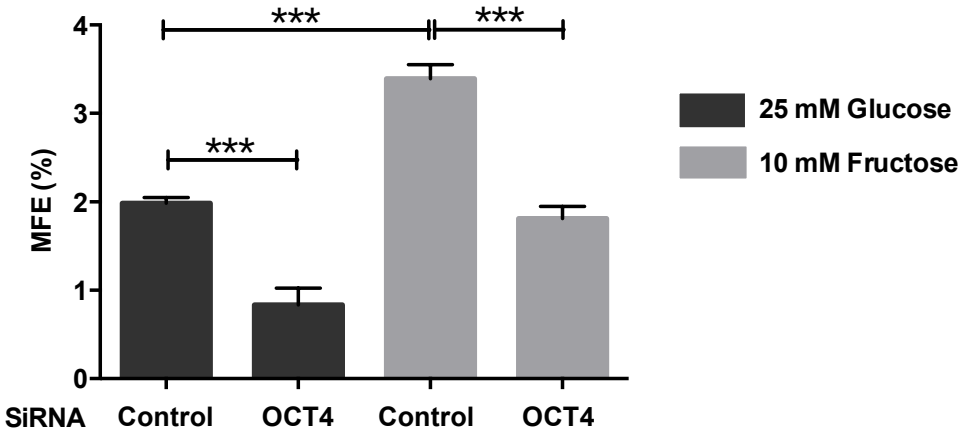

Figure 4.28 The evaluation of MFE following OCT4 silencing in MCF-7 cell line. MCF-7 cells were transfected with OCT4 full length siRNA for 48 hours. 5000 single cells were seeded to form mammospheres, cultured for five days under mammosphere conditions. Each experiment was repeated three times and performed in triplicate. Results were presented as mean ± SEM. Statistical analysis was performed using GraphPad Prism. *** $P \leq 0.001$. n=3

4.3.3.2.2 Effect of silencing OCT4A and OCT4B (OCT4A/B) in mammosphere formation

To further investigate whether the attenuation of MFE following OCT4 knockdown was related to OCT4 isoforms, OCT4 was silenced using a specific siRNA targeting against the C-terminus of the gene to target both isoforms, A and B. Results show that the absence of these OCT4 isoforms significantly reduced the MFE in fructose adapted cells by ~5 folds. However, the reduction in MFE was not significant under glucose conditions (Figure 4.29).

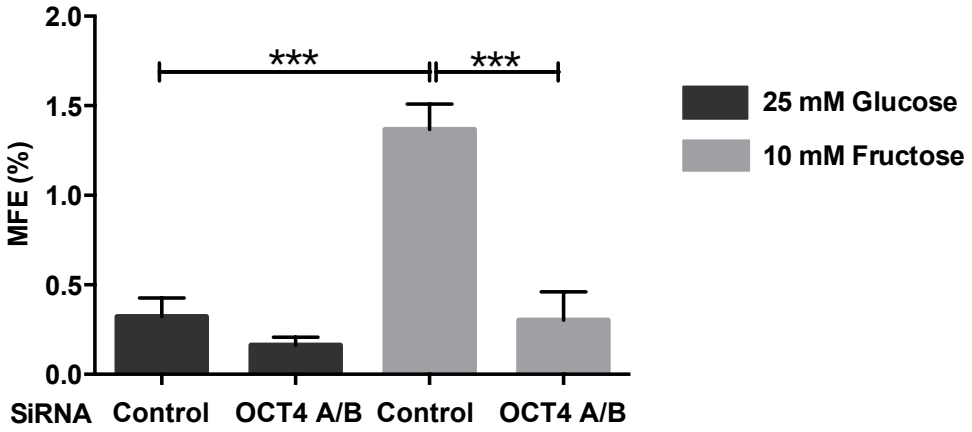

Figure 4.29 The evaluation of MFE following OCT4 silencing in MCF-7 cell line. MCF-7 cells were transfected with OCT4 specific siRNA targeting two main isoforms A and B for 48 hours. 5000 single cells were seeded to form mammospheres, cultured for five days under mammosphere conditions. Each experiment was repeated 3 times and performed in triplicate. Results were presented as mean ± SEM. Statistical analysis was performed using GraphPad Prism. *** $P \leq 0.001$. n=3

4.3.3.2.3 Effect of silencing OCT4 PG1 in mammosphere formation

Detection of OCT4 and its efficacy as a marker of pluripotency in breast cancer cell lines has been challenged recently but could be due to artefacts generated by pseudogene transcripts. OCT4 PG1 is known to be transcribed in cancer cell lines and is absent or expressed at lower levels in embryonic carcinoma cells. This is consistent with our previous data shown by RT-PCR and Western blot analysis. Therefore the role of OCT4 PG1 in tumorigenicity was investigated in the stem cell population of MCF-7 breast cancer cell line via mammosphere assay. Results revealed that knocking down OCT4 PG1 using specific siRNA significantly attenuated mammosphere formation in MCF-7 cells in both groups (Figure 4.30).

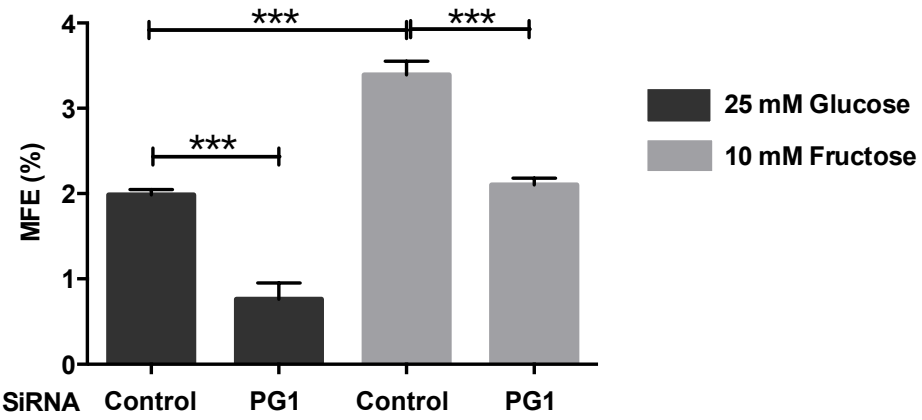

Figure 4.30 The evaluation of MFE following OCT4 PG1 silencing in MCF-7 cell line. MCF-7 cells were transfected with OCT4 PG1 specific siRNA for 48 hours. 5000 single cells were seeded to form mammospheres, cultured for five days under mammosphere culture. Each experiment was repeated three times and performed in triplicate. Results were presented as mean ± SEM. Statistical analysis was performed using GraphPad Prism. *** $P \leq 0.001$. n=3

To sum up, this result chapter points out some important highlights regarding the role of stem cell markers in breast cancer. Most importantly, we have shown that OCT4A is not expressed in breast cancer cells line, while evidence indicated the presence of an isoform/pseudogene of OCT4 in MCF-7 cells, which is also involved in the formation of tumour initiating cells and, therefore, are important in stemness maintenance. Moreover, another highlight of this chapter was the higher expression of OCT4 and SOX2 in glycolytic restriction which is also beneficial to the CSLC population.

4.4 Discussion

Different *in vitro* studies have been carried out in this project to investigate the role of stem cell factors SOX2 and OCT4 in breast cancer cell lines and the breast CSL population.

Like other studies, a standard RT-PCR technique was initially applied to assess the mRNA expression of OCT4 and SOX2 in different breast cancer cell lines, using specific primer sets. Consistent with the results from Ling *et al.* 2012 (193), we have shown both at the protein and mRNA levels that SOX2 is expressed in breast cancer cell lines. A greater intensity of expression was seen in less aggressive luminal-like MCF-7 and T-47D as opposed to basal-like MDA-MB-231 and SkBr-3 cells (Figure 4.1). However, this finding was contradicted by others, indicating that SOX2 was preferentially expressed in tumours with basal-like phenotype and also was significantly and more frequently detected in basal-like breast carcinomas (194) (195). This contradiction may be due to the use of primary tissues in these studies, rather than cell lines.

The investigation of SOX2 expression levels in different glycolytic conditions showed that in restricted glycolytic conditions (fructose conditions), MCF-7 cells expressed higher levels of SOX2 by about three fold. As SOX2 is well known as a key stem cell marker, these results could therefore suggest that contrary to the literature, fructose could provide a better energy source (compared to glucose) for stem cells. In the No-RT experiment, the Ct values obtained for SOX2 were sufficiently different between the "with RT" (Ct ~30) and "without RT" (Ct ~35) in fructose cultured cells, suggesting that the increase in SOX2 mRNA in fructose cultured cells is true.

Using an OCT4 full length primer set, OCT4 mRNA was found to be more highly expressed in NT2 cells (positive control for OCT4) compared with breast cancer cells. Importantly we have shown that OCT4A was not present in somatic MCF-7 cells both at protein and mRNA levels which aligns with the data obtained in other studies (196) (190). Conversely, OCT4B was detected at very low levels in MCF-7 cells (196) (190), confirming observations in other studies. Additionally, the OCT4 PG1 transcript can produce a protein similar to OCT4A, containing N, C- terminal and POU domain. Therefore, the mouse anti-OCT3/4 (Sc-5279) monoclonal antibody (raised against amino acids 1-134 of OCT-3/4 of human origin) could experimentally detect the protein

expression of OCT4 PG1. However, OCT4 PG1 could be discriminated from OCT4A according to the size differences in Western blot analysis. Accordingly, using an OCT4 (Ab19857) antibody against OCT4A and OCT4B, a protein was detected in breast cancer cells at ~48 kDa. The detected band appeared larger than OCT4A in NT2 cells, suggesting that the identified protein did not belong to OCT4A as was proved previously. Moreover, OCT4B has a lower molecular weight (~35 kDa) compared to that of OCT4A. Therefore, the identified protein could not belong to OCT4B either. The higher density of the bands in MCF-7 and MDA-MB-231 cell lines and the weaker signal in NT2 cells were comparable with Warthemann *et al*. observation (66). This band is thought to belong to an OCT4-related protein (OCT4 PG1) that is likely to have higher expression in breast cancer cell lines (Figure 4.14B). An additional band at ~50 kDa was detected using the OCT4 (Ab19857) antibody in NT2 cells which was also in concordance with the results obtained by Warthemann *et al*. (66) and Bhartiya *et al*. (197). Alternative forms of protein variation in OCT4 (OCT4B, OCT4 pseudogenes, could be the possible reasons behind the size shifts on western blot.)

To further decipher the expression of OCT4, a different antibody targeting the full length OCT4 was used to assess whether any isoforms/pseudogenes of OCT4 was expressed in breast cancer cell lines. Hu *et al*. (89) showed that OCT4 was expressed at high levels in human breast cancer MCF-7 cells. Moreover, they reported a successful reduction in OCT4 expression levels, using an siRNA which eventually resulted in cell apoptosis (89). To discover which OCT4 isoforms were expressed in MCF-7 cells, cells were transfected with an siRNA, targeting OCT4A and OCT4 PG1, and an OCT4 (MAB1759) antibody was used to detect the full length OCT4. Neither siRNAs silenced OCT4 in NT2 cells when probing with OCT4 (MAB1759) antibody. However, siRNA2 showed that the protein was silenced in NT2 cells when OCT4 (Ab19857; raised against OCT4A and OCT4B) was used, suggesting that the silenced protein in the lower band in NT2 cells (~43 kDa) was related to the OCT4A isoform due to its molecular weight. The upper unaffected band might be associated with an OCT4 related protein which was not targeted with siRNA2 (Figure 4.15B). Moreover, as was previously concluded, the OCT4 PG1 expression appeared weaker in NT2 cells than in MCF-7, suggesting that the targeted mRNA in NT2 cells was more likely to be related to OCT4A than OCT4 PG1.

In MCF-7 cells, the intensity of OCT4 band was reduced following application of siRNA10, using both OCT4 antibodies. Although it was not possible to distinguish the OCT4A protein from the OCT4 PG1, based on the predicted molecular masses and previous results showing that OCT4A was not expressed in breast cancer cell lines, the silenced protein is thought to be related to OCT4 PG1 (Figure 4.17B). Moreover, the unaffected bands in MCF-7 cells could be related to a protein that was not silenced and targeted by OCT4 (Ab19857) antibody, indicating the potential expression of alternatively transcribed OCT4 isoforms (OCT4 B1) and translated pseudogenes in MCF-7 cells (Figure 4.17).

In addition to the two main OCT4 isoforms, the expression and transcription of OCT4 pseudogenes in different cancers was detected by Suo *et al.* (198). Different studies also reported the same observations (70) (198). A year later in 2006, de Jong and Looijenga announced that highly homologous pseudogenes and other OCT4-related genes may have been the cause of false positive artefacts arising in RT-PCR analysis (73). According to Zhao *et al.* OCT4 PGs can produce protein products; all may be localized to the nucleus. OCT4 PG3 can also be localized in the cytoplasm. The positive staining of OCT4 using an anti-OCT4 antibody (Ab18976) also indicated the expression of OCT4 PGs in tumour cell lines and tumour tissues (62). Due to high levels of homology between OCT4A and OCT4 PG1, it was intriguing to further investigate the expression of OCT4 PG1 in breast cancer cell lines. Moreover, since it was practically difficult to entirely eliminate genomic DNA from RNA preparations, the No-RT method was included in the experiments. Since many of the papers that claim to show OCT4 PG1 expression did not include such controls, the inclusion of such controls was important to test OCT4 PG1 expression in this study. The RT-PCR results (including the RT enzyme) showed a higher expression of OCT4 PG1 in breast cancer cell lines compared with NT2 cells. However, in the No-RT experiment, the Ct values for OCT4 PG1 were obtained at similar levels between with and without RT in both glycolytic conditions, while this value was clearly different for actin. This indicated that the detected products could possibly be due to the contaminating DNA.

Metabolic adaptation is considered one of the hallmarks of cancer cells. Moreover, cancer cells are believed to be highly reliant on glycolysis for energy production. Therefore, the potential changes following alteration in metabolic state of cells was assessed in MCF-7 proliferation and the expression levels of OCT4 were evaluated following this change. At the protein level, nuclear and perinuclear staining from OCT4 was detected in MCF-7 cells using an OCT4 full-length antibody. The perinuclear staining was detected with higher intensity under fructose conditions, suggesting that less glycolytic cells have enhanced expression of OCT4 in their population. This provides possible evidence that OCT4 is regulated similarly to SOX2 by glycolysis in breast cancer cells. Further, it was clear that OCT4A was not expressed in breast cancer cell lines. However, the nuclear staining of OCT4 was intriguing so investigation of the role of other isoforms/pseudogenes in MCF-7 cells was performed. OCT4 protein was detected with the same intensity to those in control groups following OCT4 PG1 siRNA transfection (Figure 4.26). Furthermore, when probing with the OCT4 full-length antibody, a large portion of NT2 cells had been silenced using an siRNA targeting the full length OCT4, while almost all of the cells were detectable with the same intensity to those in control groups following OCT4 PG1 siRNA transfection. In MCF-7 cells, almost all OCT4 and OCT4 PG1 siRNA transfected cells displayed no expression of OCT4-related protein when probing with the full-length antibody. This suggests that an isoform/pseudogene with high homology to OCT4A, likely OCT4 PG1, is absent in NT2 cells. Together with the previous finding, this suggests that in NT2 cells the silenced protein could be related to OCT4A and that the expressed protein in MCF-7 cells is likely to be OCT4-related. Similar results were obtained with Western blot analysis in NT2 cells when probing with the OCT4 full-length antibody following OCT4 and OCT4 PG1 siRNA transfection. The OCT4 protein was silenced only in the population transfected with OCT4 siRNA targeting the full-length OCT4. Consistent with the previous data, OCT4 was silenced in MCF-7 cells using an siRNA against the full length OCT4 and OCT4 PG1, using an OCT4 (MAB1759) antibody. However, it was only under fructose conditions that OCT4 was silenced (no expression of protien was detected) using an OCT4 PG1 specific siRNA. The OCT4B variant was only detected in MCF-7 cells at about 23 kDa when probed with the OCT4 (MAB1759) antibody. Similar silencing pattern at about 23 kDa was seen as at 48 kDa indicating that less OCT4 protein was expressed following OCT4 siRNA transfection compared with OCT4

PG1 siRNA transfection when probing with OCT4 (MAB1759) antibody. It can be concluded that the detected protein at about 48 kDa in MCF-7 cells was more likely to be OCT4-related.

To determine the identification of the expressed protein and to clarify the protein is not OCT4A or OCT4B related, an additional siRNA targeting against the two main OCT4 isoforms were used and the expression levels of OCT4 assessed subsequently in glucose and fructose conditions.

Glucose condition: knowing that OCT4A was not expressed in MCF-7 cells, and OCT4B was cytoplasmically localised, a similar expression pattern to those of control cells following OCT4A/B silencing suggest that the expressed protein could be either non-OCT4 related or related to a new isoform/pseudogene. Moreover, it was shown that when OCT4 PG1 was silenced, almost all the cells in the population displayed very low or no protein expression when probing with OCT4 full length antibody. This suggests that the expressed protein could be likely related to OCT4 PG1.

Fructose condition: the OCT4-related protein was more highly expressed under fructose conditions using all three siRNAs which was similar to the observation with SOX2, that fructose improved the conditions for stem cell population.

It is noteworthy to mention again that the CSLC population of MCF-7 cells preferred fructose conditions as confirmed by MFE. Leis *et al*. reported that not only did SOX2 overexpression lead to enhanced ability of sphere formation, its expression seemed to induce stem-like features in MCF-7 cells (58). They also reported that silencing SOX2 reduced the tumour size and delayed tumour formation in a mouse xenograft model (58). In contrast, results here indicated that SOX2 did not significantly affect mammosphere formation in MCF-7 cells, suggesting that although SOX2 is a stem cell marker, it was not an essential factor in inducing CSLC growth.

CSLCs have been found in tumours expressing OCT4 (89). OCT4A was shown to be mainly expressed in a rare population with $ALDH^+$ phenotype, while OCT4B was reported to be expressed in differentiated tumorspheres (199). Moreover, OCT4 might maintain the survival of CSLCs partly through Oct4/Tcl1/Akt1 by inhibiting apoptosis which strongly indicates that targeting OCT4 may have important clinical applications in cancer therapy (89). In cervical cancer, OCT4A appeared to be responsible for stemness in CSLCs and induced carcinogenesis. Whereas OCT4B triggered tumour

growth by promoting apoptosis and EMT. This increased the probability that OCT4A and OCT4B were involved in regulating cancer development (199). There is a high probability that OCT4 positive cells represented CSLCs and that OCT4 expression was required for the self-renewal property of this rare population (200) (201). Data in this thesis were consistent with this assumption, showing that OCT4 expression was required for mammosphere formation, which is a stem-like functional assay, representing CSL properties. Furthermore, these findings suggest that silencing OCT4 may reverse cancer development.

There has not been an agreement on the metabolic features of CSLCs. Many believe that CSLCs are mainly glycolytic and others indicated that mitochondrial metabolism is instead the main source of energy in this population (202). CSLCs may adapt to their microenvironmental changes by shifting from one metabolic pathway to another or by attaining an intermediate metabolic phenotype when convenient. Therefore, the role of metabolism in CSLC population in carcinogenesis has become one of the major focuses in cancer research (202).

We have shown that the absence of two main isoforms, OCT4A and OCT4B, significantly reduced the MFE under fructose conditions. Additionally, we have shown that there was no expression of the OCT4 protein following OCT4 PG1 siRNA transfection under fructose conditions. Moreover, OCT4 and OCT4 PG1 siRNA transfection significantly decreased the population of CSLCs by reducing the MFE, leading to the conclusion that OCT4 is a critical factor for CSLC activity in MCF-7 cells and OCT4 PG1 could be involved in tumorigenicity. Our results, when taken along with others, suggest that investigations of OCT4 expression in cancers and stem cells could be an important step towards gaining a better knowledge of cancer stem cell biology.

Due to OCT4 artefacts and false positive results, there are several conflicting reports from OCT4 in the literature. Therefore, to avoid such problems leading to false interpretation in science, caution and careful interpretation of different experimental methods is required.

RT-PCR: during RT-PCR, artefacts derived from different splice variants of OCT4 can confuse analysis. Exon 1 is unique to the OCT4A transcript. Therefore, to discriminate OCT4A from other splice variants of OCT4, one of the primers should lie in exon 1 and primers should be intron spanning to avoid false PCR amplifications from OCT4

genome sequence and to make it possible to distinguish between the two main isoforms, A and B (203). Moreover, applying a No-RT additional step is of benefit to discriminate between false and real results. OCT4 PCR products need to be sequenced as an ideal step to determine which OCT4 isoform/pseudogene was expressed in the cell line. And to confirm the identity of the amplified PCR product.

Immunochemistry: the two main splice variants (A and B) are identical in their C-terminal domain. Therefore, the more accurate antibody to discriminate between the two isoforms has to be raised against the N-terminal domain which is specific to OCT4A. The OCT4A isoform seems to be localised in the nucleus, and is responsible for stem cell properties, while OCT4B mainly localises to the cytoplasm.

Western blot: in Western blot analysis, the C and N-terminus domain has to be taken into account when using antibodies. The signals from OCT4A will be larger in size due to the higher molecular weight compared with OCT4B. However, to be sure, it is highly recommended to use only monoclonal antibodies that recognize a single epitope in the N-terminal part of the protein (203). In this study, the results revealing no expression of OCT4A in breast cancer cell lines were obtained using a monoclonal antibody (Sc-5279 Santa Cruz).

It is noteworthy that, in OCT4 experiments, there were some contradictory results at protein and mRNA levels. A gap between the mRNA and protein levels exists due to different levels of post-transcriptional and post-translational regulation and the amount of transcript does not always correlate with the amount of protein products. The gene expression measured by qRT-PCR could be uncorrelated with the protein levels sometimes. qRT-PCR is quantitative, while Western blotting or even Immunofluorescence, will be at best semi-quantitative. Therefore, it is not easy to compare these methods directly.

Chapter 5

Metabolic modulation in breast cancer stem-like cells

5.1 Introduction

In mammals, after digestion, food is broken down into glucose, glutamine, and lipids to provide energy for differentiated and proliferating tissues (130). To survive, cells require sufficient energy and this is provided by cellular metabolism. Recent findings on how cancer cells display different metabolisms from that of differentiated cells have opened new insights into the possibility of targeting metabolic pathways to inhibit the tumour growth. An altered metabolic phenotype is a hallmark of highly proliferative tissues such as cancer cells and stem cells that may serve as promising targets for novel therapeutic intervention. ES cells and cancer cells share common metabolic shifts to increased glycolysis and decreased mitochondria respiration (133). Metabolic pathways in stem cells shift between glycolysis, mitochondrial respiration, and fatty acid oxidation (176) (204). Primary and metastatic cancers are defined as highly glycolytic as confirmed by PET image analysis (134). Hence, reducing glycolysis (e.g. fructose condition) could provide a less beneficial growing environment for these cells. Moreover, as already mentioned in the previous chapters, CSLCs are found to be involved in cancer recurrence. A successful treatment for the elimination of tumours has to target both cancer cells and CSLCs. Appropriate alterations in the balance of different metabolic pathways may create a better understanding of how the whole-body metabolism interacts with tumour metabolism (130). Therefore, modulation of metabolic pathways in CSLC population would be a promising approach to prevent tumour relapse.

CtBPs are of interest in metabolic studies as they maintain the metabolic homeostasis. Additionally, CtBPs are extensively expressed in tumour samples from breast cancer patients compared with surrounding non-tumour tissues. A possible way to reduce the metabolic activity of CSLCs could be to reduce CtBPs activity.

5.2 Aims

The specific aims of this chapter are:

- To investigate the effects of modulating different metabolic pathways in the bCSLC population of MCF-7 cells *in vitro* via mammosphere formation assay. This section was specifically aiming to assess the effect of different metabolic treatments on the survival of MCF-7 cells in 2D culture and to see whether these treatments affect the stem cell population of MCF-7 cells when analysing mammosphere forming ability.
- To investigate the role of CtBP and its inhibitor MTOB in sensing glycolysis to control stem-like cell formation.
- To investigate the expression levels of stem cell markers (SOX2, OCT4, and OCT4 PG1) in fructose and glucose adapted cells following different metabolic treatments.

5.3 Experimental outline

Variation in the number of mammospheres (stem cell population) is due to the effect of treatments applied in 2D culture. Therefore, a number of possible combinations of treatment in 2D and 3D culture were chosen to evaluate and compare each set. To obtain effective results, an optimum duration of treatment was necessary. Initially, prior to the mammosphere assay, MCF-7 cells were exposed to the desired treatments for 48 hours followed by 24 hours incubation without treatment. However, this 24 hour incubation between the treatment and data evaluation affected the results and eliminated the impact of treatment on the cell population. To overcome this problem, a 72 hour treatment without additional 24 hours with fresh media was chosen as an optimum treatment time. A 72 hour treatment was applied to the previously adapted cells (to either 25 mM glucose or 10 mM fructose) followed by five days in mammosphere culture with and without treatment. Mammospheres ≥50 μm were counted and MFE was calculated.

5.4 Glycolytic inhibition

5.4.1 Sodium oxamate, a glycolytic inhibitor

Cancers rely primarily on aerobic glycolysis with a high uptake of glucose compared with non-cancerous cells, leading to higher lactate production and therefore environmental acidification (130). High acidification causes an increase in the expression levels of a key glycolysis enzyme, lactate dehydrogenase (LDH), in the very last step of glycolysis where pyruvate is converted to lactate (132). High expression of LDH has also been reported in CSLC metabolic phenotypes. Moreover, LDH was shown to be an effective anti-cancer target (153). Therefore, one possible way to decrease the metabolic rates of CSLCs was to inhibit LDH activities. Blocking lactate production would increase the pyruvate flux into the mitochondrial glucose oxidation, leading to inhibition of glycolysis. Suppressing glycolysis leads to increased cancer apoptosis and tumour growth, mediated by oxidative stress in cancer cells (153).

In this study, sodium oxamate was used as a classic inhibitor of LDH. To assess the effect of sodium oxamate in the population of bCSLCs, an initial density of 250,000 cells were plated, treated with 25 mM oxamate for 72 hours in 2D culture, and counted following treatment. This concentration was determined to inhibit glycolysis in MCF-7 without disturbing mitochondrial function.

As expected, the growth rate was significantly reduced from ~2.8 to ~1.2 (~2 fold) following oxamate treatment in more glycolytic cells; while under fructose conditions, cells did not show sensitivity to oxamate (Figure 5.1).

Cells treated with oxamate were plated at a density of 5000 cells per well of a 12 well-plate for mammosphere culture for five days. One group received 25 mM oxamate in the condition media, while the other group was only fed with conditioned media. The control group received no treatment in either cultures. Following five days, mammospheres ≥50 μm were counted using an Olympus IX81 microscope fitted with a graticule.

Consistent with the previous results, MFE was significantly higher under fructose conditions by approximately three fold. Following 2D treatment only, MFE decreased significantly by two fold in more glycolytic cells. Moreover, comparing with the non-treated cells, sodium oxamate markedly reduced the stem cell population of glucose

adapted cells and prevented mammosphere formation by three fold when presented in 3D culture.

In the glycolysis restriction group (fructose), MCF-7 cells did not prove to be as sensitive to sodium oxamate for mammosphere formation as they were under glucose adaptation. Under fructose conditions, the MFE appeared higher compared with the control cells without any treatment in 2D and 3D culture. However, in the presence of oxamate in the conditioned media, the level of MFE dropped significantly around 1.5 fold which was less remarkable compared with the decrease observed in more glycolytic cells (Figure 5.2).

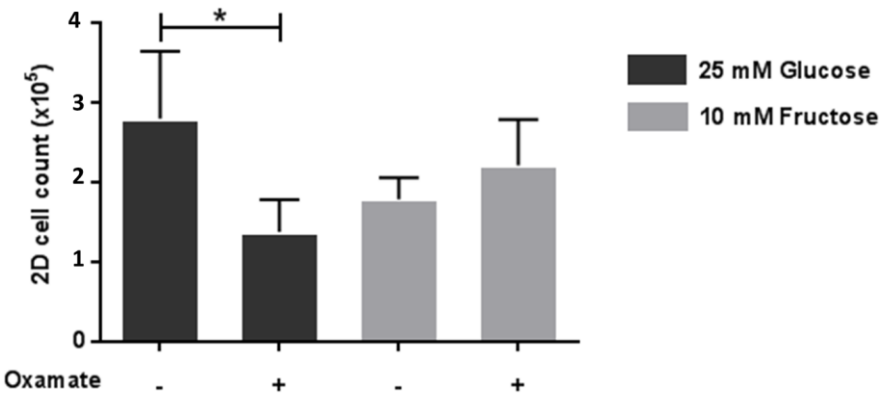

Figure 5.1 72 hour oxamate treatment in MCF-7 cell line. MCF-7 cells were adapted to either 25 mM glucose or 10 mM fructose for about three weeks in culture and were plated at an initial density of 250,000 cells per 60 mm dishes for 48 hours. Cells were treated with 25 mM oxamate for 72 hours in 2D culture and counted following treatment. The graph shows a combination of three independent experiments. Results are presented as mean ± SEM.

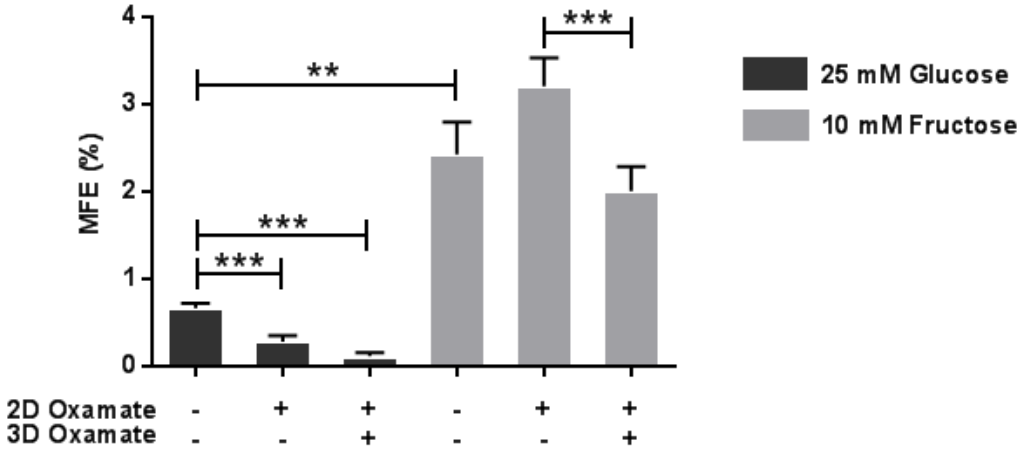

Figure 5.2 Mammsophere formation following oxamate treatment. Previously adapted MCF-7 cells were treated with oxamate for 72 hours in 2D culture followed by five days mammosphere culture (3D) with and without treatment. Non-treated and oxamate treated cells were plated at an initial density of 5000 cells for five days under mammosphere culture. Each experiment was repeated three times and performed in triplicate. Results are presented as mean ± SEM. ** $P \leq 0.01$, *** $P \leq 0.001$. n=3

5.4.2 2-Deoxy-D-glucose (2DG), glycolytic inhibition

One of the key glycolytic regulating enzymes is hexokinase II (HKII) which is upregulated in many cancers and competitively inhibits the production of glucose-6-phosphate (glucose-6-PO4) (the first step of glycolysis) from glucose (141). One possible way to prevent glycolysis is to inhibit such glycolytic enzymes. 2DG is a glycolytic inhibitor which inhibits the HKII enzyme. 2DG enters the cell through the glucose transporters (GLUTs), accumulates in cells and competes for glucose (204). It is known that cancer cells keenly up take up 2DG. During this process, the level of ATP drops and leads to cell death under hypoxia (135). Moreover, it has been reported that 2DG inhibits bCSLC proliferation (204). To investigate the effect of reducing glycolysis in breast cancer, MCF-7 cells were exposed to 10 mM 2DG for 72 hours in 2D culture and the effect of treatment was assessed on the cell growth. In more glycolytic cells, 2DG decelerated the growth of cancer cells by around 2.6 fold in 2D culture. The decrease was more striking in fructose adapted cells reducing from 2.2×10^5 to 0.3×10^5 cells (Figure 5.3).

Following 2D treatment, 5000 cells were plated under mammosphere culture conditions for five days and 2DG was added to the conditioned media. Mammospheres ≥50 μm were counted and MFE was calculated. The control group received no treatment. 2DG, when only applied in 2D culture, resulted in a downward trend in the MFE by around three fold under glucose conditions and by around two fold in fructose adapted cells ($P \leq 0.001$). Cells that received treatment in 2D culture were found to be more sensitive to the additional treatment in the 3D culture. The presence of 2DG in the conditioned media reduced mammosphere formation in this population irrespective of the type of sugar adaptation. However, the ability of forming mammospheres was entirely prevented in fructose adapted cells following 2DG treatment in 3D culture ($P \leq 0.001$) (Figure 5.4).

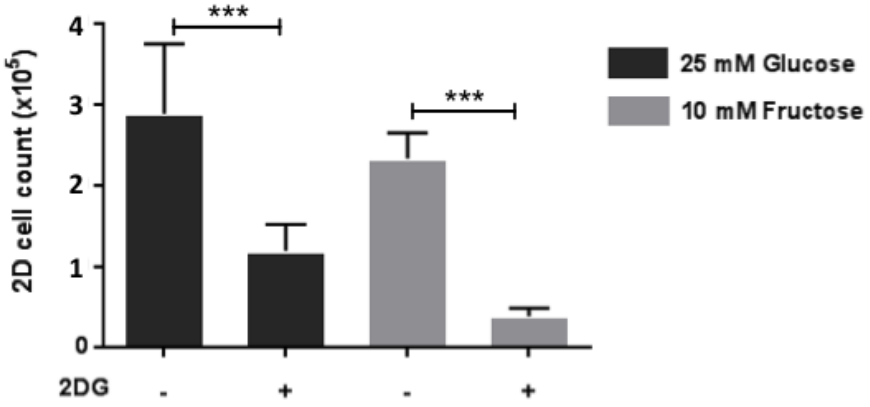

Figure 5.3 72 hour 2DG treatment in MCF-7 cell line. MCF-7 cells were adapted to either 25 mM glucose or 10 mM fructose for about three weeks in culture and were plated at an initial density of 250,000 cells per 60 mm dishes for 48 hours. Cells were treated with 10 mM 2DG for 72 hours in 2D culture and counted following treatment. The graph shows a combination of three independent experiments. Results are presented as mean ± SEM. *** $P \leq 0.001$. n=3

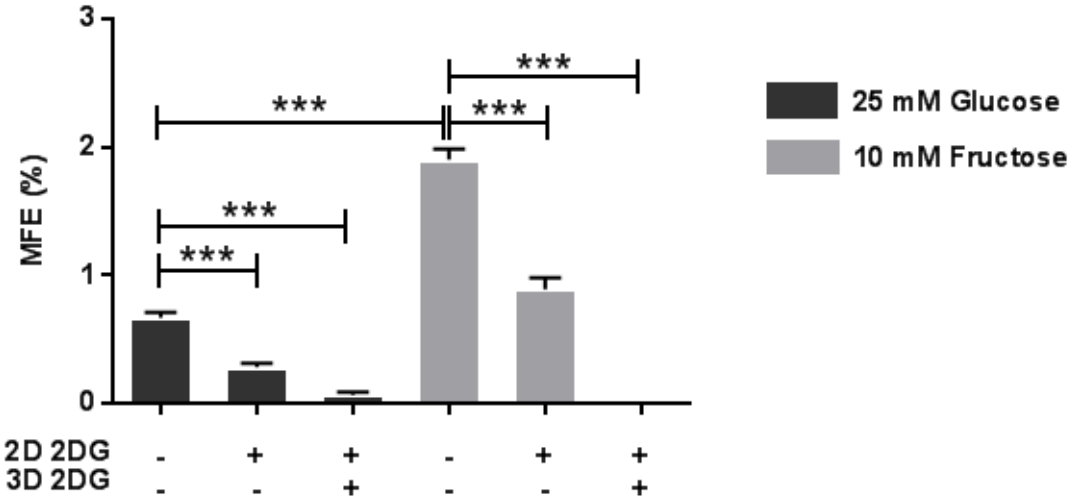

Figure 5.4 Mammosphere formation following 2DG treatment. Previously adapted MCF-7 cells to glucose and fructose, were treated with 10 mM 2DG for 72 hours in 2D culture followed by five days mammosphere culture (3D) with and without treatment. Non-treated and 2DG treated cells were plated at an initial density of 5000 cells for five days under mammosphere culture. Each experiment was repeated three times and performed in triplicate. Results are presented as mean ± SEM. ** $P \leq 0.01$, *** $P \leq 0.001$. n=3

5.5 Alternative nutrient sources

5.5.1 Glutamine starvation

Glutamine is a critical amino acid for the biosynthesis of proteins, lipids, and fatty acid synthesis. Some cancer cells rely on glutamine for their growth, survival, and to provide intermediates for the TCA cycle. Glutamine provides energy for cancer cells through the first step of the TCA cycle. Thus, glutamine withdrawal may reduce TCA cycle flux and ATP production, causing cell death (130). Moreover, the lack of glutamine has been reported to reduce the tumour growth rate both *in vitro* and *in vivo* (135). Considering the importance of glutamine in cancer cell survival, the effect of glutamine starvation was assessed in breast cancer MCF-7 cells.

MCF-7 cells were subjected to glutamine deprivation in 2D culture, adapted to grow in no glutamine DMEM including either glucose or fructose for approximately two weeks. Following adaptation, 250,000 cells were plated in media without glutamine for 72 hours. According to the growth rate, the absence of glutamine in 2D culture did not significantly reduce the cell numbers in either glycolytic conditions (similarly affected) (Figure 5.5).

A 72 hour glutamine deprivation in 2D culture was the only treatment to reduce the MFE significantly under fructose conditions ($P \leq 0.05$). However, when glutamine was eliminated from both 2D and 3D culture, the reduction in the MFE was found to be more striking; from 2.3×10^5 to 1.9×10^5 cells ($P \leq 0.001$). However, under glucose conditions, the absence of glutamine did not significantly reduce the mammosphere forming ability (Figure 5.6).

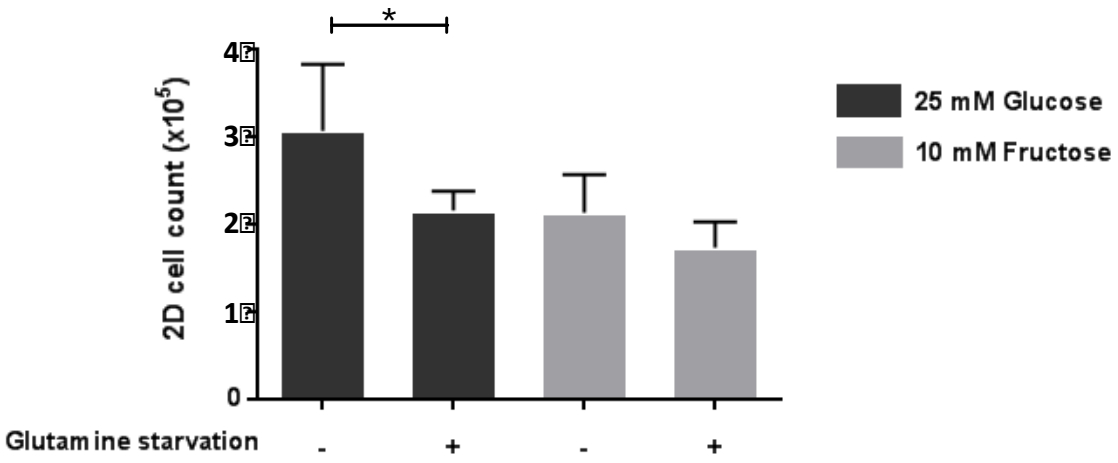

Figure 5.5 72 hour glutamine starvation in MCF-7 cell line. MCF-7 cells were cultured in the presence or absence of glutamine for approximately two weeks. Following adaptation, cells were plated at an initial density of 250,000 cells per 60 mm dishes in the presence or absence of glutamine for 72 hours in 2D culture, and cell number was counted. The graph shows a combination of three independent experiments. Results are presented as mean ± SEM.

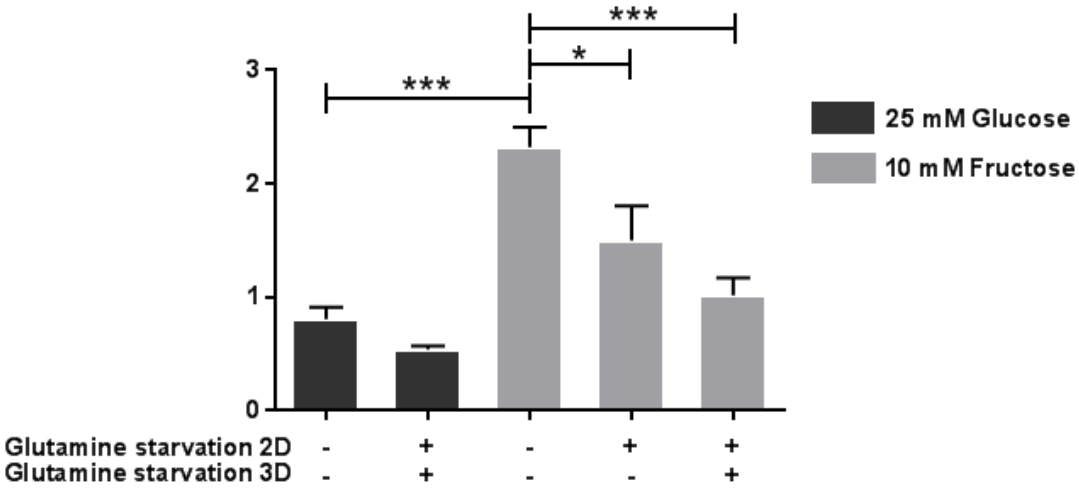

Figure 5.6 Mammosphere formation following glutamine starvation. MCF-7 cells were cultured in the presence or absence of glutamine for approximately two weeks. Following adaptation, non-treated and treated cells were plated at an initial density of 5000 cells and induced to form mammospheres for five days either in the presence of or the absence of glutamine. Each experiment was repeated three times and performed in triplicate. Each experiment was repeated three times and performed in triplicate. Results are presented as mean ± SEM. * $P \leq 0.05$, *** $P \leq 0.001$. n=3

5.6 Mitochondrial respiration

5.6.1 Metformin, inhibition of mitochondrial respiration

Metformin inhibits metabolism from different aspects. The inhibitory action of metformin on glucose metabolism comes from a combination of effects on glycolysis, fatty acid oxidation, and signalling pathways. Metformin impairs glycolysis by inhibiting the enzymatic activity of HK, resulting in less pyruvate production. Moreover, metformin inhibits the AKT signalling pathway which also reduces HK expression and mitochondrial interaction (162).

Metformin enters the cell through the OCT1 transporter and then enters the mitochondria and inhibits complex I of the electron transport chain, resulting in decreased NADH oxidation, TCA Cycle, and ATP synthesis. This results in reduced gluconeogenesis (less glucose formation from pyruvate) and increased glycolysis (more pyruvate formation from glucose). Metformin also inhibits CPT1, resulting in less acetyl CoA production and reduced fatty acid oxidation.

The following series of experiments were designed to test the hypothesis that metformin inhibits the growth of breast cancer cells and supresses the self-renewal of breast CSLCs (205). Different concentrations of metformin (10 µM and 50 µM) were used.

10 µM metformin: in 2D culture, under glucose conditions, metformin did not remarkably change the growth rates of treated cells compared with non-treated cells. However, under fructose conditions, the growth rate appeared higher for those receiving the treatment; although, the difference did not reach the statistical significance (Figure 5.7A).

50 µM metformin: similar results were obtained with 50 µM concentration under glucose conditions. Higher dose of metformin caused no difference in the growth rate of fructose adapted cells before and after treatment (Figure 5.7B).

The mammosphere assay was performed following 72 hour treatment with different concentrations of metformin for five days. 10 µM metformin significantly reduced the MFE at similar rates in both glycolytic conditions when presented in either culture systems (2D and 3D) (Figure 5.8A). Increasing the dose of metformin to 50 µM, the MFE dropped significantly when metformin was only present in the 2D culture (in both glycolytic conditions). However, in the presence of metformin in the mammosphere

culture, the MFE remained at similar levels to that of control and 2D treatment group (Figure 5.8B). It is noteworthy that under fructose conditions, in the presence of metformin in the conditioned media, the MFE was significantly higher compared with the group with 2D treatment only.

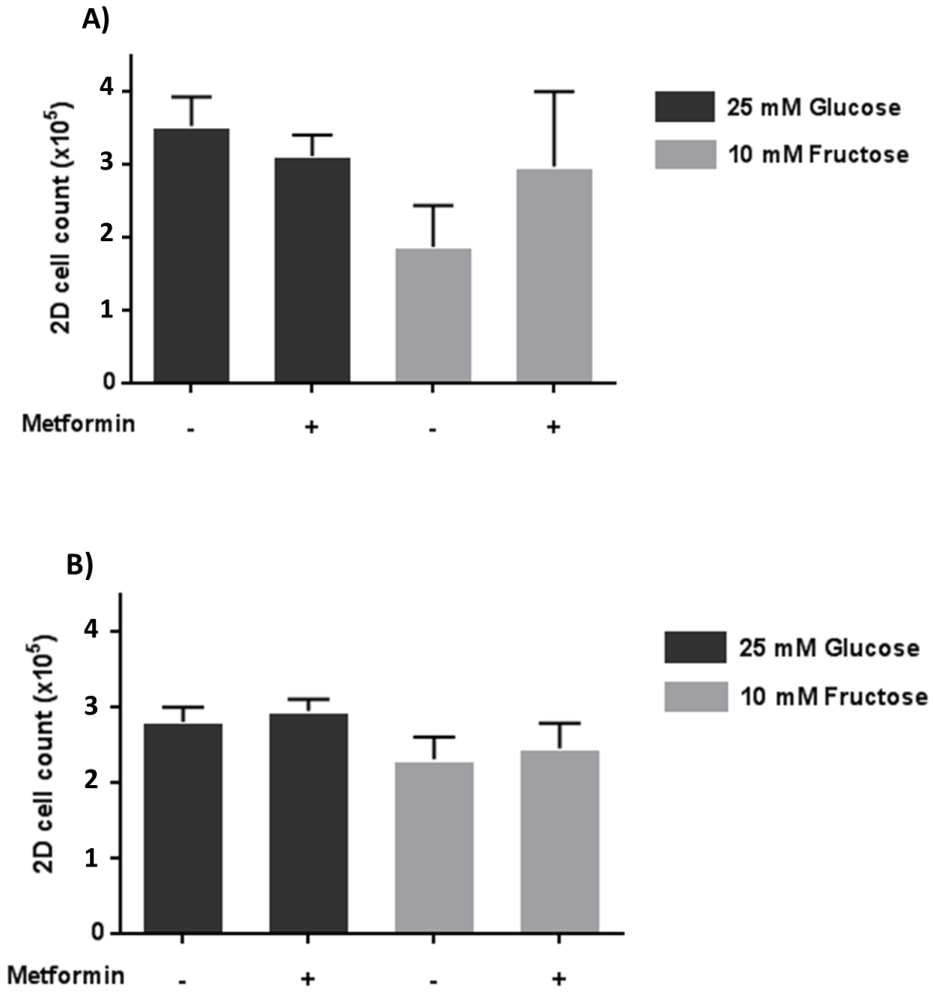

Figure 5.7 72 hour treatment with metformin in MCF-7 cell line. MCF-7 cells were adapted to either 25 mM glucose or 10 mM fructose for about three weeks in culture and were plated at an initial density of 250,000 cells per 60 mm dishes for 48 hours and were then expose to (A) 50 µM and (B) 10 µM metformin for 72 hours in 2D culture. The graph shows a combination of three independent experiments. Results are presented as mean ± SEM.

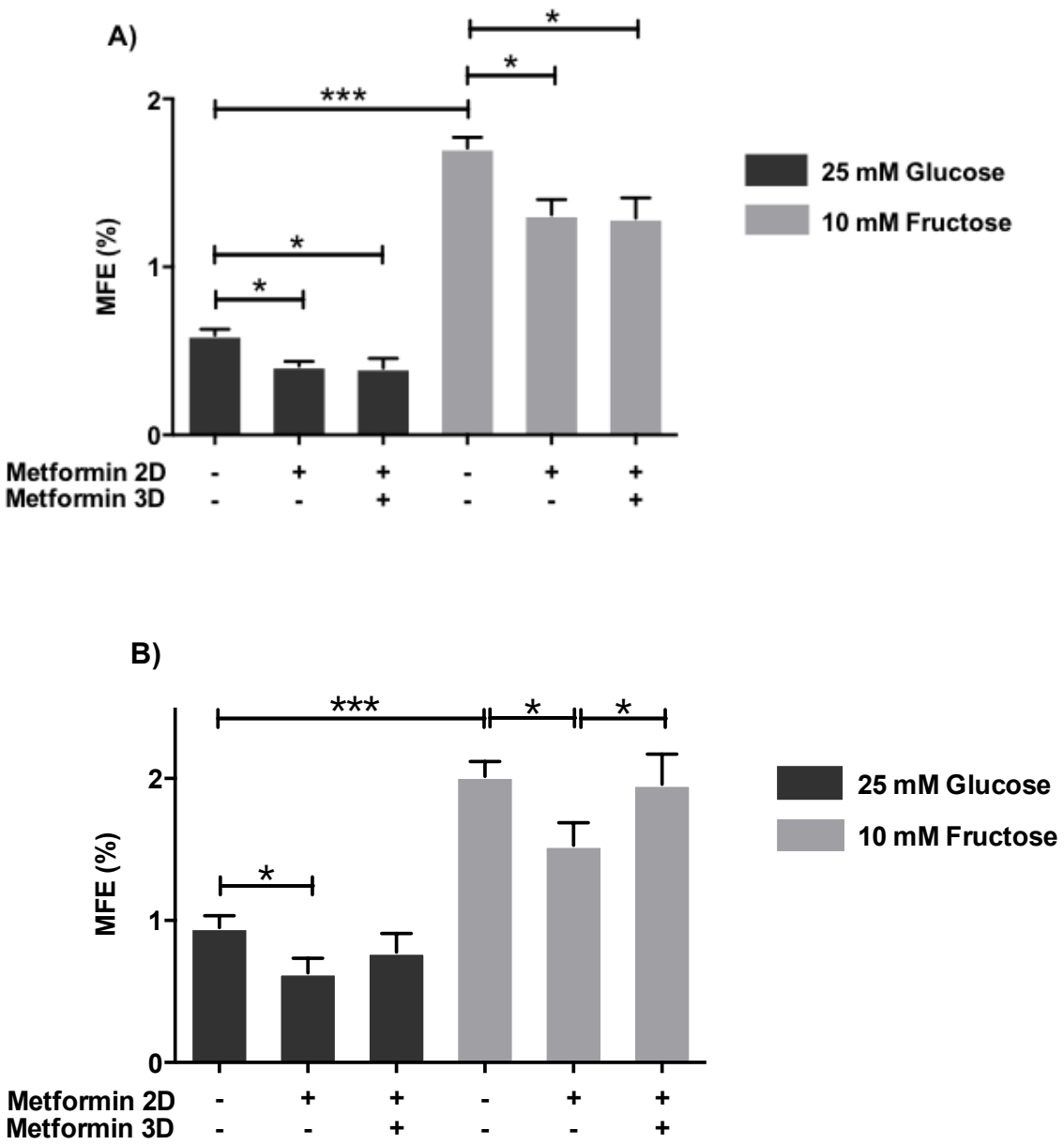

Figure 5.8 Mammosphere formation following metformin treatment. Previously adapted MCF-7 cells with glucose and fructose were exposed to 10 µM (A) and 50 µM metformin (B) for 72 hours. Non-treated and metformin treated MCF-7 cells were plated at an initial density of 5000 cells and were induced to form mammospheres for five days. MFE was calculated subsequently. Each experiment was repeated three times and performed in triplicate. Results are presented as mean ± SEM. * $P \leq 0.05$, *** $P \leq 0.001$. n=3

5.6.2 Dichloroacetate (DCA), mitochondria reactivation

Mitochondrial respiration consists of a set of metabolic reactions with the aim of generating ATP which is impaired in the majority of cancers (206). DCA is a mitochondria-targeting molecule that shifts glycolysis to glucose oxidation by inhibiting mitochondrial PDKI (138). This action increases the pyruvate flux into the mitochondria and therefore mitochondrial respiration (135). This could be more toxic to glycolytic cells that normally try to avoid channelling pyruvate into the mitochondria. Therefore, MCF-7 cells were exposed to 10 mM DCA for 72 hours which was reported to be a sufficient dose to activate mitochondria metabolism (207). As expected, more glycolytic cells showed a greater sensitivity to DCA. However, this result did not reach statistical significance (Figure 5.9). MFE was calculated following five days of mammosphere culture. Data demonstrated that DCA significantly reduced the MFE in more glycolytic cells when presented in both cultures. Under fructose conditions, DCA did not reduce the MFE when it was only applied to the cells in 2D culture. Adding DCA to the mammosphere culture resulted in MFE levels dropping significantly compared with other two conditions (Figure 5.10).

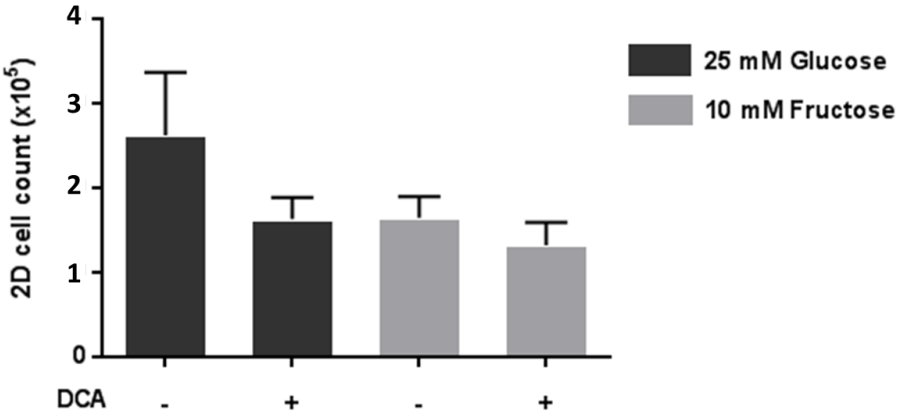

Figure 5.9 72 hour treatment with DCA in MCF-7 cells. MCF-7 cells were adapted to either 25 mM glucose or 10 mM fructose for about three weeks in culture and were plated at an initial density of 250,000 cells per 60 mm dishes for 48 hours. Cells were treated with 10 mM DCA for 72 hours in 2D culture and counted following treatment. The graph shows a combination of three independent experiments. Results are presented as mean ± SEM.

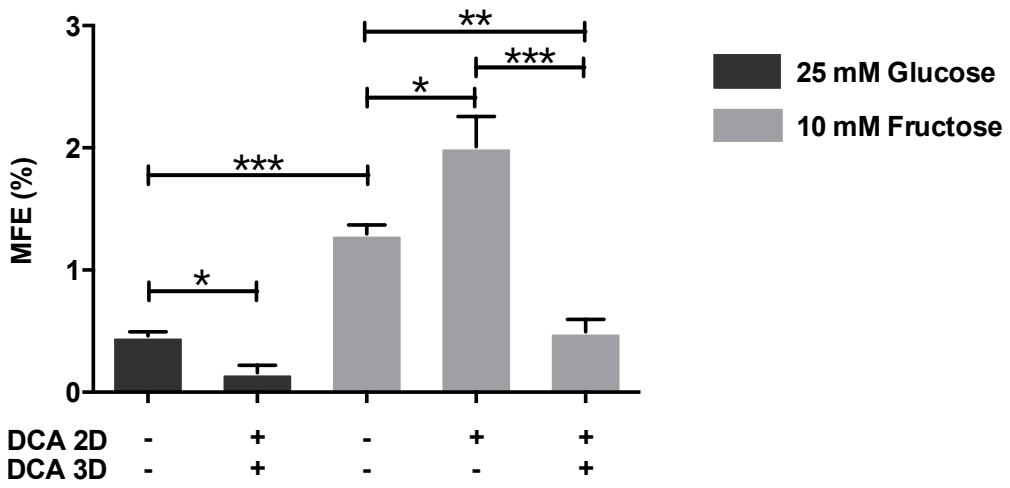

Figure 5.10 Mammosphere formation following DCA treatment. Previously adapted MCF-7 cells were treated with 10 mM DCA for 72 hours in 2D culture followed by five days mammosphere culture (3D) with and without treatment. Non-treated and DCA treated cells were plated at an initial density of 5000 cells for five days under mammosphere culture. Each experiment was repeated three times and performed in triplicate. Results are presented as mean ± SEM. * $P \leq 0.05$, ** $P \leq 0.01$, *** $P \leq 0.001$. n=3

5.7 Fatty acid oxidation (FAO)

5.7.1 Etomoxir, inhibitor of fatty acid oxidation

Fatty acids are required for cellular proliferation and cancer cell survival (208) (131). More differentiated cells rely primarily on OXPHOS to generate ATP, using three major sources: glucose, glutamine, and fatty acids (131). In non-cancerous cells long chain fatty acids are synthesized from glucose and stored as lipids. They enter the mitochondria through CPTl mitochondrial enzyme and converted to acetyl CoA through OXPHOS FAO to generate ATP. In cancers, fatty acid synthesis is at a higher rate to provide NADPH. In stem cells there is a shift between glycolysis, OXPHOS, and fatty acid synthesis during the maturation of adult stem cells. Therefore, fatty acid synthesis is an important metabolic pathway in many cell types. To control this metabolic pathway, etomoxir was used as an inhibitor of mitochondrial CPT1. Inhibition of CPT1 reduces the fatty acid flux into the mitochondria and therefore inhibits FAO (208). To investigate the effect of reducing FAO in breast cancer, MCF-7 cells were treated with 100 µM etomoxir in 2D culture for 72 hours (209). Results showed that etomoxir equally affected cell growth in both metabolic conditions by reducing the cell number (Figure 5.11).

Under glucose conditions, etomoxir reduced mammosphere formation by about three fold. In a low-glycolytic state, under fructose conditions, following the 2D-only treatment, etomoxir reduced the MFE from 3 to 1.5 (two fold). However, the presence of etomoxir in both cultures (2D and 3D) more dramatically reduced the MFE in this group. The MFE significantly dropped regardless of the presence of etomoxir in the conditioned media (3D culture) ($P \leq 0.001$) (Figure 5.12).

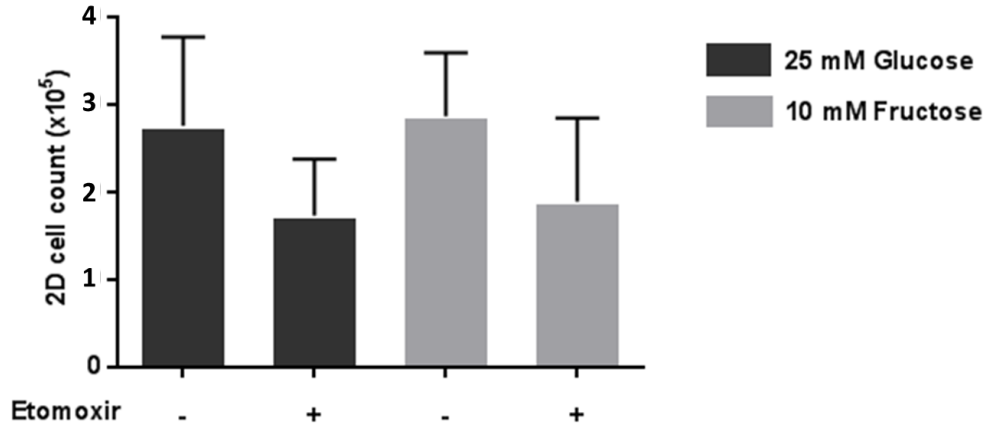

Figure 5.11 72 hour treatment with etomoxir in MCF-7 cells. MCF-7 cells were adapted to either 25 mM glucose or 10 mM fructose for about three weeks in culture and were then plated at an initial density of 250,000 cells per 60 mm dishes for 48 hours. Cells were treated with 100 µM etomoxir for 72 hours in 2D culture and counted following treatment. The graph shows a combination of three independent experiments. Results are presented as mean ± SEM.

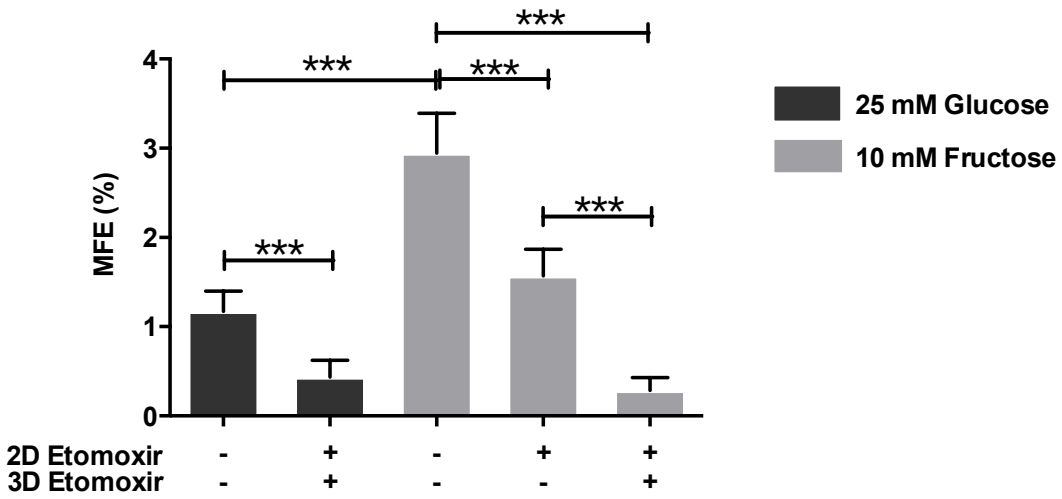

Figure 5.12 Mammosphere formation following etomoxir treatment. Previously adapted MCF-7 cells were treated with 100 µM etomoxir for 72 hours in 2D culture followed by five days mammosphere culture (3D) with and without treatment. Non-treated and etomoxir treated cells were plated at an initial density of 5000 cells for five days under mammosphere culture. Each experiment was repeated three times and performed in triplicate. Results are presented as mean ± SEM. *** $P \leq 0.001$ n=3

5.8 C-terminal binding protein (CtBP), a metabolic sensor

The CtBP transcriptional corepressors stimulate survival of cancer cells and promote their migration and invasion. Metabolic imbalance is often associated with over-activating metabolic sensors such as CtBPs. CtBP proteins are of interest as they bind to NAD^+/NADH and respond to the metabolic state of the cell; maintain cancer cell growth and metabolic homeostasis (210).

CtBP was reported to supress the expression of different tumour suppressor genes and induce the EMT during the cancer cell metastasis (173). CtBP independently reduces tumour initiation, progression, and metastasis by transcriptionally regulating genes related to stem cell pathways, genome stability, EMT, and cancer cell metabolism (171).

Therefore, to investigate the role of CtBP in the stem-like population of breast cancer, we firstly studied the expression levels of CtBP in MCF-7 cells. Subsequently, the expression levels of CtBP were further assessed following fructose adaptation. Furthermore, the effect of CtBP inhibition was investigated in the mammosphere formation in MCF-7 cells (results shown together).

5.8.1 CtBP1 and CtBP2 silencing

CtBP was silenced using a single siRNA, targeting both CtBP1 and CtBP2 (CtBP1/2). The expression levels of CtBP1 and CtBP2 were assessed independently upon transfection using specific antibodies. CtBP1 and CtBP2 protein were found to be expressed in the nucleus of MCF-7 cells. Expression was reduced following silencing CtBP1/2 (Figure 5.13B).

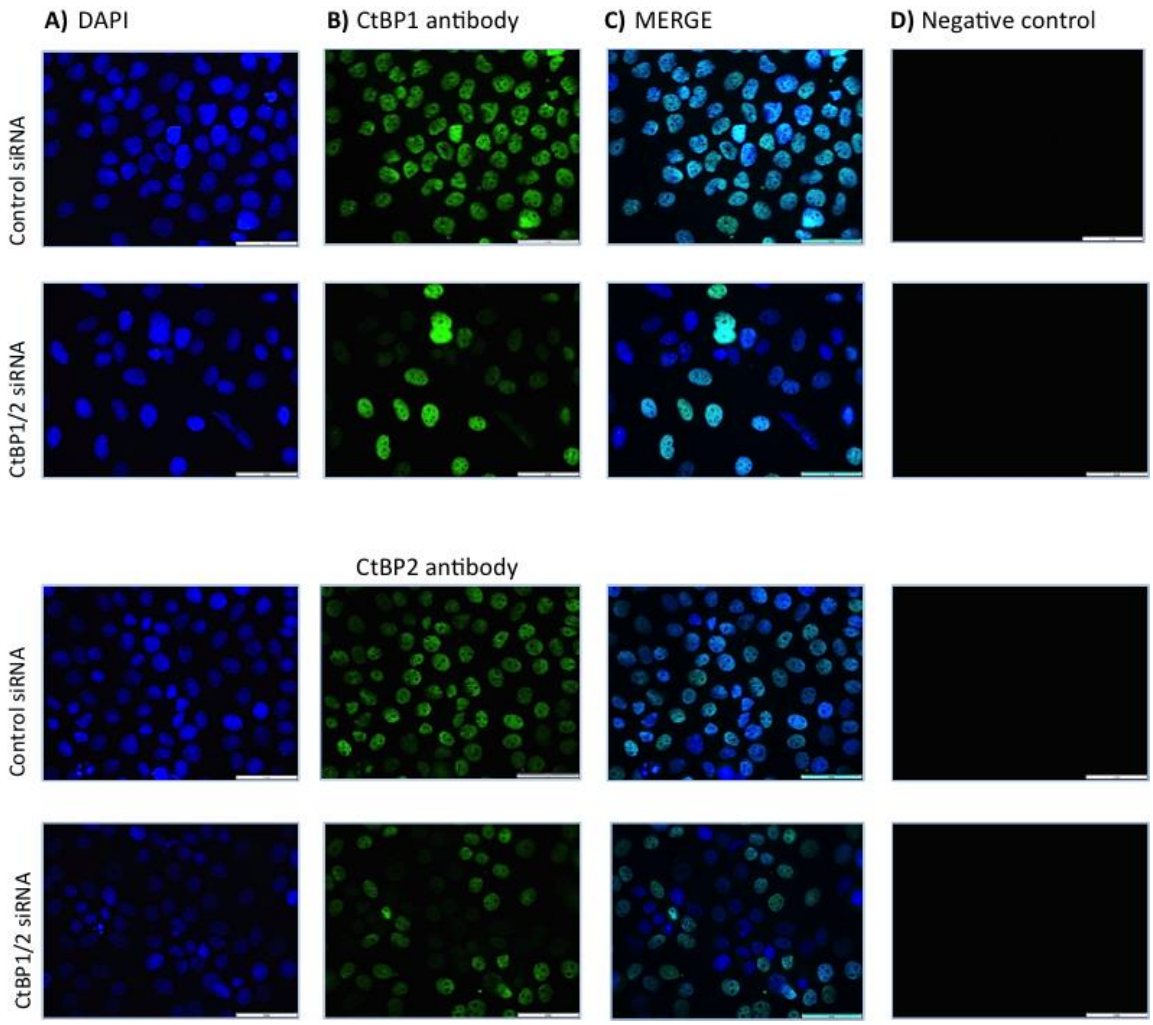

Figure 5.13 Characterisation of the intracellular localisation of CtBPs in MCF-7 cells. CtBPs were silenced using a single siRNA targeting both CtBP1 and CtBP2 (CtBP1/2). The blue staining represents DAPI-stained nuclei (A). Nuclear expression of CtBP protein (CtBP1 and CtBP2) was detected using CtBP antibodies, presented in green (B). Merge represents merge images of A and B (C). The negative control was with secondary antibody only (D). Scale bar represents 20 μm.

The expression levels of CtBP protein were further assessed by Western blot analysis in MCF-7 cells. The blot shows that CtBP1 was silenced using CtBP1 siRNA (Figure 5.14A). The blot shows that the intensity of CtBP2 protein band decreased with CtBP2 siRNA (Figure 5.14B). The loading control only shows four lanes for the top gel. However, CtBP1 was expected to knock-down following CtBP1/2 siRNA transfection.

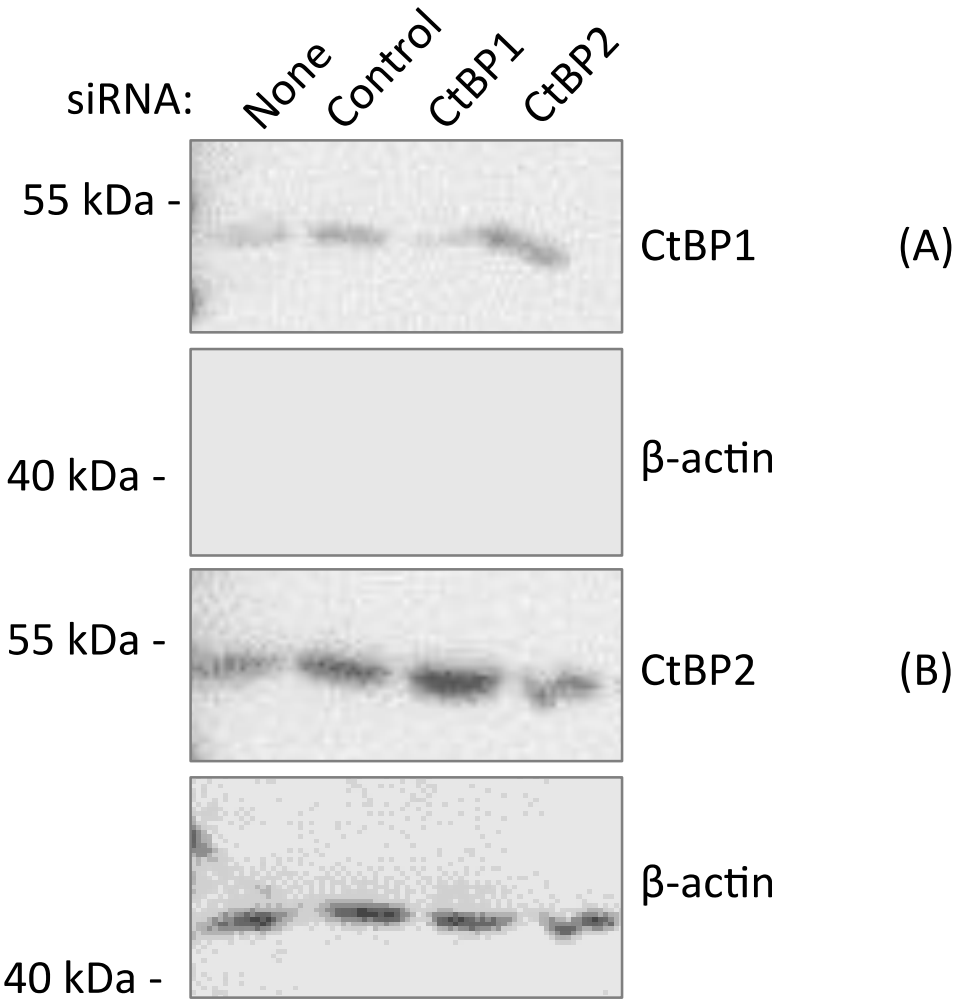

Figure 5.14 Characterisation of CtBP protein expression in MCF-7 cells by Western blot analysis. CtBP1 and CtBP2 protein were expressed in MCF-7 cells detected using CtBP1 and CtBP2 antibody respectively (A, B). CtBP1 and CtBP2 were detected using CtBP1 and CtBP2 antibodies respectively (A, B). First lane from left was served as a no treatment group (none). The control group represents control siRNA. β-actin was used as a loading control. Blots were exposed using BioRad FluoroS Multimager.

5.8.2 CtBP1 expression under glucose and fructose conditions

To investigate whether different glycolytic conditions affect CtBP expression, the expression levels of CtBP1 were further assessed under glucose and fructose conditions. CtBP1 was detected at about 48 kDa in both glycolytic conditions in MCF-7 cells. However, the intensity of the detected bands appeared either the same or slightly higher under fructose conditions. Therefore, the accuracy of the observation required further assessment (Figure 5.15).

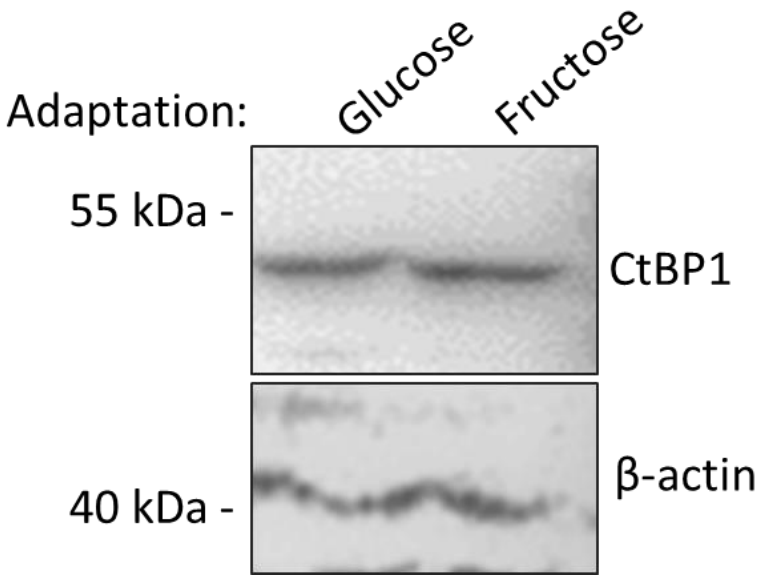

Figure 5.15 Characterisation of CtBP protein expression in MCF-7 cells adapted in either fructose or glucose by Western blot analysis. β-actin was used as a loading control. Blots were exposed using BioRad FluoroS Multimager. n=2

The expression levels of CtBP1 were further investigated using real time qPCR. CtBP1 mRNA expression was significantly increased in fructose compared with glucose adapted MCF-7 cells (Figure 5.16).

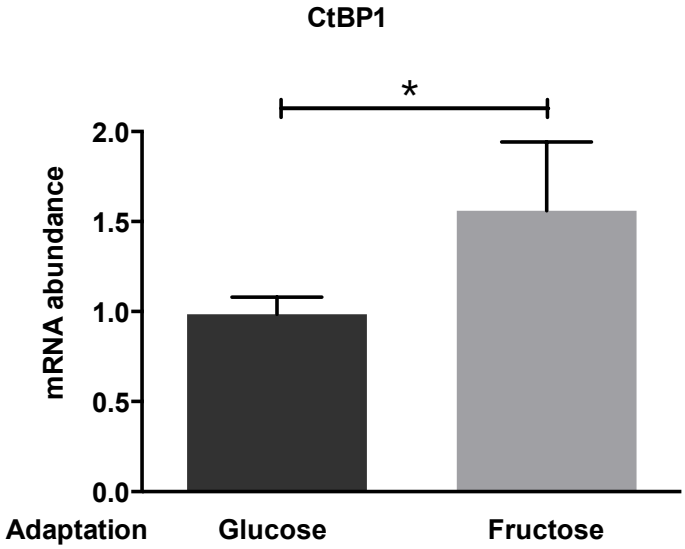

Figure 5.16 CtBP1 mRNA abundance under glucose and fructose adaptation in MCF-7 cells. CtBP1 mRNA expression levels were assessed by RT-qPCR in MCF-7 cells adapted in either fructose or glucose conditions. The Ct obtained for each cell line was normalised against the housekeeping gene β-actin. Relative mRNA abundance was calculated by normalising to β-actin. Results are presented as mean ± SEM. * $P \leq 0.05$ n=4

5.8.3 Mammosphere forming ability following CtBP siRNA transfection

To investigate the role of CtBPs in sensing glycolysis in the CSLC population of MCF-7 cells, CtBP was silenced using specific siRNAs targeting CtBP1 and CtBP2. siRNA transfected cells were seeded at a density of 5000 cells per well of 12 well-plate to form mammospheres. Mammospheres ≥50 μm were counted following five days culture. Under both metabolic conditions (fructose and glucose), the MFE declined dramatically in CtBP1/2 siRNA transfected cells with respect to the control group (Figure 5.17).

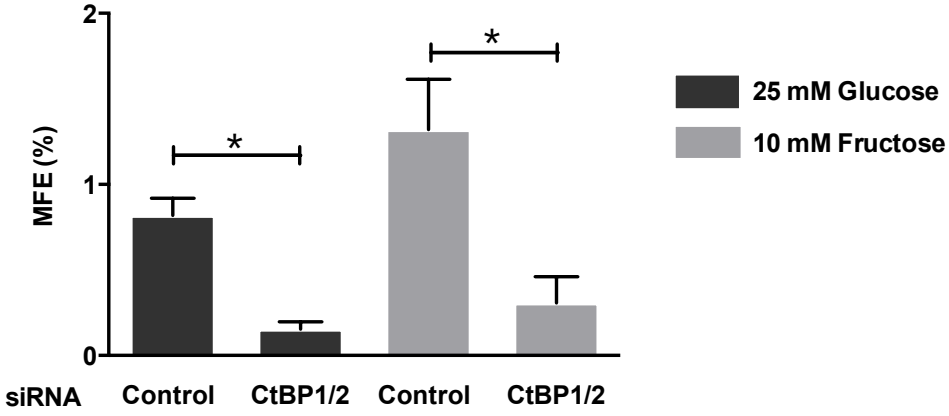

Figure 5.17 The effect of CtBP silencing on MFE in MCF-7 cells. MCF-7 cells were transfected with CtBP1/2 siRNA. 48 hours post-transfection, an initial density of 5000 cells were seeded per well and allowed to form mammospheres. Following five days culture, mammospheres ≥50 μm were counted. Each experiment was repeated three times and performed in triplicate. Results are presented as mean ± SEM. * P ≤ 0.05 n=3

5.8.4 4-methylthio-2-oxobutyric acid (MTOB), CtBP inhibitor

MTOB is a high affinity inhibitor to human CtBP which can be cytotoxic to cancer cells at high concentrations (172). Following CtBP silencing with siRNA, to investigate whether MCF-7 cells would respond to MTOB as they did to CtBP siRNA, MCF-7 cells were initially exposed to 4 mM MTOB in 2D culture for 48 hours and were allowed to form mammospheres for five days in conditioned media excluding treatment (172). Results revealed that 48 hours of treatment did not affect the mammosphere formation under either conditions (Figure 5.18).

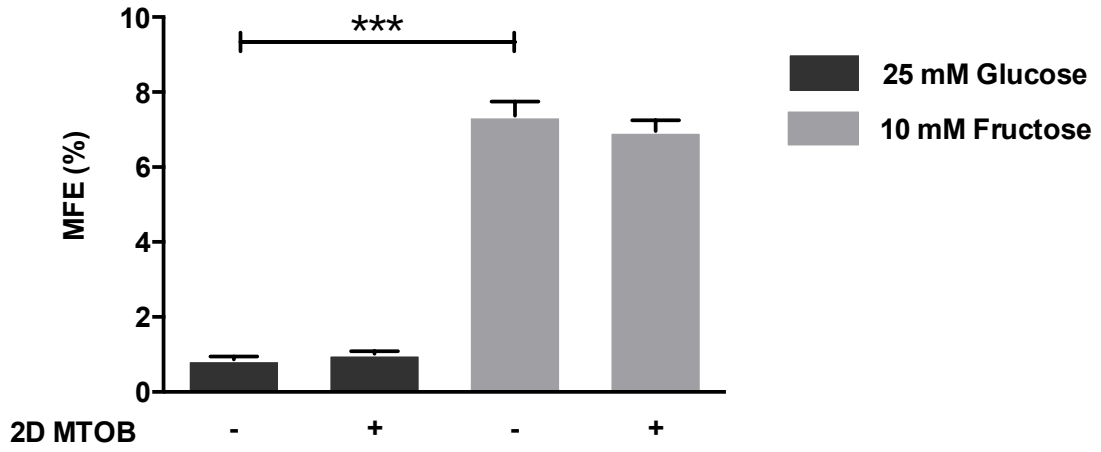

Figure 5.18 The effect of 48 hour MTOB treatment on mammosphere formation. Following 48 hour treatment with 4 mM MTOB in 2D culture, non-treated and treated cells with were seeded at an initial density of 5000 cells per well for five days under mammosphere culture. MFE was then evaluated. Each experiment was repeated three times and performed in triplicate. Results are presented as mean ± SEM. *** $P \leq 0.001$ n=3

Therefore, a longer treatment duration was considered and MCF-7 cells were exposed to MTOB for 72 hours in 2D conditions. There was a significant decrease in the cell growth following MTOB treatment (Figure 5.19). A dramatic drop was observed in the MFE by approximately 2.6 fold when cells were only exposed to MTOB in 2D culture ($P \leq 0.001$). Furthermore, MTOB was also applied to the mammosphere culture following treatment in 2D. Adding MTOB to the mammosphere culture entirely prevented the formation of mammospheres (Figure 5.20).

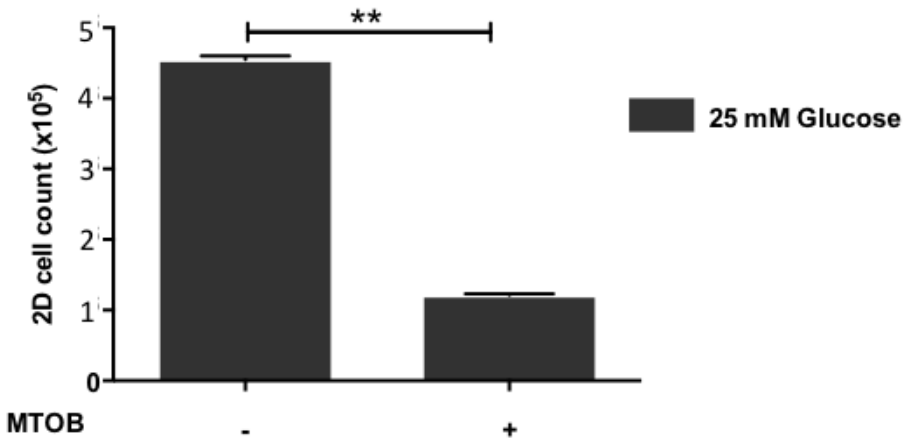

Figure 5.19 72 hour treatment with MTOB in MCF-7 cells. MCF-7 cells were plated at an initial density of 250,000 cells per 60 mm dishes for 48 hours and were treated with 4 mM MTOB for 72 hours in 2D culture. The graph shows a combination of three independent experiments. Results are presented as mean ± SEM. ** $P \leq 0.01$

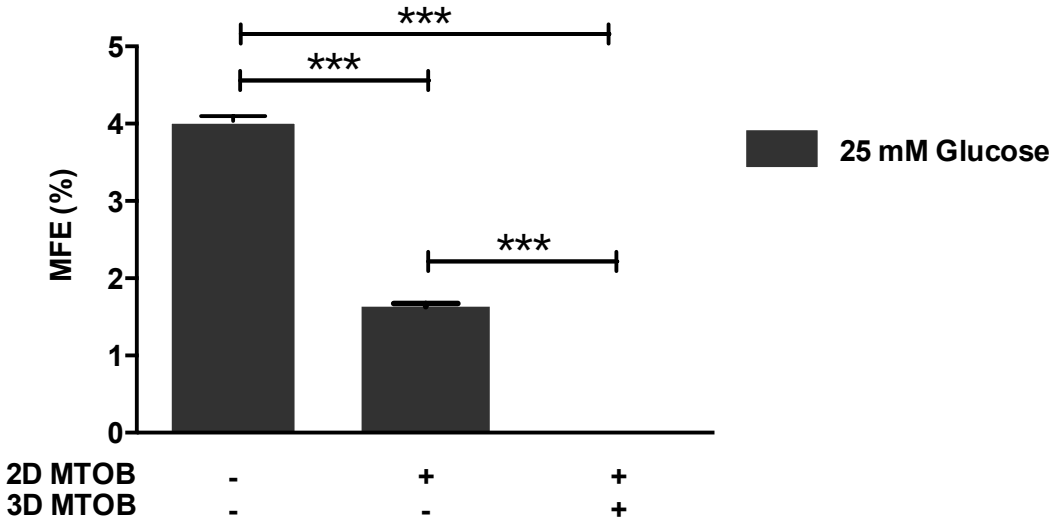

Figure 5.20 The effect of MTOB treatment on mammosphere formation in MCF-7 cells. Following 72 hour treatment with 4 mM MTOB in 2D culture, non-treated and treated cells were seeded at an initial density of 5000 cells per well for five days under mammosphere culture. MFE was then evaluated. Each experiment was repeated three times and performed in triplicate. Results are presented as mean ± SEM. *** $P \leq 0.001$ n=3

5.8.5 Preliminary analysis of CtBP1 expression levels upon different metabolic modulation

To investigate whether the expression levels of CtBP would be affected by modulating different metabolic pathways, the expression levels of CtBP were examined following different metabolic treatments in glycolytic and less-glycolytic conditions. MCF-7 cells from both groups, were treated with different inhibitors for 72 hours for Western blot analysis (Figure 5.21).

5.8.5.1 Alternative nutrient sources

CtBP1 protein appeared to be less expressed following glutamine starvation in both glycolytic groups.

5.8.5.2 Fatty acid oxidation

Etomoxir slightly reduced the expression levels of CtBP1 in both glycolytic groups.

5.8.5.3 Glycolysis

CtBP1 was clearly less expressed in cells with impaired glycolysis (oxamate and 2DG treatment). However, this effect was more extreme under fructose conditions.

5.8.5.4 Mitochondria respiration

The CtBP expression was only decreased under glucose conditions following DCA treatment. The expression of CtBP1 appeared weaker upon metformin treatment (Figure 5.21).

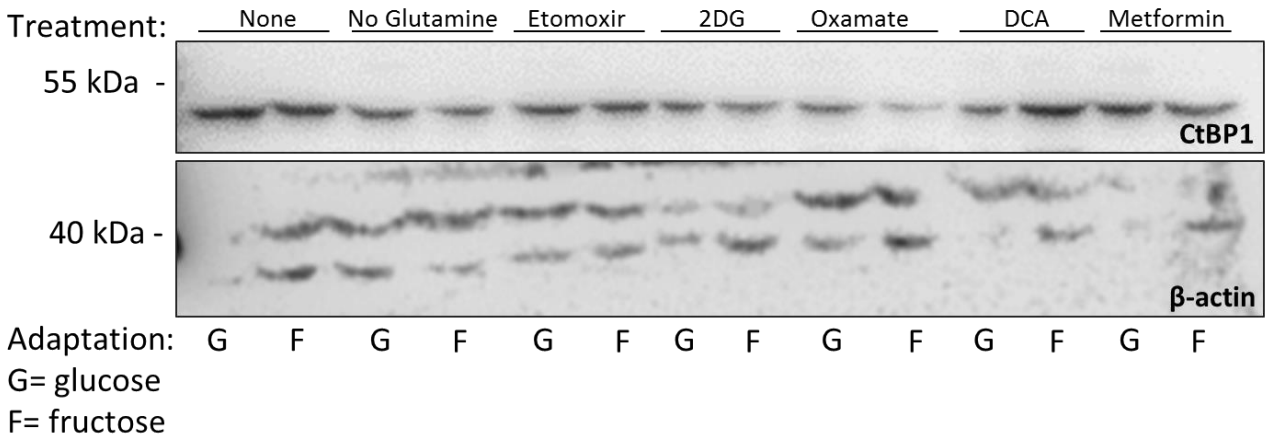

Figure 5.21 Characterisation of CtBP protein expression in MCF-7 cells following different metabolic treatments by Western blot analysis. MCF-7 cells were exposed to different metabolic treatments for 72 hours. Cells were harvested, lysed, and subjected to SDS-PAGE on a 10% gel. The expression levels of CtBP1 were assessed in fructose and glucose adapted cells following each treatment. β-actin was used as a loading control. Blots were exposed using BioRad FluoroS Multimager.

5.9 Preliminary analysis of OCT4 expression levels upon different metabolic modulation

To investigate whether different metabolic states affect the stem cell population of MCF-7 cells, the expression levels of OCT4 were assessed.

5.9.1 Alternative nutrition source

Glutamine starvation: the expression levels of OCT4 increased following glutamine deprivation under both glycolytic states (glucose and fructose) (Figure 5.22).

5.9.2 Fatty acid oxidation

Etomoxir: the expression levels of OCT4 increased following etomoxir treatment only in glucose adapted cells. However, under fructose conditions, the intensity of OCT4 band appeared weaker compared with the untreated corresponding control.

5.9.3 Glycolysis

2-Deoxy-D-glucose (2DG): the expression levels of OCT4 were considerably reduced upon 2DG treatment in both glycolytic groups.

Sodium Oxamate: oxamate did not appear to be effective enough to change the expression levels of OCT4. More glycolytic cells were found to express higher levels of OCT4 protein compared with the less glycolytic cells.

5.9.4 Mitochondrial respiration

Dichloroacetate (DCA): the OCT4 expression levels were considerably increased in both glycolytic groups when treated with DCA. However, this increase was found to be more pronounced in glucose adapted cells.

Metformin: metformin treatment entirely reduced the OCT4 expression levels regardless of fructose/glucose adaptation.

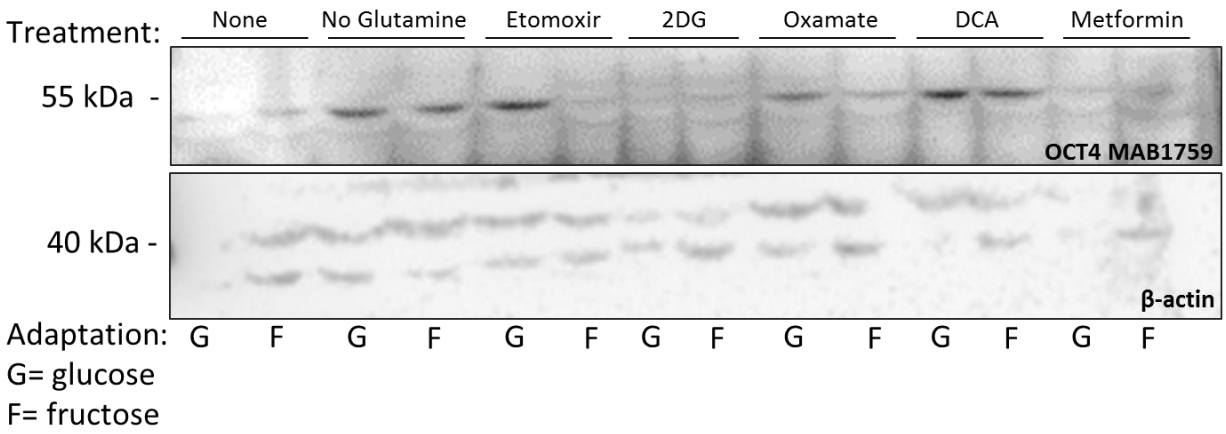

Figure 5.22 Characterisation of OCT4 protein expression in MCF-7 cells following different metabolic treatments by Western blot analysis. MCF-7 cells were exposed to different metabolic treatments for 72 hours. Cells were harvested, lysed, and subjected to SDS-PAGE and 10% gel. The expression levels of OCT4 were assessed in fructose and glucose adapted cells following each treatment. β-actin was used as a loading control. Blots were exposed using BioRad FluoroS Multimager.

5.10 Preliminary analysis of E-cadherin expression in fructose and glucose adapted MCF-7 cells

The EMT is induced by the loss of E-cadherin expression. EMT increases the stem-like properties of mammary epithelial cells in development and cancer (183). The loss of E-cadherin promotes the migratory properties of cells which leads to metastasis. It was hypothesised that E-cadherin would be reduced in fructose adapted cells with enhanced mammosphere forming ability. Furthermore, it was expected that a higher expression of E-cadherin would be seen in cells with a smaller stem cell population. Therefore, the expression levels of E-cadherin and its association with stem cell markers were assessed in MCF-7 cells. Initially, the mRNA expression levels of E-cadherin were assessed in both glycolytic groups by RT-qPCR analysis. Whilst this data is preliminary it suggests a dramatic drop of ~50% in mRNA expression of E-cadherin under fructose conditions (Figure 5.23).

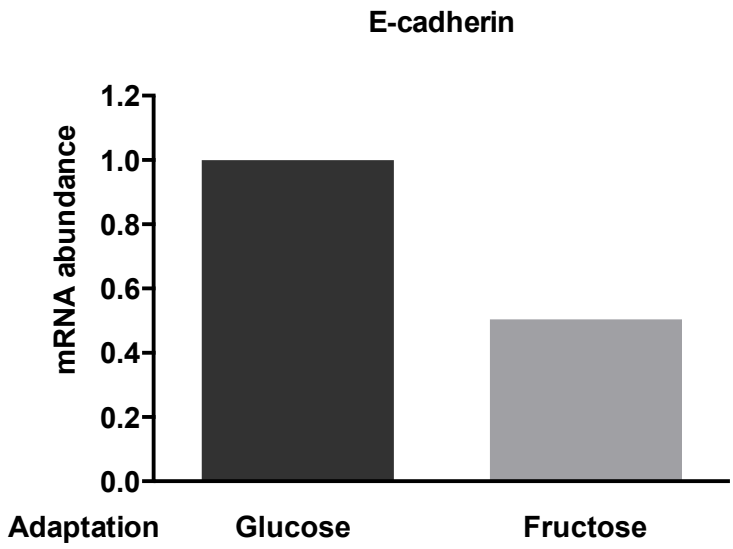

Figure 5.23 E-cadherin mRNA abundance in fructose and glucose adaptation. E-cadherin mRNA expression levels were assessed by RT-qPCR in MCF-7 cells adapted to either fructose or glucose. The Ct obtained for each cell line was normalised against the housekeeping gene β-actin. Relative mRNA abundance was calculated by normalising to β-actin. Results are presented as mean ± SEM. ** $P \leq 0.01$ n=2 Means are from any 2 technical replicates.

The expression levels of E-cadherin were investigated upon the knockdown of pluripotency markers SOX2 and OCT4 PG1. Consistent with the previous data, the mRNA expression of E-cadherin was found to be lower under fructose conditions (Figure 5.23). Whilst this data is preliminary it suggests that in glucose adapted cells, the expression levels of E-cadherin appeared to be increased following OCT4 and OCT4 PG1 silencing, noted at 1.45 and 1.15 respectively. Under fructose conditions, E-cadherin mRNA expression appeared higher following SOX2, OCT4, and OCT4 PG1 silencing (Figure 5.24).

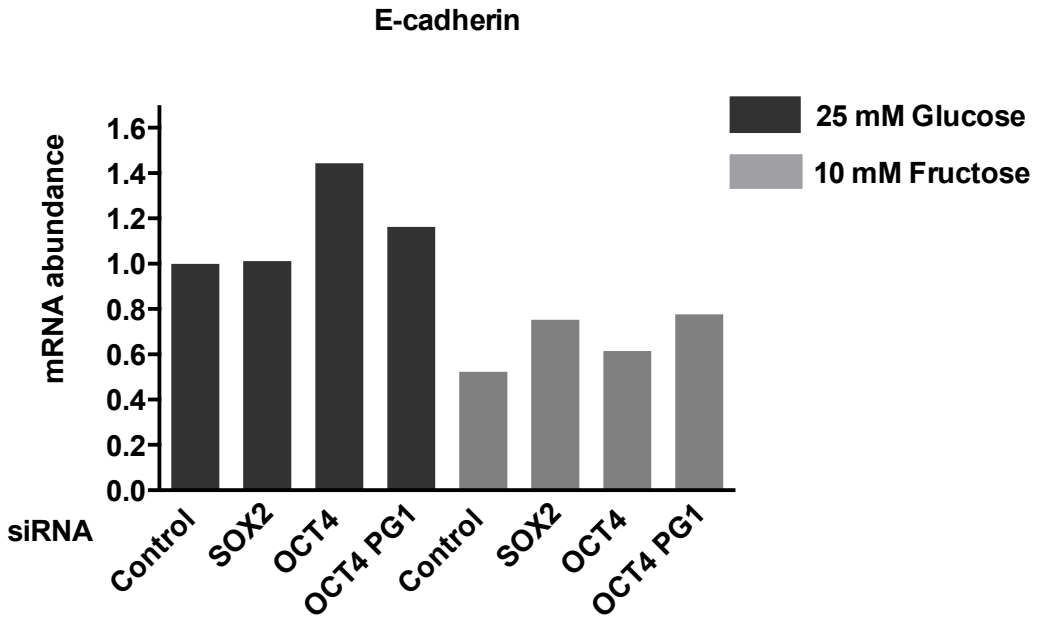

Figure 5.24 E-cadherin mRNA abundance in fructose and glucose adaptation following SOX2 and OCT4 PG1 (POU5F1B) silencing. MCF-7 cells were transfected with SOX2, OCT4, and OCT4 PG1 siRNA for 48 hours. Following transfection, E-cadherin mRNA expression levels were assessed by RT-qPCR in MCF-7 cells, adapted in either fructose or glucose. The Ct obtained for each cell line was normalised against the housekeeping gene β-actin. Relative mRNA abundance was calculated by normalising to β-actin. Results are presented as mean ± SEM. n=2 Means are from any 2 technical replicates.

5.11 Discussion

One of the most altered metabolic pathways in cancer cells and stem cells is glycolysis. Stem cells have distinctive metabolic properties such as an enhanced glycolytic phenotype which supports their activities and stemness properties (211). Malignant transformation from pre-malignant lesions to invasive cancer is associated with an increased rate of glucose uptake, leading to high rates of glycolysis (134). Constant genetic or epigenetic alterations for cellular immortalisation such as P53 mutation that causes HK dysregulation may be the reason for the enhanced glycolysis that cancer cells display *in vitro* (133). As the glycolytic phenotype appears at the early stages of carcinogenesis, targeting glycolysis could be considered as a possible target in cancer prevention and targeted therapies (134). However, targeting glycolysis for therapy has not yet been used in the clinical trials (132). Thus, the effect of reducing glycolysis on MCF-7 breast cancer cells was investigated, targeting LDH and HKII.

We have shown that sodium oxamate, a classic inhibitor of LDH, reduced the growth rate of more glycolytic cells in 2D culture as expected, while it had an opposite effect on fructose cultured cells. Oxamate significantly reduced the mammosphere formation in both glycolytic groups. The absence of oxamate in the conditioned medium (3D culture) resulted in a decrease in the MFE, only under glucose conditions suggesting that adapting cells to less glycolytic state (fructose) makes them independent of glucose for proliferation.

Another possible way to reduce glycolysis was to inhibit the HKII enzyme with 2DG. 2DG inhibited the first phase of glycolysis by directly inhibiting the conversion of fructose-6-P to glucose-6-P (212). Contrary to oxamate, 2DG significantly reduced the cell growth in both glycolytic groups. Moreover, unlike oxamate, the presence of 2DG only in 2D culture was enough to inhibit stem-like properties and reduce the MFE. It has been shown that 2DG could restrict the transportation of fructose into the cell (212). We have shown that 2DG entirely inhibited the mammosphere formation under fructose conditions when presented in the 3D culture. This could explain the higher sensitivity of fructose adapted cells to fructose restriction with 2DG treatment.

Although both oxamate and 2DG are used as glycolytic inhibitors, each targets a different stage of this pathway. Oxamate inhibits the LDH activity in the last step of glycolysis which therefore explains why glucose dependant cells were more sensitive

than fructose adapted cells to oxamate. Glucose and fructose are both phosphorylated by HKs in the first step of glycolysis where both substrates are equally present. This could explain why 2DG inhibited the cell growth and mammosphere forming ability in both groups. 2DG has been shown to decrease fructose-induced ATP levels which results in cell death. Moreover, Ciavardelli *et al.* (204) showed that 2DG inhibited bCSLCs proliferation. Contradictory results regarding the effect of 2DG brought into question the anticancer ability of 2DG in preclinical models, showing that 2DG activates pro-survival pathways in cancer cells (213) (214) (215). However, we have shown that not only did 2DG inhibit the growth of MCF-7 cells; it also targeted the CSLC population of MCF-7 cells by inhibiting mammosphere formation.

In addition to the role of glutamine in mitochondrial metabolism, glutamine also plays an important role in glycolysis by inhibiting the expression of thioredoxin-interacting protein, a negative regulator of glucose uptake. Therefore, glutamine is important in both metabolic pathways of cancer cells: oxidative phosphorylation and glycolysis (216). This feature has made glutamine metabolism an interesting target for clinical strategies to detect and treat cancer (217). Some cancer cell lines are dependent on glutamine to generate ATP. Breast cancer cells respond differently to glutamine. Basal-like cells tend to be glutamine dependent, while luminal-like cells are not (218). In contrast, we have shown that although the luminal-like MCF-7 cells did not display an entire dependency on glutamine, they had a better proliferation rate and more efficient mammosphere formation ability in the presence of glutamine. Therefore, another promising strategy for cancer treatment could be starving cancer cells of glutamine. The reliance of cancer cells on increased glucose uptake has proven glucose as the most consumed substrate by cancer cells. This observation could justify that glutamine starvation could more severely affect cells in glycolysis restriction than when glucose is available to cells. As expected, fructose adapted cells displayed more sensitivity to glutamine starvation in different culture conditions (2D and 3D). Improvements in glutamine-based investigations should soon open new insights into discriminating tumours with higher affinity to glutamine.

Despite the high reliance of cancer cells on glycolysis, the majority of tumour cells still rely on active mitochondrial respiration. As cancer cells are also characterized by decreased mitochondrial respiration and oxidative phosphorylation, different doses of metformin were applied to the cells to block this pathway. Results suggest that

mitochondrial respiration is important for glycolytic groups to display stem-like properties. Studies revealed that small doses of metformin could be used as an adjuvant therapy to prevent the EMT transition and chemoresistance (219). Together with our data, this could suggest that metformin may only be effective at a certain concentration and increasing the dose could give an unexpected result. Moreover, we have shown that metformin targeted the CSLC population but not their differentiated progenies (MCF-7 cancer cells) which is consistent with the observations in pancreatic cancer (220). Sancho *et al.* demonstrated that cancer cells are highly glycolytic while CSLCs rely on OXPHOS with very limited metabolic plasticity (220). CSLCs were not affected when metformin was deprived from the 3D culture; probably due to their intermediate glycolytic/respiratory phenotype. Furthermore, Ciavardelli *et al.* argued that bCSLCs are more reliant on anaerobic glucose metabolism compared with more differentiated cancer cells (204). In another study, Jung *et al*. showed that metformin affected the bCSLCs in the mammosphere population (205). These findings could explain the results in this thesis showing that metformin has a better impact on the stem cell population (MFE) than on more differentiated cancer cells in the 2D culture.

In addition to impairing mitochondrial function, increasing its activity by channelling pyruvate into the mitochondria could be an effective solution to destroy the more glycolytic cells. Glycolytic cells should be more sensitive to this change as they normally try to avoid channelling pyruvate into the mitochondria. Therefore, this metabolic alteration could be a promising method to eliminate highly glycolytic cells such as stem cells. DCA is involved in the downregulation of glycolysis in promoting mitochondrial glucose oxidation over glycolysis by directing pyruvate into the mitochondria, which can be toxic to the cells that are not used to this change, such as glycolytic cells (stem cells). Morfouace *et al.* demonstrated that DCA eliminated neurospheres and reduced tumour growth *in vivo* (138). They also showed that DCA efficiently caused cell death in CSLCs that are resistant to cell death inducers and thus, could be responsible for tumour recurrence (138). Therefore, the effect of DCA was assessed to see whether its toxicity also affects the stem cell population in breast cancer. As expected, DCA reduced the cell growth in more glycolytic cells while in glycolysis restriction cells did not show sensitivity to DCA treatment. We have shown that the application of DCA to both cultures (2D and 3D) significantly dropped the MFE in both glycolytic groups. However, when DCA was only applied to the cells in 2D culture,

fructose adapted cells showed more stem-like properties by forming more mammosphere, suggesting that DCA more effectively impacted cancer cells than CSLCs under glucose conditions.

Fatty acid oxidation is beneficial to cell survival independent of glycolysis. Under circumstances where glycolysis is restricted, cancer cells use fatty acid oxidation for energy production which may protect them from oxidative damage (221). Therefore, it was hypothesised that fructose adapted cells, which display more stem-like properties should be more sensitive to the inhibition of FAO. Moreover, it has been shown that inhibition of fatty acid oxidation can impair the endogenous antioxidant system resulting in ATP reduction and eventually cell death. The effect of different fatty acids on the energy metabolism, survival, and proliferation of human bone marrow stem cells has been studied. Saturated fatty acids have been found to induce apoptosis in several cell types, including bone marrow mesenchymal stem cells (222). Fillmore *et al.* reported that reducing saturated fatty acid oxidation may reduce proliferation of human bone marrow stem cells and cause cell death (223). Such observations led us to investigate the effect of inhibiting fatty acid oxidation on the stem cell population of the breast cancer cell line MCF-7 in both glycolytic groups, using etomoxir. Data from the growth rates indicated that under both glycolytic conditions, MCF-7 cells were reliant on fatty acid oxidation to maintain efficient proliferation. Consistently, restricted fatty acid oxidation, using etomoxir, significantly affected the stem cell population by reducing the MFE in both glycolytic groups, suggesting that fatty acid oxidation is important for both groups to display CSLCs. Notably, as expected, the exposure of etomoxir to cells in both culture conditions (2D and 3D) reduced the MFE in fructose adapted cells. This could suggest that the population with the potential of representing more stem-like cells is more reliant on fatty acid oxidation for their proliferation.

Studies have found that CtBP is extensively expressed in tumour samples from breast cancer patients compared with surrounding non-tumour tissues (173). Another study suggested that inhibition of CtBP by tumour-infiltrating myeloid-derived suppressor cells promoted the CSLCs phenotype (224). This is in contrast with the observations in colon and breast cancer cells as we have shown in this thesis (171). To assess whether CtBP restriction would affect the tumour initiating population (mammospheres) of MCF-7 in either glycolytic conditions, CtBP was silenced and the MFE was assessed subsequently. Considering the role of CtBP in tumour initiation, our findings revealed that at both mRNA and protein levels CtBP was more highly expressed in the population adapted to the condition that was more beneficial to CSLCs or tumour initiating cells in terms of forming mammospheres (glycolysis restriction/fructose adaptation). Moreover, we have shown that the absence of CtBP significantly reduced the stem cell population in both glycolytic groups (glucose and fructose adapted cells).

A direct consequence of MTOB is the inhibition of GDH activity which leads to increased tumour cell apoptosis. Treatment of engrafted tumours by MTOB suggested that the apoptosis induced by inhibition of the intracellular glutaminolysis pathway might be the reason behind tumour reduction induced by MTOB. Thus, these data suggest that targeting CtBP could be a possible way to treat breast cancer (225). Targeting CtBPs has long been raised as a promising approach to dysregulate the association between the metabolic and epigenetic networks leading to malignant reprogramming of cells (226). MTOB is the only currently known CtBP inhibitor that has been shown to reverses the suppression of many CtBP-targeted genes in breast cancer cells (172) (171). MTOB binds to the catalytic dehydrogenase domain of CtBPs and at high concentrations (4 mM) inhibits the recruitment of CtBPs to target promoters (172). We have shown that MTOB significantly reduced the MFE (with a 72 hour treatment). Additionally, our results indicated that MTOB could entirely eliminate the stem cell population if it remained in the conditioned media. Decreases in cell growth and mammosphere formation could indicate that MTOB affects both the stem cell population of differentiated cancer cells and the mammosphere forming ability. MTOB alone is able to induce apoptosis *in vitro*. The suppression of CtBP2, and the apparent lack of MTOB toxicity, makes it a lead compound for therapeutic research. MTOB was designed to disrupt CtBP dimerisation, which, therefore, highlights its role in preventing the recruitment of CtBPs to target promoters and antagonize CtBP transcriptional

regulation. Hence this implies MTOB does not affect CtBP metabolic sensor of redox status, suggesting that the transcriptional and not the metabolic activity of CtBP was necessary for its repressor activity.

In addition, CtBPs are of interest in metabolic studies as they maintain metabolic homeostasis (173). As NADH is known as a major indicator of glycolytic cells and CtBPs can sense the levels of free NADH. As such, the CtBP family of proteins may be considered as main regulators of highly glycolytic phenotype in cancer cells (227) (226). CtBPs are also known as metabolic sensors that control cell survival and migration in response to enhanced aerobic glycolysis and hypoxia. Increased nuclear CtBP levels have been recently shown to be associated with poor survival in breast cancer patients (228). We have shown that 2DG and oxamate clearly reduced the CtBP1 expression in MCF-7 cells. Cells under glycolysis restriction appeared to express less CtBP protein specifically following oxamate treatment, suggesting that the lower the glycolytic state is the less CtBP is expressed in the cells. This is consistent with the fact that CtBPs are regulators of highly glycolytic phenotypes.

More glycolytic cells were found to express less CtBP protein when treated with DCA, while CtBP expression levels appeared higher in fructose adapted cells. Disruption in glycolysis pathway by DCA resulted in a reduced expression of CtBP in more glycolytic cells, suggesting that CtBP expression is associated with the glycolytic state of cells. We have shown that less glycolytic cells expressed less CtBP protein when treated with metformin, while the expression levels of CtBP appeared higher in more glycolytic cells. This could also indicate a link between CtBP expression and glycolytic phenotype.

Moreover, CtBP was found to have an essential role in promoting glutaminolysis in cancer cells. Loss of CtBP leads to intracellular acidification and therefore cell apoptosis. This disruption in cancer cell metabolic homeostasis is associated with decreased glutamine consumption, oxidative phosphorylation, and ATP synthesis, suggesting CtBP as a potential therapeutic target for cancer treatment (173). We have shown that the absence of glutamine reduced the CtBP expression levels in both glycolytic groups, suggesting that the presence of glutamine is important for CtBP expression. This finding could also suggest that starving cells with glutamine together with CtBP knockdown could potentially reduce the cancer cell growth.

We have previously shown in Chapter 3 that MCF-7 cells had more CSLCs by representing higher levels of MFE under fructose conditions. Moreover, we have shown that the absence of certain pluripotency markers such as OCT4, which is a key regulator in CSLC self-renewal and differentiation, and its highly homologous pseudogene (OCT4 PG1) significantly reduced the stem cell population in both glycolytic groups. Therefore, it was felt important to investigate the expression levels of OCT4 following the application of different metabolic inhibitors in both glycolytic groups, fructose and glucose cultured cells.

Inhibiting glycolysis leads to the differentiation of pluripotent cells and thus, has a crucial role in the maintenance of the pluripotent state (229). Kim *et al.* stated that OCT4 directly controls two key glycolytic enzymes (HKII and PKMII) that determine the rate of glycolytic flux (211). This raises the possibility that OCT4 expression levels could be associated with the glycolytic state of the cells. Our results showed that inhibiting the first phase of glycolysis, using 2DG (inhibiting HKII), entirely silenced OCT4 expression in both glucose and fructose adapted cells, suggesting that glycolytic state is important for OCT4 expression. However, inhibiting the last phase of glycolysis, using oxamate, OCT4 expression was only affected (decreased) under fructose conditions. This might suggest that the first stage of glycolysis may play more important roles in differentiation state of cells and the expression of pluripotency markers such as OCT4. This observation is also supported by our previous results showing that oxamate did not reduce the stem cell population under fructose adaptation.

It has been shown that glutamine metabolism regulates the pluripotency of hESCs (230). Moreover, Marsboom *et al.* reported that OCT4 expression levels decreased following glutamine withdrawal, indicating that high levels of glutamine metabolism are critical to prevent OCT4 degradation (230). Contrary to Marsboom *et al.* findings, we have shown that glutamine starvation enhanced the expression levels of OCT4 in MCF-7 cells in either glycolytic conditions, suggesting that glutamine plays an important role in regulating OCT4 expression regardless of the glycolytic state.

Moussaieff *et al.* showed that ES cells direct pyruvate toward acetyl-CoA in the mitochondria. Therefore, preventing acetyl-CoA production could result in the loss of pluripotency, while inhibiting its consumption would delay the cell differentiation. These findings revealed an important link between metabolic states of cells and pluripotency (229). Our data showed that DCA clearly increased the expression levels of

OCT4 and therefore pluripotency in MCF-7 cells in either glycolytic conditions. Furthermore, metformin reduced OCT4 expression levels in both populations. This further confirms an association between OCT4 expression levels and glycolytic states, suggesting that OCT4 is more highly expressed in more glycolytic conditions.

In addition to the two main metabolic pathways, glycolysis and mitochondrial activity, the effect of fatty acid oxidation on the expression levels of OCT4 in MCF-7 cells was also investigated. Studies have reported a minor effect of fatty acid oxidation on the expression levels of pluripotency markers (229). However, our data indicated that under glucose conditions, inhibition of FAO increased the expression levels of OCT4, while fructose adapted cells displayed a clear knockdown of OCT4 protein following etomoxir treatment. This observation indicated the important role of FAO in pluripotency which was in agreement with our mammosphere formation data showing that both groups (fructose and glucose adapted cells) were reliant on fatty acid oxidation to represent stem cell characteristics.

In addition to maintaining the self-renewal ability of stem cells, SOX2 and OCT4 are also involved in cancer cell migration and invasion. Breast cancer metastasis is a multistep process involving several genes, including E-cadherin (231). E-cadherin expression is important for cell–cell adhesion and a reduction in its expression is critical for the incidence of metastasis (232). In epithelial malignancy such as breast cancer, the loss of E-cadherin is important in terms of the alteration of adhesive properties as well as EMT, which are considered as the key metastatic factors (233). Moreover, E-cadherin is critical for ES cell pluripotency and therefore is more highly expressed in the population with high levels of pluripotency genes such as OCT4 and SOX2. OCT4 possesses the unique capacity to suppress the EMT mediator Snail and activate the epithelial program such as inducing E-cadherin. Likewise, CSLCs are known to be involved in tumour initiation and due to their chemoresistance characteristic, they are likely to be responsible for tumour relapse and metastasis. In this regards, we have shown that fructose provides a more efficient condition for stem cells by representing significantly higher MFE compared with glucose.

To discover the link between E-cadherin expression and stem-like properties under fructose conditions, the expression levels of E-cadherin were compared in both glycolytic conditions and its relationship with stem-like properties was assessed following the silencing of tumour stem cell genes in MCF-7 cells. We found that the

expression levels of E-cadherin appeared lower under fructose conditions, suggesting that E-cadherin is less expressed in the population with higher ability to form mammospheres representing tumour initiating properties. Moreover, a correlation was identified between the expression of E-cadherin and tumour stem cell markers, indicating that E-cadherin was more highly expressed in the absence of pluripotency markers OCT4, OCT4 PG1, and SOX2 in both glycolytic groups, which is consistent with other studies showing that OCT4 promotes the EMT in lung cancer.

Chapter 6

Summary, General discussion, and Future perspectives

6.1 Summary

- In this thesis we have shown that fructose-containing media is a preferred alternative to glucose for MCF-7 cells and that a switch to a lower glycolytic state (fructose adaptation) is beneficial to the cancer stem-like population of MCF-7 breast cancer cell line. Moreover, we have shown that pluripotency markers OCT4 and SOX2 are more highly expressed in this condition.

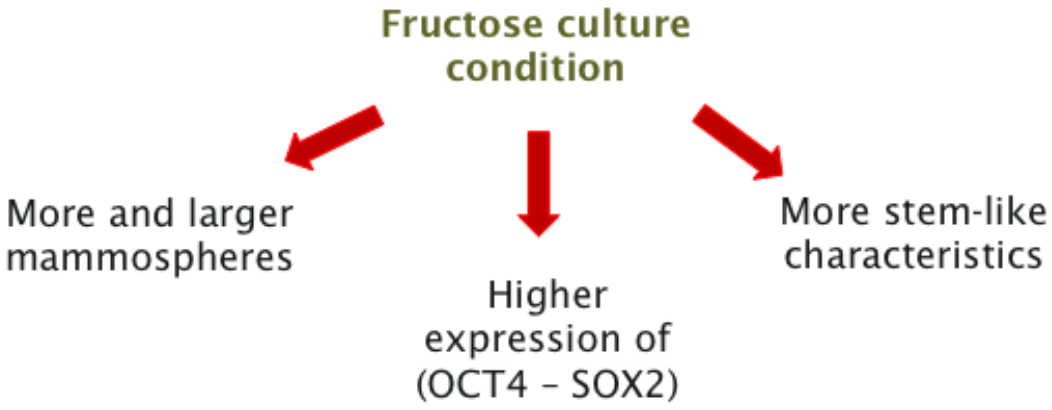

- Our data highlighted the important role of different metabolic pathways in the CSLC population. Targeting tumour metabolism is likely to have a major impact on understanding the mechanisms of cancer proliferation and could be a promising approach to stop or hold back CSLCs growth. Research on cancer cell metabolism allows us to think of cancer not only as a genetic disease but also as a disease of metabolic dysregulation.

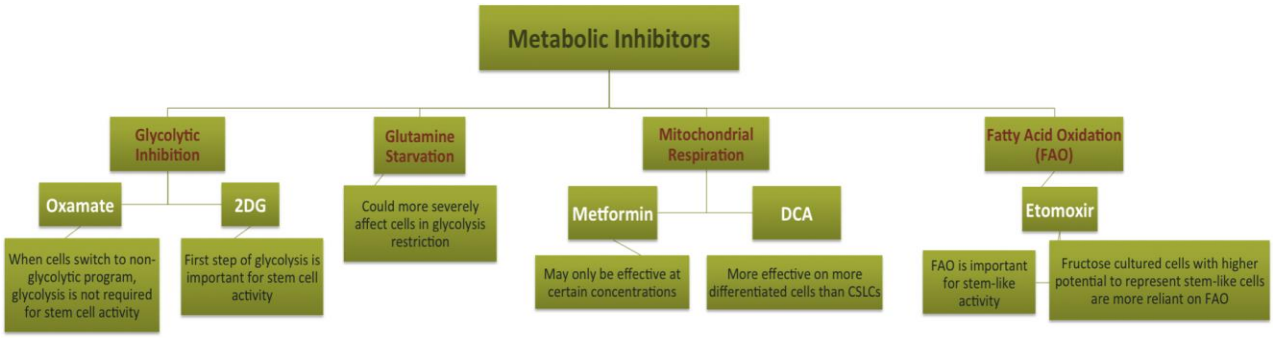

- We have shown that OCT4A is not expressed in breast cancer cell lines and a nuclear detected protein in MCF-7 cells is likely to be related to OCT4 PG1 or OCT4B1 isoform due to its molecular weight and stemness activity. Moreover, we have demonstrated that OCT4 and its homologous pseudogene OCT4 PG1, or OCT4B1 isoform are important for stemness maintenance while SOX2 is not a critical factor.

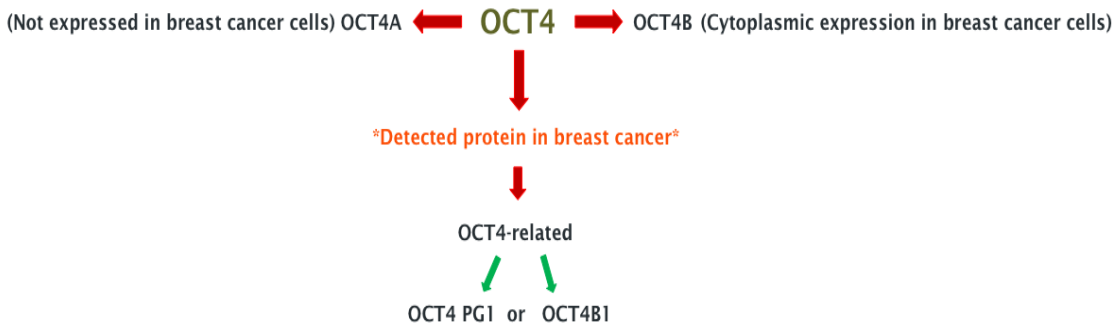

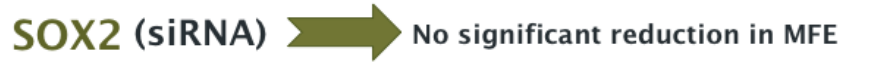

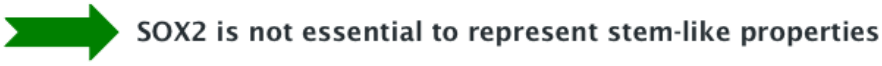

- We have shown that OCT4 and SOX2 are both more highly expressed in fructose cultured cells indicating that these genes may be regulated similarly by glycolysis in breast cancer and that fructose is a preferred metabolic condition for stem cell activity.

- CtBPs were found to be more highly expressed in the glycolytic condition which is more beneficial to CSLCs/tumour initiating cells (fructose culture conditions) in terms of forming mammospheres.

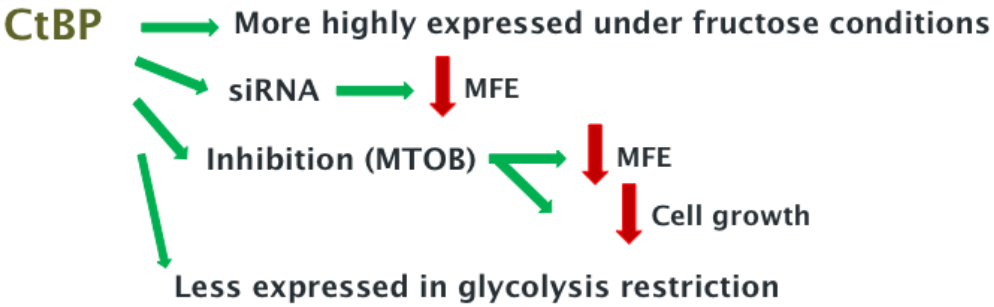

- E-cadherin seemed to be less expressed in the glycolytic condition which was more beneficial to CSLCs/tumour initiating cells (fructose culture conditions) in terms of forming mammospheres. Moreover, we have shown that targeting stem cell markers such as OCT4 and SOX2 may improve cell-cell adhesion and inhibit migration and invasion.

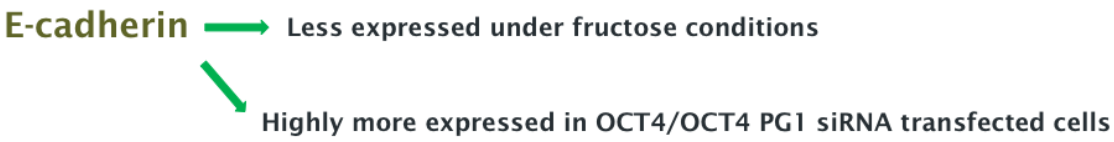

6.2 General discussion

CSLCs are likely to be the cause of cancer initiation and recurrence. Destroying this population has been suggested as a promising approach to improve cancer survival or even to cure cancer patients. Identifying the mechanisms underlying characteristics specific to CSLCs is required to target these cells and eliminate them and completely eradicate tumours. To be able to accurately target this rare population, it is of importance for cancer stem cell research to overcome methodological limitations. The successful methodological improvements could be a switch in the culture environment from 2D to 3D conditions. This thesis attempted to provide a representative overview of the 3D cell culture model of breast cancer cells by performing mammosphere formation assays.

Cancer metabolism alteration in is an important hallmark for many types of human tumours (234). Notably, the metabolic state of CSLCs appears to be remarkably different from the metabolic state of differentiated breast cancer cells and it is associated with adaptation to low glycolytic states such as fructose (235). Most importantly, we have shown for the first time that fructose compensated for the absence of glucose in MCF-7 cells by providing a better condition for cancer cell growth and stem cell population. This interesting finding offers new insights into recent studies that found a high glycolytic phenotype for all cancers, suggesting that cancer cells are capable of adapting to substrates other than glucose. CSLCs are capable of using alternative metabolic pathways for energy production, and thus, targeting individual pathways may not be an efficient therapeutic approach (235). One challenge in targeting the right pathways for effective therapies is the modulation of the altered tumour metabolism toward that of un-transformed cells through the use of different metabolic treatments.

As expected, oxamate had a more effective impact on more-glycolytic cells and inhibited the mammosphere formation and therefore stem-like activity of this group. Contrary to oxamate that increased the MFE in fructose adapted cells, 2DG entirely inhibited the stem-like properties of less-glycolytic cells, probably due to restricting the transport of fructose into the cell. Furthermore, the reliance of cancer cells on glucose could explain why in glucose restricted conditions (fructose conditions), cells displayed more sensitivity to the absence of glutamine in different culture conditions and displayed less stemness properties (2D and 3D). In other words, depriving glucose and glutamine

from the growing medium had a more striking effect on the stem cell population of MCF-7 cells.

Despite the high reliance of cancer cells on glucose and some on glutamine, the majority of tumour cells still require active mitochondrial respiration. However, cancer cells are also characterised by decreased mitochondrial respiration and oxidative phosphorylation. In this regards, metformin proved to be effective in modulating the metabolism of cancer cells even in that rare population with cancer stem like features (mammosphere formation) under both glycolytic conditions. Studies showed that small doses of metformin could be used as an adjuvant therapy to prevent the EMT (219). Together with our data, there is the suggestion that metformin may only be efficient at a certain concentration. In addition, it is thought that cancer cells suppress their mitochondrial activity and therefore avoid apoptosis. As expected, DCA more effectively impacted cells under glucose conditions and reduced the MFE. However, DCA did not affect the stem cell population of fructose adapted cells, suggesting that DCA is only effective on cancer cells and might not be an optimum therapeutic agent for targeting CSLCs.

Alternatively, inhibitory agents of fatty acid oxidation have proved to have a better therapeutic outcome and may therefore represent a more effective alternative to DCA. With this in mind, etomoxir was used in this study to inhibit FAO. FAO proved to be important for both glycolytic groups containing CSLCs. Notably, as expected, etomoxir has more strikingly reduced the MFE in fructose adapted cells, suggesting that population of cells with more stem-like features are more reliant on FAO. Moreover, etomoxir proved to be effective on the stem cell population of MCF-7 cells, and may therefore represent a promising agent to target CSLCs.

In addition to findings on metabolic inhibitors, CtBP was more highly expressed in low-glycolytic conditions that are more beneficial to CSLCs or tumour initiating cells in terms of forming mammospheres (glycolysis restriction/fructose adaptation). Moreover, silencing CtBP significantly reduced the MFE in both glucose as well as fructose adapted cells. Targeting CtBPs has long been raised as a promising approach to dysregulate the association between the metabolic and epigenetic networks leading to malignant reprogramming of cells (226). We showed that MTOB as the only currently known CtBP inhibitor, affected both the stem cell population of differentiated cancer cells and the mammosphere forming ability. This thesis also highlighted the salient

aspects of CtBP family proteins, which is that they are regulators of highly glycolytic phenotypes. We have shown that cells under glycolysis restriction appear to express less CtBP protein, suggesting that the lower the glycolytic state, the less CtBP is expressed in the cells. Cells that received DCA treatment displayed less expression of CtBP under more glycolytic conditions, suggesting that CtBP expression is associated with the glycolytic state of cells. We have further proved a link between CtBP expression and the glycolytic phenotype by showing less expression of CtBP in cells treated with metformin under more glycolytic conditions, while the expression levels of CtBP appeared higher in more glycolytic cells.

Considering the involvement of mesenchymal stem cells in cancer progression and metastases and that EMT confers mesenchymal properties and is associated with CSLC properties, this thesis partially focused on investigating the expression levels of the epithelial marker E-cadherin in the population with a greater ability to form mammospheres. Loss of E-cadherin is associated with EMT and is thought to be associated with CSLC phenotypes. We have shown that the expression levels of E-cadherin appeared lower in the population with the higher ability to form mammospheres (fructose conditions), representing tumour initiating/CSLC properties. Moreover, E-cadherin appeared to be more highly expressed in the absence of pluripotency markers, such as OCT4, OCT4 PG1, and SOX2. Furthermore, OCT4 and OCT4 PG1 were proven to be essential factors for mammosphere formation and we have therefore demonstrated their involvement in CSLC self-renewal. Therefore, reducing the expression levels of pluripotency markers could be associated with a reduction in CSLC properties and decreased possibility of disease recurrence. However, in OCT4A/B silenced cells, the MFE was only significantly reduced under fructose conditions. Knowing that OCT4A is not present in MCF-7 cells and OCT4B has no stemness features, while it has been claimed that OCT4B1 may be related to stemness (236), it can be concluded that OCT4B1 is therefore associated with CSLC model.

6.3 Future perspectives

The results of this thesis point to several interesting directions for future research. To further expand our knowledge of the importance of stem cell biology in cancer research and metabolic processes in the maintenance of CSLC activity, the following studies would be useful:

1. To evaluate the influence of genes involved in cell migration, invasion, and metastasis such as EPCAM, E-cadherin (epithelial cell adhesion molecules) and ITGB4 (integrin β4) in the survival of breast CSLCs,

- siRNA could be used to silence EPCAM, E-cadherin, and ITGB4 in MCF-7 cells cultured in fructose-including media (glycolysis restriction); the ability of cells to form mammospheres would be measured subsequently.

2. To investigate whether the transcription of pluripotency markers (OCT4 and SOX2) is regulated by adherent-related genes, such as E-cadherin in different glycolytic conditions.

- OCT4 and SOX2 expression levels would then be quantified in population with silenced adherent genes in glycolysis restricted condition with Western blotting and qPCR analysis.

➢ These two aims could provide a general approach to characterise the preferred glycolytic condition for expression of stem cell markers and identify the clinically relevant genes in cancer metastasis. If an interaction were to be demonstrated, it is possible that glycolysis and cell adhesion genes regulate the transcriptional activity of OCT4 and SOX2.

3. To determine whether stem cell markers are responsible for the increased stemness properties in different glycolytic conditions,

- The gene expression analysis on OCT4 and SOX2 could be perform in the mammosphere population of breast cancer cells under fructose conditions with Western blotting and qPCR.

➢ This would provide an overall overview of the preferred glycolytic conditions for the expression of stem cell markers and the involvement of such markers in the self-renewal of CSLCs.

➢ To more accurately estimate the outcome of different biological functional assays, the use of further breast cancer cell lines, such as the MCF10A, a human

breast epithelial cell line which is arguably the most commonly used normal breast cell model, could be useful. Moreover, using more aggressive cell lines parallel to the main used cell lines, such SkBr3 and MDA-MA-231, as they represent a different molecular subtype to that of MCF-7 cells and have different clinical outcome.

- This could provide a broader view of how different subtypes of breast cancer respond to different therapies.

4. Using *in vivo* studies as more clinically relevant models to:

- Analyse the gene expression patterns of stem cell markers (OCT4, SOX2, and NANOG) and cell adhesion related genes (E-cadherin) in the tissue sections from xenografts from different stages of cancer development.
- Grow mammospheres from the above sections following the injection of mammospheres in mice to investigate the tumour initiating ability. This could possibly provide an optimisation of developing new cancer therapeutic strategies and providing a more reliable insight into clinical trials.

5. To investigate the identification of detected bands using different OCT4 antibodies in breast cancer cell lines,

- Mass spectrometry technique could be used to significantly characterise the protein.
- RNA sequencing could be used to enable highly sensitive analysis of expression across the transcriptome.
- Different specific antibodies targeting against different OCT4 isoforms/pseudogenes could be used to better specify the identification of expressed OCT4 isoforms/pseudogenes in stem cell population of breast cancer (mammospheres) and to investigate their possible involvement in tumorigenicity.

- This will provide a more clear understanding of the involvement of OCT4 in breast cancer progression and a novel cancer therapeutic target, as transcriptional regulatory roles of OCT4 appeared to be important in breast cancer.

Bibliography

1. Schneider, K. Counseling about cancer: Strategies for genetic counseling. second edition. New York: John Wiley & Sons; 2001.
2. Bahls, C. Reining in a killer disease. The scientist. 2002;16.
3. Cooper, G. M. Elements of human cancer: Jones and Bartlett; 1992.
4. Bloom HJG, Richardson WW. Histological Grading and Prognosis in Breast Cancer: A Study of 1409 Cases of which 359 have been Followed for 15 Years. British journal of cancer. 1957;11(3):359-77.
5. Key TJ, Verkasalo PK, Banks E. Epidemiology of breast cancer. The Lancet Oncology. 2001;2(3):133-40.
6. Bartkova J, Horejsi Z, Koed K, Kramer A, Tort F, Zieger K, et al. DNA damage response as a candidate anti-cancer barrier in early human tumorigenesis. Nature. 2005;434(7035):864-70.
7. Jennifer F. Wilson. Elucidating the DNA damage pathway. The Scientist. 2002;16.
8. Alfred G. Knudson Two genetic hits (more or less) to cancer. Nature reviews Cancer. 2001;1:157-62.
9. López-Lázaro M. A New View of Carcinogenesis and an Alternative Approach to Cancer Therapy. Molecular Medicine. 2010;16(3-4):144-53.
10. Brand KA, Hermfisse U. Aeobic glycolysis by proliferating cells: a protective strategy against reactive oxygen species'. FASEB. 1997;11.
11. Hanahan D, Weinberg RA. Hallmarks of cancer: the next generation. Cell. 2011;144.
12. Scully OJ, Bay B-H, Yip G, Yu Y. Breast Cancer Metastasis. Cancer Genomics - Proteomics. 2012;9(5):311-20.
13. Gelao L, Criscitiello C, Fumagalli L, Locatelli M, Manunta S, Esposito A, et al. Tumour dormancy and clinical implications in breast cancer. Ecancermedicalscience. 2013;7:320.
14. Nguyen DX MJ. Genetic determinants of cancer metastasis. Nat Rev Genet. 2007;8:341-52.
15. Li DM, Feng YM. Signaling mechanism of cell adhesion molecules in breast cancer metastasis: potential therapeutic targets. Breast cancer research and treatment. 2011;128(1):7-21.
16. Savagner P. The epithelial-mesenchymal transition (EMT) phenomenon. Annals of oncology : official journal of the European Society for Medical Oncology / ESMO. 2010;21 Suppl 7:vii89-92.
17. Samatov TR, Tonevitsky AG, Schumacher U. Epithelial-mesenchymal transition: focus on metastatic cascade, alternative splicing, non-coding RNAs and modulating compounds. Molecular cancer. 2013;12(1):107.
18. Wang Y, Zhou BP. Epithelial-mesenchymal transition in breast cancer progression and metastasis. Chinese Journal of Cancer. 2011;30(9):603-11.
19. Kumar S, Das A, Sen S. Extracellular matrix density promotes EMT by weakening cell-cell adhesions. Molecular bioSystems. 2014;10(4):838-50.
20. Hulpiau P, van Roy F. Molecular evolution of the cadherin superfamily. The international journal of biochemistry & cell biology. 2009;41(2):349-69.
21. Kalluri R, Weinberg RA. The basics of epithelial-mesenchymal transition. The Journal of clinical investigation. 2009;119(6):1420-8.

22. Mani SA, Guo W, Liao MJ, Eaton EN, Ayyanan A, Zhou AY, et al. The epithelial-mesenchymal transition generates cells with properties of stem cells. Cell. 2008;133(4):704-15.
23. Dykxhoorn DM, Wu Y, Xie H, Yu F, Lal A, Petrocca F, et al. miR-200 enhances mouse breast cancer cell colonization to form distant metastases. PloS one. 2009;4(9):e7181.
24. Kimberly Stone, Amanda Wheeler. Breast Anatomy and Basic Histology, Physiology, and Pathology; 2007.
25. David J. Winchester, David P. Winchester. Breast Cancer; 2006.
26. Li CI. Incidence of Invasive Breast Cancer by Hormone Receptor Status From 1992 to 1998. Journal of Clinical Oncology. 2003;21(1):28-34.
27. Cowin P, Wysolmerski J. Molecular mechanisms guiding embryonic mammary gland development. Cold Spring Harbor perspectives in biology. 2010;2(6):a003251.
28. Van Keymeulen A, Rocha AS, Ousset M, Beck B, Bouvencourt G, Rock J, et al. Distinct stem cells contribute to mammary gland development and maintenance. Nature. 2011;479(7372):189-93.
29. Noel Weidmer MD JPS, M.D., Wiliam R. Welch, M.D., and Judah Folkma, M.D. Tumor angiogenesis and metastasis - Correlation in invasive breast carcinoma. Journal of medicine. 1991.
30. Catherine de Martel JF SF, Jérôme Vignat, Freddie Bray, David Forman, Martyn Plummer. Global burden of cancers attributable to infections in 2008: a review and synthetic analysis. 2012;13:607–15.
31. Bombonati A, Sgroi DC. The molecular pathology of breast cancer progression. The Journal of pathology. 2011;223(2):307-17.
32. Casarsa C, Oriana S, Coradini D. The controversial clinicobiological role of breast cancer stem cells. Journal of oncology. 2008;2008:492643.
33. Polyak K. Heterogeneity in breast cancer. The Journal of clinical investigation. 2011;121(10):3786-8.
34. Eini R, Stoop H, Gillis AJ, Biermann K, Dorssers LC, Looijenga LH. Role of SOX2 in the etiology of embryonal carcinoma, based on analysis of the NCCIT and NT2 cell lines. PloS one. 2014;9(1):e83585.
35. Stewart BW, Wild CP. World Cancer Report 2014. World Health Organization; 2014.
36. Eheman CR, Shaw KM, Ryerson AB, Miller JW, Ajani UA, White MC. The changing incidence of in situ and invasive ductal and lobular breast carcinomas: United States, 1999-2004. Cancer epidemiology, biomarkers & prevention : a publication of the American Association for Cancer Research, cosponsored by the American Society of Preventive Oncology. 2009;18(6):1763-9.
37. Wellings SR, Jensen HM. On the Origin and Progression of Ductal Carcinoma in the Human Breast. JNCI J. 1973;50:1111-8.
38. CWEaIO E. Histopathology2002.
39. Oyama T MH, Koerner F. Atypical cystic lobules: an early stage in the formation of low-grade ductal carcinoma in situ. an international journal of pathology. 1999;435:413-21.
40. Strauss, Jonathan, Small Jr., William, Woloschak, Gayle E. Breast Cancer Biology for the Radiation Oncologist. Berlin: Springer-Verlag; 2015
41. Pece S, Tosoni D, Confalonieri S, Mazzarol G, Vecchi M, Ronzoni S, et al. Biological and molecular heterogeneity of breast cancers correlates with their cancer stem cell content. Cell. 2010;140(1):62-73.

42. Sotiriou C PL. Gene-Expression Signatures in Breast Cancer. New England Journal of Medicine. 2009;360:790-800.
43. Polyak K. Breast cancer: origins and evolution. The Journal of clinical investigation. 2007;117(11):3155-63.
44. Dey D SM, Paranjape AN, Krishnan V, Giraddi R, Kumar MV. Phenotypic and functional characterization of human mammary stem/progenitor cells in long term culture. PloS one. 2009;4.
45. Rippon HJ, Bishop AE. Embryonic stem cells. Cell Proliferation. 2004;37(1):23-34.
46. Schöler HR. The Potential of Stem Cells: An Inventory. Humanbiotechnology as Social Challenge. 2007;28.
47. Reya T, Morrison SJ, Clarke MF, Weissman IL. Stem cells, cancer, and cancer stem cells. Nature. 2001;414(6859):105-11.
48. stem cells and cancer2009.
49. Al-Hajj M, Clarke MF. Self-renewal and solid tumor stem cells. Oncogene. 2004;23(43):7274-82.
50. Zhao W, Ji X, Zhang F, Li L, Ma L. Embryonic stem cell markers. Molecules. 2012;17(6):6196-236.
51. Takahashi K, Yamanaka S. Induction of pluripotent stem cells from mouse embryonic and adult fibroblast cultures by defined factors. Cell. 2006;126.
52. Evans MJ, Kaufman MH. Establishment in culture of pluripotential cells from mouse embryos. Nature. 1981;292(5819):154-6.
53. Thomson JA, Itskovitz-Eldor, J., Shapiro, S.S., Waknitz, M.A., Swiergiel, J.J., Marshall, V.S., and Jones, J.M. Embryonic stem cell lines derived from human blastocysts. Science. 1998;282.
54. Niwa H, Miyazaki J, Smith AG. Quantitative expression of Oct-3/4 defines differentiation, dedifferentiation or self-renewal of ES cells. Nature genetics. 2000;24(4):372-6.
55. Jaenisch R YR. Stem Cells, the Molecular Circuitry of Pluripotency and Nuclear Reprogramming. Cell. 2008;132:567-82.
56. Masui S NY, Toyooka Y, Shimosato D, Yagi R, Takahashi K. Pluripotency governed by Sox2 via regulation of Oct3/4 expression in mouse embryonic stem cells. Nature cell biology. 2007;9:625-35.
57. Ferletta M, Caglayan D, Mokvist L, Jiang Y, Kastemar M, Uhrbom L, et al. Forced expression of Sox21 inhibits Sox2 and induces apoptosis in human glioma cells. International journal of cancer Journal international du cancer. 2011;129(1):45-60.
58. Leis O, Eguiara A, Lopez-Arribillaga E, Alberdi MJ, Hernandez-Garcia S, Elorriaga K, et al. Sox2 expression in breast tumours and activation in breast cancer stem cells. Oncogene. 2012;31(11):1354-65.
59. Weiren Luo1, Siyi Li1, Bailu Peng2, Yanfen Ye2, Xubin Deng2, Kaitai Yao2*. Embryonic Stem Cells Markers SOX2, OCT4 and Nanog Expression and Their Correlations with Epithelial- Mesenchymal Transition in Nasopharyngeal Carcinoma. PLoS genetics. 2013;8(2).
60. Han X, Fang X, Lou X, Hua D, Ding W, Foltz G, et al. Silencing SOX2 induced mesenchymal-epithelial transition and its expression predicts liver and lymph node metastasis of CRC patients. PloS one. 2012;7.
61. Chiou SH, Wang ML, Chou YT, Chen CJ, Hong CF, Hsieh WJ, et al. Coexpression of Oct4 and Nanog enhances malignancy in lung adenocarcinoma by inducing cancer stem cell-like properties and epithelial-mesenchymal transdifferentiation. Cancer research. 2010;70(24):10433-44.

62. Zhao S, Yuan Q, Hao H, Guo Y, Liu S, Zhang Y, et al. Expression of OCT4 pseudogenes in human tumours: lessons from glioma and breast carcinoma. The Journal of pathology. 2011;223(5):672-82.
63. Zeineddine D, Hammoud AA, Mortada M, Boeuf H. The Oct4 protein: more than a magic stemness marker. American Journal of Stem Cells. 2014;3(2):74-82.
64. Klemm JD PC. Oct-1 POU domain-DNA interactions: cooperative binding of isolated subdomains and effects of covalent linkage. Genes & development. 1996;10:27-36.
65. Yeom YI, Ha HS, Balling R, Scholer HR, Artzt K. Structure, expression and chromosomal location of the Oct-4 gene. Mechanisms of development. 1991;35(3):171-9.
66. Warthemann R, Eildermann K, Debowski K, Behr R. False-positive antibody signals for the pluripotency factor OCT4A (POU5F1) in testis-derived cells may lead to erroneous data and misinterpretations. Molecular human reproduction. 2012;18(12):605-12.
67. Rizzino A. Sox2 and Oct-3/4: a versatile pair of master regulators that orchestrate the self-renewal and pluripotency of embryonic stem cells. Wiley interdisciplinary reviews Systems biology and medicine. 2009;1(2):228-36.
68. Baselga J, Norton L. Focus on breast cancer. Cancer Cell.2002; (4): 319-22
69. Takeda J, Seino S, Bell GI. Human Oct3 gene family: cDNA sequences, alternative splicing, gene organization, chromosomal location, and expression at low levels in adult tissues. Nucleic Acids Res. 1992;20(17):4613-20.
70. Atlasi Y, Mowla SJ, Ziaee SA, Gokhale PJ, Andrews PW. OCT4 spliced variants are differentially expressed in human pluripotent and nonpluripotent cells. Stem cells. 2008;26(12):3068-74.
71. Cheong CY, Lufkin T. Alternative splicing in self-renewal of embryonic stem cells. Stem cells international. 2011;2011:560261.
72. Young Il Y HH-S, Balling R, Schöler HR, Artzt K. Structure, expression and chromosomal location of the Oct-4 gene. Mechanisms of development. 1991;35:171-9.
73. de Jong J LL. Stem cell marker OCT3/4 in tumor biology and germ cell tumor diagnostics: history and future. Critical reviews in oncogenesis. 2006;12:171-203.
74. Glinsky GV, Berezovska O, Glinskii AB. Microarray analysis identifies a death-from-cancer signature predicting therapy failure in patients with multiple types of cancer. The Journal of clinical investigation. 2005;115(6):1503-21.
75. Liedtke S, Enczmann J, Waclawczyk S, Wernet P, Kogler G. Oct4 and its pseudogenes confuse stem cell research. Cell stem cell. 2007;1(4):364-6.
76. Harrison PM, Milburn D, Zhang Z, Bertone P, Gerstein M. Identification of pseudogenes in the Drosophila melanogaster genome. Nucleic Acids Res. 2003;31(3):1033-7.
77. Xie G, Zhan J, Tian Y, Liu Y, Chen Z, Ren C, et al. Mammosphere cells from high-passage MCF7 cell line show variable loss of tumorigenicity and radioresistance. Cancer letters. 2012;316(1):53-61.
78. Marie Dewannieux CETH. LINE-mediated retrotransposition of marked Alu sequences. Nature. 2003;35:45-8.
79. Graur D, Shuali Y, Li WH. Deletions in processed pseudogenes accumulate faster in rodents than in humans. Journal of molecular evolution. 1989;28(4):279-85.
80. Max EE. Plagiarized Errors and Molecular Genetics: Another Argument in the Evolution-Creation Controversy. Creation/Evolution Journal. 1986;6:34–46.

81. Hayashi H, Arao T, Togashi Y, Kato H, Fujita Y, De Velasco MA, et al. The OCT4 pseudogene POU5F1B is amplified and promotes an aggressive phenotype in gastric cancer. Oncogene. 2015;34(2):199-208.
82. Weina K, Utikal J. SOX2 and cancer: current research and its implications in the clinic. Clinical and Translational Medicine. 2014;3(1):1-10.
83. Giorgetti A, Montserrat N, Rodriguez-Piza I, Azqueta C, Veiga A, Izpisua Belmonte JC. Generation of induced pluripotent stem cells from human cord blood cells with only two factors: Oct4 and Sox2. Nature protocols. 2010;5(4):811-20.
84. Dong C WD, Koopman P. Sox genes and cancer. Cytogenetic and Genome Research. 2004;105:442-7.
85. Sussman RT, Stanek TJ, Esteso P, Gearhart JD, Knudsen KE, McMahon SB. The epigenetic modifier ubiquitin-specific protease 22 (USP22) regulates embryonic stem cell differentiation via transcriptional repression of sex-determining region Y-box 2 (SOX2). The Journal of biological chemistry. 2013;288.
86. Koo BS, Lee SH, Kim JM, Huang S, Kim SH, Rho YS, et al. Oct4 is a critical regulator of stemness in head and neck squamous carcinoma cells. Oncogene. 2015;34(18):2317-24.
87. Wang Q, He W, Lu C, Wang Z, Wang J, Giercksky KE, et al. Oct3/4 and Sox2 are significantly associated with an unfavorable clinical outcome in human esophageal squamous cell carcinoma. Anticancer Res. 2009;29.
88. Ben-Porath I, Thomson MW, Carey VJ, Ge R, Bell GW, Regev A, et al. An embryonic stem cell-like gene expression signature in poorly differentiated aggressive human tumors. Nature genetics. 2008;40(5):499-507.
89. Hu T, Liu S, Breiter DR, Wang F, Tang Y, Sun S. Octamer 4 small interfering RNA results in cancer stem cell-like cell apoptosis. Cancer research. 2008;68(16):6533-40.
90. Nowell PC. The clonal evolution of tumor cell populations. Science. 1976;194(4260):23-8.
91. Li XL, Hara T, Choi Y, Subramanian M, Francis P, Bilke S, et al. A p21-ZEB1 complex inhibits epithelial-mesenchymal transition through the microRNA 183-96-182 cluster. Molecular and cellular biology. 2014;34(3):533-50.
92. Yohei Shimono 1, *, Junko Mukohyama 1, Shun-ichi Nakamura 1,2 and Hironobu Minami 3. MicroRNA Regulation of Human Breast Cancer Stem Cells. Clinical Medicine. 2015;5.
93. Velasco-Velazquez MA PV, Lisanti MP, Pestell RG. The role of breast cancer stem cells in metastasis and therapeutic implications. The American journal of pathology. 2011;179:2-11.
94. Wicha MS, Liu S, Dontu G. Cancer stem cells: an old idea--a paradigm shift. Cancer research. 2006;66(4):1883-90; discussion 95-6.
95. Clevers H. The cancer stem cell: premises, promises and challenges. Nature medicine. 2011;17(3):313-9.
96. Vazquez-Martin A, Cufí S, López-Bonet E, Corominas-Faja B, Cuyàs E, Vellon L, et al. Reprogramming of non-genomic estrogen signaling by the stemness factor SOX2 enhances the tumor-initiating capacity of breast cancer cells. Cell cycle. 2013;12.
97. Muhammad Al-HajjMSW, Adalberto Benito-Hernandez, Sean J. Morrison a, ClarkeMF. Prospective identification of tumorigenic breast cancer cells. pnas. 2003;100:3983–8.
98. Ginestier C, Hur MH, Charafe-Jauffret E, Monville F, Dutcher J, Brown M, et al. ALDH1 is a marker of normal and malignant human mammary stem cells and a predictor of poor clinical outcome. Cell stem cell. 2007;1(5):555-67.

99. Alvi AJ, Clayton H, Joshi C, Enver T, Ashworth A, Vivanco MdM, et al. Breast Cancer Research. 2002;5(1):R1.
100. Dontu G, Abdallah WM, Foley JM, Jackson KW, Clarke MF, Kawamura MJ, et al. In vitro propagation and transcriptional profiling of human mammary stem/progenitor cells. Genes & development. 2003;17(10):1253-70.
101. Liu H, Patel MR, Prescher JA, Patsialou A, Qian D, Lin J, et al. Cancer stem cells from human breast tumors are involved in spontaneous metastases in orthotopic mouse models. Proceedings of the National Academy of Sciences of the United States of America. 2010;107(42):18115-20.
102. Liu S, Dontu G, Wicha MS. Mammary stem cells, self-renewal pathways, and carcinogenesis. Breast cancer research : BCR. 2005;7(3):86-95.
103. Welch DR. Technical considerations for studying cancer metastasis in vivo. Clinical & Experimental Metastasis. 1997;15:272.
104. Tsvee Lapldot CS, Josef Vormoor, Barbara Caceres-Cortes, Mark Minden, Bruce Paterson, Michael A. Caligiuri, & John E. Dick. A cell initiation human acute myeloid leukaemia after transplantation into SCID mice. Nature. 1994;367.
105. Bjerkvig R, Tysnes BB, Aboody KS, Najbauer J, Terzis AJ. Opinion: the origin of the cancer stem cell: current controversies and new insights. Nature reviews Cancer. 2005;5(11):899-904.
106. Andrzejewski S, Gravel SP, Pollak M, St-Pierre J. Metformin directly acts on mitochondria to alter cellular bioenergetics. Cancer & Metabolism. 2014;2:12.
107. Kise K, Kinugasa-Katayama Y, Takakura N. Tumor microenvironment for cancer stem cells. Advanced drug delivery reviews. 2016;99(Pt B):197-205.
108. Smalley M, Piggott L, Clarkson R. Breast cancer stem cells: obstacles to therapy. Cancer letters. 2013;338(1):57-62.
109. GonÁalves NdN, Colombo J, Lopes JR, Gelaleti GB, Moschetta MG, Sonehara NlM, et al. Effect of Melatonin in Epithelial Mesenchymal Transition Markers and Invasive Properties of Breast Cancer Stem Cells of Canine and Human Cell Lines. PloS one. 2016;11(3):e0150407.
110. Dick JE. Stem cell concepts renew cancer research. Blood. 2008;112(13):4793-807.
111. Fox RG, Park FD, Koechlein CS, Kritzik M, Reya T. Musashi signaling in stem cells and cancer. Annual review of cell and developmental biology. 2015;31:249-67.
112. Chang JT, Mani SA. Sheep, wolf, or werewolf: cancer stem cells and the epithelial-to-mesenchymal transition. Cancer letters. 2013;341(1):16-23.
113. Birgersdotter A, Sandberg R, Ernberg I. Gene expression perturbation in vitro--a growing case for three-dimensional (3D) culture systems. Seminars in cancer biology. 2005;15(5):405-12.
114. Van der Worp HB, Howells DW, Sena ES, Porritt MJ, Rewell S, O'Collins V, et al. Can animal models of disease reliably inform human studies? PLoS medicine. 2010;7(3):e1000245.
115. Hait WN. Anticancer drug development: the grand challenges. Nat Rev Drug Discov. 2010;9(4):253-4.
116. Nelson CM, Bissell MJ. Modeling dynamic reciprocity: engineering three-dimensional culture models of breast architecture, function, and neoplastic transformation. Seminars in cancer biology. 2005;15(5):342-52.
117. Edmondson R, Broglie JJ, Adcock AF, Yang L. Three-Dimensional Cell Culture Systems and Their Applications in Drug Discovery and Cell-Based Biosensors. Assay and Drug Development Technologies. 2014;12(4):207-18.

118. Tibbitt MW, Anseth KS. Hydrogels as extracellular matrix mimics for 3D cell culture. Biotechnology and bioengineering. 2009;103(4):655-63.
119. Huang H, Ding Y, Sun XS, Nguyen TA. Peptide hydrogelation and cell encapsulation for 3D culture of MCF-7 breast cancer cells. PloS one. 2013;8(3):e59482.
120. Perche F, Torchilin VP. Cancer cell spheroids as a model to evaluate chemotherapy protocols. Cancer biology & therapy. 2012;13(12):1205-13.
121. Berx G, Raspé E, Christofori G, Thiery JP, Sleeman JP. Pre-EMTing metastasis? Recapitulation of morphogenetic processes in cancer. Clin Exp Metastasis. 2007;24(8):587-97
122. Palomeras S, Rabionet M, Ferrer I, Sarrats A, Garcia-Romeu ML, Puig T, et al. Breast Cancer Stem Cell Culture and Enrichment Using Poly(epsilon-Caprolactone) Scaffolds. Molecules. 2016;21(4).
123. Charafe-Jauffret E, Ginestier C, Birnbaum D. Breast cancer stem cells: tools and models to rely on. BMC cancer. 2009;9:202.
124. Grimshaw MJ, Cooper L, Papazisis K, Coleman JA, Bohnenkamp HR, Chiapero-Stanke L, et al. Mammosphere culture of metastatic breast cancer cells enriches for tumorigenic breast cancer cells. Breast cancer research : BCR. 2008;10(3):R52.
125. Shaw FL, Harrison H, Spence K, Ablett MP, Simoes BM, Farnie G, et al. A detailed mammosphere assay protocol for the quantification of breast stem cell activity. Journal of mammary gland biology and neoplasia. 2012;17(2):111-7.
126. Pastrana E, Silva-Vargas V, Doetsch F. Eyes wide open: a critical review of sphere-formation as an assay for stem cells. Cell stem cell. 2011;8(5):486-98.
127. Marie SKN, Shinjo SMO. Metabolism and brain cancer. Clinics. 2011;66:33-43.
128. Bonanni MCaB. Breast Cancer Metabolism and Mitochondrial Activity: The Possibility of Chemoprevention with Metformin. BioMed Research International. 2015;2015.
129. Patergnani S, Baldassari F, De Marchi E, Karkucinska-Wieckowska A, Wieckowski MR, Pinton P. Chapter Sixteen - Methods to Monitor and Compare Mitochondrial and Glycolytic ATP Production. In: Lorenzo G, Guido K, editors. Methods in Enzymology. Volume 542: Academic Press; 2014. p. 313-32.
130. Vander Heiden MG, Cantley LC, Thompson CB. Understanding the Warburg effect: the metabolic requirements of cell proliferation. Science. 2009;324(5930):1029-33.
131. Pike LS, Smift AL, Croteau NJ, Ferrick DA, Wu M. Inhibition of fatty acid oxidation by etomoxir impairs NADPH production and increases reactive oxygen species resulting in ATP depletion and cell death in human glioblastoma cells. Biochimica et Biophysica Acta (BBA) - Bioenergetics. 2011;1807(6):726-34.
132. Shanmugasundaram Ganapathy-Kanniappan1 and Jean-Francois H Geschwind1. Tumor glycolysis as a target for cancer therapy: progress and prospects. Molecular cancer. 2013;12.
133. Kondoh H. Cellular life span and the Warburg effect. Experimental cell research. 2008;314(9):1923-8.
134. Gatenby RA, Gillies RJ. Why do cancers have high aerobic glycolysis? Nature reviews Cancer. 2004;4(11):891-9.
135. Pecqueur C, Oliver L, Oizel K, Lalier L, Vallette FM. Targeting metabolism to induce cell death in cancer cells and cancer stem cells. International journal of cell biology. 2013;2013:805975.
136. Michelakis ED, Webster L, Mackey JR. Dichloroacetate (DCA) as a potential metabolic-targeting therapy for cancer. British journal of cancer. 2008;99(7):989-94.

137. Angelides KJ, Hammes GG. Mechanism of action of the pyruvate dehydrogenase multienzyme complex from Escherichia coli. Proceedings of the National Academy of Sciences of the United States of America. 1978;75(10):4877-80.
138. Morfouace M, Lalier L, Bahut M, Bonnamain V, Naveilhan P, Guette C, et al. Comparison of spheroids formed by rat glioma stem cells and neural stem cells reveals differences in glucose metabolism and promising therapeutic applications. The Journal of biological chemistry. 2012;287(40):33664-74.
139. Cantor JR, Sabatini DM. Cancer cell metabolism: one hallmark, many faces. Cancer discovery. 2012;2(10):881-98.
140. Ferreira LMR. Cancer metabolism: The Warburg effect today. Experimental and Molecular Pathology. 2010;89(3):372-80.
141. Zhang J, Nuebel E, Daley GQ, Koehler CM, Teitell MA. Metabolic regulation in pluripotent stem cells during reprogramming and self-renewal. Cell stem cell. 2012;11(5):589-95.
142. Gatenby RA, Gawlinski ET. A reaction-diffusion model of cancer invasion. Cancer research. 1996;56(24):5745-53.
143. Chen JL, Lucas JE, Schroeder T, Mori S, Wu J, Nevins J, et al. The genomic analysis of lactic acidosis and acidosis response in human cancers. PLoS genetics. 2008;4(12):e1000293.
144. Puspa RP, Wen L, Fei X, Koji F, Kounosuke W. Anti-Cancer Drugs Targeting Fatty Acid Synthase (FAS). Recent Patents on Anti-Cancer Drug Discovery. 2012;7(2):185-97.
145. Heddleston JM, Li Z, Lathia JD, Bao S, Hjelmeland AB, Rich JN. Hypoxia inducible factors in cancer stem cells. British journal of cancer. 2010;102(5):789-95.
146. DeBerardinis RJ, Sayed N, Ditsworth D, Thompson CB. Brick by brick: metabolism and tumor cell growth. Current Opinion in Genetics & Development. 2008;18(1):54-61.
147. Choi J, Kim do H, Jung WH, Koo JS. Metabolic interaction between cancer cells and stromal cells according to breast cancer molecular subtype. Breast cancer research : BCR. 2013;15(5):R78.
148. Erickson JW, Cerione RA. Glutaminase: a hot spot for regulation of cancer cell metabolism? Oncotarget. 2010;1(8):734-40.
149. Zhao Y, Butler EB, Tan M. Targeting cellular metabolism to improve cancer therapeutics. Cell death & disease. 2013;4:e532.
150. Mathupala SP, Heese C, Pedersen PL. Glucose catabolism in cancer cells. The type II hexokinase promoter contains functionally active response elements for the tumor suppressor p53. The Journal of biological chemistry. 1997;272(36):22776-80.
151. Maher JC, Krishan A, Lampidis TJ. Greater cell cycle inhibition and cytotoxicity induced by 2-deoxy-d-glucose in tumor cells treated under hypoxic vs aerobic conditions. Cancer Chemotherapy and Pharmacology. 2003;53(2):116-22.
152. Fantin VR, St-Pierre J, Leder P. Attenuation of LDH-A expression uncovers a link between glycolysis, mitochondrial physiology, and tumor maintenance. Cancer Cell. 2006;9(6):425-34.
153. Yang Y, DS, LZ, et al. Different effects of LDH-A inhibition by oxamate in non-small. Oncotarget. 2014;5.
154. Ioanna Papandreou TG, and Nicholas C. Denko. Anticancer drugs that target metabolism: is dichloroacetate. International Journal of Cancer. 2011;128.
155. Bode BP. Recent molecular advances in mammalian glutamine transport. The Journal of nutrition. 2001;131(9 Suppl):2475S-85S; discussion 86S-7S.

156. Wise DR, Thompson CB. Glutamine Addiction: A New Therapeutic Target in Cancer. Trends in biochemical sciences. 2010;35(8):427-33.
157. Curi R, Lagranha CJ, Doi SQ, Sellitti DF, Procopio J, Pithon-Curi TC, et al. Molecular mechanisms of glutamine action. Journal of cellular physiology. 2005;204(2):392-401.
158. Lu CW, Lin SC, Chen KF, Lai YY, Tsai SJ. Induction of pyruvate dehydrogenase kinase-3 by hypoxia-inducible factor-1 promotes metabolic switch and drug resistance. The Journal of biological chemistry. 2008;283(42):28106-14.
159. Papandreou I, Cairns RA, Fontana L, Lim AL, Denko NC. HIF-1 mediates adaptation to hypoxia by actively downregulating mitochondrial oxygen consumption. Cell Metab. 2006;3(3):187-97.
160. Huqi A. cancer and inhibition of fatty acid oxidation. Heart Metab. 2011;51.
161. Wong JYY, Huggins GS, Debidda M, Munshi NC, De Vivo I. Dichloroacetate induces apoptosis in endometrial cancer cells. Gynecologic Oncology.109(3):394-402.
162. Salani B, Del Rio A, Marini C, Sambuceti G, Cordera R, Maggi D. Metformin, cancer and glucose metabolism. Endocrine-related cancer. 2014;21(6):R461-71.
163. Liu X, Chhipa RR, Pooya S, Wortman M, Yachyshin S, Chow LM, et al. Discrete mechanisms of mTOR and cell cycle regulation by AMPK agonists independent of AMPK. Proceedings of the National Academy of Sciences of the United States of America. 2014;111(4):E435-44.
164. Birsoy K, Possemato R, Lorbeer FK, Bayraktar EC, Thiru P, Yucel B, et al. Metabolic determinants of cancer cell sensitivity to glucose limitation and biguanides. Nature. 2014;508(7494):108-12.
165. Lopaschuk GD, Ussher JR, Folmes CD, Jaswal JS, Stanley WC. Myocardial fatty acid metabolism in health and disease. Physiological reviews. 2010;90(1):207-58.
166. Chinnadurai G. Transcriptional regulation by C-terminal binding proteins. The international journal of biochemistry & cell biology. 2007;39(9):1593-607.
167. Zhang Q, Wang SY, Nottke AC, Rocheleau JV, Piston DW, Goodman RH. Redox sensor CtBP mediates hypoxia-induced tumor cell migration. Proceedings of the National Academy of Sciences of the United States of America. 2006;103(24):9029-33.
168. Bergman L, Blaydes J. Loss of C-terminal binding protein transcriptional corepressor leads to aberrant mitosis and cell death in breast cancer cells: Breast Cancer Res. 2006;8(Suppl 2):P1. Epub 2006 Nov 1 doi:10.1186/bcr1556.
169. Hildebrand JD, Soriano P. Overlapping and unique roles for C-terminal binding protein 1 (CtBP1) and CtBP2 during mouse development. Molecular and cellular biology. 2002;22(15):5296-307.
170. Byun JS, Gardner K. C-Terminal Binding Protein: A Molecular Link between Metabolic Imbalance and Epigenetic Regulation in Breast Cancer. International journal of cell biology. 2013;2013:647975.
171. Di LJ, Byun JS, Wong MM, Wakano C, Taylor T, Bilke S, et al. Genome-wide profiles of CtBP link metabolism with genome stability and epithelial reprogramming in breast cancer. Nature communications. 2013;4:1449.
172. Straza MW, Paliwal S, Kovi RC, Rajeshkumar B, Trenh P, Parker D, et al. Therapeutic targeting of C-terminal binding protein in human cancer. Cell cycle. 2010;9(18):3740-50.
173. Wang L, Zhou H, Wang Y, Cui G, Di LJ. CtBP maintains cancer cell growth and metabolic homeostasis via regulating SIRT4. Cell death & disease. 2015;6:e1620.
174. Patel J, Baranwal S, Love IM, Patel NJ, Grossman SR, Patel BB. Inhibition of C-terminal binding protein attenuates transcription factor 4 signaling to selectively target colon cancer stem cells. Cell cycle. 2014;13(22):3506-18.

175. Tan BT, Park CY, Ailles LE, Weissman IL. The cancer stem cell hypothesis: a work in progress. Lab Invest. 2006;86(12):1203-7.
176. Shyh-Chang N, Daley GQ, Cantley LC. Stem cell metabolism in tissue development and aging. Development. 2013;140(12):2535-47.
177. Sakamoto R, Rahman MM, Shimomura M, Itoh M, Nakatsura T. Time-lapse imaging assay using the BioStation CT: a sensitive drug-screening method for three-dimensional cell culture. Cancer science. 2015;106(6):757-65.
178. Reitzer LJ, Wice BM, Kennell D. Evidence that glutamine, not sugar, is the major energy source for cultured HeLa cells. The Journal of biological chemistry. 1979;254(8):2669-76.
179. Marvin T. Nieman RSP, Keith R. Johnson, and Margaret J. Wheelock. N-Cadherin Promotes Motility in Human Breast Cancer Cells Regardless of Their E-Cadherin Expression. The Journal of cell biology. 1999;147.
180. Annibaldi A, Widmann C. Glucose metabolism in cancer cells. Current opinion in clinical nutrition and metabolic care. 2010;13(4):466-70.
181. Liu H, Huang D, McArthur DL, Boros LG, Nissen N, Heaney AP. Fructose induces transketolase flux to promote pancreatic cancer growth. Cancer research. 2010;70(15):6368-76.
182. Visvader JE, Lindeman GJ. Cancer stem cells in solid tumours: accumulating evidence and unresolved questions. Nature reviews Cancer. 2008;8(10):755-68.
183. Manuel Iglesias J, Beloqui I, Garcia-Garcia F, Leis O, Vazquez-Martin A, Eguiara A, et al. Mammosphere formation in breast carcinoma cell lines depends upon expression of E-cadherin. PloS one. 2013;8(10):e77281.
184. Liu A, Yu X, Liu S. Pluripotency transcription factors and cancer stem cells: small genes make a big difference. Chinese Journal of Cancer. 2013;32(9):483-7.
185. Kumar SM, Liu S, Lu H, Zhang H, Zhang PJ, Gimotty PA, et al. Acquired cancer stem cell phenotypes through Oct4-mediated dedifferentiation. Oncogene. 2012;31(47):4898-911.
186. Jez M, Ambady S, Kashpur O, Grella A, Malcuit C, Vilner L, et al. Expression and differentiation between OCT4A and its Pseudogenes in human ESCs and differentiated adult somatic cells. PloS one. 2014;9(2):e89546.
187. Liang J, Wan M, Zhang Y, Gu P, Xin H, Jung SY, et al. Nanog and Oct4 associate with unique transcriptional repression complexes in embryonic stem cells. Nat Cell Biol. 2008;10(6):731-9.
188. Kim RJ, Nam JS. OCT4 Expression Enhances Features of Cancer Stem Cells in a Mouse Model of Breast Cancer. Laboratory Animal Research. 2011;27(2):147-52.
189. Liu CG, Lu Y, Wang BB, Zhang YJ, Zhang RS, Lu Y, et al. Clinical implications of stem cell gene Oct-4 expression in breast cancer. Annals of surgery. 2011;253(6):1165-71.
190. Wang Y, Meng L, Hu H, Zhang Y, Zhao C, Li Q, et al. Oct-4B isoform is differentially expressed in breast cancer cells: hypermethylation of regulatory elements of Oct-4A suggests an alternative promoter and transcriptional start site for Oct-4B transcription. Bioscience reports. 2011;31(2):109-15.
191. Piva M, Domenici G, Iriondo O, Rabano M, Simoes BM, Comaills V, et al. Sox2 promotes tamoxifen resistance in breast cancer cells. EMBO molecular medicine. 2014;6(1):66-79.
192. Castillo SD, Sanchez-Cespedes M. The SOX family of genes in cancer development: biological relevance and opportunities for therapy. Expert Opinion on Therapeutic Targets. 2012;16(9):903-19.

193. Ling G, Chen D, Wang B, Zhang L. Expression of the pluripotency markers Oct3/4, Nanog and Sox2 in human breast cancer cell lines. Oncology Letters. 2012;4(6):1264-8.
194. Rodriguez-Pinilla SM, Sarrio D, Moreno-Bueno G, Rodriguez-Gil Y, Martinez MA, Hernandez L, et al. Sox2: a possible driver of the basal-like phenotype in sporadic breast cancer. Mod Pathol. 2007;20(4):474-81.
195. Stem cells and cancer stem cells. Kean University, Union, NJ, USA: Springer.
196. Cantz T, Key G, Bleidissel M, Gentile L, Han DW, Brenne A, et al. Absence of OCT4 expression in somatic tumor cell lines. Stem cells. 2008;26(3):692-7.
197. Bhartiya D, Kasiviswanathan S, Unni SK, Pethe P, Dhabalia JV, Patwardhan S, et al. Newer insights into premeiotic development of germ cells in adult human testis using Oct-4 as a stem cell marker. The journal of histochemistry and cytochemistry : official journal of the Histochemistry Society. 2010;58(12):1093-106.
198. Suo G, Han J, Wang X, Zhang J, Zhao Y, Zhao Y, et al. Oct4 pseudogenes are transcribed in cancers. Biochemical and biophysical research communications. 2005;337(4):1047-51.
199. Shao-Wen Li X-LW, Chun-Li Dong, Xiu-Ying Xie, Jin-Fang Wu, Xin Zhang. The Differential Expression of OCT4 Isoforms in Cervical Carcinoma. PLoS genetics. 2015;10.
200. Gibbs CP, Kukekov VG, Reith JD, Tchigrinova O, Suslov ON, Scott EW, et al. Stem-Like Cells in Bone Sarcomas: Implications for Tumorigenesis. Neoplasia (New York, NY). 2005;7(11):967-76.
201. Chiou SH, Yu CC, Huang CY, Lin SC, Liu CJ, Tsai TH, et al. Positive correlations of Oct-4 and Nanog in oral cancer stem-like cells and high-grade oral squamous cell carcinoma. Clinical cancer research : an official journal of the American Association for Cancer Research. 2008;14(13):4085-95.
202. Maria Peiris-Pagès UEM-O, Richard G. Pestell, Federica Sotgia and Michael P. Lisanti. Cancer stem cell metabolism
. Breast Cancer Research. 2016;10.
203. Liedtke S, Stephan M, Kogler G. Oct4 expression revisited: potential pitfalls for data misinterpretation in stem cell research. Biological chemistry. 2008;389(7):845-50.
204. Ciavardelli D, Rossi C, Barcaroli D, Volpe S, Consalvo A, Zucchelli M, et al. Breast cancer stem cells rely on fermentative glycolysis and are sensitive to 2-deoxyglucose treatment. Cell death & disease. 2014;5:e1336.
205. Ji-Won Jung1.¤ S-BP, Soo-Jin Lee1, Min-Soo Seo1, James E. Trosko1,2, Kyung-Sun Kang1. Metformin Represses Self-Renewal of the Human Breast
Carcinoma Stem Cells via Inhibition of Estrogen
Receptor-Mediated OCT4 Expression. PloS one. 2011;6(11).
206. Wang X, Moraes CT. Increases in mitochondrial biogenesis impair carcinogenesis at multiple levels. Molecular Oncology.5(5):399-409.
207. Gang BP, Dilda PJ, Hogg PJ, Blackburn AC. Targeting of two aspects of metabolism in breast cancer treatment. Cancer biology & therapy. 2014;15(11):1533-41.
208. Currie E, Schulze A, Zechner R, Walther Tobias C, Farese Robert V, Jr. Cellular Fatty Acid Metabolism and Cancer. Cell Metabolism. 2013;18(2):153-61.
209. María Cristina Estañ EC, 1 Susana Calvo,1,2 Beatriz Guillén-Guío,1 María del Carmen Boyano-Adánez,2 Elena de Blas,1 Eduardo Rial,1,* and Patricio Aller1,*. Apoptotic Efficacy of Etomoxir in Human Acute Myeloid Leukemia Cells. Cooperation with Arsenic Trioxide and Glycolytic Inhibitors, and Regulation by Oxidative Stress and Protein Kinase Activities. PloS one. 2014;9.

210. Jack BH, Pearson RC, Crossley M. C-terminal binding protein: A metabolic sensor implicated in regulating adipogenesis. The international journal of biochemistry & cell biology. 2011;43(5):693-6.
211. Kim H, Jang H, Kim TW, Kang BH, Lee SE, Jeon YK, et al. Core Pluripotency Factors Directly Regulate Metabolism in Embryonic Stem Cell to Maintain Pluripotency. Stem cells. 2015;33(9):2699-711.
212. Kuo SC, Lampen JO. Inhibition by 2-deoxy-D-glucose of synthesis of glycoprotein enzymes by protoplasts of Saccharomyces: relation to inhibition of sugar uptake and metabolism. Journal of bacteriology. 1972;111(2):419-29.
213. Diansheng Zhong LX, Tongrui Liu, Xiuju Liu, Xiangguo Liu, Jing Chen, Shi-Yong Sun, Fadlo R. Khuri, Yaping Zong‖, Qinghua Zhou and Wei Zhou,1,2. The Glycolytic Inhibitor 2-Deoxyglucose Activates Multiple Prosurvival Pathways through IGF1R. jbc. 2009.
214. Kurtoglu M, Gao N, Shang J, Maher JC, Lehrman MA, Wangpaichitr M, et al. Under normoxia, 2-deoxy-D-glucose elicits cell death in select tumor types not by inhibition of glycolysis but by interfering with N-linked glycosylation. Molecular cancer therapeutics. 2007;6(11):3049-58.
215. Zhong D, Liu X, Schafer-Hales K, Marcus AI, Khuri FR, Sun SY, et al. 2-Deoxyglucose induces Akt phosphorylation via a mechanism independent of LKB1/AMP-activated protein kinase signaling activation or glycolysis inhibition. Molecular cancer therapeutics. 2008;7(4):809-17.
216. Kaadige MR, Looper RE, Kamalanaadhan S, Ayer DE. Glutamine-dependent anapleurosis dictates glucose uptake and cell growth by regulating MondoA transcriptional activity. Proceedings of the National Academy of Sciences of the United States of America. 2009;106(35):14878-83.
217. Hensley CT. Glutamine and cancer: cell biology, physiology, and clinical opportunities. 2013;123(9):3678-84.
218. Kung HN, Marks JR, Chi JT. Glutamine synthetase is a genetic determinant of cell type-specific glutamine independence in breast epithelia. PLoS genetics. 2011;7(8):e1002229.
219. Diana Hatoum1 and Eileen M. McGowan1. Recent Advances in the Use of Metformin: Can Treating Diabetes Prevent Breast Cancer? BioMed Research International
. 2015;2015.
220. Sancho P, Burgos-Ramos E, Tavera A, Bou Kheir T, Jagust P, Schoenhals M, et al. MYC/PGC-1α Balance Determines the Metabolic Phenotype and Plasticity of Pancreatic Cancer Stem Cells. Cell Metabolism.22(4):590-605.
221. Zaugg K, Yao Y, Reilly PT, Kannan K, Kiarash R, Mason J, et al. Carnitine palmitoyltransferase 1C promotes cell survival and tumor growth under conditions of metabolic stress. Genes & development. 2011;25(10):1041-51.
222. Lu J, Wang Q, Huang L, Dong H, Lin L, Lin N, et al. Palmitate causes endoplasmic reticulum stress and apoptosis in human mesenchymal stem cells: prevention by AMPK activator. Endocrinology. 2012;153(11):5275-84.
223. Fillmore N, Huqi A, Jaswal JS, Mori J, Paulin R, Haromy A, et al. Effect of Fatty Acids on Human Bone Marrow Mesenchymal Stem Cell Energy Metabolism and Survival. PloS one. 2015;10(3).
224. Cui TX, Kryczek I, Zhao L, Zhao E, Kuick R, Roh MH, et al. Myeloid-derived suppressor cells enhance stemness of cancer cells by inducing microRNA101 and suppressing the corepressor CtBP2. Immunity. 2013;39(3):611-21.

225. DeBerardinis RJ, Mancuso A, Daikhin E, Nissim I, Yudkoff M, Wehrli S, et al. Beyond aerobic glycolysis: transformed cells can engage in glutamine metabolism that exceeds the requirement for protein and nucleotide synthesis. Proceedings of the National Academy of Sciences of the United States of America. 2007;104(49):19345-50.
226. Chinnadurai G. The Transcriptional Corepressor CtBP: A Foe of Multiple Tumor Suppressors. Cancer research. 2009;69(3).
227. Chiarugi A, Dolle C, Felici R, Ziegler M. The NAD metabolome [mdash] a key determinant of cancer cell biology. Nature reviews Cancer. 2012;12(11):741-52.
228. Kim JH, Youn HD. C-terminal binding protein maintains mitochondrial activities. Cell Death Differ. 2009;16(4):584-92.
229. Moussaieff A, Rouleau M, Kitsberg D, Cohen M, Levy G, Barasch D, et al. Glycolysis-Mediated Changes in Acetyl-CoA and Histone Acetylation Control the Early Differentiation of Embryonic Stem Cells. Cell Metabolism.21(3):392-402.
230. Marsboom G, Zhang G-F, Pohl-Avila N, Zhang Y, Yuan Y, Kang H, et al. Glutamine Metabolism Regulates the Pluripotency Transcription Factor OCT4. Cell Reports.16(2):323-32.
231. Ding L, Ellis MJ, Li S, Larson DE, Chen K, Wallis JW, et al. Genome remodelling in a basal-like breast cancer metastasis and xenograft. Nature. 2010;464(7291):999-1005.
232. Nijkamp MM, Span PN, Hoogsteen IJ, van der Kogel AJ, Kaanders JH, Bussink J. Expression of E-cadherin and vimentin correlates with metastasis formation in head and neck squamous cell carcinoma patients. Radiotherapy and oncology : journal of the European Society for Therapeutic Radiology and Oncology. 2011;99(3):344-8.
233. Fan L, Wang H, Xia X, Rao Y, Ma X, Ma D, et al. Loss of E-cadherin promotes prostate cancer metastasis via upregulation of metastasis-associated gene 1 expression. Oncology Letters. 2012;4(6):1225-33.
234. Pulito C, Donzelli S, Muti P, Puzzo L, Strano S, Blandino G. microRNAs and cancer metabolism reprogramming: the paradigm of metformin. Annals of Translational Medicine. 2014;2(6).
235. Erina Vlashia, Chann Lagadeca,1, Laurent Vergnesb, TM, KM, MP, , Popescua R, et al. metabolic state of glioma stem cells and nontumorigenic cells. PNAS. 2011;108.
236. Mikkers H, Frisen J. Deconstructing stemness. The EMBO journal. 2005;24(15):2715-9.